PINCER-METAL COMPLEXES

Applications in Catalytic Dehydrogenation Chemistry

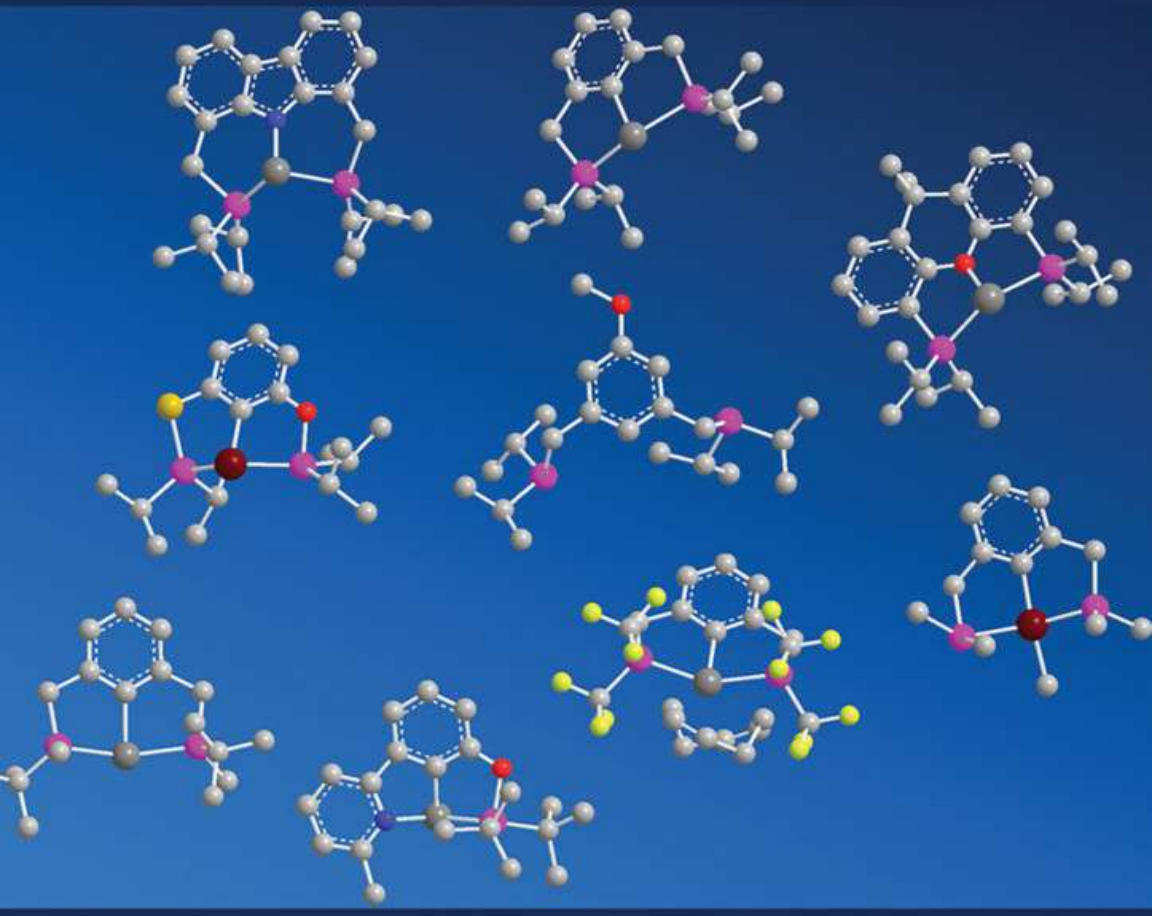

ELSEVIER

Edited by
Akshai Kumar

Pincer—Metal Complexes

Pincer–Metal Complexes

Applications in Catalytic Dehydrogenation Chemistry

Edited by

AKSHAI KUMAR

Department of Chemistry, Centre for Nanotechnology, School of Health Science and Technology, Indian Institute of Technology, Guwahati, Guwahati, India

ELSEVIER

Elsevier
Radarweg 29, PO Box 211, 1000 AE Amsterdam, Netherlands
The Boulevard, Langford Lane, Kidlington, Oxford OX5 1GB, United Kingdom
50 Hampshire Street, 5th Floor, Cambridge, MA 02139, United States

Notices
Knowledge and best practice in this field are constantly changing. As new research and experience broaden our understanding, changes in research methods, professional practices, or medical treatment may become necessary.

Practitioners and researchers must always rely on their own experience and knowledge in evaluating and using any information, methods, compounds, or experiments described herein. In using such information or methods they should be mindful of their own safety and the safety of others, including parties for whom they have a professional responsibility.

To the fullest extent of the law, neither the Publisher nor the authors, contributors, or editors, assume any liability for any injury and/or damage to persons or property as a matter of products liability, negligence or otherwise, or from any use or operation of any methods, products, instructions, or ideas contained in the material herein.

British Library Cataloguing-in-Publication Data
A catalogue record for this book is available from the British Library

Library of Congress Cataloging-in-Publication Data
A catalog record for this book is available from the Library of Congress

ISBN: 978-0-12-822091-7

Publisher: Susan Dennis
Acquisitions Editor: Emily M. McCloskey
Editorial Project Manager: Lena Sparks
Production Project Manager: Paul Prasad Chandramohan
Cover Designer: Victoria Pearson

Typeset by MPS Limited, Chennai, India

Contents

List of contributors

Vinay Arora
Department of Chemistry, Indian Institute of Technology Guwahati, Guwahati, India

Ekambaram Balaraman
Department of Chemistry, Indian Institute of Science Education and Research (IISER), Tirupati, India

Prosenjit Daw
Department of Chemical Sciences, Indian Institute of Science Education and Research Berhampur, Berhampur, India

Akshai Kumar
Department of Chemistry, Indian Institute of Technology Guwahati, Guwahati, India; Center for Nanotechnology, Indian Institute of Technology Guwahati, Guwahati, India; School of Health Science & Technology, Indian Institute of Technology Guwahati, Guwahati, India

Sabuj Kundu
Department of Chemistry, Indian Institute of Technology Kanpur, Kanpur, India

Aisa Mohanty
Department of Chemical Sciences, Indian Institute of Science Education and Research Berhampur, Berhampur, India

Pran Gobinda Nandi
Department of Chemistry, Indian Institute of Technology Guwahati, Guwahati, India

Bhaskar Paul
Department of Chemistry, Indian Institute of Technology Kanpur, Kanpur, India; University of California at Riverside, Riverside, CA, United States

Raju Sharma
Department of Chemical Sciences, Indian Institute of Science Education and Research Berhampur, Berhampur, India

Sujan Shee
Department of Chemistry, Indian Institute of Technology Kanpur, Kanpur, India

Ganesan Sivakumar
Department of Chemistry, Indian Institute of Science Education and Research (IISER), Tirupati, India

Vinita Yadav
Organic Chemistry Division, CSIR—National Chemical Laboratory (CSIR—NCL), Pune, India; Academy of Scientific and Innovative Research (AcSIR), Ghaziabad, India

Eileen Yasmin
Department of Chemistry, Indian Institute of Technology Guwahati, Guwahati, India

Foreword

A typical pincer ligand consists of three donor atoms stabilizing a planar, meridional, or occasionally facial metal scaffold, with the central donor moiety being neutral or anionic, resulting in two five-membered chelate rings. Although PCP type of pincer ligands with central anionic carbon-donor atom flanked by soft phosphorus donors was first established by Shaw in the 1970s, it took center stage much later and was subsequently established as a novel ligand system to promote several challenging catalytic reactions and showed its superiority in metal-mediated organic synthesis. As a result, pincer framework witnessed tremendous growth in the last two decades with a variety of combinations of donor atoms, preferably having an aromatic or pyridyl bridging units and became an integral part of inorganic and organometallic chemistry and homogeneous catalysis. Relatively easy synthetic methodologies, six-electron donor capability, availability of numerous P, N, O, and S donor moieties for incorporation, options for tuning steric and electronic properties, and robust nature made pincer ligands one of the most invincible systems in the field of applied science.

Presently researchers are using a variety of pincer platforms to perform challenging and unusual organic transformations under mild conditions, for example, ammonia production from dinitrogen, conversion of CO_2 into useful organic molecules, and alkane dehydrogenation. Metal-mediated dehydrogenation is a green and environmentally benign system valuable in several synthetic processes and possibly for hydrogen generation and storage for future energy requirements.

In this context, Akshai Kumar's efforts to bring a consolidated monograph on various dehydrogenation processes utilizing pincer ligands are commendable. I am sure that this book will receive a very good response from synthetic chemists and all readers.

M.S. Balakrishna
Phosphorus Laboratory, Department of Chemistry, IIT Bombay, Mumbai, India

Preface

Ever since the discovery of the first organometallic complex, ligands have been systematically modified to attain better control on the stability and reactivity of organometallic systems. This has led to interesting findings that metal complexes containing monodentate ligands are less stable than bidentate, which in turn are less stable than tridentate systems and so on. No surprisingly, the enhanced stability comes as a trade-off to the reduced reactivity. It has been widely accepted that tridentate systems (those binding the metal center in a meridional fashion, in particular) strike an optimal balance between the stability and reactivity. These "Pincer" systems offer numerous avenues to tailor the reactivity via the steric and the electronic control. The typically rigid framework provides robustness to the complex thereby enhancing its thermal stability. On the other hand, the catalytic versatility is provided by the ease of ligand tailoring to suit one's steric and electronic requirements.

Several modifications of the pincer motif have been reported owing to the easily tailorable ligand backbone leading to five- or six-membered chelate rings that have a common metal-hetero atom bond. Pincer complexes with desired catalytic properties have been obtained by varying either the ligating groups or by changing the linker atoms apart from the possibility of having the pincer platform itself as a noninnocent ligand. Furthermore, the aryl backbone offers the possibility of introducing several polar functionalities, which not only helps in controlling the electronics remotely but also facilitates the heterogenization of the molecular catalysts on many solid supports. The chemistry of pincer complexes is very vast and owes a lot to the outstanding contributions to pioneers such as Shaw, van-Koten, Kaska, Jensen, Goldman, Milstein, and Brookhart among several others. Rightly, this interesting chemistry has been reviewed several times in various contexts and for scattered applications. This book discusses the chemistry of pincer–metal complexes in the context of a single application of dehydrogenation of various hydrocarbon derivatives catalyzed by pincer–metal complexes.

Hitherto, the dehydrogenation of hydrocarbons and their derivatives have been discussed separately. This stems from the fact that the operating mechanisms and catalyst compatibility for pure hydrocarbons are distinctly different from their functionalized analogs. However, in recent years,

there has been a surge in the lookout for hydrocarbon dehydrogenation catalytic systems that are compatible with polar substituents. This would facilitate formulation of tandem processes that are not only limited to hydrocarbon transformation but also to hydrocarbon functionalization in a single pot. In this context, this book provides a good understanding on the operating mechanisms and dehydrogenation catalyst compatibility in both (functionalized and unfunctionalized) hydrocarbon systems. This unified approach would not only shed light on the distinct differences of these catalytic systems but also would reveal the subtle similarities in the reactivity.

Accordingly, it is a great pleasure to start the book with Chapter 1 on Application of Pincer–Metal Complexes in Catalytic Transformations by Daw. Chapter 2, Pincer-Group(8) and Pincer-Group(9) Metal Complexes for Catalytic Alkane Dehydrogenation Reactions, reviews the chemistry of group-8 and group-9 pincer–metal complexes in alkane dehydrogenation. In Chapter 3, Transition Metal Catalyzed Dehydrogenation of Methanol and Related Transformations, Kundu provides an overview on the pincer–metal catalyzed dehydrogenation of methanol and related reactions. This is followed by Chapter 4, Transition Metal Pincer Complexes in Acceptorless Dehydrogenation Reactions, from Balaraman who comment on the applicability of pincer–metal complexes in acceptorless dehydrogenation of functionalized hydrocarbons. Chapter 5, An Outlook on the Applications of Pincer–Metal Complexes in Catalytic Dehydrogenation Chemistry, summarizes the current state-of-art in the pincer–metal catalyzed dehydrogenation chemistry of hydrocarbons and their derivatives. It is hoped that the knowledge churned out from this whole exercise would be beneficial and enjoyable for the authors and the audience alike. This concept offers immense potential of leading to exciting future innovations in the dehydrogenation chemistry. It is envisaged that the audience who read this book would develop their own perception on this fascinating chemistry, which could result in diverse new research endeavors and exciting possibilities.

My heartfelt appreciation to the authors for their excellent contribution of science. I have been fortunate to have the support from a very able, professional, and cooperative editorial team comprising Emily M. McCloskey and Lena Sparks. The periodic discussions with Lena have been of immense help in producing this volume in a timely manner.

Akshai Kumar

CHAPTER 1

Application of pincer metal complexes in catalytic transformations

Aisa Mohanty, Raju Sharma and Prosenjit Daw*
Department of Chemical Sciences, Indian Institute of Science Education and Research Berhampur, Berhampur, India
*Corresponding author. e-mail address: pdaw@iiserbpr.ac.in

1.1 Introduction

Ligand's versatility plays a significant role in the sensitive design of metal complexes to display interesting reactivity toward the field of catalysis. A wide variety of ligands are developed that tune the metal center reactivity based on steric and electronic properties. Pincer ligands have gained special interests in catalysis due to their specific properties [1]. The term "Pincer" was first coined by G. Van Koten in 1989, and it was noted that the rigidity of such ligands can tune the stability of the metal complexes [2]. The synthesis of pincer complexes has been started in the early 1970s by Moulton and Shaw [3], and in present days, various new architectural designs continue to come out. The modern definition of pincer complexes is associated with rigid binding with the three adjacent coplanar sites of metal in a meridional configuration [4]. In general, a central aromatic backbone with two Lewis basic donor groups attached in the sidearm by spacers group is the more frequently observed system that makes a tridentate ligand. Although various kinds of pincer systems are also known without having the aromatic backbone. Pincer ligands offer a valuable scope toward steric and electronic properties of the complexes, therefore providing high stability due to its chelating nature and can increase its potential value toward catalysis. Crabtree and Peris described the classification of the pincer ligands based on their symmetry (palindromic or nonpalindromic) and neutral or ionic nature of its binding motifs, which is depicted in Fig. 1.1 [5].

Due to the thermal stability, the pincer complexes are used as catalysts in various kinds of organic transformations [6]. The specific architectural design and their different properties like non-innocent nature, outer

Pincer–Metal Complexes
DOI: https://doi.org/10.1016/B978-0-12-822091-7.00003-8

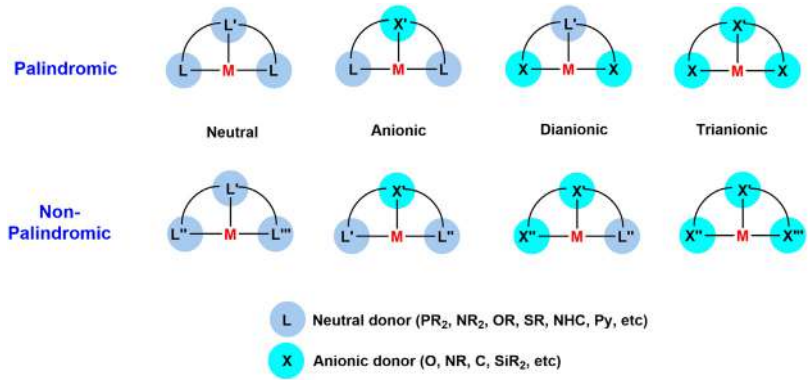

Figure 1.1 Common types of pincer ligands and their classification.

sphere effects on ligand frameworks [7], metal–ligand cooperation [8], hemilability of pendant arms [9], and redox-active behavior, which facilitates single electron transfer [10] of such complexes, serve as an unique platform for introducing their role in homogeneous catalysis. Along with pincer systems are enable to activate the small organic molecule such as CO_2, H_2, N_2, water, acids, dihalides, oxidizing, and reducing agents at elevated temperature without hampering the pincer coordination geometry [11]. Except for catalysis, some species are also used for multiple purposes ranging from application in nanoscience to the development of chemical sensors and chemical switches [12]. Moreover, pincer complexes have been used to investigate C–C, C–H, and C–O bond activation processes [13] or serve as building blocks for the synthesis of self-assembled supramolecular structures [14]. The major application of such kind of pincer complexes is in the field of homogeneous catalysis reaction involving hydrogenation and dehydrogenation reaction of organic molecules. A vast literature presents on the dehydrogenation of organic substrates [15], transfer hydrogenation [16], acceptorless dehydrogenation [17], dehydrogenative coupling reaction [18], borrowing hydrogenation reaction [19], and alkane dehydrogenation reaction using such pincer complexes [20].

In this book, other chapters are dedicated to the topics of olefin dehydrogenation, alcohol dehydrogenative coupling reaction, and methanol dehydrogenation reaction. In this chapter, we present general applications of the pincer complexes in the homogeneous catalysis reaction such as ammonia borane dehydrogenation and its application in the hydrogen storage, dinitrogen activation and its application to the ammonia synthesis,

coupling reactions, hydrogenation of challenging organic molecules like urea, carbonate, carbamate, amide, ester, and the redox-active pincer ligand and its application in the organic transformation.

1.2 Dehydrogenation of ammonia borane and its derivatives

In search of alternatives to fossil fuels, hydrogen is probably the most promising as the energy source for the future, which does not produce any common pollutant of greenhouse gases [21–24]. Due to its low volumetric energy density, the storage of hydrogen is the major challenge in the hydrogen economy. Hydrogen can be stored in two forms: physical and chemical. Apart from the physical form of storage (like compressed gas to liquid hydrogen and adsorbent materials, having some major limitation), the chemical form has emerged as a good alternative, consisting of the releasing of molecular hydrogen from organic compounds with high hydrogen density, such as HCOOH, CH_3OH, organic heterocycles [25–27].

Ammonia borane is often considered as a promising chemical hydrogen storage material due to its high hydrogen content as low molecular weight ammonia boranes can offer up to 19.6 wt% storage capacity theoretically. A protic and hydridic hydrogen atoms adjacent to each other present in the ammonia boranes that are Lewis acid-base adducts and make the release of hydrogen gas favorable. Ammonia boranes can dehydrogenate thermally in the absence of a catalyst, although the use of a catalyst affords the dehydrogenation process under mild conditions. The hydrogen storage capacity depends on the final dehydrogenated product distribution and the catalyst plays a vital role here. Poly(aminoborane) $[H_2BNH_2]_n$, borazine $[HBNH]_3$, or polyborazylene (hydrogen storage capacity 6.8–12.96 wt%) can be formed by the dehydropolymerization process of ammonia borane $H_3B \cdot NH_3$ by eliminating more than 1 equivalent of hydrogen gas. Whereas the substituted amine-boranes like $H_3B \cdot NMeH_2$, $H_3B \cdot NMe_2H$, and $MeH_2B \cdot NH_2R$ exhibit a relatively lower hydrogen storage capacity after the dehydrocoupling to form poly (aminoborane) derivative. The vast amount of research attempts to maximize the hydrogen yield to implement these compounds as hydrogen storage material along with detailed mechanistic studies were performed to understand the transition metal complexes interaction with such substrates containing protic and hydridic hydrogens [28–37]. Several pincer

complexes have also been used for the dehydrogenation of ammonia borane derivatives as describe here.

In 2006, the Goldberg group first explored the (POCOP)Ir$(H)_2$ (C1) pincer complex as a catalyst for the ammonia borane dehydrogenation [38]. Treatment of 0.5 M ammonia borane solution with a 0.5 mol% catalyst afforded quantitative conversion and 1 equivalent of hydrogen gas was released. During the reaction, a white solid was deposited that after analyzed by NMR, IR, and X-ray powder diffraction identified as the cyclic pentamer, $[H_2NBH_2]_5$. To describe the mechanistic insight, they reported that a tetrahydride complex (POCOP)Ir$(H)_4$ (C2) was observed initially from complex C1 during the dehydrogenation of H_3NBH_3, and after long reaction times, a new BH_3 adduct iridium dihydride complex (C3) was formed.

Later, the Manner group reported the same Ir pincer C1 catalyst for the dehydropolymerization of the N-methylamine-borane, which afforded a poly(N-methylaminoborane) with weight average molecular weight of 160,000 (P1) as an off-white solid in high yield (60%) with the vigorous bubbling of hydrogen generation (Fig. 1.2) [39]. Parallelly, the same catalyst was also used for the catalytic dehydrocoupling reaction of ammonia borane and afforded a polymeric white solid product (P2) and corresponding copolymer (P3) was synthesized by a mixture of N-methylamine-borane and ammonia borane. The linear polymeric structure was reported by detailed structural analysis of polymers P1, using various mass spectrometric techniques, such as high-resolution ESI and nanospray MS, solution and solid-state NMR, and IR spectroscopy methods.

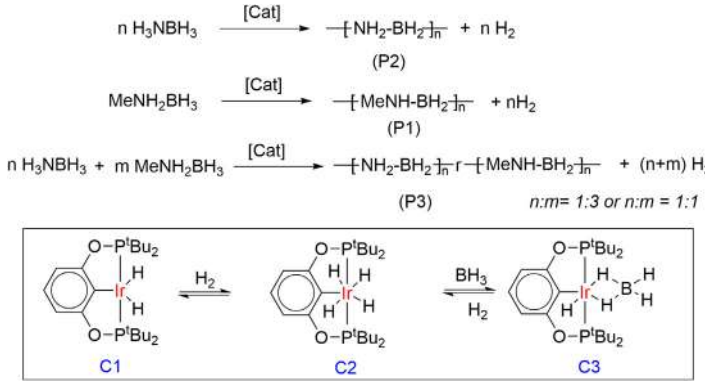

Figure 1.2 Dehydropolymerization of amine-borane derivatives using Ir(POCOP) pincer complex.

Schneider group reported Ru–amido complex [Ru(PNP)(H)(PMe_3)] (PNP = $N(CH_2CH_2P^iPr_2)_2$) C4 (0.01 mol%) as catalyst in the dehydrogenation of ammonia borane with 0.83 equivalent of H_2 formation (TON = 8300) and a pseudo-first-order reaction with 21 s^{-1} TOF value (Fig. 1.3) [40] whereas catalyst loadings of 0.1 mol% (C4) produce slightly more than one equivalent of H_2. A MAS-^{11}B NMR and IR spectra predicted the formation of a polymeric dehydrocoupling product $(BH_2NH_2)_n$ along with small amounts of borazine. A concerted mechanism of the NH and BH bond cleavages is predicted in the rate-determining step. The mechanistic studies disclosed that at the early stage of the reaction only trans-dihydro amino complex (C5) was formed. The same group later explored the details of the mechanism of the reaction based on the kinetic studies, control experiments, and the DFT calculation [41].

Yamashita group developed a boron-based pincer ligand with iridium catalyst for the AB dehydrogenation reaction [42]. In the presence of KO^tBu, a stoichiometric amount of dimethyl amine-borane (DMAB) converted into cyclic dimer $(Me_2N–BH_2)_2$, with a trace amount of BH $(NMe_2)_2$. Under catalytic condition 2 mol% of C6/KO^tBu (1/1.5) undergoes dehydrogenation of DMAB with quantitative conversion within 10 min and H_2 was evolved immediately upon mixing the substrate and catalyst. Reducing the catalyst loading to 0.5 mol% resulted in 65% of the conversion after 3 h at 23°C whereas at 60°C improved to 83%. Although the quantitative conversion of DMAB to a cyclic product at 60°C after 3 h was observed in a concentrated reaction medium by reducing the volume of THF solvent. Monitoring the catalysis reaction by ^{11}B NMR spectroscopy depicted that DMAB, dehydrogenated cyclic dimer, linear dimer ($HMe_2N–BH_2–NMe_2–BH_3$), monomer ($Me_2N=BH_2$),

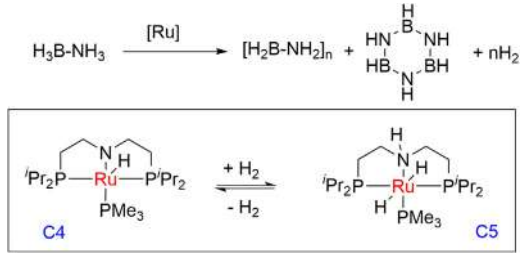

Figure 1.3 Dehydrogenation of ammonia borane to the polymeric dehydrocoupling product using Ru(PNP) pincer complex.

and a small amount of $BH(NMe_2)_2$ were formed. In the first 5 min, conversion of DMAB to the linear dimer and subsequent cyclization to the cyclic dimer was observed with 77%, and almost full conversion was achieved after 3 h. The complex C6 shows an initial TOF of 3400 h^{-1} in 2 min using 0.5 mol% catalyst loading.

A probable mechanism was proposed where complex C6 was activated by KO^{t}Bu to generate the three-coordinated "T-shaped" (PBP) iridium(I) species (C7) and followed by coordination to a DMAB molecule through its nucleophilic B–H ended in a η^2 fashion forming C8. The N–H proton in coordinated DMAB was transferred to the iridium center formed an iridium hydride intermediate (C9) and followed by dissociation of the dehydrogenated monomer $Me_2N=BH_2$ and generated the dihydride complex C11 via tetrahydride intermediate C10. A coupling reaction of DMAB and the dehydrogenated monomer to produce the linear dimer ($HMe_2N–BH_2–NMe_2–BH_3$) and spontaneously transformed into the cyclic dimer by releasing an additional equivalent of H_2 was proposed (Fig. 1.4).

In 2016, the Velez group reported RhH{xant(P^iPr_2)$_2$} complex (C12) for the same reaction where 1 mol of molecular hydrogen was released per mole of ammonia borane and dimethylamine borane with TOF at 50% conversion of 3150 h^{-1} and 1725 h^{-1}, respectively [43]. The dehydrogenation of ammonia borane yielded poly(aminoborane) as a white, insoluble product whereas dimethylamine borane dehydrogenation

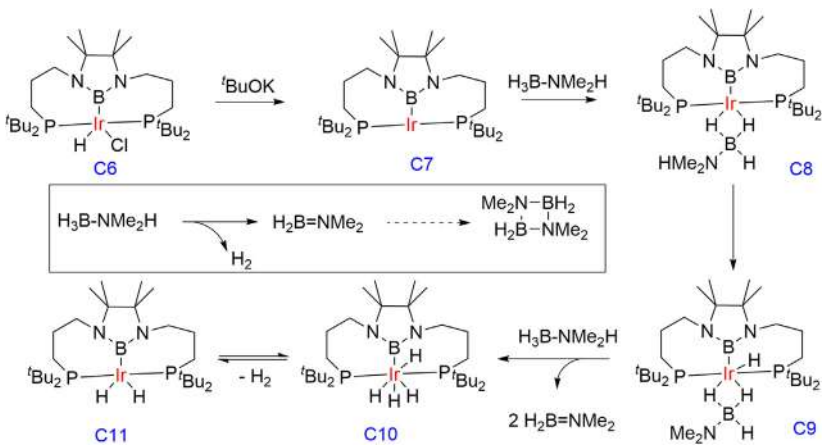

Figure 1.4 Dehydrogenation of dimethylamine borane to a cyclic product using Ir (PBP) complex.

afforded the dimer $[H_2BNMe_2]_2$ and no traces of the linear diborazane $H_3B{-}NMe_2{-}BH_2{-}NHMe_2$ were observed at any point of the reaction, which suggests an off-metal dimerization of $H_2B=NMe_2$. Additionally, the same catalyst also used for the transfer hydrogenation reaction where 1:1 ammonia borane/cyclohexene mixture initially undergoes the selective dehydrocoupling of ammonia borane, and subsequently the generated molecular hydrogen reduces the olefin with a TOF 50% value of 12 h^{-1}. During the tandem process, no formation of any borylation product was observed, which is also consistent with the release of H_2BNH_2 and experiences polymerization out of the coordination sphere of the metal, initiated by a nucleophile.

The detailed DFT calculation revealed the mechanism wherein the initial step complex C12 dissociated the oxygen atom of the diphosphine ligand to afford the tricoordinated T-shaped intermediate C13 followed by the subsequent coordination of ammonia borane to form C14, which homolytically added the coordinated B − H bond, to afford the dihydride intermediate C15, and contained a stabilized boryl ligand. The five coordinated rhodium(III) complex C15 evolved into the hydride − dihydrogen intermediate C16, which upon release of the dihydrogen ligand regenerates C13 to complete the cycle (Fig. 1.5).

Weller group in 2019 showed that the $[Rh(PONOP)(\eta^2\text{-}H_2)][BAr^F{}_4]$ precatalyst C17 (2 mol%) can quantitatively dehydrogenate $H_3B\text{-}NMe_2H$ to $[H_2BNMe_2]_2$ [44]. In the proposed mechanism, first the deprotonation of the Shimoi-type amine-borane σ-complex (C18) occurred by amines to form a metal−hydride intermediate (C19) and ammonium salt along with the dehydrogenated aminoborane product, which then formed a cyclic final product in either of two pathways, which includes a nucleophilic attack on boron via a boronium route or deprotonation of the σ-bound amine-borane via an ammonium route. Lastly, the ammonium salt transferred the proton to Rh-H intermediate (C19) to form dihydrogen complex C17 (Fig. 1.6).

In addition to catalysts of 2nd- and 3rd-row transition metals, a variety of earth-abundant metal-based catalysts have also been employed for the dehydrogenation of ammonia borane.

Schneider Group in 2015 reported iron pincer complex [FeH(CO)(PNP)] (PNP = $N\text{-}(CH_2CH_2P^iPr_2)_2$) C20 for ammonia borane dehydrocoupling reaction [45]. One equivalent of H_2 was released with TOF of 30 h^{-1} from AB at room temperature without any additional activation, such as base or irradiation. The full conversion was obtained with catalyst

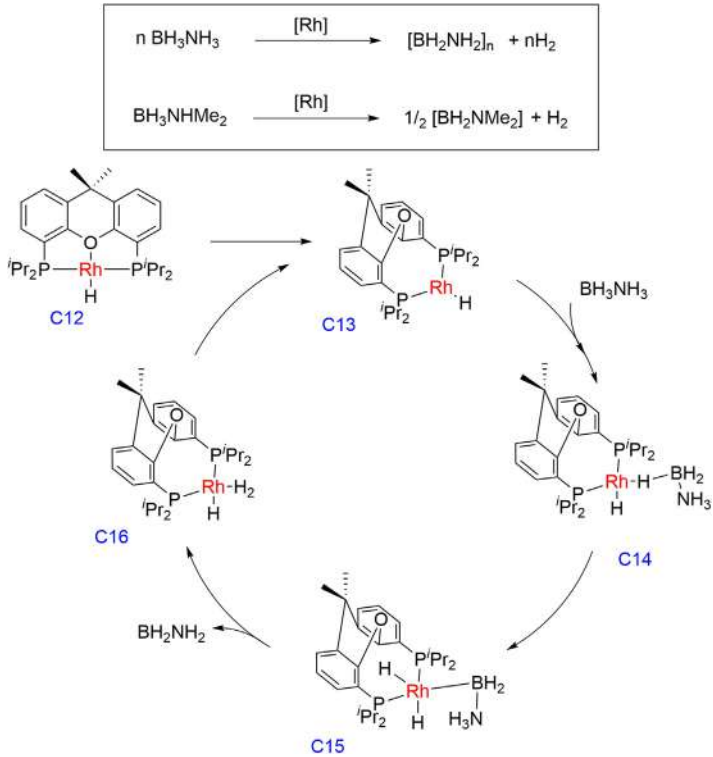

Figure 1.5 Dehydrogenation of ammonia borane using Rh(xantphos) pincer complex and proposed mechanism.

loadings of 0.5 mol% and a maximum TON of 200 was achieved with 0.1 mol% catalyst loading where poly(aminoborane) was obtained as a major product along with small amounts of borazine, polyborazylene, cyclotriaminoborane, cyclodiaminoborane, and B-(cyclotriborazanyl)-amine-borane. ^{31}P and ^{11}B NMR spectroscopy revealed that free boron moiety is coordinated by the dihydride intermediate (C23), which undergoes the catalyst deactivation process. To improve the catalyst activities, additional NMe_2Et (Cat/ NMe_2Et/AB = 1/4/500) was added and a higher TON of 330 was observed without affecting the selectivity of the reaction. Complex C20 reacted with AB and formed resting state iron–dihydride complex C22, which further dehydrogenated the ammonia borane to H_2, and transient aminoborane ($H_2B=NH_2$), which underwent the polymerization via the intermediate C21. Catalyst C22 was also observed to form a deactivated product C23 with the addition of free BH_3 (Fig. 1.7).

Guan group reported a series of iron bis(phosphinite) pincer complexes employed for the same reaction and observed an immediate gas evolution when a solution of catalyst C24 in THF was mixed with a solution of AB (20 equivalents) in diglyme at 60°C (Fig. 1.8) [46]. After 24 h, 2.5

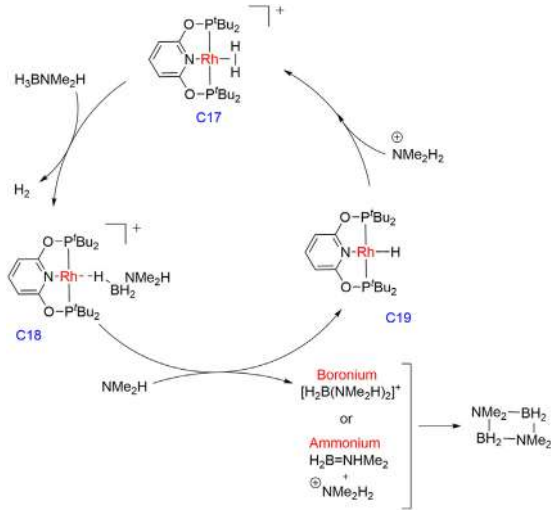

Figure 1.6 Dehydrogenation of amine-borane using Rh(PONOP) pincer complex and proposed mechanism.

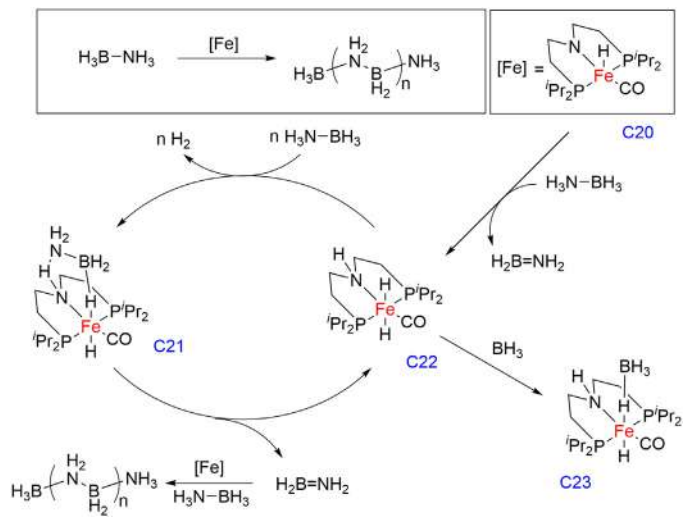

Figure 1.7 Ammonia borane dehydrogenation using Fe(PNP) pincer complex.

equivalents of H_2 per AB was released. Complex C25 shows improved catalytic activity whereas complex C26 is a superior catalyst in terms of both rate and the extent of H_2 released. The ^{11}B NMR spectrum of the soluble materials shows the formation of borazine and polyborazylene as products with cyclotriborazane (CTB) and B-(cyclodiborazanyl)aminoborohydride (BCDB) in minor portions. The H_2 evolution from this process using catalyst C26 gives 1.0, 2.0, and 2.5 equivalents of H_2 per AB in 1.5, 7, and 16 h, respectively. However, the amount of released H_2 still increases after 12 h, suggesting that the lifetime of the catalytically active species is longer. It was proposed that the active intermediate was formed by removing one PMe_2Ph unit from catalyst C26. Compared to the uncatalyzed thermal reaction, the rate for the dehydrogenation of AB catalyzed by C26 is about 50 times faster. The proposed rate-determining step involves simultaneously breaking the N − H and B − H bonds of AB, which results in the protonation of the ipso carbon and the transfer of a hydride ligand from B to Fe, which is followed by the formation of a dihydride species. At the final stage, the simultaneous C − H bond activation to restore the pincer framework completes the cycle by eliminating one molecule of hydrogen, which is facile even at room temperature.

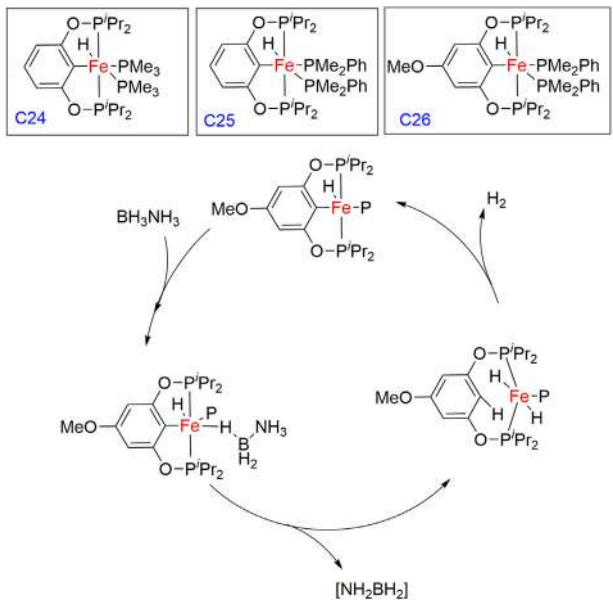

Figure 1.8 Ammonia borane dehydrogenation using Fe(POCOP) pincer complex and proposed mechanism.

Baker group in 2019 reported that the reaction of Fe pincer complex C27 with 20 equivalents of AB in THF at 60°C resulted in the immediate observation of gas evolution and formation of insoluble poly(aminoborane) [47]. After 2 h, the $^{11}B\{^{1}H\}$ NMR spectrum revealed the formation of borazine and polyborazylene along with a mixture of linear and branched aminoborane oligomers. Dehydrogenation of methylamine-borane (MeAB) also proceeded smoothly with the C27 precatalyst, albeit with poor selectivity. Interestingly, ammonia borane dehydrogenation reactions using precatalyst C28 showed lower activity but much greater selectivity, yielding only the branched cyclic aminoborane tetramer [B-(cyclotriborazanyl)amine-borane] in addition to borazine and polyborazylene. Furthermore, C28 was also reused for multiple times, although longer reaction times were required to consume the second and third batches of AB while maintaining high selectivity of the cyclic products. Also, the same was employed for dehydrogenation of MeAB and trimethylamine borane (TMAB), which was selective for the cyclic products with primarily CTB [$(MeNHBH_2)_3$], whereas no reaction was observed with TMAB, suggesting that bifunctional N − H activation is integral to the dehydrogenation pathway. The reaction of C29 with 20 equivalents of AB at room temperature showed the same reactivity; however, after 1 h, a black precipitate was observed, indicative of catalyst decomposition. Overall amido complex C29 was the most active catalyst but least stable and complex C27 also showed limited catalyst lifetime, while less active Fe−thiolate complex C28 proved to be the most robust under the optimized conditions of amine-borane dehydrogenation (Fig. 1.9).

Peter group reported the dehydrogenation of HMe_2N-BH_3 catalyzed by the Co pincer complex [48]. The reaction of C30 with Me_2NH-BH_3 in a 1:2 stoichiometric ratio afforded the quantitative

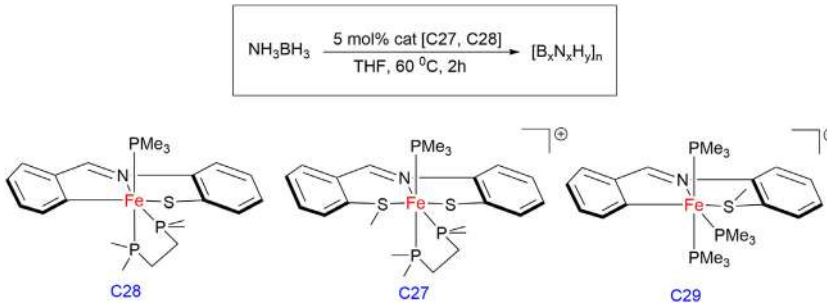

Figure 1.9 Ammonia borane dehydrogenation using Fe(SNS) pincer complexes.

formation of a hydridoborane tetrahydridoborate cobalt complex (C31) accommodating a bridging hydride and an η^2-BH_4 ligands confirmed by NMR and X-ray crystallography. Me_2NH-BH_3 stirred in C_6D_6 with 2 mol% of C30 or C31 under inert atmosphere underwent initial dehydrogenation to a linear product ($HMe_2N-BH_2-Me_2N-BH_3$), which fully converted into $(Me_2N-BH_2)_2$ in 6 h (TOF $\approx$ 8 h^{-1}). C31 effectively catalyzed both olefin hydrogenation and amine − borane dehydrogenation and together afforded a transfer hydrogenation reaction. Equal amounts of styrene and HMe_2N-BH_3 were reacted in C_6D_6 at 25°C with 2 mol% of catalyst and after 24 h, styrene was hydrogenated to ethylbenzene quantitatively, and the dehydrogenated product $(Me_2N-BH_2)_2$ was observed (Fig. 1.10).

Weller group reported that the $CoCl_2(R_2PCH_2CH_2)_2NH$ (R = ^{i}Pr, Cy) C32, C33 respectively complexes used for the H_3B-$NMeH_2$ dehydrogenation under mild condition (0.4 mol% catalyst, 25°C, 1,2-$F_2C_6H_4$ as solvent) in presence of 2 equivalents of an amine ($NMeH_2$) with respect to [Co], a linear $(H_2BNMeH)_n$, medium molecular weight polymer was formed (47600 g mol^{-1} and Đ = 1.5) in 60% yield with TOF of 750 h^{-1} for complex C32 and 3700 h^{-1} for C33 [49]. A 10 g scale reaction was performed under the optimized condition using precatalyst C33 which afforded an off-white polymer of molecular weight of 74200 g mol^{-1}. The mechanism was proposed where metal–ligand cooperativity played a significant role in the substrate activation and dehydrogenation process (Fig. 1.11).

Fout and Melchor group explored a Co complex (C34) with monoanionic bis(carbene) aryl pincer ligand for the dehydrogenation of AB

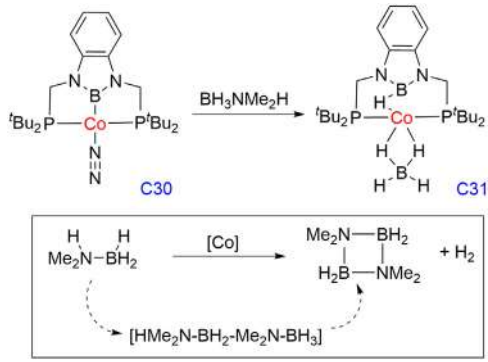

Figure 1.10 Amine-borane dehydrogenation using Co(PBP) pincer complex.

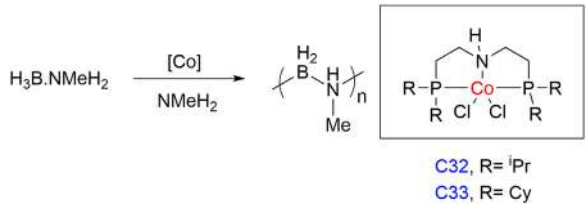

Figure 1.11 Amine-borane dehydrogenation using Co(PNP) pincer complex and proposed mechanism.

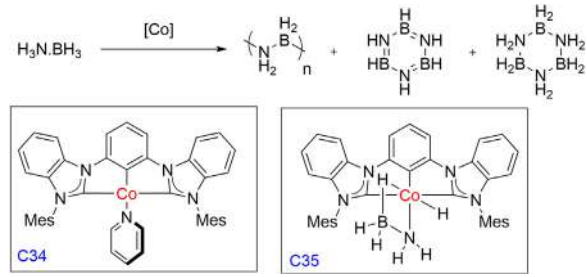

Figure 1.12 Ammonia borane dehydrogenation using Co(CCC) pincer complex and proposed mechanism.

catalytically and reported that 1.7 equivalents of H_2 per AB was released in THF at 60°C and afforded both soluble (borazine and polyborazylene) and insoluble (poly(aminoborane)) BN-containing species [50]. The controlled reaction of C34 with a stoichiometric amount of AB in THF yielded a hydride–amidoborane Co complex (^{Mes}CCC)CoH(NH_2BH_3) (C35), which was isolated and characterized (Fig. 1.12).

1.3 Dinitrogen activation using pincer ligands

Nitrogen is one of the most abundant elements in the earth's atmosphere; however, due to the chemical inertness, its high bond dissociation energy (945 KJ/mol), low proton affinity, nonpolar character and high HOMO-LUMO gap, its fixation or transformation to functionalized molecules such as ammonia, hydrazine or other fine chemicals are thermodynamically very demanding [51,52]. Ammonia production from dinitrogen is one of the most important chemical transformations that have a direct impact on human society. Ammonia is used for the production of fertilizers, which are essential to provide feedstocks for the world's expanding

population [53,54]. Industrially, ammonia is synthesized by the Haber–Bosch process, from the reaction of dinitrogen and dihydrogen gases in the presence of a heterogeneous catalyst in harsh reaction conditions (high temperature and high pressure) [55]. Therefore the development of more energy-efficient and ambient conditions for the reduction of dinitrogen to ammonia is one of the most important and challenging chemical transformations in the century.

In contrast to the many reports on the stoichiometric reactivity of transition metal-bound dinitrogen complexes, there are only a few examples reporting the catalytic transformation of dinitrogen using these complexes under ambient reaction conditions [52,56–70]. In 2003, the Schrock group reported the successful catalytic reduction of dinitrogen into ammonia under ambient conditions using a molybdenum–dinitrogen complex bearing a bulky HIPT-substituted triamidoamine ligand as a catalyst, along with 2,6-lutidiniumtetrakis[3,5-bis(triflurometh yl) phenylborate]([LutH]BAr^{F}_{4}) as a proton source and $CrCp_2^*$ as a reducing agent [71]. Recently, pincer-based metal compounds have attracted their application in dinitrogen activation chemistry, which is developing with time. In this section, we have disclosed the important dinitrogen activation reactions by using several reported transition metal pincer complexes.

1.3.1 Catalytic dinitrogen activation using Mo pincer catalyst

After the Schrock's report, in 2010, a significant breakthrough has been achieved in this field by Nishibayashi and co-workers using Mo–PNP-based pincer ligand [72]. Mo–PNP–N_2 bridged binuclear pincer catalyst C36 (0.01 mmol) (PNP = 2, 6-bis(di-tert-butylphosphinomethyl)pyridine), under excess proton source as [LutH]OTf (0.96 mmol) and reductant as $CoCp_2$ (0.72 mmol) afforded 12 equivalents of ammonia with respect to catalyst whereas by increasing the [LutH]OTf (2.88 mmol) and $CoCp_2$ (2.16 mmol), it afforded 23 equivalents of ammonia; however, dihydrogen is also detected as a side product. In 2012, the same group reported that substitution of the tert-butyl (^{t}Bu) group by adamantyl (Ad) group to one of the P-arm of catalyst C37 afforded 14 equivalents of ammonia under similar condition [[LutH] OTf (0.96 mmol) and $CoCp_2$ (0.72 mmol)] while with a large excess of reagents [LutH]OTf (288 equivalents) and $CoCp_2$ (216 equivalents), it afforded only 16 equivalents of ammonia based on the catalyst C37. Other system containing –Ph (C38), –Cy (C39), and –^{i}Pr (C40) substituents were found to be a less effective catalyst (Fig. 1.13) [73].

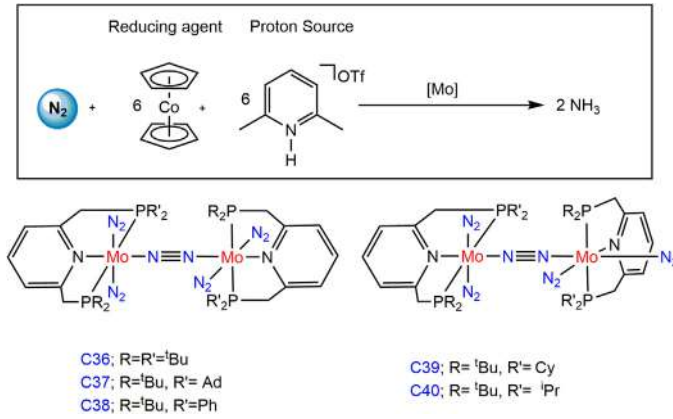

Figure 1.13 N_2 bridged binuclear Mo(PNP) pincer complexes.

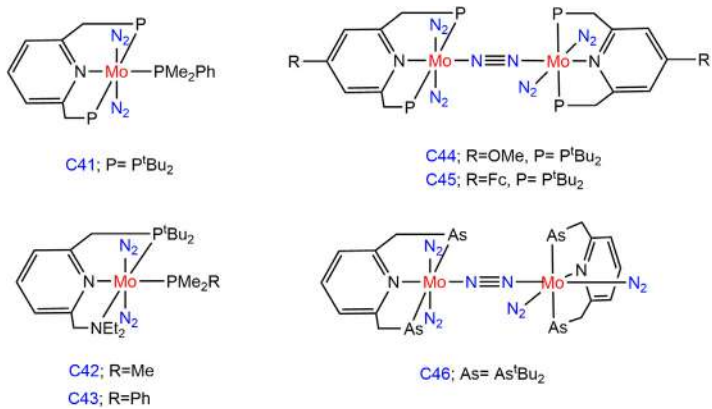

Figure 1.14 Mononuclear N_2 bound Mo pincer complexes and N_2 bridged binuclear Mo pincer complexes.

The mononuclear–molybdenum complex bearing PNP pincer ligand C41 (0.04 mmol) reported by the Nishibayashi group yielded 1.38 equivalents of NH_3 based on Mo using H_2SO_4 as proton source at room temperature (Fig. 1.14) [74]. The complexes C42 and C43 bearing PNN ligand also afforded ammonia in a lower amount (0.20, 0.25 equivalents/Mo respectively) compared to C41 under the similar condition [75]. Nishibayashi group observed that the introduction of electron-donating methoxy(-OMe) group at the 4-position of pyridine moiety of catalyst C36 dramatically increased the yield of ammonia [76]. Up to 52 equivalents of ammonia were produced based on the catalyst C44 together with

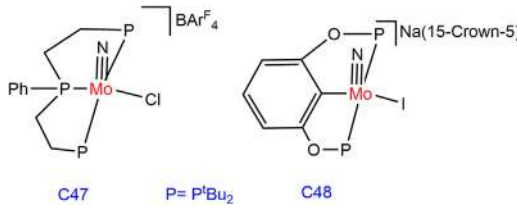

Figure 1.15 Mononuclear Mo–nitride pincer complexes.

dihydrogen as a side product using 360 equivalents of $CoCp_2$ and 480 equivalents of [LutH]OTf, while the introduction of the ferrocene group at the 4-position of PNP moiety of catalyst C36 gave up to 45 equivalents of NH_3 based on catalyst C45 (using 288 and 384 equivalents of $CoCp_2$ and [LutH]OTf, respectively) [77]. This two subsequence studies depicted that the introduction of an electron-donating moiety, –OMe group, onto the pyridine ring of the PNP-pincer ligand likely accelerates the protonation step of dinitrogen, while the introduction of a redox-active ferrocene site to the pyridine ring of PNP-ligand likely accelerates the reduction steps in catalytic nitrogen fixation. A modified ligand system was reported by Nishibayashi where the ligand pincer phosphine donor was replaced by arsine donors C46, which feature a large element and bearing poorer σ-donating/π-accepting ability. 0.6 equivalent/Mo of NH_3 was formed when complex C46 was treated with an excess amount of H_2SO_4 (0.94 mmol), and the maximum 1 equivalent/Mo of NH_3 was formed when the reaction was performed with varying equivalents of $CoCp_2$ and [LutH]OTf [78].

In 2015, the Nishibayashi group synthesized a series of Mo–nitride complexes (Fig. 1.15), among which catalyst C47 containing mer-tridentate triphosphine (PPP) ligand was found to be a more effective catalyst for dinitrogen reduction where up to 63 equivalents of NH_3/Mo was yielded using $CoCp^*_2$ (540 equivalents), [CoIH]OTf (720 equivalents) under atmospheric dinitrogen pressure [79]. The anionic POCOP–Mo–nitride complex C48 reported by Schrock and co-workers afforded only 0.3 equivalent/Mo of ammonia by treatment with [LutH]BAr$^F_4$ and $CrCp^*_2$ and 0.34 equivalent/Mo by treatment with [LutH]OTf and $CoCp_2$ [80].

[MoI_3(PNP)] C49 complex was reported by the Nishibayashi group, which afforded up to 830 equivalents of ammonia based on the catalyst, when 0.001 mmol of the catalyst was treated with [CoIH]OTf (2880 equivalents) and $CoCp^*_2$ (2160 equivalents) under 1 atm dinitrogen pressure [81].

PCP-type pincer ligands, comprise both diphosphine donors and N-heterocyclic carbene, a Mo complex C50, afforded up to 200 equivalents of ammonia based on the catalyst, whereas the electron-donating methyl group in the benzene ring, C51, gave a slightly higher yield of ammonia than C50 (230 equivalents of ammonia based on the catalyst) using $CrCp^*_2$ (1440 equivalents) and [LutH]OTf (1920 equivalents) under dinitrogen atmospheric pressure [82].

Nishibayashi and co-workers designed a Mo−triiodide complex C52 bearing PCP ligand, which afforded 49 equivalents/Mo of NH_3 upon treatment with 180 equivalents of $CoCp^*_2$ and 240 equivalents of [CoIH]OTf. The halide congeners [$MoCl_3$(PCP)] (C53) showed less reactivity (34 equivalents/Mo of NH_3) under similar reaction conditions. However, the addition of 3 equivalents of NaI to C53 showed better catalytic activity (50 equivalents/Mo of NH_3) and selectivity for ammonia formation. The reaction of C53 with 3 equivalents of NaI with large excess of $CoCp^*_2$ (720 equivalents) and [CoIH]OTf (960 equivalents) afforded 167 equivalents/Mo of NH_3 [83].

As an extension of their work, the introduction of EWG (-Ph) and redox-active (Fc) group onto the 4-position of catalyst C49 substantially increased the ammonia formation where catalyst C54 and C55 worked as a more effective catalyst than C49 under the similar reaction conditions, and using 360 equivalents $CoCp_2$ and 480 equivalents [CoIH]OTf, up to 90, 83 equivalents/Mo of ammonia was formed on catalyst C54 and C55, respectively, while C49 gave slightly lower yield (66 equivalents/Mo) of ammonia formation [84]. While the use of ferrocene-linked bis(molybdenum-triiodide) ligand C56 afforded a lower catalytic yield of ammonia (up to 45 equivalents/Mo) than the corresponding mononuclear complex C49 or C55, under similar reaction conditions (Fig. 1.16) [85].

Tuczek group reported the catalytic ammonia synthesis from dinitrogen using Mo complex supported by PN^3P pincer ligand where 3.12 equivalents of ammonia were formed using catalyst C59 (0.01 mmol), $CrCp^*_2$ (36 equivalents) as reductant and [LutH]OTf (48 equivalents) as a proton source, while with catalyst C57 and C58, only a stoichiometric yield of ammonia (0.51 and 0.44) was formed [86]. No improvement was observed with large excess of reagents $CrCp^*_2$ (110 equivalents) and [LutH]OTf (146 equivalents).

In place of a strong acid, an effort to use H_2O as a proton source was employed by the Nishibayashi who recently explored the coupling of water oxidation with dinitrogen fixation [87]. Upon water oxidation with

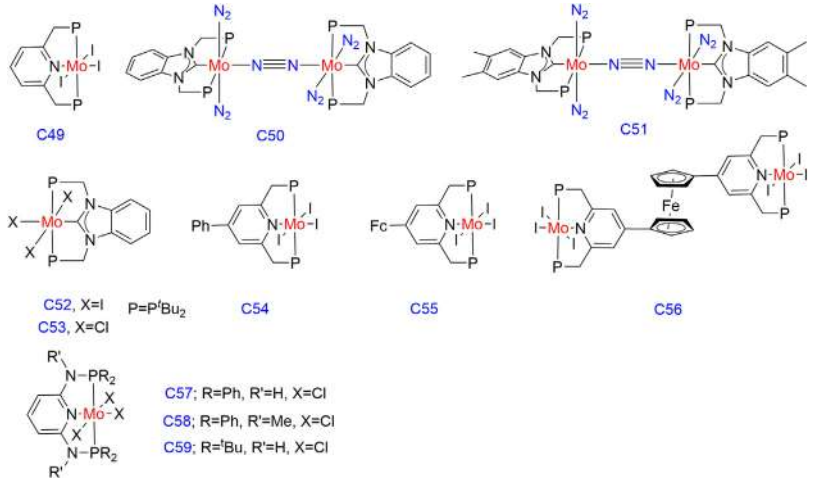

Figure 1.16 Mononuclear and binuclear Mo pincer complexes employed for N_2 activation.

[Ru] complex, [Ru(bda)(isoq)$_2$] (bda = 2,2′-bipyridine-6,6′-dicarboxylate, isoq = isoquinoline), H^+ was generated that combined with [Lut] to form $[LutH]^+$ and it further combined with C36 and yielded 8.5 equivalents/Mo of NH_3 and this yield was similar to that with purified [LutH]OTf (9.7 equivalents of NH_3). Using a large excess of reagents up to 17.1 equivalents of NH_3 was generated.

Visible light-driven water oxidation was also studied using [Ru(bpy)$_3$](OTf)$_2$ (bpy = 2,2′-bipyridine) as the photosensitizer and $Na_2S_2O_8$ as a sacrificial oxidizing agent. The catalytic reaction of dinitrogen gas with in situ generated proton source $[LutH]^+$, reductant as $CoCp_2$, and Mo–catalyst C36 was examined, and 6 equivalents of NH_3 was formed (Fig. 1.17).

On the continuation of the previous work, they utilized SmI_2 as a reductant source with polar protic H^+ donors (alcohols or water) [88]. The reaction of N_2 with ethylene glycol, SmI_2, and catalyst C60 generated NH_3 at a TOF of 117 min^{-1}. Treatment of N_2 with catalyst C60, SmI_2 (14,400 equivalents), and H_2O in THF for 4 h at room temperature afforded 4350 equivalents of NH_3 in 91% yield. This catalytic system using SmI_2/H_2O, efficient reduction, and protonation was proposed to proceed via a proton-coupled electron transfer (PCET) mechanism.

In 2020, Nishibayashi and co-workers have synthesized mononuclear Mo complexes bearing anionic pyrrole-based pincer ligands C61, C62, and dimeric Mo–PNP complex C63 and explored for dinitrogen

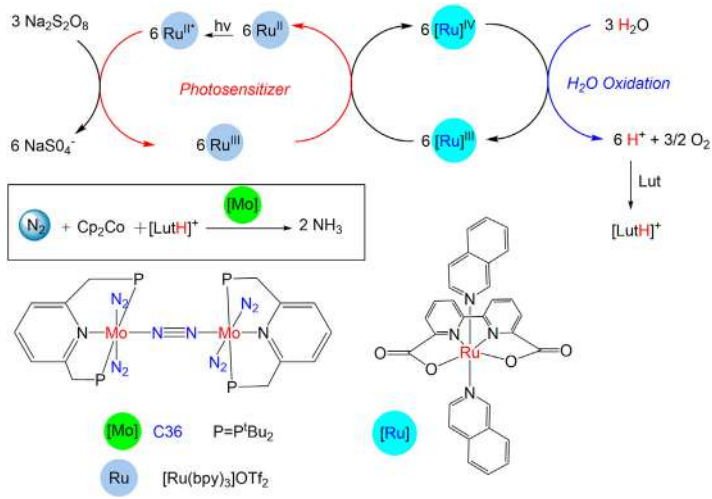

Figure 1.17 Ammonia synthesis from N_2 using water as a proton source.

activation, employing SmI_2 as reductant and H_2O or alcohol as a proton source, where up to 12.2 and 11.2 equivalents/Mo of NH_3 was formed using C61 as a catalyst with ethylene glycol and H_2O, respectively (using 180 equivalents each of reductant and proton source). While complex C62 and C63 afforded slightly lower yield of NH_3 (7.3 and 6.9 equivalents of NH_3 on C62 and C63 using ethylene glycol and 2.6 equivalents of NH_3 each on C62 and C63 using water as proton source based on Mo atom of catalyst respectively) under the similar reaction conditions (Fig. 1.18) [89].

1.3.2 Catalytic dinitrogen activation using 3d metal pincer catalyst

In 2016, the Nishibayashi group reported the catalytic nitrogen fixation using Fe–dinitrogen complex C64 containing anionic pyrrole-based PNP pincer ligand [90]. Although no fixed N products were obtained using conditions similar for their Mo system (i.e., [LutH]OTf and $CoCp_2$) but up to 14.3 equivalents/Fe of NH_3 was formed, using 184 equivalents of $[H(Et_2O)_2][BAr^F{}_4]$ and 200 equivalents KC_8 with 37% efficiency. The N_2H_4 was also formed during the process but the ratio of NH_3 versus N_2H_4 depends mainly on the nature of the solvent like in THF, hydrazine was formed in the major amount relative to Et_2O. The Fe–H complex C65 and the protonated pyrrole–backbone complex C66 were also

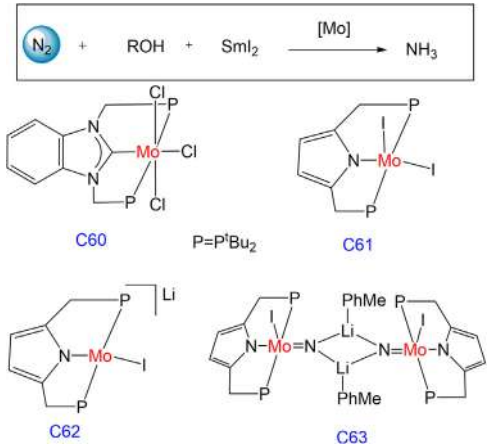

Figure 1.18 Ammonia synthesis from N_2 using SmI_2 as a reducing agent and water or alcohol as a proton source.

used as a catalyst for the same reaction but yielded a lower amount of NH_3 as compared to C64 (3.0 and 2.6 equivalents of NH_3 was formed per Fe using 38 and 40 equivalents of proton source and reductant, respectively).

Later on, the same group also reported that the introduction of −Me group at 3, 4−position of pyrrole ring C67 can inhibit the protonation at the pyrrole backbone, which produced a higher yield 22.7 equivalents/Fe of ammonia (using 184 and 200 equivalents of proton source and reductant, respectively) [91]. Although the introduction of −Me substituents to pyrrole backbone improved the yield of ammonia formation, the electron-rich pyrrole remained the thermodynamically favored site for protonation. Further effort to prevent protonation by replacing electron-rich pyrrole ring by carbazole moiety C68 yielded only 3.2 equivalents/Fe of NH_3 (using 76 and 80 equivalents of proton source and reductant, respectively) (Fig. 1.19) [92].

Nishibayashi group also studied the Co pincer complex catalyzed dinitrogen fixation using the same bis-(phosphino)pyrrole system [93]. The efficiency of Co-congener C69 was found to be similar for that Fe complex C64, where up to 15.9 equivalents of NH_3 were formed based on the catalyst C69 by using a large excess of 200 equivalents of KC_8 and 184 equivalents of $[H(Et_2O)_2]BAr^F{}_4$, while the other Co-congeners (C70, C71, C72) produced a lower yield of NH_3 (3.1, 2.2, 2.0 equivalents/Co of NH_3, respectively using 40 equivalents of reductant and 38 equivalents of proton source).

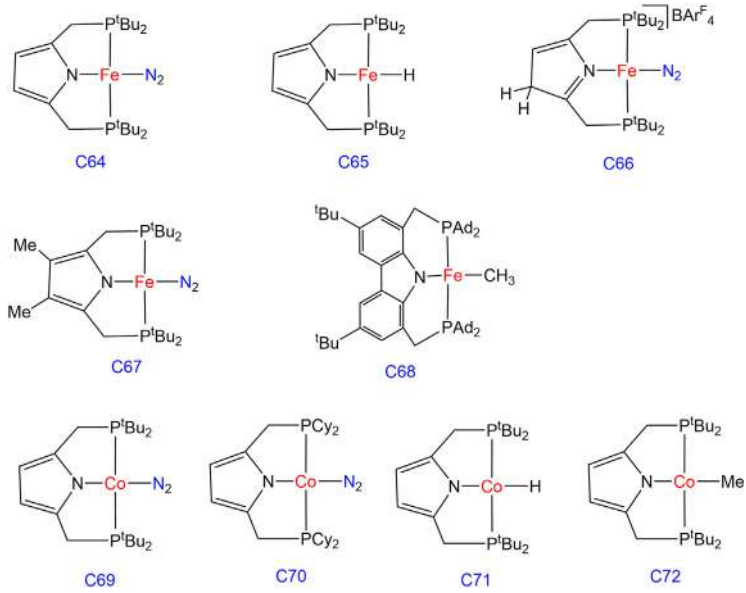

Figure 1.19 Ammonia synthesis from N_2 using Co and Fe pincer complexes.

Budzellar and co-workers reported the bridging dinitrogen–chromium diiminepyridine complex C73 [94], which underwent a further two-electron reduction followed by one-hydrogen-atom transfer from one of the four imine methyl group to the dinitrogen moiety to afford complex C74, which on further reduction with 3 equivalents of NaH under dinitrogen pressure afforded complex C75. Complex C75 upon acidic hydrolysis with HCl and $NaBPh_4$ finally produced ammonium ion. The formation of monosodium and disodium amide complexes C76 and C77 were further observed by eventual cleavage of complex C74 with 1 equivalent of NaH (Fig. 1.20).

1.3.3 Catalytic dinitrogen fixation using earlier transition metals (V, Ti, Zr)

In addition to molybdenum and late transition metal–dinitrogen complexes, earlier transition metal complexes (vanadium, titanium, and zirconium) also show catalytic activities for the reduction of dinitrogen to ammonia. Nishibayashi and co-workers reported the mononuclear vanadium–aryloxy complex C80 bearing anionic pyrrole-based PNP ligand, which showed the best catalytic activity among all other V complexes (C78–81) and produced 12 equivalents of ammonia and 1.8

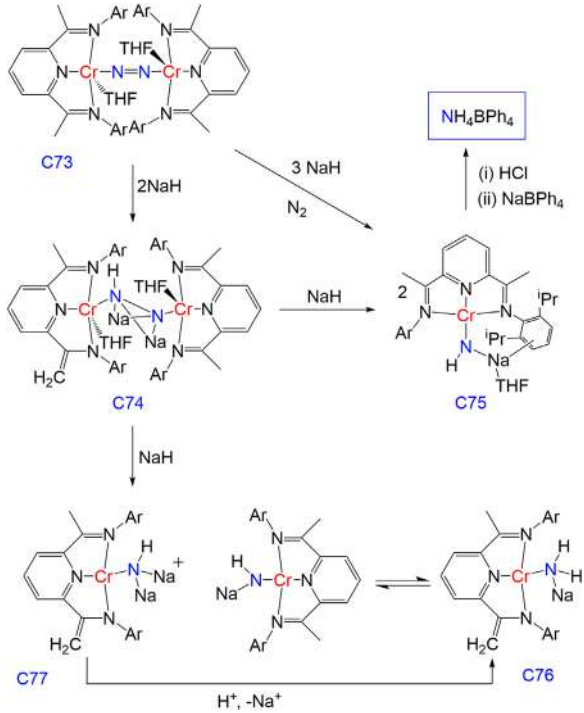

Figure 1.20 Dinitrogen activation and partial reduction using Cr pincer complex.

equivalents of hydrazine based on the vanadium atom using 200 equivalents of KC_8 and 184 equivalents of $[H(Et_2O)_2]BAr^F{}_4$ while other V complexes produced a lower yield of ammonia (3.5, 4.6, and 6.6 equivalents/V of NH_3 on catalyst C78, C79, and C81, respectively) [95].

In contrast, mononuclear and dinitrogen-bridged titanium and zirconium complexes (C82–C85) bearing anionic pyrrole pincer ligand and Cp ligand gave only stoichiometric amount of ammonia and hydrazine under similar reaction conditions. The dinitrogen-bridged Zr complex C85 gave a slightly higher yield of ammonia (1.3 equivalents/Zr) as compared to dinitrogen-bridged Ti complex C83 (one equivalent/Ti). While mononuclear Ti complex C82 and dichloro-bridged Ti complex C84 gave very lower yield, 0.13 and 0.31 equivalents/Ti of NH_3, respectively, using 40 equivalents of KC_8 and 38 equivalents of $[H(Et_2O)_2]BAr^F{}_4$ (Fig. 1.21) [96].

Hou and co-workers reported that PNP-ligated titanium complex C86 can serve as an unique platform for dinitrogen activation [97]. DFT

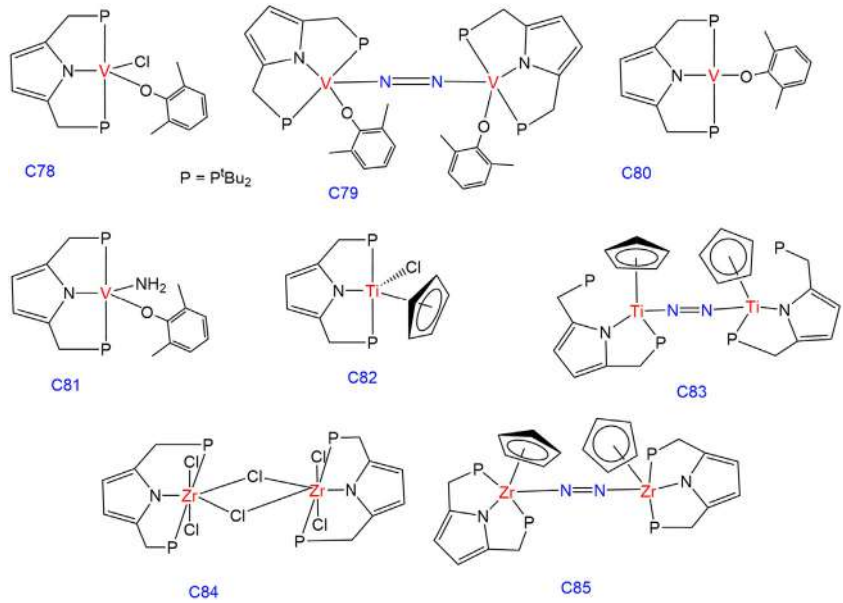

Figure 1.21 Ammonia synthesis from N_2 using Ti, V, and Zr pincer complexes.

calculations revealed that the transformation of the dinitrogen unit in C87−$^{15}N_2$ to the imidio/nitrido species in C88−$^{15}N_2$ is initiated by the hydrogenation of the dinitrogen unit with an external H_2 with subsequent release of another molecule of H_2 from the Titanium framework and subsequent cleavage of the N−N bond, which constitutes the first example of N_2 cleavage and hydrogenation by H_2 without the preactivation of N_2 by other reducing agents (Fig. 1.22).

1.3.4 N−X bond formation with metal nitride in pincer complexes

Schneider group reported that the addition of alkyl triflates to Re−nitride complex C90 leads to N_2 functionalization [98]. DFT calculation suggests that the reduction of complex C89 forms a dimer [(PNP)ClRe(N_2)ReCl(PNP)], which is the reasonable intermediate that undergoes subsequent N−N scission to afford Re−nitride complex C90. The high stability of the Re−nitride bond did not allow for ammonia formation by hydrolysis or hydrogenolysis; however, nitride functionalization can be achieved by an electrophilic attack of MeOTf to afford C−N bond formation product C91. Later the same group also reported the synthetic cycle for the

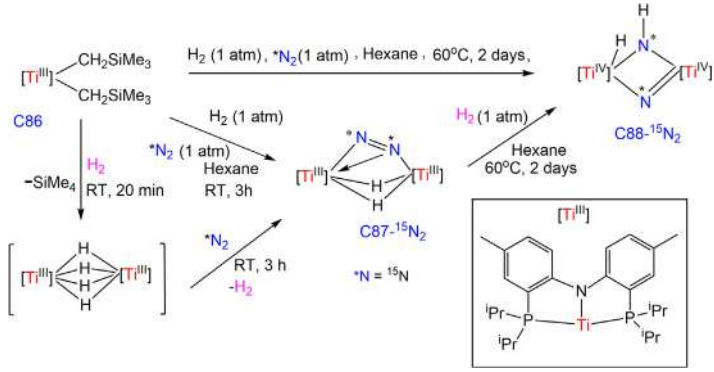

Figure 1.22 Activation and hydrogenation of N_2 by H_2 at a PNP-ligated titanium platform.

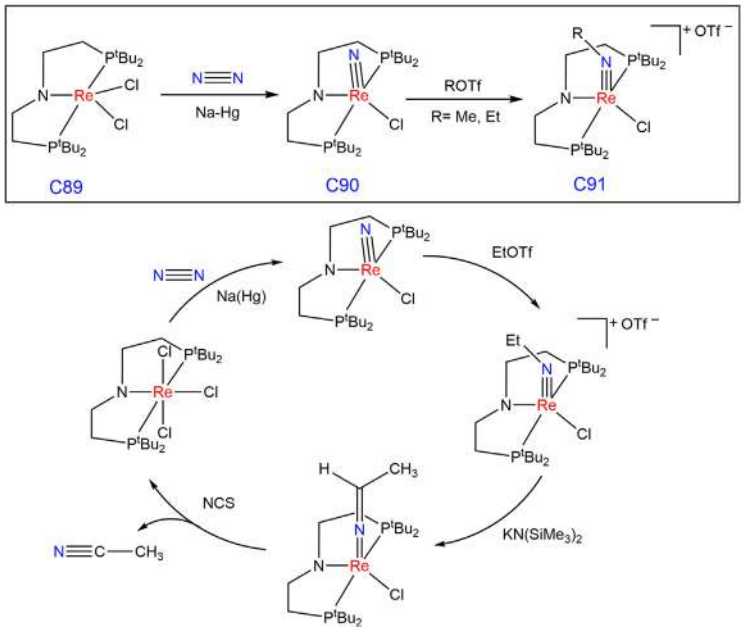

Figure 1.23 N_2 functionalization with Re–nitride catalyst.

transformation of N_2 to acetonitrile in the presence of base [$KN(SiMe_3)_2$] and chlorinating agent N-chlorosuccinimide (NCS), which describes a new strategy for dinitrogen functionalization to valuable chemicals beyond ammonia (Fig. 1.23) [99].

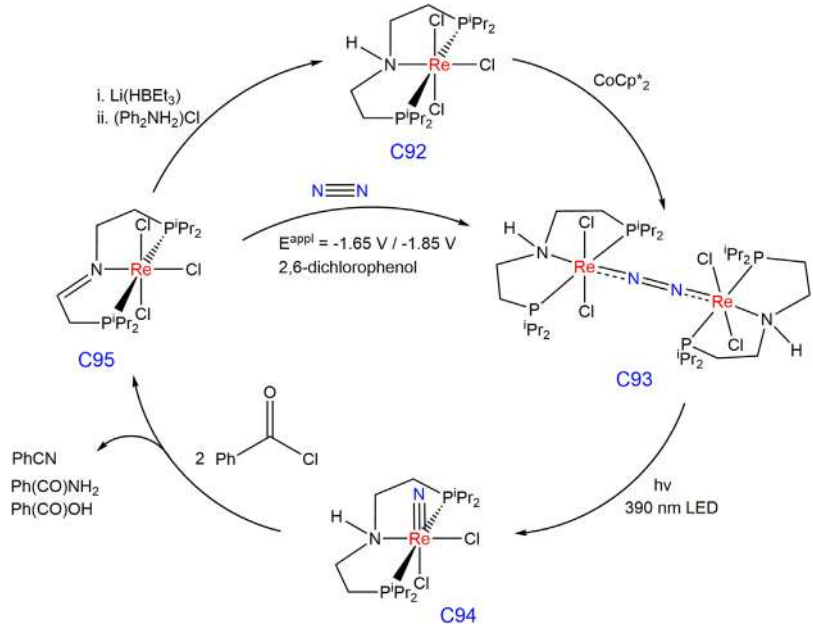

Figure 1.24 Photolytic and electrochemical splitting of N_2 to nitride and formation of benzonitrile/benzamide.

In 2018, the Schneider group reported the electrochemical and photolytic splitting of N_2 to corresponding benzonitrile/benzamide in an overall 61% yield with respect to nitrogen [100]. The reduction of [(PNP^{i}Pr)$ReCl_3$] [PNP^{i}Pr = HN($CH_2CH_2P^iPr_2$)$_2$], C92 under N_2 atmosphere did not yield nitride species and a bridging dinitrogen complex [(PNP^{i}Pr)$ReCl_2$]$_2$(μ-N_2) C93 was isolated in presence of $CoCp^*_2$, which upon irradiation with visible light undergoes photolytic N−N triple bond scission and nitrido complex (PNP^{i}Pr)Re(N)Cl_2 (C94) was formed. Subsequent heating of C94 with 2 equivalents of PhC(O)Cl at 80°C in 1,4-dioxane over 15 h yielded rhenium(III) complex C95 along with benzamide (30%) and a benzonitrile (64%), which accounts for 94% of the nitride ligand. The products PhCN and $PhCO_2H$ were formed by the reaction of benzamide with benzoyl chloride, which reveals that $PhC(O)NH_2$ is the possible intermediate product of nitride benzoylation and $2e^-/2H^+$ transfer from the pincer ligand (Fig. 1.24).

Miller and co-workers in 2019 reported the ammonia (74% yield) synthesis from the N_2-derived rhenium nitride complex upon treatment with SmI_2/H_2O [101]. The reaction pathway involved the reductive formation

of a bridging N_2 complex from (PONOP)$ReCl_3$ C96, photolytic N_2 splitting, and PCET reduction of metal nitride bond to form C99 and the ammonium ion in 74% yield (Fig. 1.25).

1.3.5 Catalytic silylation of dinitrogen using transition metal pincer complexes

The silylation of the metal-bound N_2 to functionalizing silyl amines $N(SiR_3)_3$, which can be hydrolyzed to NH_3, is an alternative approach. In place of using proton and electron equivalents, the commonly available silylating reagents and any strong reductant (e.g., Li, Na, K, KC_8) play a significant role.

Mézailles and co-workers reported the catalytic reduction of dinitrogen into silyl amines [102], using Mo complex bearing tridentate PPP-pincer ligand and cyclic silylated hydrazido complex C100 produced up to 39 equivalents of NH_4^+ per Mo after acid hydrolysis using 400 equivalents of K and 200 equivalents of $SiMe_2ClCH_2CH_2SiMe_2Cl$. The Fe-congeners were also found to be an effective catalyst for the same reaction where up to 32 equivalents of $N(SiMe_3)_3$ were yielded using catalyst C101 and 600 equivalents each of K and Me_3SiCl, respectively [103].

Iron- and cobalt–dinitrogen complexes bearing PSiP-type pincer ligand C102 and C103 reported by Nishibayashi yielded up to 26 and 41 equivalents of $N(SiMe_3)_3$ using 600 equivalents each of K and $SiMe_3Cl$, respectively [104]. The anionic pyrrole Fe–PNP pincer complex C64 afforded up to 33 equivalents of $N(SiMe_3)_3$. The Rh–dinitrogen congener C104 yielded up to 23.2 equivalents/Rh of NH_3 after acid hydrolysis (using 1.5 mmol of KC_8 and Me_3SiCl, at −40°C) [105]. Fenske group reported the dinitrogen silylation catalyzed by bis(silylene)-based [SiCSi] pincer hydrido Fe(II) dinitrogen complex C105, which afforded up to 74.4 equivalents/Fe of $N(SiMe_3)_3$ using 1800 equivalents/catalyst each of KC_8 and Me_3SiCl, respectively, in dioxane at 25°C for 150 h (Fig. 1.26) [106].

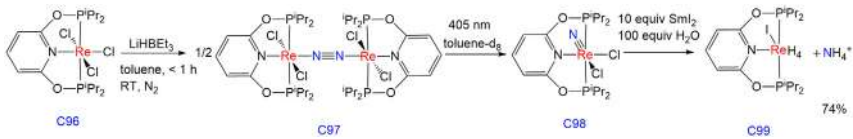

Figure 1.25 SmI_2/H_2O proton-coupled electron transfer (PCET) reduction of Re − nitride complex to NH_4^+.

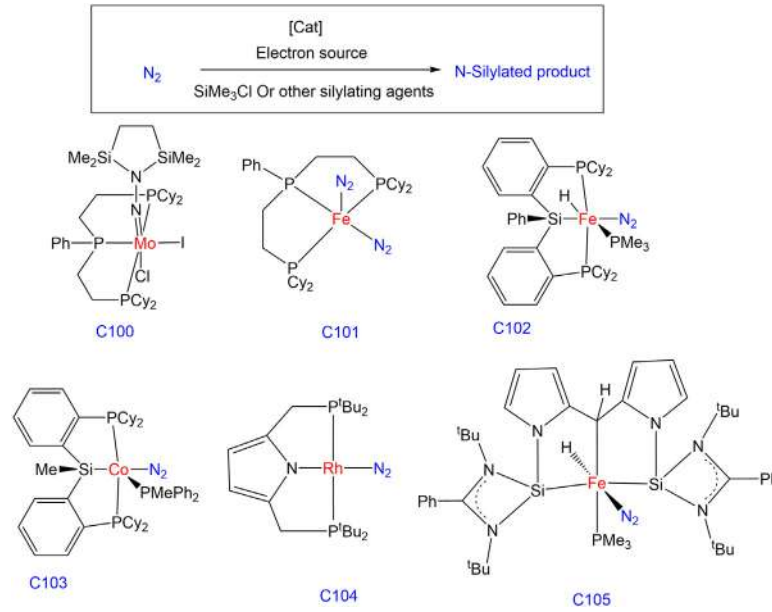

Figure 1.26 Catalytic silylation using various transition metal pincer complexes.

1.4 Pincer complexes as hydrogenation catalyst

Apart from the dehydrogenation reaction, pincer complexes have also been employed as catalysts for the hydrogenation reaction. Under hydrogen pressure, a different type of organic molecular functionality undergoes hydrogenation that has several advantages over the classical hydrogenation reaction like atom economic process, sustainable, and less waste. The pincer ligand having a proton-responding arms or the metal ligand cooperativity plays a significant role in the hydrogenation reaction of the small organic molecule, where molecular dihydrogen cleaves heterolytically to proton and hydride and transfers to the organic substrate. This section describes the catalytic hydrogenation of ester, amides, carbamate, urea, nitriles, and alkyne groups mediated by pincer complexes.

1.4.1 Ester hydrogenation

The hydrogenation of ester was first demonstrated by the Milstein group in 2006 using Ru–PNN pincer complex C106 as a catalyst under the hydrogen pressure of only 5.3 bar and base-free condition [107]. Various ester substrates are hydrogenated to corresponding alcohols, although later Robertson group employed the same catalyst for the hydrogenation of

polyesters that have significant development in terms of practical application [108]. Several other Ru-based pincer complexes are reported in the literature [109–112]. Beller group reported the Ir–MACHO complex (C107) for the hydrogenation of a variety of esters, including heterocyclic esters in the presence of a catalytic amount of base and under a hydrogen pressure of 50 bar at 130°C for 18 h [113].

In 2014, Milstein group reported hydrogenation of trifluoroacetic esters using nonprecious transition metals of a Fe–PNP pincer complex trans-[Fe(PNP)$(H)_2$(CO)] C108 under mild reaction conditions, which produced corresponding trifluoroethanol with 0.05 mol% of catalyst loading corresponded to a TON of 1280 [114]. Beller [115] and Guan [116] independently reported broad-scope hydrogenation of nonactivated esters catalyzed by an iron aliphatic pincer complex [Fe(PNHP)(H)(CO)(BH_4)] C109 with no added base. Beller and co-workers studied the catalytic activity of Fe complex with a "MACHO" ligand with different substituents on the P arms and showed that ethyl substituted complex C110 was the most active one [117]. No additional base was required and several aromatic cycles, heterocyclics, and olefins functionality along with lactones and diesters were also suitable for hydrogenation. In 2015, the Milstein group first reported the ester hydrogenation reaction to alcohol catalyzed by Co–PNNH pincer complex C111 where a 25 mol% of base was required to activate the substrate via the formation of enolate intermediate [118]. Jones group reported the Co–MACHO complex C112 as catalyst under H_2 (55 bar) in THF at 120°C for the hydrogenation of esters without any additive where the biomass-derived cyclic ester efficiently converted to corresponding diol product with a TOF of 3890 [119]. In 2016, the Beller group first reported the ester hydrogenation reaction using the Mn pincer complex [120]. A Mn–MACHO pincer catalytic system C113 enabled the effective and selective hydrogenation of various aromatic and aliphatic esters as well as diesters and lactones. In 2017, the Milstein group also reported Mn(PNNH) catalyst C114 for the same transformation under mild reaction conditions (100°C, 20 bar) (Fig. 1.27) [121].

1.4.2 Amide hydrogenation

In 2010, the Milstein group first reported the efficient hydrogenation of amides to form corresponding amines and alcohols by N–C cleavage, using a dearomatized Ru pincer complex C115 (1 mol%) with 10 atm of hydrogen pressure, in THF at 140°C [122]. Various types of heterocyclic

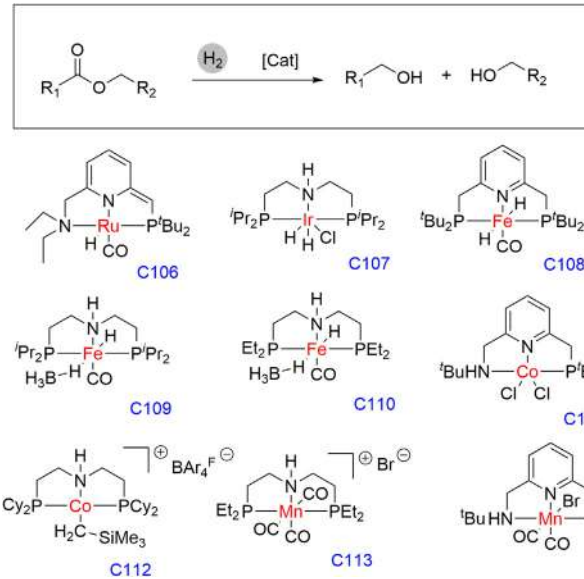

Figure 1.27 Catalytic hydrogenation of ester to alcohol using various transition metal pincer complexes.

and aromatic functionalized amide substrates were tolerated under the catalytic condition. The very recently same group also reported the amide hydrogenation under extremely milder condition (RT, 5 − 10 bar of H_2) catalyzed by well-defined ruthenium−PNNH pincer complex C116 (0.5 mol%), which shows potential dual modes of metal − ligand cooperation [123]. Beller group also reported a Ru−PNN catalyst C117 bearing an imidazolylaminophosphino ligand for the hydrogenation of a range of amides under base-free conditions in high yields [124].

In 2016, Langer reported the iron pincer (Fe−MACHO−BH_3) catalyst C110 for amide hydrogenation with a hydrogen pressure of 50 bar in THF at 70°C−100°C without any external additives [125]. Whereas Milstein group employed Fe−PNP complex C118 under 60 bar hydrogen pressure and catalytic amounts of KHMDS as a base in dioxane at 140°C for the hydrogenation of activated amides to corresponding amines and alcohols via N−C bond cleavage [126]. Bernskoetter group reported an iron(II) hydride amido complex (^{i}PrPNP)Fe(H)CO (^{i}PrPNP = N[$CH_2CH_2(P^iPr_2)]_2$) C119 for the selective catalytic deaminating hydrogenation of amides with TONs over 1000 for multiple substrates and more than 4000 TONs was obtained for activated formanilides [127].

In 2017, the Beller group reported an Mn–PNN pincer catalyst C120 containing an imidazolyaminolphosphino ligand that showed high activity and selectivity in the hydrogenation of a wide range of secondary and tertiary amides via deamination pathways under mild conditions [128].

Deoxygenated hydrogenation of amides (C–O bond cleavage) is an efficient method to access the corresponding amines in a single-step process, although the low electrophilicity of the amide carbonyl group and the competitive C–N bond cleavage make this transformation more challenging. Zhou group reported a well-defined iridium catalyst C121 bearing a (POCOP) pincer ligand combined with $B(C_6F_5)_3$ as Lewis acid for the chemoselective deoxygenated hydrogenation of amides to amine under mild reaction conditions [129]. Later Milstein group reported the same reaction with high efficiency and selectivity using an dearomatized Mn–PNP pincer complex C122 in presence of Lewis acid $B(C_6F_5)_3$ under 50 bar of hydrogen pressure (Fig. 1.28) [130].

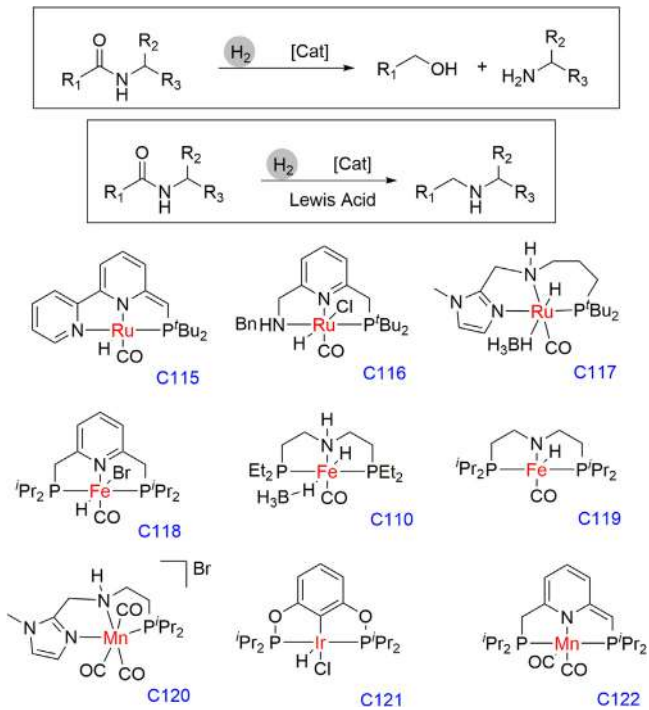

Figure 1.28 Catalytic hydrogenation of amide using various transition metal pincer complexes.

1.4.3 Hydrogenation of urea, carbamate, carbonate, and imides derivatives

In 2011, the Milstein group reported the first example of catalytic hydrogenation of urea derivatives. Selective formation of methanol and the corresponding amines takes place by the cleavage of the robust C−N bonds under mild and neutral conditions [131]. Using dearomatized bipyridine-based Ru−PNN pincer complex C115, urea derivative underwent hydrogenation in presence of H_2 (13.6 atm) at 110°C for 72 h afforded high yield of methanol and corresponding amines. Later the same group also reported the hydrogenation of cyclic urea (ethylene urea) to methanol and ethylenediamine in quantitative amounts using aromatized Ru−PNN complex C115a in the presence of 60 bar H_2 pressure for 1.5 days under elevated temperature [132]. In the same year, they also reported that by the hydrogenation of organic carbonate derivatives by using the same complex C115 as well as with Ru−PNN dearomatized complex C106a, C−O bond was cleaved to afford methanol and the corresponding alcohol derivatives with higher TON up to 4700 [133]. The same catalyst was also active for the hydrogenation of the carbamate derivatives and afforded the methanol and corresponding amine with alcohol derivative under the mild condition in good yields. Ding group also reported the hydrogenation of the cyclic carbonate using Ru−MACHO catalyst C123 under 50 bar of hydrogen pressure and afforded methanol and diol in good yields. Highest TON of 87,000 and a TOF of 1200 h^{-1} were achieved on decreasing the catalyst loading to 0.001 mol% [134].

Milstein group also reported the hydrogenation of organic carbonates to the corresponding alcohol and methanol using Mn−PNNH complex C114 under 30 bar of H_2 pressure in the presence of a catalytic amount of base at 110°C for 30 h [135]. Leitner group reported the hydrogenation of the cyclic carbonate using the Mn−PNHP C124 catalyst under 30 bar of hydrogen pressure where turnover numbers up to 620 and 400 were obtained for the formation of the diol and methanol, respectively [136]. Rueping group also reported the hydrogenation of the cyclic carbonate using Mn−PNHN C125 catalyst under mild condition (140°C, 50 bar of H_2) and low catalyst loading up to 0.25 mol% [137]. In 2019, Milstein group reported the hydrogenation of urea derivatives by using Mn−PNN complex C126 via MLC involved dearomatized complex [138]. Catalyst C126 (0.02 mmol), ^{t}BuOK (0−3 mol%), urea derivatives in toluene, and H_2 (20−40 bar) at 130°C afforded good conversion with methanol

formation. The detailed mechanism is also described based on the controlled experiments where the dearomatized pincer complex plays an active role in the H_2 activation and the substrate hydrogenation process. The same complex was also used for the hydrogenation of carbamate derivatives and afforded methanol and corresponding amine and alcohol.

Milstein group also reported the hydrogenation of cyclic imides to diols and amines using a ruthenium pincer catalyst C127 [139]. Cyclic imides treated with complex C127 with ^{t}BuOK under H_2 pressure (40 bar) afforded good to moderate yields of the corresponding diol and amines. Very recently, the same group also explored the same reaction with the earth-abundant Mn-based pincer complex C126 under H_2 pressure (30 bar), 130°C for 48 h in basic condition, which afforded diol and primary amines in very good yields (Fig. 1.29) [140].

1.4.4 Nitrile hydrogenation

The hydrogenation of nitrile provides primary or secondary imines as well as primary, secondary, or tertiary amines. The hydrogenation of nitriles to secondary imines is reported by Milstein group in 2011 where a bipyridine-based Ru–PNN pincer complex C115 effectively hydrogenated nitrile under mild and neutral conditions at only 4 bar of H_2 displaying various functional groups tolerance [141]. Prechtl group demonstrated the coupling of nitriles with amines catalyzed by a Ru–amido complex C128 in the

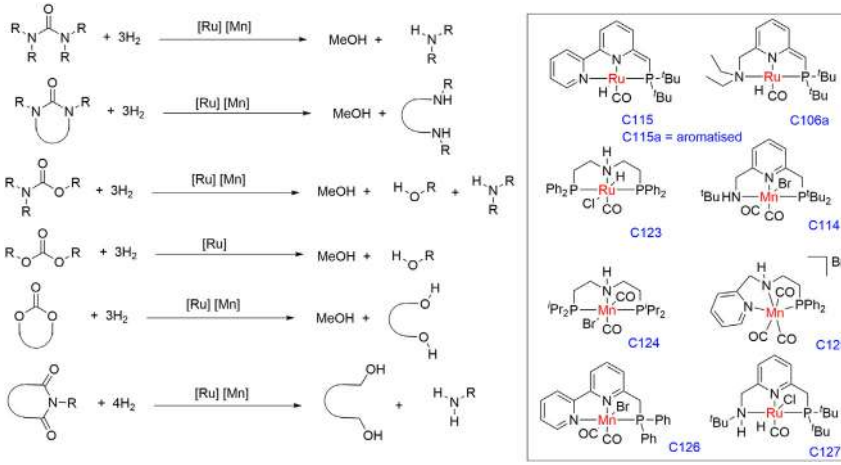

Figure 1.29 Catalytic hydrogenation of urea, carbonate, carbamate, imides derivatives using various transition metal pincer complexes.

presence of only 0.4 MPa of H_2 pressure and catalyst loading of 0.5−1 mol %, which proceeded with high selectivity [142]. In 2017, Milstein group reported the earth-abundant iron pincer complex C129 for selective homocoupling-hydrogenation of nitriles under catalytic base concentration and mild hydrogen pressure [143,144].

The complete hydrogenation of nitrile to amine is one of the significant reactions due to the various applications of the final amine products. In 2011, Leitner group reported the hydrogenation of aliphatic and aromatic nitriles using 0.4 mol% ruthenium pincer complex C130 under the hydrogen pressure of 75 bar at 135°C afforded good yields [145]. The presence of catalytic amounts of water (2 mol%) enhanced the catalytic activity, and the increased rate of the reactions was also noticed. Beller group reported one of the most active catalytic systems based on imidazolylphosphine PNN pincer with ruthenium complex C117 for the nitrile hydrogenation reaction [146]. The maximum TON of 2000 was reported at 0.05 mol% of catalyst loading for the benzonitrile to benzylamine transformation; along with this, various kind of aromatic and aliphatic nitrile substrate scope was also checked under the base-free, mild reaction condition (30 bar H_2 pressure). Milstein group reported the same reaction at low H_2 pressure (3 bar), using Ru−PNP pincer complex C131 (0.3 mol %), with a variety of nitriles derivatives under neutral conditions and without any additives [147].

The catalysts with nonprecious metals were reported by Beller using 1 mol% of Fe pincer complex C109 under the hydrogen pressure of 30 bar in isopropanol. A series of aliphatic, aromatic, and heterocyclic nitriles was hydrogenated with tolerating esters, amides functional groups [148]. Milstein group reported the Co−PNNH catalyst C111 using $NaBEt_3H$ and NaOEt as an additive for the hydrogenation of nitriles to primary amines [149]. Beller group reported Mn pincer complex C124 for the hydrogenation of nitrile to the primary amine. In presence of 3 mol% catalyst, 10 mol% base, and 50 bar H_2 pressure at 120°C in isopropanol afforded almost quantitative yields and a wide range of substrate scope was achieved (Fig. 1.30) [150].

1.4.5 Hydrogenation of alkynes

The partial hydrogenation of the C−C triple bond to selective alkene formation is one of the important transformations in organic chemistry. Chirik group reported the hydrogenation of hindered olefins catalyzed by

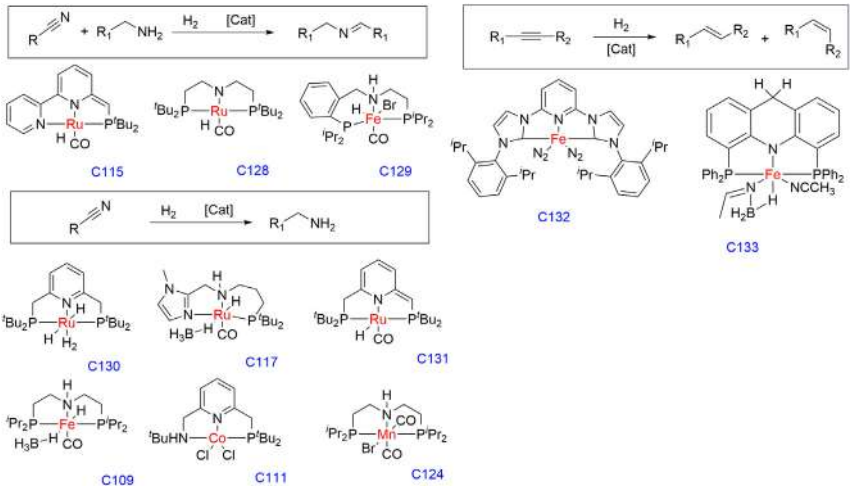

Figure 1.30 Catalytic hydrogenation of nitrile and alkyne using various transition metal pincer complexes.

electron-rich bis(arylimidazol-2-ylidene) iron pincer complex (C132) at 4 bar of hydrogen and 23°C afforded good yield [151]. Milstein group also employed an acridine-based iron PNP pincer complex C133 for the hydrogenation of alkynes to olefins with a high E-selectivity under mild and base-free conditions (Fig. 1.30) [152].

1.5 Coupling reaction: C–C bond formation reaction

The carbon–carbon bond formation reaction is one of the most important transformations in organic chemistry with its various applications in industries as well as in pharmaceuticals [153–155]. Several palladium-based pincer complexes as well as nonprecious transition metal-based pincer complexes were explored as a catalyst for the Heck-Mizoroki, Negishi, Suzuki-Miyaura, Kumada, Stille coupling reaction [13,14,156–165].

1.5.1 Mizoroki-Heck reaction

In 1997, Milstein group reported the Pd–PCP pincer complex C134 for the coupling reaction between aryl halides and olefins, which afforded good yields with an excellent selectivity of E-product using a catalyst loading of 9×10^{-5} mol% at 140°C and a maximum TON of 528700 was achieved [166]. Jensen group later employed a Pd–POCOP pincer complex C135 (0.67 mol%) for the coupling of relatively less reactive

chlorobenzenes substrates and styrene in presence of CsOAc as base afforded selectively trans-configured product with >99% of yields [167]. In 2014, the Albrecht group reported a carboxylic acid functionalized (NHC)-based Pd–N(NHC)O pincer complex C136 for the coupling of bromobenzenes derivatives and styrene under mild reaction conditions (Fig. 1.31) [168]. Depending on the reaction condition, catalyst showed the "turn on" and "turn off" switchable catalytic activity, which represented the active role of the carboxylate arm of the ligand. Tu group reported a NHC-based pincer complex of palladium (C137) for the coupling of aryl halides with alkyl acrylates in presence of K_2CO_3 as base, and maximum TON of 1.32×10^8 was achieved [169]. Whereas catalyst C138 works in water as a solvent for coupling of iodobenzenes derivatives, tert-butyl acrylate derivatives in presence of triethylamine and tetra-n-butylammonium iodide (TBAI), which released quantitative yields of the coupled product [170]. The number of contributions of different research groups around the world has enabled the preparation of pincer catalysts with several topologies and applied for Mizoroki–Heck coupling reaction [171–182].

1.5.2 Suzuki–Miyaura reaction

Bedford group reported a Pd–POCOP pincer catalyst C139 for the Suzuki–Miyaura couplings of phenylboronic acid and aryl halides derivatives, and maximum TONs of 190000 was recorded for the p-bromo derivative with very low catalyst loading (0.0001 mol%), and a maximum

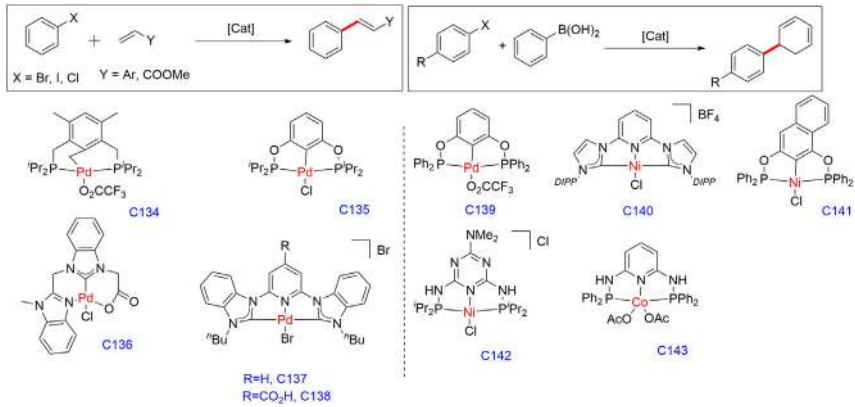

Figure 1.31 Catalytic Mizoroki–Heck and Suzuki–Miyaura coupling reaction using various transition metal pincer complexes.

92% yield was achieved [183]. Several other palladium pincer compounds were used successfully for the same reactions [184–210]. Apart from Pd, few earth-abundant metal pincer complexes also function as a catalyst for the same transformation. Inamoto group successfully employed a pyridine backbone with NHC arms Ni(II) pincer complex C140 for the Suzuki–Miyaura coupling reactions of aryl halides or aryl tosylates with phenyl boronic acids and afforded the corresponding coupling products in good yields [211–213]. Morales–Morales group reported a Ni(II)–POCOP pincer catalyst C141 for the coupling of bromobenzenes derivatives with phenylboronic acid, which showed quantitative conversions to the biphenyl product [214]. Kirchner group scanned various kinds of Ni–PN^5P pincer complexes where catalyst C142 showed the best reactivity for the Suzuki–Miyaura coupling in term of yields [215]. The similar ligand scaffold with PNNNP ligand with Co(II) pincer complex C143 reported by the Bhat group was successfully employed for the same reaction under mild conditions and observed the improvement of catalytic activity (Fig. 1.31) [216].

1.5.3 Sonogashira, Negishi, Kumada-Corriu, Stille cross-coupling

Crabtree and faller group reported a Pd–CNC pincer complex C144 for the Sonogashira cross-coupling reaction with maximum TON of 75000 using 2×10^{-4} mol% of catalyst loading [217]. Dominguez and San-Martin group scanned a series of Pd(II) pincer catalysts for the coupling of 4-chlorobenzene derivatives and phenylacetylene where C145 showed a very good catalytic performance using a catalyst loading of only 0.1 mol% in pyrrolidine at 100°C for 6 h [187,197]. Frech group reported Sonogashira cross-coupling reactions with $\{[C_6H_3–2,6\text{-}(NHP\{piperidinyl\}_2)_2]Pd(Cl)\}$ C146, which required low catalyst loadings (0.005 mol%) under additive and amine-free reaction conditions [218]. Maximum of 2×10^6 TON and 400000 h^{-1} TOFs were observed under the optimized reaction condition in the coupling reaction of iodobenzene and ethynylbenzene. Xu group reported a Ni(II)–POCOP pincer complex C147 as a catalyst for the couplings of alkyl halides and lithium acetylides where 99% of highest yield was achieved in presence of N-methyl-2-pyrrolidine (NMP) as solvent and 0.5 mol% of catalyst loading [219] (Fig. 1.32).

Lei group reported a bis(thioamide)pyridine ligand-based Pd(II)–SNS pincer complex C148 for the Negishi cross-coupling reaction with aryl halides and alkyl zinc under mild reaction conditions affording good yields

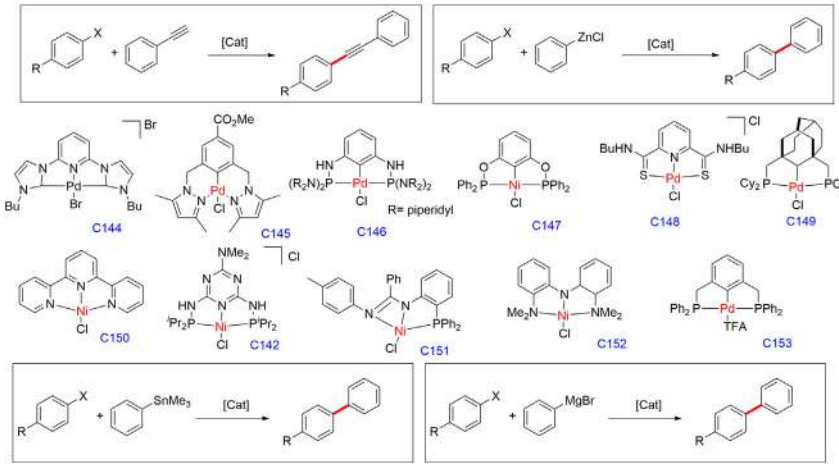

Figure 1.32 Catalytic Sonogashira, Negishi, Kumada-Corriu, Stille cross-coupling using various transition metal pincer complexes.

with the maximum TON of 6.1×10^6 and TOF of $6.4 \times 10^4\ h^{-1}$ [220, 221]. Frech group employed an aliphatic PCP–Pd pincer complex C149 for the same coupling reaction of aryl bromides derivatives with diarylzinc reagents in NMP with high functional groups tolerance and only 0.1 mol% of catalyst loading [222]. Biscoe group reported the Negishi cross coupling reaction between aryl/heteroaryl iodides and secondary alkyl zinc halides to get the retention product without competitive isomerization of the nucleophile by using Ni(Cl)(tpy) pincer catalyst C150. To get the higher selective branched product over the linear product, 1 equivalent of salt additives such as $LiBF_4$ was also used [223]. Kirchner group also employed the Ni-catalyst (C142) for the Negishi cross-coupling reaction and revealed that various activated and inactivated aryl halides including chlorides as well as phenol derivatives such as tosylates and mesylates were well tolerated under the optimized reaction condition [224]. Wang group reported a Ni–NNP pincer complex C151 for the Kumada coupling reaction involving between a Grignard reagent and an aryl-halide using low catalyst loadings under mild reaction conditions, achieving high yields [225,226]. Hu group also described a Ni–NNN pincer complex C152 in the Kumada-Corriu cross-coupling reaction with excellent activities for the secondary alkyl halides [227,228]. Wendt group employed PCP–Pd complex (C153) in the Stille coupling reaction between aryl bromide and trimethyl(phenyl)tin and a maximum TON of

690000 and TOF of 38000 h^{-1} were achieved under the optimized reaction conditions (Fig. 1.32) [229].

1.6 Redox-Active Pincer Complexes

The pincer ligands have a strong influence on the reactivity and selectivity of metal complexes by modifying the steric and electronic properties at metal centers. Ligand motif subclassification with this delight are trans-spanning ligands [230], ambidentate ligand [231], bridging ligand, binucleating ligand, spectator ligand, a bulky ligand, chiral ligand, hemilabile ligand [232], and non-innocent ligand [233]. Among all these, metal complexes based on "non-innocent ligands" have displayed excellent catalytic activities and exposed many exciting catalytic reactions as mentioned above.

In 1966, C.K. Jørgensen first described that ligands are called innocent when they allow to distinguish the exact oxidation state of a central metal atom without any ambiguity [10]. Non-innocent ligands are redox-active that have energetically favorable levels that can reduce or oxidize themselves to change their oxidation state and can act as electron reservoirs, which are pointed out by Chirik and Wieghardt later [234]. Often these ligands upon binding with transition metals can easily transform into ligand radicals. Redox non-innocent ligand motif is gaining much more importance due to its effective strategy in catalysis [235]. Electron deposition or dissipation of a redox-active ligand have a significant impact in the reactivity to the adjacent metal complex by permitting it to adopt different resonance structure with or without changing the oxidation state of the metal, thus facilitating bond making and bond-breaking processes (Fig. 1.33).

The redox-active ligand is an "actor ligand" that generates reactive ligand radicals that actively participate in the catalysis reaction process. The redox non-innocent ligand and the metal allow chemical reaction by the cooperative substrate activation pathway (Fig. 1.33a). It also involves modification of the substrate reactivity where the substrate itself acts as a redox non-innocent ligand (Fig. 1.33b). Another classification of the non-innocent ligand is a "spectator ligand" that modifies the Lewis acidity of the metal by the redox reaction of the ligand and influences the substrate affinity of subsequent reactions (Fig. 1.33c) or ligands as an electron-reservoir allows the metal to store electrons in the ligand in elementary steps thus avoiding the uncommon oxidation state of the metal (Fig. 1.33d) [236,237].

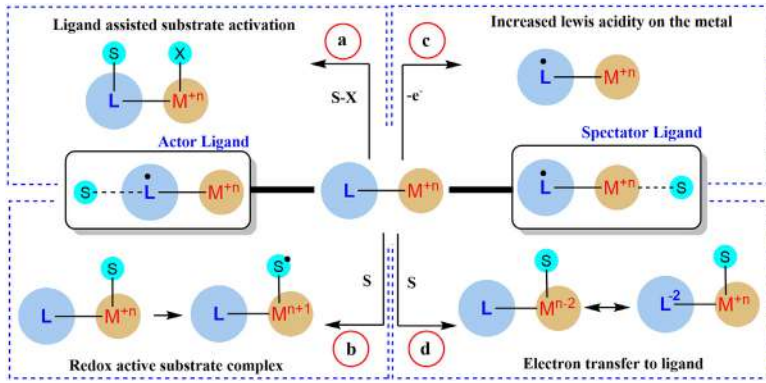

Figure 1.33 Different pathways of the redox-active ligand for the substrate activation in the catalytic process.

To overcome high-energy barriers, the use of redox-active pincer complex in various multielectron transformations by using relatively abundant, nontoxic, and 3d transition metals is an eye-catching strategy [238]. This multielectron transformation requires an aid of transition metal complex with redox-active ligands, which can supply reducing or oxidizing equivalents. A redox-active ligand works together with a metal ion that was observed in various metalloenzymes in the natural processes [239,240]. However, recent developments optimize the versatile nature of redox-active non-innocent ligands in both catalytic activities of transition metal coordination sphere and substrate activation. This section provides an overview of highlighting research directions of the redox-active pincer complex and uncover its modes of reactivity and catalytic pathways as well.

The iron pincer complex containing pyridine−bisimine ligand functionalized by bulky ortho-substituted aryl amines C154 was developed by Brookhart [241] and Gibson [242] and employed for the olefin polymerization reaction [243].

Later Chirik group developed a cationic Fe^{II}−dimpy complex C155 and revealed its importance as a propagating species in the polymerization of olefin [244,245]. A redox activity of the bis(imino)pyridine iron bis (dinitrogen) complexes (^{i}PrPDI)Fe$(N_2)_2$ C156 was used for catalytic intramolecular $[2\pi + 2\pi]$ cycloaddition reactions of α, ω dienes. The formation of strained four-membered rings is thermally forbidden and photochemically allowed. The iron complex supported by redox-active ligand showed the same reaction with high catalytic turnover and high yield at room temperature. The formal oxidative addition underwent after

the coordination of two-terminal diene accepted two electrons from the ligand and simultaneous reduction of the 2,6-diiminepyridine moiety, which allowed iron to maintain the energetically favorable Fe(II) oxidation state. The N-tert-butyl derivatives of diene delivered the yield of the reactions up to 95% with TOF $> 450\ h^{-1}$ in <5 min (Fig. 1.34) [246].

Chirik et al. proposed a C–C coupling transformation aided by the same iron complex C156. This hydrogen mediated catalytic cycloaddition of 1,6-enynes were conducted with 5 mol% of C156 at 23°C under 4 atm H_2 in benzene solution, afforded high turnover frequency. Tosyl-, benzyl-, and tert-butyl-protected terminal aminoenynes showed catalytic conversion to yield facile hydrogen-mediated cyclization with the formation of the cis diastereomers over the trans ones (Fig. 1.35A) [247].

The same complex C156 also showed excellent catalytic activity for the regioselective anti-Markovnikov alkene-hydrosilylation reaction. Transformation of 1-octene was carried out in the presence of 0.05 mol% of catalyst and tertiary silane [$(Me_3SiO)_2MeSiH$] with yield up to 98%. The reaction intermediate formed after loss of 2 equivalents of dinitrogen from C156 yielded iron(II) complex with a dianionic tridentate N_3^{-2} ligand, which inserted into the Si–H bond by accepting two electrons from the ligand and simultaneous reduction of the 2,6-diiminepyridine moiety without hampering iron(II) oxidation state. Further on, subsequent anti-Markovnikov addition of electrophilic Si-species and hydride

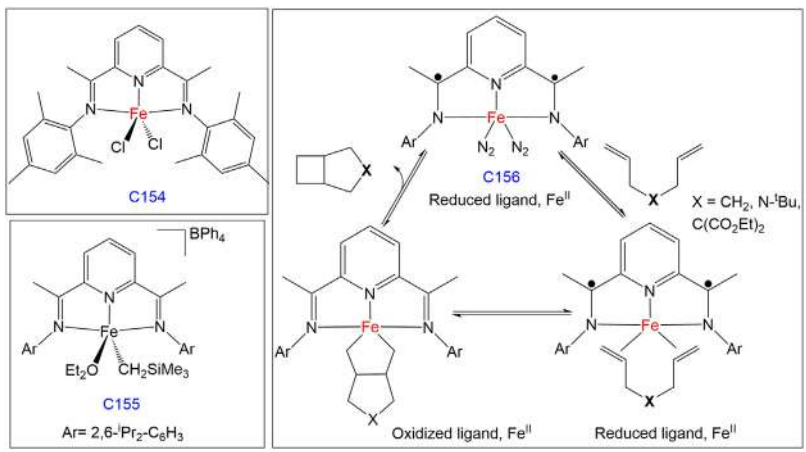

Figure 1.34 Redox non-innocent 2,6-diiminepyridine ligand in Fe-catalyzed [2 + 2] cycloaddition ring-closure reactions.

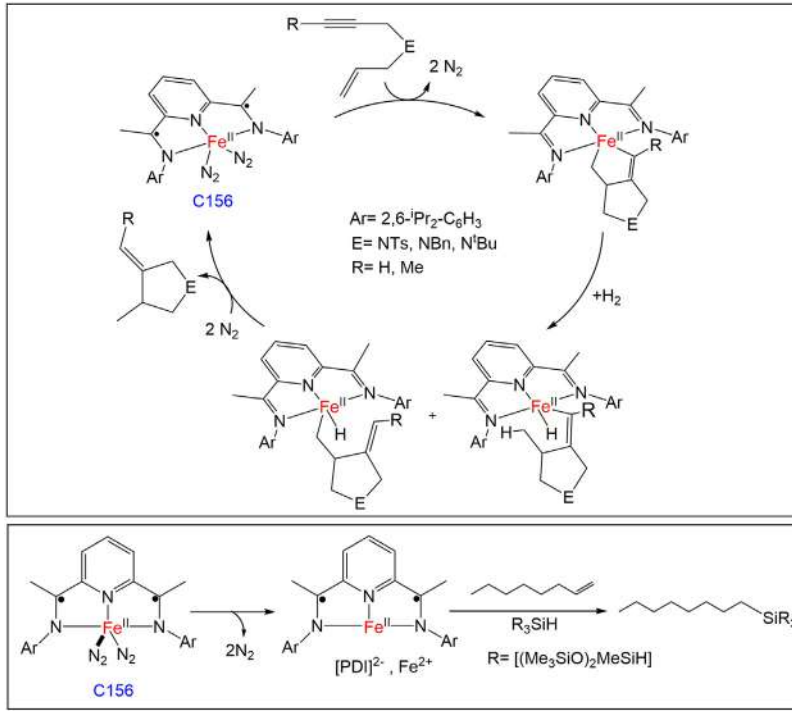

Figure 1.35 (A) 1,6-Enyne cycloaddition with a redox-activated bis-aryl iminopyridine Fe^{+2} complex. (B) Selective terminal alkene hydrosilylation.

across the double bond of substrate facilitated the conversion of the desired product (Fig. 1.35B) [248].

In 2008, Mindiola et al. reported an electron-rich Ni complex C157 bearing a redox-active PNP pincer ligand (PNP = N[2-P($CHMe_2$)$_2$−4-methylphenyl]$_2$), which acts as an electron source. With the combination of structural, spectroscopic, and theoretical techniques, C157 and its radical cation counterpart C158 in presence of ferrocenium ion have exposed the presence of redox-active sites of ligand and spectroscopically depicted that the electron hole resides mostly at the nitrogen and aryl carbon atoms of the pincer type PNP ligand where nickel was in +2 oxidation state (Fig. 1.36) [249].

In 2012, Heyduk et al. reported the formation of aryl diazenes from the aniline derivatives via the four-electron oxidation using a tantalum(V) complex bearing a tridentate trianionic redox-active ligand, N,N-bis(3,5-di-tertbutyl-2-phenoxide)amide ($[ONO^{red}]^{3-}$). The dimethyl tantalum complex ($[ONO^{red}]TaMe_2$) C159 on treatment with p-toluidine and

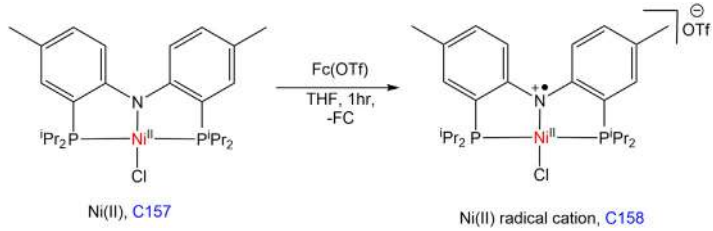

Figure 1.36 Chemical oxidation of Ni(II) with Fc(OTf).

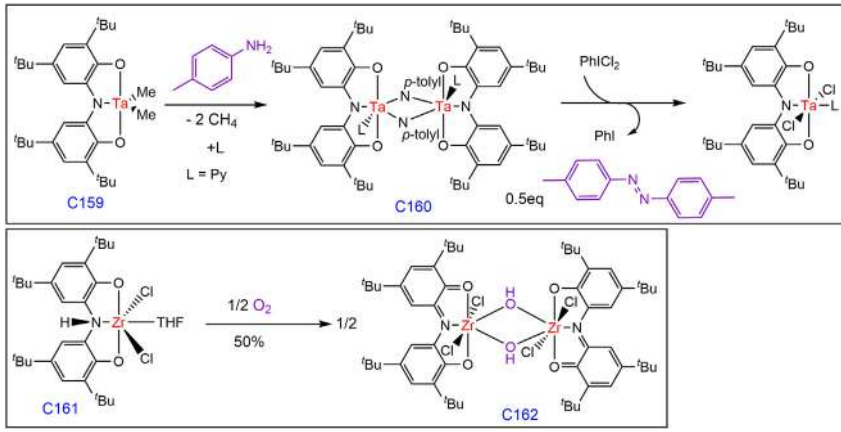

Figure 1.37 (A) Organic diazene elimination from tantalum (V) bridging imido dimer. (B) Synthesis of zirconium hydroxide bridged dimer complex.

pyridine (L) resulted into the bridging imido tantalum(V) dimer C160, which upon oxidation with iodobenzene dichloride ($PhICl_2$) quantitatively eliminated the aryl diazene (p-tolyl)N = N(p-tolyl) from tantalum (V) bridging imido dimer. The trianionic $[ONO^{red}]^{3-}$ ligand motif subsequently participated in one- and two-electron oxidations of complexes to form dianionic $[ONO^{sq}]^{2-}$ and monoanionic $[ONO^{q}]^{-}$, respectively, which lead to the formation of N = N bond (Fig. 1.37A) [250].

The same [ONO] ligand platform is also capable of serving as both an electron and proton donor for the reduction of O_2 at a zirconium(IV) coordination complex. The reduction of O_2 is a four-electron, two-proton process that was achieved from dianionic $[ONHO]^{2-}$ linked Zr (IV) complex $[(ONHO)ZrCl_2(THF)]$ C161 to form the bis(hydroxo) complex $[(ONO^{q})ZrCl_2(\mu\text{-}OH)]_2$ C162 revealed by Heyduk group (Fig. 1.37B) [251].

Heyduk et al. presented tantalum(V) complex coordinated to trianionic $(NNN^{cat})^{3-}$ redox-active pincer ligand, which showed one- and two-electron oxidations to form dianionic semiquinone form $[NNN^{sq}]^{2-}$ and monoanionic form $[NNN^{q}]^{-}$, respectively. Five coordinated tantalum(V) complex $[(NNN^{cat})TaCl_2]$ C163 showed different kinds of reactivity involving one- and two-electron oxidation at the metal coordination sphere by the redox activity of ligand motif. Complex C163 underwent one-electron oxidation in the presence of 0.5 equivalent of iodobenzene dichloride ($PhICl_2$) afforded the redox-active ligated $[(NNN^{sq})TaCl_3]$ complex. Also, the same complex C163 showed two-electron oxidations by the reaction with organic azides (ArN_3) and diazoalkane (N_2CPh_2) to form tantalum imido species accommodating monoanionic pincer ligand form. This was the first example of a two-electron nitrene transfer from an organic azide to tantalum(V) complex C163 (Fig. 1.38) [252].

Zargarian group developed the nickel complexes having a phosphinite-amine pincer ligand framework (POCN). The $16e^-$ complexes (POCN) $Ni^{II}Br$ C164 (a–c) complexes with different amine substituted ligand like $NR_2 =$ 3-morpholine (a), NMe_2 (b), NEt_2 (c) gave $17e^-$ $(POCN)Ni^{III}Br_2$ C165 (a–c) complexes when treated with Br_2, N-bromosuccinimide or CBr_4. The non-innocent nature of ligand was observed in cyclic

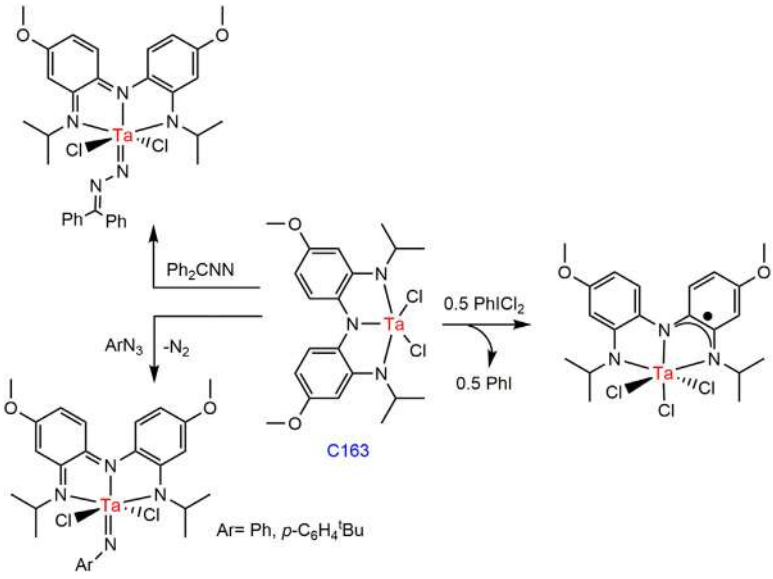

Figure 1.38 Reactions of Ta pincer complex with $PhICl_2$, ArN_3, and Ph_2CNN.

voltammogram studies where a clean irreversible one-electron oxidation at higher potential was observed. (POCN)$Ni^{III}Br_2$ C165 complexes also catalyzed the Kharasch anti-Markovnikov addition reaction of CCl_4 to olefin at 80°C affording up to 50 catalytic turnovers (Fig. 1.39) [253].

Heyduk et al. reported the catalytic nitrene transfer reactions from organic azides to tert-butyl isocyanide to form non-symmetrical carbodiimides with the aid of zirconium(IV) complex C166. The ligand dissociation of an isonitrile ligand from coordinatively saturated Zr complex C166 thus generated a vacant site for coordination of azide with the expulsion of N_2. The redox-active ligand is oxidized by two electrons to the quinone form, consistent with the formation of zirconium nitrogen multiple bonds. The later steps involved migratory insertion and reductive elimination that reduce the ligand with subsequent formation of the carbodiimide C = N bond. The reductive elimination is associated with no change of metal d-electron count, which again proved the role of redox non-innocence nature of the ligand. Adamantyl and tert-butyl azides proceeded with complete conversion into carbodiimide with the reaction of ^{t}BuNC in 10 h, using 10 mol% of the C166 catalyst loading (Fig. 1.40) [254].

Luca reported the redox-active bis(imino)pyridine Ni pincer complex C167 for catalytic hydrogen production. The NNN pincer ligand underwent one-electron reduction at low overpotential due to the presence of low-lying LUMO, which is easily reducible. The ligand reduced metal complex intermediate further underwent PCET yielded a Ni(II) hydride with a neutral ligand. The H_2 release step has involved the protonation of a Ni(II) hydride with water substitution to regenerate the catalyst. The exploration of reactivity of the redox-active ligand for such catalytic process tends to increase the hydrogen production with a rate of 105 s^{-1} (Fig. 1.41) [255].

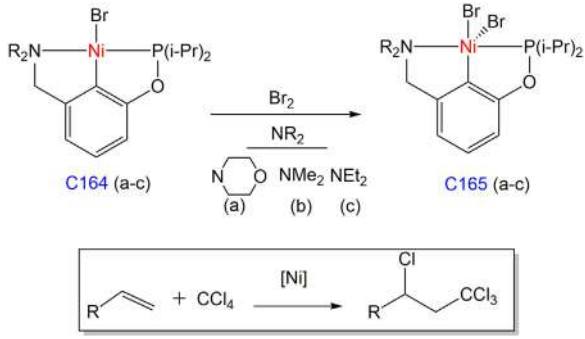

Figure 1.39 Kharasch addition reaction using Ni pincer complexes.

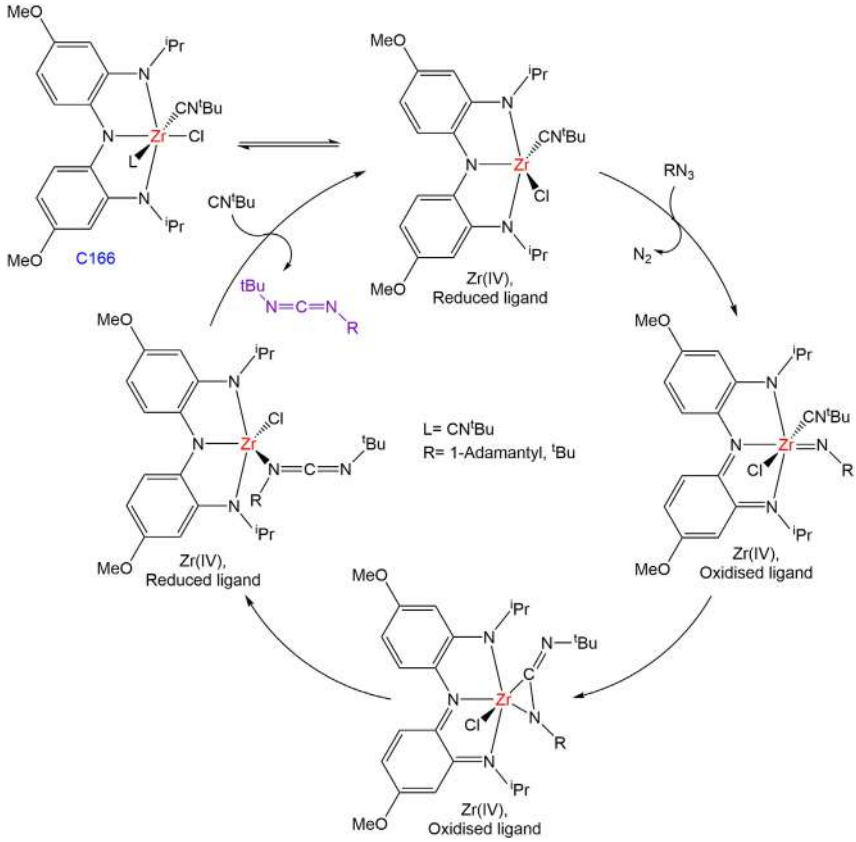

Figure 1.40 Redox active ligand participation in catalytic formation of carbodiimides from Isocyanides and organic azides.

Heyduk demonstrated the disulfide reductive elimination from an iron (III) dithiolate complex C168 coordinated with the monoanionic redox-active pincer ligand [ONO^{q}]. The monoanionic quinolate synthon of the ligand [ONO^{q}]K was treated with diamido iron(III) precursor FeCl[N(SiMe$_3$)$_2$]$_2$(THF) and afforded [ONO^{q}]Fe[N(SiMe$_3$)$_2$]$_2$ C168, which upon protonolysis with tert-butyl thiol and pyridine underwent two-electron reduction of ligand to result in the [ONO^{cat}]Fe(Py)$_3$ complex. This transformation witnessed the expulsion of ditertbutyldisulfide, which was confirmed by GC-MS and quantified to 81% yield with respect to the initial quantity of C168. The presence of a redox-active platform can influence the reductive elimination of disulfide without disturbing any changes to the metal oxidation state (Fig. 1.42) [256].

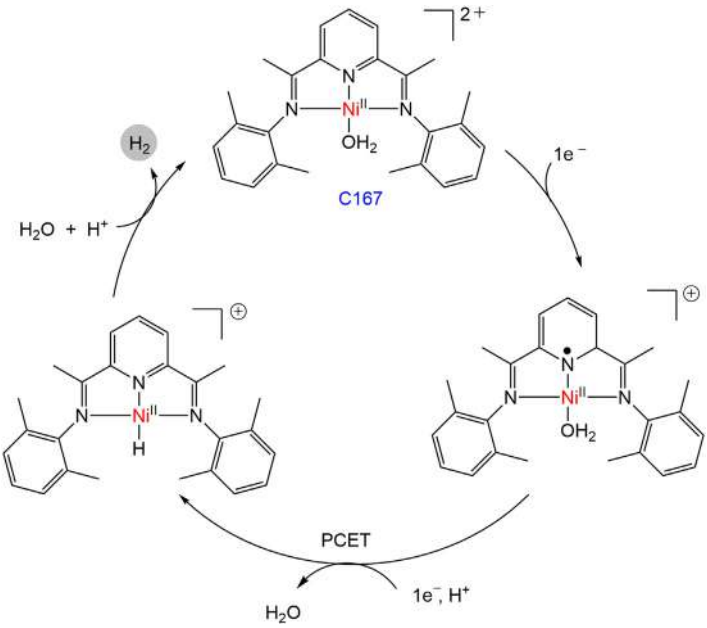

Figure 1.41 Proton reduction with a Ni bis-aryl-iminopyridine electrocatalyst.

Van der Vlugt group reported a redox-active aminophenol phosphine ligand (PNO^{H2}) ligated with Pd^{II} complex for the homolytic cleavage of S–S bond by releasing a thiyl(sulfanyl) radical. The complex generated two spin states of the ligand: dianionic PNO^{AP} (AP = amidophenolato) and monoanionic PNO^{ISQ} (ISQ = iminosemiquinoate). Air-sensitive diamagnetic Pd^{II} complex $[CoCp_2]$ $[PdCl(PNO^{AP})]$ C169 with addition to halide-abstracting agent $TlPF_6$ generated $Pd(PNO^{AP})$ complex C170, which underwent homolytic bond fission of diphenyldisulphide inducing the single-electron transfer from the fully reduced aminophenolate ligand to form metal-bound thiolate $Pd(PNO^{ISQ})$ complex C171. Both the complexes C170 and C171 bearing two different forms of ligand (PNO^{AP}) and (PNO^{ISQ}), respectively, were combined to produce monothiolate-bridged ligand-based mixed valent binuclear Pd^{II} complex C172 (Fig. 1.43) [257].

Van der Vlugt group also reported the intramolecular C–H amination of azides to form pyrrolidines derivatives using a Pd complex with redox-active $[NNO^{H2}]$ pincer ligand. The paramagnetic Pd^{II} complex C173 with coordination to monoanionic NNO^{ISQ} pincer ligand radical underwent one-electron oxidation in presence of cobaltocene to generate diamagnetic Pd^{II} complex C174 with coordination to dianionic NNO^{AP}

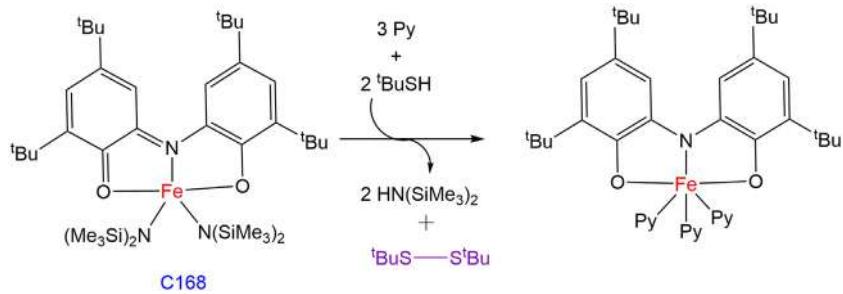

Figure 1.42 Redox-active ligand facilitated the reductive elimination of a disulfide from Fe(III).

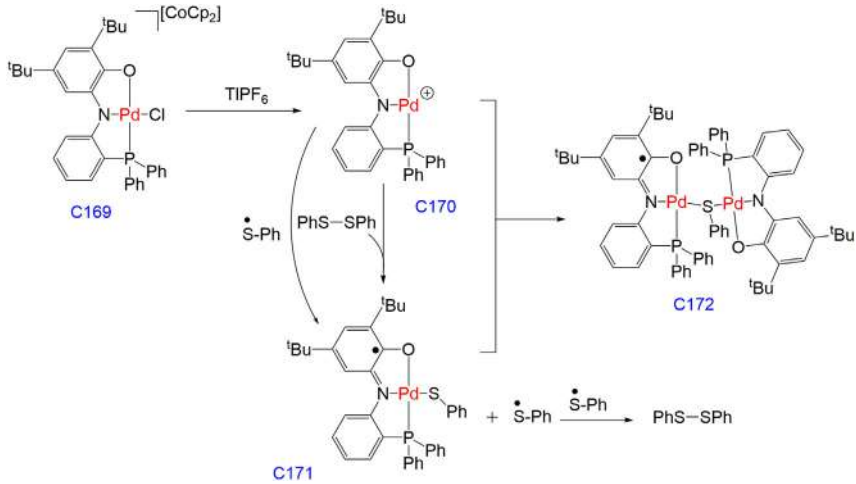

Figure 1.43 Formation of a μ-thiolato-bridged dinuclear Pd(II) complex bearing two redox-active PNO pincer ligands in two different oxidation states.

ligand, which thermally activated organic azide followed by the ligand to substrate electron transfer formed an unusual "nitrene-substrate radical, ligand-radical" Pd^{II} intermediate. The intermediate on subsequent hydrogen atom abstraction to generate a C-centered radical and rebound to make a C—N bond in presence of Boc_2O resulted in desired Boc-protected pyrrolidine with 10% of yield (Fig. 1.44) [258].

Later, the same group improved the catalytic yield by using a paramagnetic high spin $Fe^{III}(Cl)_2(NNO^{ISQ})$ complex C175 for the synthesis of N-heterocycles via direct $C(sp^3)$-H amination of a wide range of organic azides. This reaction condition afforded TON of 620 under the optimized catalytic conditions (Fig. 1.45) [259].

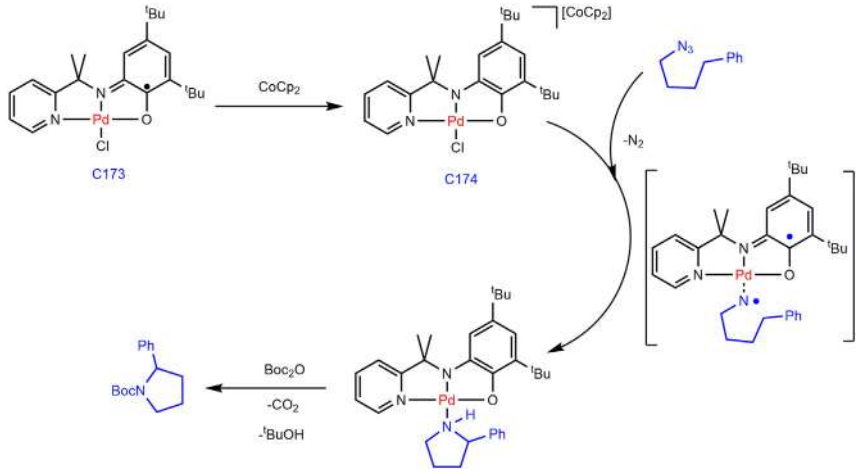

Figure 1.44 C–H amination of azide complex to pyrrolidine complex.

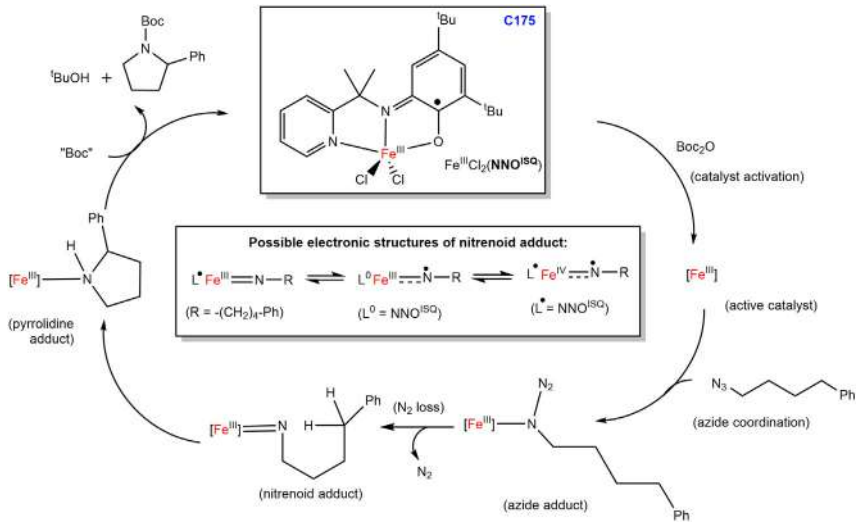

Figure 1.45 Postulated cycle for the C–H amination.

Paul group reported a catalytic substituted benzyl alcohol oxidation to corresponding carbonyl compounds mediated by the iron complex with a redox non-innocent azo-pincer ligand. The redox non-innocent azo aromatic ligand, 2-(arylazo)-1,10-phenanthroline (L^1), was employed in these studies, where the ligand was tridentate and having one easily reducible

azo moiety. The FeL^1Cl_2 complex C176 formed an azo anion radical active catalyst **I** after $1e^-$ reduction and followed by the addition of deprotonated alcohol formed intermediate **II**. A hydrogen atom abstraction from the α-carbon of the coordinated alcohol by the ligand generated an O-coordinated ketyl radical ion intermediate **III**. This is followed by rapid one-electron oxidation-afforded intermediate **IV** and the corresponding carbonyl compound. **IV** underwent alcohol coordination and proton abstraction by ligand-formed intermediate **V** and followed by aerial oxidation of **V**-formed azo chromophore **VI**, which underwent an intramolecular electron transfer in presence of the redox-active pincer ligand to regenerate the intermediate **II** (Fig. 1.46) [260].

Goswami group also reported the same reaction using Ru(II) complex C177 containing redox-active non-innocent ligand of 2,6-bis(phenylazo) pyridine and ancillary ligands. The benzyl alcohol was oxidized to benzaldehyde with 86% of the isolated yield. Complex C177 in presence of a base and alcoholic substrate formed a Ru alkoxide intermediate **I**, which afforded a Ru−H intermediate **II** upon the hydride migration with loss of the corresponding aldehyde. The Ru−H intermediate on subsequent H-walking from metal to redox-active ligand **III** and alcohol coordination followed by hydrogen migration from alcohol to the same redox-active ligand formed intermediate **IV**. The reaction is further assisted in the presence of O_2 to regenerate the catalyst via oxidation of hydrazo intermediate (Fig. 1.47) [261].

In 2019, Zhang, Mao and Dub group reported the V^{III} complex C178/C178-H featured with a redox non-innocent ligand, that is, π-radical monoanionic tpy species ($R\text{-tpy}^{\cdot-}$, R = CH_2SiMe_3), utilized for catalytic reduction of ketone, aldehyde, imine, ester, and carboxamide through hydroboration and/or hydrosilylation. Complex C178/C178-H mixture was employed for such chemoselective reduction, tolerated many functional groups, and yielded TONs and TOFs up to 1000 and $\sim 500\ h^{-1}$, respectively (Fig. 1.48) [262].

In 2020, Rosca et al. demonstrated the formation of a long carbon-carbon bond by bis(imino)pyrazine-supported iron complex. Synthesized pyrazine diimine ligand ($P^{Pz}DI$)-coordinated iron complex ($P^{Pz}DI$)Fe $(CO)_2$ in presence of mild methylating agent afforded the N-methylated complex C179, which showed one irreversible potential at −2.10 V in cyclic voltammetry study, hence thought to undergo easy ligand-based imine reduction. In addition of cobaltocene to a benzene suspension of N-methylated complex underwent an easy reduction at pyrazinium core

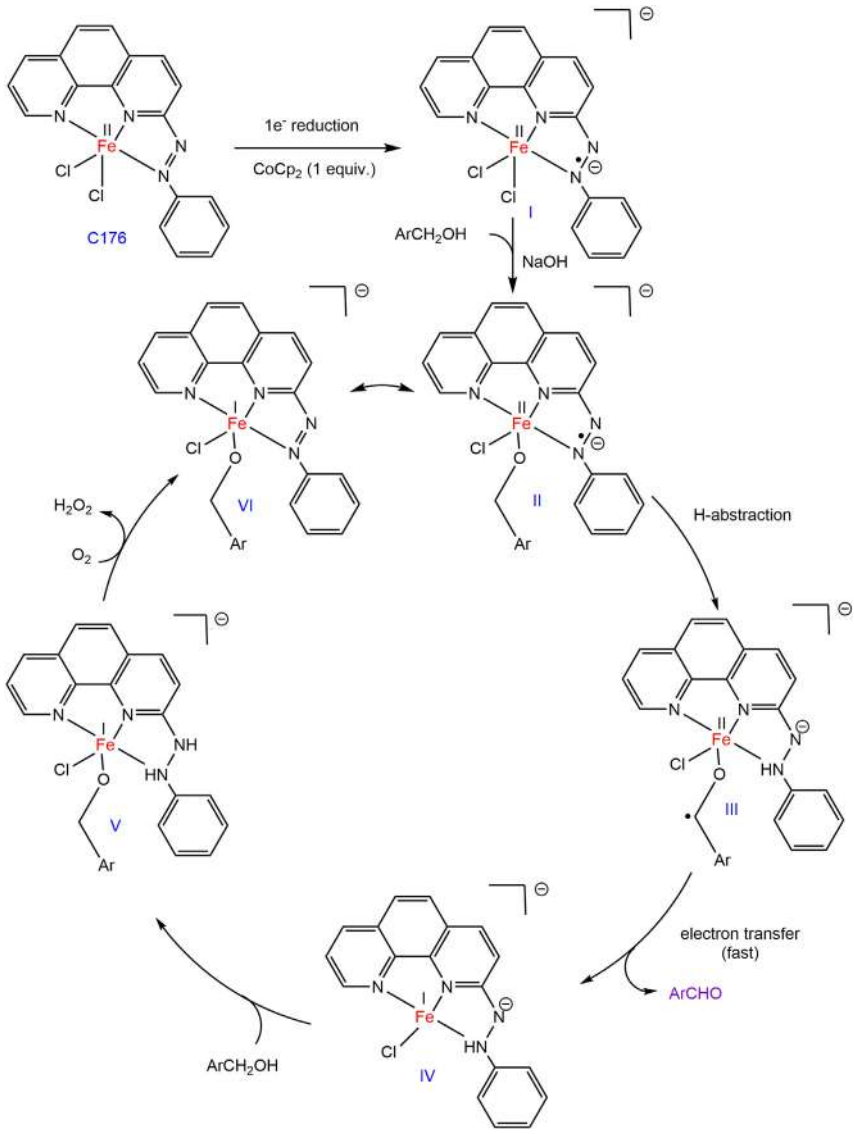

Figure 1.46 Mechanistic overview for the alcohol oxidation catalyzed by $[Fe(L_1)Cl_2]$.

to generate a radical at carbon atom α to the cationic N-atom, which immediately dimerize to form weak C—C bond. Further it can be cleaved under relatively mild oxidative conditions such as $Fc[PF_6]$ to regenerate parent N-methylated complex C179 (Fig. 1.49A) [263].

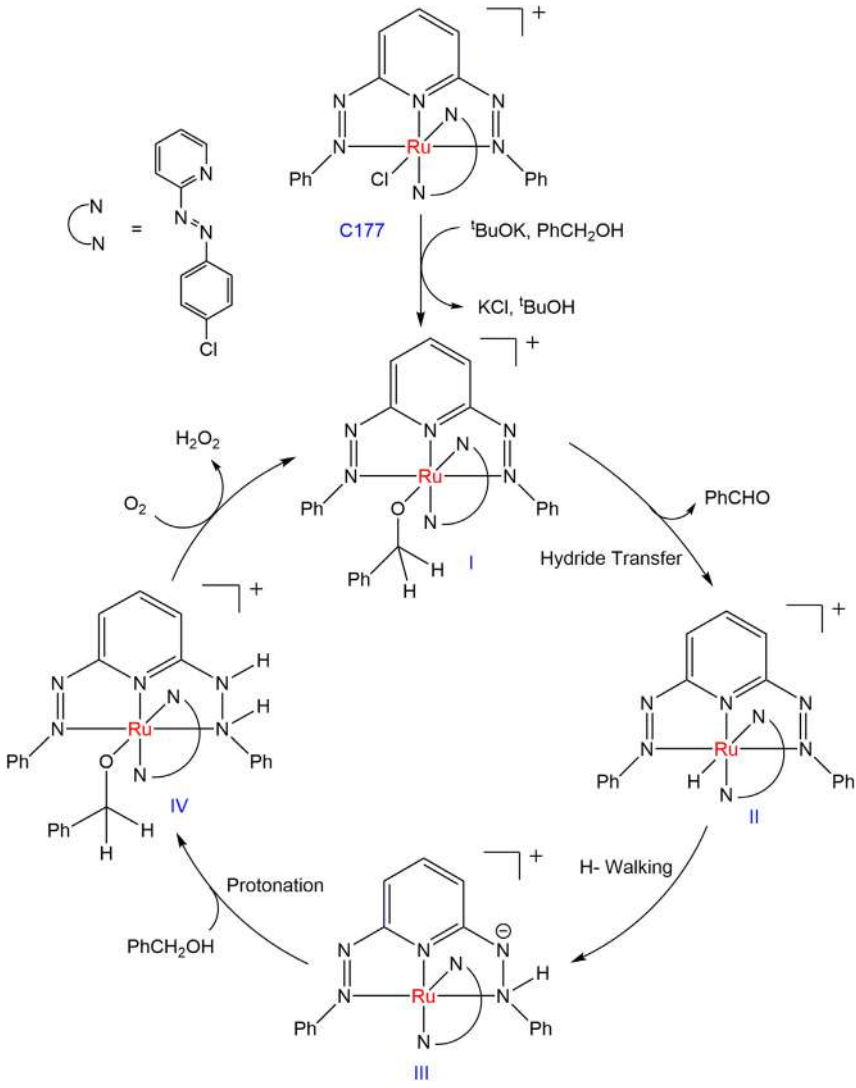

Figure 1.47 Mechanism for the alcohol oxidation reaction with catalyst C177.

More recently in 2020, Milstein group utilized the redox-active acridine-based PNP pincer ligand in coordination with inexpensive, earth-abundant base metals such as Fe (C180), Co, Ni, and Mn, which showed the irreversible C−C bond formation at the electrophilic C9 position of the acridine-based ligand containing radical using suitable redox reagent (Fig. 1.49B) [264].

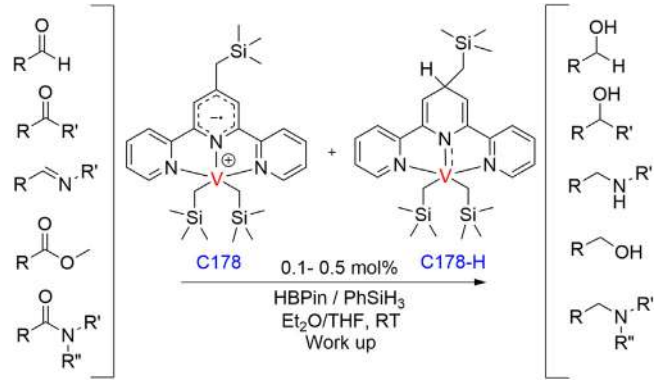

Figure 1.48 Representation of hydroboration/hydrosilylation of aldehydes/keytones, esters, imine, and carboxamides catalyzed by a C178/C178-H mixture.

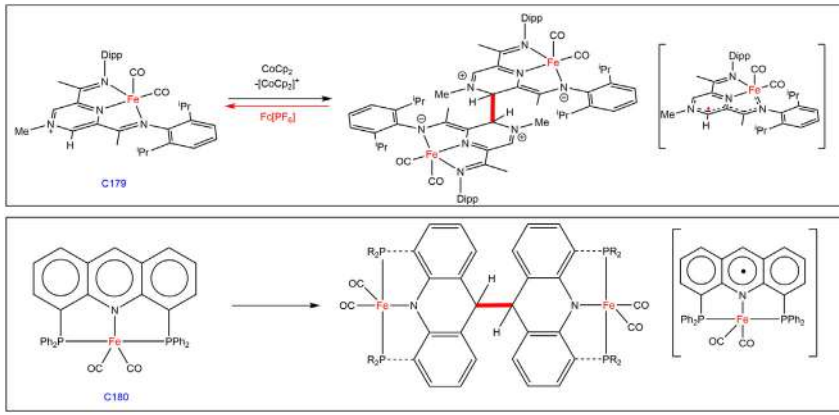

Figure 1.49 (A) Bis(imino)pyrazine supported iron complex to mediate C—C bond formation. (B) Redox-active pincer iron complex to mediate C—C bond formation.

1.7 Conclusion

The pincer system serves as a ligand and readily coordinated with various metal centers. The synthesized metal complexes are applied as catalysts in the different homogeneous catalytic processes where the value-added products are synthesized from the readily available organic substrates under sustainable and ambient reaction conditions. Many homogeneous catalysts are used for the various acceptorless dehydrogenation or dehydrogenative coupling reactions and in the hydrogenation or the transfer hydrogenation reaction in the organic synthesis. These systems are also applied in small

molecule activation and bond activation chemistry and employed them for the value-added product formation. This book chapter describes few important topics where the pincer complexes are directly used as catalysts efficiently. Dehydrogenation of aminoborane is applied as the hydrogen storage material and the pincer complexes are used as a catalyst for this process, which has a direct impact on the renewable energy harvesting process. The ammonia synthesis from the dinitrogen under the ambient condition is also one of the greatest challenges in the current time where pincer complexes play a significant role. The hydrogenation of the very stable and unreactive bonds like urea, carbamate, and direct methanol synthesis from them have a direct impact on the methanol economy, which is also considered as an alternative renewable fuel. The C−C coupling reaction forms various kinds of organic molecules used in the pharmaceuticals and drug industries where the Pd pincer complexes are used as a catalyst efficiently and achieve the high TON value. The redox-active pincer complexes open a new avenue in the organic synthesis where the interesting and sophisticated organic synthesis can be done under mild conditions. Although other challenges remain like water splitting to hydrogen synthesis, absolute atom economic reaction, degradation of polymers, or plastics, which have a direct impact on human society. The pincer complexes are currently used as catalysts for these kinds of challenging projects, and preliminary success is already achieved whereas more developments are required.

References

[1] M.A.W. Lawrence, K.A. Green, P.N. Nelson, S.C. Lorraine, Pincer ligands—tuneable, versatile and applicable, Polyhedron 143 (2018) 11−27.
[2] G. van Koten, Tuning the reactivity of metals held in a rigid ligand environment, Pure Appl. Chem. 61 (10) (1989) 1681−1694.
[3] C.J. Moulton, B.L. Shaw, Transition metal-carbon bonds. Part XLII. Complexes of nickel, palladium, platinum, rhodium, and iridium with the tridentate ligand 2,6-bis [(di-t-butylphosphino)methyl]phenyl, J. Chem. Soc. Dalton Trans. (11)(1976) 1020−1024.
[4] G. Bauer, X. Hu, Recent developments of iron pincer complexes for catalytic applications, Inorg. Chem. Front. 3 (6) (2016) 741−765.
[5] E. Peris, R.H. Crabtree, Key factors in pincer ligand design, Chem. Soc. Rev. 47 (6) (2018) 1959−1968.
[6] C. Gunanathan, D. Milstein, Bond activation, and catalysis by ruthenium pincer complexes, Chem. Rev. 114 (24) (2014) 12024−12087.
[7] T.J. Schmeier, G.E. Dobereiner, R.H. Crabtree, N. Hazari, Secondary coordination sphere interactions facilitate the insertion step in an iridium(III) CO_2 reduction catalyst, J. Am. Chem. Soc. 133 (24) (2011) 9274−9277.

[8] J.R. Khusnutdinova, D. Milstein, Metal–ligand cooperation, Angew. Chem. Int. (Ed.) 54 (42) (2015) 12236–12273.
[9] C.S. Slone, D.A. Weinberger, C.A. Mirkin, The transition metal coordination chemistry of hemilabile ligands, Prog. Inorg. Chem. 48 (2007) 233–350.
[10] C.K. Jørgensen, Differences between the four halide ligands, and discussion remarks on trigonal-bipyramidal complexes, on oxidation states, and on diagonal elements of one-electron energy, Coord. Chem. Rev. 1 (1–2) (1966) 164–178.
[11] M.E. O'Reilly, A.S. Veige, Trianionic pincer and pincer-type metal complexes and catalysts, Chem. Soc. Rev. 43 (17) (2014) 6325–6369.
[12] D. Morales-Morales, Pincer complexes: applications in catalysis, Rev. Soc. Quím. Méx. 48 (4) (2004) 338–346.
[13] M. van der Boom, D. Milstein, Cyclometalated phosphine-based pincer complexes: mechanistic insight in catalysis, coordination, and bond activation, Chem. Rev. 103 (5) (2003) 1759–1792.
[14] M. Albrecht, G. van Koten, Platinum group organometallics based on "pincer" complexes: sensors, switches, and catalysts. In memory of Prof. Dr. Luigi M. Venanzi and his pioneering work in organometallic chemistry, particularly in PCP pincer chemistry, Angew. Chem. Int. (Ed.) 40 (20) (2001) 3750–3781.
[15] G.A. Filonenko, R.V. Putten, E.J.M. Hensen, E.A. Pidko, Catalytic (de)hydrogenation promoted by non-precious metals—Co, Fe and Mn: recent advances in an emerging field, Chem. Soc. Rev. 47 (4) (2018) 1459–1483.
[16] J. Ito, H. Nishiyama, Recent topics of transfer hydrogenation, Tetrahedron Lett. 55 (20) (2014) 3153–3166.
[17] C. Gunanathan, D. Milstein, Applications of acceptorless dehydrogenation and related transformations in chemical synthesis, Science 341 (6143) (2013) 1229712.
[18] S. Waiba, B. Maji, Manganese catalyzed acceptorless dehydrogenative coupling reactions, ChemCatChem 12 (7) (2020) 1891–1902.
[19] A. Corma, J. Navas, M.J. Sabater, Advances in one-pot synthesis through borrowing hydrogen catalysis, Chem. Rev. 118 (4) (2018) 1410–1459.
[20] J. Choi, A.H.R. MacArthur, M. Brookhart, A.S. Goldman, Dehydrogenation and related reactions catalyzed by iridium pincer complexes, Chem. Rev. 111 (3) (2011) 1761–1779.
[21] R. Griessen, I.A.M.E. Giebels, B. Dam, Hydrogen functionalized materials, in: A. Züttel, A. Borgschulte, L. Schlapbach (Eds.), Hydrogen as a Future Energy Carrier, Wiley, Weinheim, Germany, 2008. Available from: https://doi.org/10.1002/9783527622894.
[22] C.C. Elam, C.E.G. Padró, G. Sandrock, A. Luzzi, P. Lindblad, E.F. Hagen, Realizing the hydrogen future: the International Energy Agency's efforts to advance hydrogen energy technologies, Int. J. Hydrog. Energy 28 (6) (2003) 601–607.
[23] S. Niaz, T. Manzoor, A.H. Pandith, Hydrogen storage: materials, methods and perspectives, Renew. Sust. Energ. Rev. 50 (2015) 457–469.
[24] U. Eberle, M. Felderhoff, F. Schüth, Chemical and physical solutions for hydrogen storage, Angew. Chem. Int. (Ed.) 48 (36) (2009) 6608–6630.
[25] R.H. Crabtree, Nitrogen-containing liquid organic hydrogen carriers: progress and prospects, ACS sustain, Chem. Eng. 5 (6) (2017) 4491–4498.
[26] E. Gianotti, M. Taillades-Jacquin, J. Rozière, D.J. Jones, High-purity hydrogen generation via dehydrogenation of organic carriers: a review on the catalytic process, ACS Catal. 8 (5) (2018) 4660–4680.
[27] F. Uhrig, J. Kadar, K. Müller, Reliability of liquid organic hydrogen carrier-based energy storage in a mobility application, Energy Sci. Eng. 8 (6) (2020) 2044–2053.
[28] C.W. Hamilton, R.T. Baker, A. Staubitz, I. Manners, B-N compounds for chemical hydrogen storage, Chem. Soc. Rev. 38 (1) (2009) 279–293.

[29] A. Staubitz, A.P.M. Robertson, M.E. Sloan, I. Manners, Amine- and phosphine-borane adducts: new interest in old molecules, Chem. Rev. 110 (7) (2010) 4023–4078.
[30] A. Staubitz, A.P.M. Robertson, I. Manners, Ammonia-borane and related compounds as dihydrogen sources, Chem. Rev. 110 (7) (2010) 4079–4124.
[31] D.H.A. Boom, A.R. Jupp, J.C. Slootweg, Dehydrogenation of amine–boranes using P-block compounds, Chem. Eur. J. 25 (39) (2019) 9133–9152.
[32] A. Rossin, M. Peruzzini, Ammonia-borane and amine-borane dehydrogenation mediated by complex metal hydrides, Chem. Rev. 116 (15) (2016) 8848–8872.
[33] H.C. Johnson, T.N. Hooper, A.S. Weller, The catalytic dehydrocoupling of amine–boranes and phosphine–boranes, Top. Organomet. Chem. 49 (2015) 153–220.
[34] X. Zhang, L. Kam, R. Trerise, T.J. Williams, Ruthenium-catalyzed ammonia borane dehydrogenation: mechanism and utility, Acc. Chem. Res. 50 (1) (2017) 86–95.
[35] D. Han, F. Anke, M. Trose, T. Beweries, Recent advances in transition metal catalysed dehydropolymerisation of amine boranes and phosphine boranes, Coord. Chem. Rev. 380 (2019) 260–286.
[36] S. Bhunya, T. Malakar, G. Ganguly, A. Paul, Combining protons and hydrides by homogeneous catalysis for controlling the release of hydrogen from ammonia-borane: present status and challenges, ACS Catal. 6 (11) (2016) 7907–7934.
[37] A.L. Colebatch, A.S. Weller, Amine-borane dehydropolymerization: challenges and opportunities, Chem. Eur. J. 25 (6) (2019) 1379–1390.
[38] M.C. Denney, V. Pons, T.J. Hebden, D.M. Heinekey, K.I. Goldberg, Efficient catalysis of ammonia borane dehydrogenation, J. Am. Chem. Soc. 128 (37) (2006) 12048–12049.
[39] A. Staubitz, M.E. Sloan, A.P.M. Robertson, A. Friedrich, S. Schneider, P.J. Gates, J. S. auf der Günne, I. Manners, Catalytic dehydrocoupling/dehydrogenation of N-methylamine-borane and ammonia-borane: synthesis and characterization of high molecular weight polyaminoboranes, J. Am. Chem. Soc. 132 (38) (2010) 13332–13345.
[40] M. Käss, A. Friedrich, M. Drees, S. Schneider, Ruthenium complexes with cooperative PNP ligands: bifunctional catalysts for the dehydrogenation of ammonia–borane, Angew. Chem. Int. (Ed.) 48 (5) (2009) 905–907.
[41] A.N. Marziale, A. Friedrich, I. Klopsch, M. Drees, V.R. Celinski, J.S. auf Der Günne, et al., The mechanism of borane-amine dehydrocoupling with bifunctional ruthenium catalysts, J. Am. Chem. Soc. 135 (36) (2013) 13342–13355.
[42] E.H. Kwan, H. Ogawa, M. Yamashita, A highly active PBP–iridium catalyst for the dehydrogenation of dimethylamine–borane: catalytic performance and mechanism, ChemCatChem 9 (13) (2017) 2457–2462.
[43] M.A. Esteruelas, P. Nolis, M. Oliván, E. Oñate, A. Vallribera, A. Vélez, Ammonia borane dehydrogenation promoted by a pincer-square-planar rhodium(I) monohydride: a stepwise hydrogen transfer from the substrate to the catalyst, Inorg. Chem. 55 (14) (2016) 7176–7181.
[44] E.A.K. Spearing-Ewyn, N.A. Beattie, A.L. Colebatch, A.J. Martinez-Martinez, A. Docker, T.M. Boyd, et al., The role of neutral Rh(PONOP)H, free NMe_2H, boronium and ammonium salts in the dehydrocoupling of dimethylamine-borane using the cationic pincer $[Rh(PONOP)(\eta^2\text{-}H_2)]^+$ catalyst, Dalton Trans. 48 (39) (2019) 14724–14736.
[45] A. Glüer, M. Förster, V.R. Celinski, J. Schmedt Auf Der Günne, M.C. Holthausen, S. Schneider, Highly active iron catalyst for ammonia borane dehydrocoupling at room temperature, ACS Catal. 5 (12) (2015) 7214–7217.
[46] P. Bhattacharya, J.A. Krause, H. Guan, Mechanistic studies of ammonia borane dehydrogenation catalyzed by iron pincer complexes, J. Am. Chem. Soc. 136 (31) (2014) 11153–11161.

[47] M.R. Elsby, K. Ghostine, U.K. Das, B.M. Gabidullin, R.T. Baker, Iron-SNS and -CNS complexes: selective C_{aryl}—S bond cleavage and amine-borane dehydrogenation catalysis, Organometallics 38 (19) (2019) 3844—3851.
[48] T.P. Lin, J.C. Peters, Boryl-mediated reversible H_2 activation at cobalt: catalytic hydrogenation, dehydrogenation, and transfer hydrogenation, J. Am. Chem. Soc. 135 (41) (2013) 15310—15313.
[49] T.M. Boyd, K.A. Andrea, K. Baston, A. Johnson, D.E. Ryana, A.S. Weller, A simple cobalt-based catalyst system for the controlled dehydropolymerisation of $H_3B \cdot NMeH_2$ on the gram-scale, Chem. Commun. 56 (3) (2020) 482—485.
[50] J.W. Nugent, M. G.-Melchor, A.R. Fout, Cobalt-catalyzed ammonia borane dehydrogenation: mechanistic insight and isolation of a cobalt hydride-amidoborane complex, Organometallics 39 (15) (2020) 2917—2927.
[51] H.P. Jia, E.A. Quadrelli, Mechanistic aspects of dinitrogen cleavage and hydrogenation to produce ammonia in catalysis and organometallic chemistry: relevance of metal hydride bonds and dihydrogen, Chem. Soc. Rev. 43 (2) (2014) 547—564.
[52] A.E. Shilov, Catalytic reduction of molecular nitrogen in solutions, Russ. Chem. Bull. 52 (2003) 2555—2562.
[53] J.N. Galloway, A.R. Townsend, J.W. Erisman, M. Bekunda, Z. Cai, J.R. Freney, et al., Transformation of the nitrogen cycle: recent trends, questions, and potential solutions, Science 320 (5878) (2008) 889—892.
[54] D. Fowler, M. Coyle, U. Skiba, M.A. Sutton, J.N. Cape, S. Reis, et al., The global nitrogen cycle in the twenty-first century, Philos. Trans. R. Soc. Lond. Biol. Sci. 368 (1621) (2013) 20130164.
[55] T. Kandemir, M.E. Schuster, A. Senyshyn, M. Behrens, R. Schlogl, The Haber-Bosch process revisited: on the real structure and stability of "ammonia iron" under working conditions, Angew. Chem. Int. (Ed.) 52 (48) (2013) 12723—12726.
[56] T.A. Bazhenova, A.E. Shilov, Nitrogen-fixation in solution, Coord. Chem. Rev. 144 (1995) 69—145.
[57] K. Shiina, Reductive silylation of molecular nitrogen via fixation totris(trialkylsilyl) amine, J. Am. Chem. Soc. 94 (26) (1972) 9266—9267.
[58] K. Komori, H. Oshita, Y. Mizobe, M. Hidai, Catalytic conversion of molecular nitrogen into silylamines using molybdenum and tungsten dinitrogen complexes, J. Am. Chem. Soc. 111 (5) (1989) 1939—1940.
[59] K. Komori, S. Sugiura, Y. Mizobe, M. Yamada, M. Hidai, Syntheses and some reactions of trimethylsilylated dinitrogen complexes of tungsten and molybdenum, Bull. Chem. Soc. Jpn. 62 (9) (1989) 2953—2959.
[60] H. Oshita, Y. Mizobe, M. Hidai, Preparation and properties of molybdenum and tungsten dinitrogen complexes XLI: silylation and germylation of a coordinated dinitrogen in cis-$[M(N_2)_2(PMe_2Ph)_4]$ (M = Mo, W) usingR_3ECl/NaI and R_3ECl/Na mixtures (E = Si, Ge). X-ray structure of trans-$WI[(NNGePh_3)(PMe_2Ph)_4].C_6H_6$, J. Organomet. Chem. 456 (2) (1993) 213—220.
[61] M. Mori, Activation of nitrogen for organic synthesis, J. Organomet. Chem. 689 (24) (2004) 4210—4227.
[62] S. Kim, F. Loose, P.J. Chirik, Beyond ammonia: nitrogen − element bond forming reactions with coordinated dinitrogen, Chem. Rev. 120 (12) (2020) 5637—5681.
[63] M.J. Chalkley, M.W. Drover, J.C. Peters, Catalytic N_2-to-NH_3 (or -N_2H_4) conversion by well-defined molecular coordination complexes, Chem. Rev. 120 (12) (2020) 5582—5636.
[64] Y. Tanabe, Y. Nishibayashi, Recent advances in catalytic silylation of dinitrogen using transition metal complexes, Coord. Chem. Rev. 389 (2019) 73—93.
[65] J.L. Crossland, D.R. Tyler, Iron-dinitrogen coordination chemistry: dinitrogen activation and reactivity, Coord. Chem. Rev. 254 (2010) 1883—1894.

[66] S. Kuriyama, Y. Nishibayashi, Catalytic transformations of molecular dinitrogen by iron and cobalt-dinitrogen complexes as catalysts, Top. Organomet. Chem. 60 (2017) 215–234.
[67] K.C. MacLeod, P.L. Holland, Recent developments in the homogeneous reduction of dinitrogen by molybdenum and iron, Nat. Chem. 5 (7) (2013) 559–565.
[68] S. Hinrichsen, H. Broda, C. Gradert, L. Söncksen, F. Tuczek, Recent developments in synthetic nitrogen fixation, Annu. Rep. Prog. Chem., Sect. A: Inorg. Chem. 108 (2012) 17–47.
[69] I. Klopsch, E.Y. Yuzik-Klimova, S. Schneider, Functionalization of N_2 by mid to late transition metals via N − N bond cleavage, Top. Organomet. Chem. 60 (2017) 71–112.
[70] M.D. Fryzuk, S.A. Johnson, The continuing story of dinitrogen activation, Coord. Chem. Rev. 200 − 202 (2000) 379–409.
[71] D.V. Yandulov, R.R. Schrock, Catalytic reduction of dinitrogen to ammonia at a single molybdenum center, Science 301 (5629) (2003) 76–78.
[72] K. Arashiba, Y. Miyake, Y. Nishibayashi, A molybdenum complex bearing PNP-type pincer ligands leads to the catalytic reduction of dinitrogen into ammonia, Nat. Chem. 3 (2) (2011) 120–125.
[73] E. Kinoshita, K. Arashiba, S. Kuriyama, Y. Miyake, R. Shimazaki, H. Nakanishi, et al., Synthesis and catalytic activity of molybdenum − dinitrogen complexes bearing unsymmetric PNP-type pincer ligands, Organometallics 31 (23) (2012) 8437–8443.
[74] K. Arashiba, K. Sasaki, S. Kuriyama, Y. Miyake, H. Nakanishi, Y. Nishibayashi, Synthesis and protonation of molybdenum- and tungsten-dinitrogen complexes bearing PNP-type pincer ligands, Organometallics 31 (5) (2012) 2035–2041.
[75] K. Arashiba, K. Nakajima, Y. Nishibayashi, Synthesis and reactivity of molybdenum-dinitrogen complexes bearing PNN-type pincer ligand, Z. Anorg. Allg. Chem. 641 (1) (2015) 100–104.
[76] S. Kuriyama, K. Arashiba, K. Nakajima, H. Tanaka, N. Kamaru, K. Yoshizawa, et al., Catalytic formation of ammonia from molecular dinitrogen by use of dinitrogen-bridged dimolybdenum − dinitrogen complexes bearing PNP-pincer ligands: remarkable effect of substituent at PNP-pincer ligand, J. Am. Chem. Soc. 136 (27) (2014) 9719–9731.
[77] S. Kuriyama, K. Arashiba, K. Nakajima, H. Tanaka, K. Yoshizawa, Y. Nishibayashi, Nitrogen fixation catalyzed by ferrocene substituted dinitrogen-bridged dimolybdenum–dinitrogen complexes: unique behavior of ferrocene moiety as redox active site, Chem. Sci. 6 (7) (2015) 3940–3951.
[78] Y. Tanabe, S. Kuriyama, K. Arashiba, Y. Miyake, K. Nakajima, Y. Nishibayashi, Preparation and reactivity of molybdenum–dinitrogen complexes bearing an arsenic-containing ANA-type pincer ligand, Chem. Commun. 49 (81) (2013) 9290–9292.
[79] K. Arashiba, E. Kinoshita, S. Kuriyama, A. Eizawa, K. Nakajima, H. Tanaka, et al., Catalytic reduction of dinitrogen to ammonia by use of molybdenum-nitride complexes bearing a tridentate triphosphine as catalysts, J. Am. Chem. Soc. 137 (17) (2015) 5666–5669.
[80] T.J. Hebden, R.R. Schrock, M.K. Takase, P. Müller, Cleavage of dinitrogen to yield a (t-BuPOCOP)molybdenum(iv) nitride, Chem. Commun. 48 (13) (2012) 1851–1853.
[81] K. Arashiba, A. Eizawa, H. Tanaka, K. Nakajima, K. Yoshizawa, Y. Nishibayashi, Catalytic nitrogen fixation via direct cleavage of nitrogen–nitrogen triple bond of molecular dinitrogen under ambient reaction conditions, Bull. Chem. Soc. Jpn. 90 (10) (2017) 1111–1118.
[82] A. Eizawa, K. Arashiba, H. Tanaka, S. Kuriyama, Y. Matsuo, K. Nakajima, et al., Remarkable catalytic activity of dinitrogen-bridged dimolybdenum complexes

bearing NHC-based PCP-pincer ligands toward nitrogen fixation, Nat. Commun. 8 (14874) (2017).
[83] A. Eizawa, K. Arashiba, A. Egi, H. Tanaka, K. Nakajima, K. Yoshizawa, et al., Catalytic reactivity of molybdenum—trihalide complexes bearing PCP-type pincer ligands, Chem. Asian J. 14 (12) (2019) 2091—2096.
[84] T. Itabashi, I. Mori, K. Arashiba, A. Eizawa, K. Nakajima, Y. Nishibayashi, Effect of substituents on molybdenum triiodide complexes bearing PNP-type pincer ligands toward catalytic nitrogen fixation, Dalton Trans. 48 (10) (2019) 3182—3186.
[85] T. Itabashi, K. Arashiba, H. Tanaka, A. Konomi, A. Eizawa, K. Nakajima, et al., Synthesis and catalytic reactivity of bis(molybdenum-trihalide) complexes bridged by ferrocene skeleton toward catalytic nitrogen fixation, Organometallics 38 (14) (2019) 2863—2872.
[86] N. Stucke, J. Krahmer, C. Näther, F. Tuczek, Molybdenum complexes supported by PN^3P pincer ligands: synthesis, characterization and application to synthetic nitrogen fixation, Eur, J. Inorg. Chem. 47 (2018) 5108—5116.
[87] Y. Tanabe, K. Arashiba, K. Nakajima, Y. Nishibayashi, Catalytic conversion of dinitrogen into ammonia under ambient reaction conditions by using proton source from water, Chem. Asian J. 12 (19) (2017) 2544—2548.
[88] Y. Ashida, K. Arashiba, K. Nakajima, Y. Nishibayashi, Molybdenum-catalysed ammonia production with samarium diiodide and alcohols or water, Nature 568 (7753) (2019) 536—540.
[89] Y. Tanabe, Y. Sekiguchi, H. Tanaka, A. Konomi, K. Yoshizawa, S. Kuriyama, et al., Preparation and reactivity of molybdenum complexes bearing pyrrole-based PNP-type pincer ligand, Chem. Commun. 56 (51) (2020) 6933—6936.
[90] S. Kuriyama, K. Arashiba, K. Nakajima, Y. Matsuo, H. Tanaka, K. Ishii, et al., Catalytic transformation of dinitrogen into ammonia and hydrazine by iron-dinitrogen complexes bearing pincer ligand, Nat. Commun. 7 (12181) (2016).
[91] Y. Sekiguchi, S. Kuriyama, A. Eizawa, K. Arashiba, K. Nakajima, Y. Nishibayashi, Synthesis and reactivity of iron − dinitrogen complexes bearing anionic methyl- and phenyl-substituted pyrrole-based PNP-type pincer ligands toward catalytic nitrogen fixation, Chem. Commun. 53 (88) (2017) 12040—12043.
[92] J. Higuchi, S. Kuriyama, A. Eizawa, K. Arashiba, K. Nakajima, Y. Nishibayashi, Preparation and reactivity of iron complexes bearing anionic carbazole-based PNP-type pincer ligands toward catalytic nitrogen fixation, Dalton Trans. 47 (4) (2018) 1117—1121.
[93] S. Kuriyama, K. Arashiba, H. Tanaka, Y. Matsuo, K. Nakajima, K. Yoshizawa, et al., Direct transformation of molecular dinitrogen into ammonia catalyzed by cobalt dinitrogen complexes bearing anionic PNP pincer ligands, Angew. Chem. Int. (Ed.) 55 (46) (2016) 14291—14295.
[94] I. Vidyaratne, J. Scott, S. Gambarotta, P.H.M. Budzelaar, Dinitrogen activation, partial reduction, and formation of coordinated imide promoted by a chromium diiminepyridine complex, Inorg. Chem. 46 (17) (2007) 7040—7049.
[95] Y. Sekiguchi, K. Arashiba, H. Tanaka, A. Eizawa, K. Nakajima, K. Yoshizawa, et al., Catalytic reduction of molecular dinitrogen to ammonia and hydrazine using vanadium complexes, Angew. Chem. Int. (Ed.) 57 (29) (2018) 9064—9068.
[96] Y. Sekiguchi, F. Meng, H. Tanaka, A. Eizawa, K. Arashiba, K. Nakajima, et al., Synthesis and reactivity of titanium- and zirconium-dinitrogen complexes bearing anionic pyrrole-based PNP-type pincer ligands, Dalton Trans. 47 (33) (2018) 11322—11326.
[97] B. Wang, G. Luo, M. Nishiura, A. Hu, T. Shima, Y. Luo, et al., Dinitrogen activation by dihydrogen and a PNP ligated titanium complex, J. Am. Chem. Soc. 139 (5) (2017) 1818—1821.

[98] I. Klopsch, M. Finger, C. Würtele, B. Milde, D. Werz, S. Schneider, Dinitrogen splitting and functionalization in the coordination sphere of rhenium, J. Am. Chem. Soc. 136 (19) (2014) 6881–6883.
[99] I. Klopsch, M. Kinauer, M. Finger, C. Würtele, S. Schneider, Conversion of dinitrogen into acetonitrile under ambient conditions, Angew. Chem. Int. (Ed.) 55 (15) (2016) 4786–4789.
[100] F. Schendzielorz, M. Finger, J. Abbenseth, C. Würtele, V. Krewald, S. Schneider, Metal-ligand cooperative synthesis of benzonitrile by electrochemical reduction and photolytic splitting of dinitrogen, Angew. Chem. Int. (Ed.) 58 (3) (2019) 830–834.
[101] Q.J. Bruch, G.P. Connor, C. Chen, P.L. Holland, J.M. Mayer, F. Hasanayn, et al., Dinitrogen reduction to ammonia at rhenium utilizing light and proton-coupled electron transfer, J. Am. Chem. Soc. 141 (51) (2019) 20198–20208.
[102] Q. Liao, N. Saffon-Merceron, N. Mezailles, N2 reduction into silylamine at tridentate phosphine/Mo center: catalysis and mechanistic study, ACS Catal. 5 (11) (2015) 6902–6906.
[103] A. Cavaillé, B. Joyeux, N. Saffon-Merceron, N. Nebra, M. Fustier-Boutignon, N. Mézailles, Triphos – Fe dinitrogen and dinitrogen – hydride complexes: relevance to catalytic N2 reductions, Chem. Commun. 54 (84) (2018) 11953–11956.
[104] R. Imayoshi, K. Nakajima, J. Takaya, N. Iwasawa, Y. Nishibayashi, Synthesis and reactivity of iron- and cobalt-dinitrogen complexes bearing PSiP-type pincer ligands toward nitrogen fixation, Eur. J. Inorg. Chem. 2017 (32) (2017) 3769–3778.
[105] R. Kawakami, S. Kuriyama, H. Tanaka, K. Arashiba, A. Konomi, K. Nakajima, et al., Catalytic reduction of dinitrogen to tris(trimethylsilyl)amine using rhodium complexes with a pyrrole-based PNP-type pincer ligand, Chem. Commun. 55 (99) (2019) 14886–14889.
[106] S. Li, Y. Wang, W. Yang, K. Li, H. Sun, X. Li, et al., N_2 silylation catalyzed by a bis(silylene)-based [SiCSi] pincer hydrido iron(II) dinitrogen complex, Organometallics 39 (5) (2020) 757–766.
[107] J. Zhang, G. Leitus, Y. Ben-David, D. Milstein, Efficient homogeneous catalytic hydrogenation of esters to alcohols, Angew. Chem. Int. (Ed.) Engl. 45 (7) (2006) 1113–1115.
[108] E.M. Krall, T.W. Klein, R.J. Andersen, A.J. Nett, R.W. Glasgow, D.S. Reader, et al., Controlled hydrogenative depolymerization of polyesters and polycarbonates catalyzed by ruthenium(II) PNN pincer complexes, Chem. Commun. 50 (38) (2014) 4884–4887.
[109] Y. Sun, C. Koehler, R. Tan, V.T. Annibale, D. Song, Esterhydrogenation catalyzed by Ru-CNN pincer complexes, Chem. Commun. 47 (49) (2011) 8349–8351.
[110] E. Fogler, E. Balaraman, Y. Ben-David, G. Leitus, L.J.W. Shimon, D. Milstein, New CNN-type ruthenium pincer NHC complexes. Mild, efficient catalytic hydrogenation of esters, Organometallics 30 (14) (2011) 3826–3833.
[111] E. Balaraman, E. Fogler, D. Milstein, Efficient hydrogenation of biomass-derived cyclic di-esters to 1,2-diols, Chem. Commun. 48 (8) (2012) 1111–1113.
[112] W. Kuriyama, T. Matsumoto, O. Ogata, Y. Ino, K. Aoki, S. Tanaka, et al., Catalytic hydrogenation of esters. development of an efficient catalyst and processes for synthesising (R)-1,2-propanediol and 2-(l-menthoxy)ethanol, Org. Process. Res. Dev. 16 (1) (2012) 166–171.
[113] K. Junge, B. Wendt, H. Jiao, M. Beller, Iridium-catalyzed hydrogenation of carboxylic acid esters, ChemCatChem 6 (10) (2014) 2810–2814.
[114] T. Zell, Y. Ben-David, D. Milstein, Unprecedented iron-catalyzed ester hydrogenation. Mild, selective, and efficient hydrogenation of trifluoroacetic esters to alcohols catalyzed by an iron pincer complex, Angew. Chem. 126 (18) (2014) 4773–4777.

[115] S. Werkmeister, K. Junge, B. Wendt, E. Alberico, H. Jiao, W. Baumann, et al., Hydrogenation of esters to alcohols with a well-defined iron complex, Angew. Chem. Int. (Ed.) 53 (33) (2014) 8722–8726.
[116] S. Chakraborty, H. Dai, P. Bhattacharya, N.T. Fairweather, M.S. Gibson, J.A. Krause, et al., Iron-based catalysts for the hydrogenation of esters to alcohols, J. Am. Chem. Soc. 136 (22) (2014) 7869–7872.
[117] S. Elangovan, B. Wendt, C. Topf, S. Bachmann, M. Scalone, A. Spannenberg, et al., Improved second generation iron pincer complexes for effective ester hydrogenation, Adv. Synt. Catal. 358 (5) (2016) 820–825.
[118] D. Srimani, A. Mukherjee, A.F.G. Goldberg, G. Leitus, Y. Diskin-Posner, L.J.W. Shimon, et al., Cobalt catalyzed hydrogenation of esters to alcohols. Unexpected reactivity trend indicates ester enolate intermediacy, Angew. Chem. Int. (Ed.) 54 (42) (2015). 12537-12360.
[119] J. Yuwen, S. Chakraborty, W.W. Brennessel, W.D. Jones, Additive free cobalt catalyzed hydrogenation of esters to alcohols, ACS Catal. 7 (5) (2017) 3735–3740.
[120] S. Elangovan, M. Garbe, H. Jiao, A. Spannenberg, K. Junge, M. Beller, Hydrogenation of esters to alcohols catalyzed by defined manganese pincer complexes, Angew. Chem. Int. (Ed.) 55 (49) (2016) 15364–15368.
[121] N.A. Espinosa-Jalapa, A. Nerush, L.J.W. Shimon, G. Leitus, L. Avram, Y. Ben-David, et al., Manganese catalyzed hydrogenation of esters to alcohols, Chem. Eur. J. 23 (25) (2017) 5934–5938.
[122] E. Balaraman, B. Gnanaprakasam, L.J.W. Shimon, D. Milstein, Direct hydrogenation of amides to alcohols and amines under mild conditions, J. Am. Chem. Soc. 132 (47) (2010) 16756–16758.
[123] S. Kar, M. Rauch, A. Kumar, G. Leitus, Y. Ben-David, D. Milstein, Selective room-temperature hydrogenation of amides to amines and alcohols catalyzed by a ruthenium pincer complex and mechanistic insight, ACS Catal. 10 (10) (2020) 5511–5515.
[124] J.R. Cabrero-Antonino, E. Alberico, H.-J. Drexler, W. Baumann, K. Junge, H. Junge, et al., Efficient base free hydrogenation of amides to alcohols and amines catalyzed by well defined pincer imidazolyl ruthenium complexes, ACS Catal. 6 (1) (2016) 47–54.
[125] F. Schneck, M. Assmann, M. Balmer, K. Harms, R. Langer, Selective hydrogenation of amides to amines and alcohols catalyzed by improved iron pincer complexes, Organometallics 35 (11) (2016) 1931–1943.
[126] J.A. Garg, S. Chakraborty, Y. Ben-David, D. Milstein, Unprecedented iron-catalyzed selective hydrogenation of activated amides to amines and alcohols, Chem. Commun. 52 (30) (2016) 5285–5288.
[127] U. Jayarathne, Y. Zhang, N. Hazari, W.H. Bernskoetter, Selective iron catalyzed deaminative hydrogenation of amides, Organometallics 36 (2) (2017) 409–416.
[128] V. Papa, J.R. Cabrero-Antonino, E. Alberico, A. Spanneberg, K. Junge, H. Junge, et al., Efficient and selective hydrogenation of amides to alcohols and amines using a well-defined manganese − PNN pincer complex, Chem. Sci. 8 (5) (2017) 3576–3585.
[129] M.L. Yuan, J.-H. Xie, S.F. Zhu, Q.L. Zhou, Deoxygenative hydrogenation of amides catalyzed by a well-defined iridium pincer complex, ACS Catal. 6 (6) (2016) 3665–3669.
[130] Y.Q. Zou, S. Chakraborty, A. Nerush, D. Oren, Y. Diskin-Posner, Y. Ben-David, et al., Highly selective, efficient deoxygenative hydrogenation of amides catalyzed by a manganese pincer complex via metal-ligand cooperation, ACS Catal. 8 (9) (2018) 8014–8019.
[131] E. Balaraman, Y. Ben-David, D. Milstein, Unprecedented catalytic hydrogenation of urea derivatives to amines and methanol, Angew. Chem. Int. (Ed.) 50 (49) (2011) 11702–11705.

[132] Y. Xie, P. Hu, Y. Ben-David, D. Milstein, A. Reversible, Liquid organic hydrogen carrier system based on methanol-ethylenediamine and ethylene urea, Angew. Chem. Int. (Ed.) 58 (15) (2019) 5105–5109.
[133] E. Balaraman, C. Gunanathan, J. Zhang, L.J.W. Shimon, D. Milstein, Efficient hydrogenation of organic carbonates, carbamates and formates indicates alternative routes to methanol based on CO_2 and CO, Nat. Chem. 3 (8) (2011) 609–614.
[134] Z. Han, L. Rong, J. Wu, L. Zhang, Z. Wang, K. Ding, Catalytic hydrogenation of cyclic carbonates: a practical approach from CO_2 and epoxides to methanol and diols, Angew. Chem. Int. (Ed.) 51 (52) (2012) 13041–13045.
[135] A. Kumar, T. Janes, N.A. Espinosa-Jalapa, D. Milstein, Manganese catalyzed hydrogenation of organic carbonates to methanol and alcohols, Angew. Chem. Int. (Ed.) 57 (37) (2018) 12076–12080.
[136] A. Kaithal, M. Hölscher, W. Leitner, Catalytic hydrogenation of cyclic carbonates using manganese complexes, Angew. Chem. 130 (41) (2018) 13637–13641.
[137] V. Zubar, Y. Lebedev, L.M. Azofra, L. Cavallo, O. El-Sepelgy, M. Rueping, Hydrogenation of CO_2 derived carbonates and polycarbonates to methanol and diols by metal – ligand cooperative manganese catalysis, Angew. Chem. Int. (Ed.) 57 (41) (2018) 13439–13443.
[138] U.K. Das, A. Kumar, Y. Ben-David, M.A. Iron, D. Milstein, Manganese catalyzed hydrogenation of carbamates and urea derivatives, J. Am. Chem. Soc. 141 (33) (2019) 12962–12966.
[139] A. Kumar, T. Janes, N.A. Espinosa-Jalapa, D. Milstein, Selective hydrogenation of cyclic imides to diols and amines and its application in the development of a liquid organic hydrogen carrier, J. Am. Chem. Soc. 140 (24) (2018) 7453–7457.
[140] U.K. Das, T. Janes, A. Kumar, D. Milstein, Manganese catalyzed selective hydrogenation of cyclic imides to diols and amines, Green. Chem. 22 (10) (2020) 3079–3082.
[141] D. Srimani, M. Feller, Y. Ben David, D. Milstein, Catalytic coupling of nitriles with amines to selectively form imines under mild hydrogen pressure, Chem. Commun. 48 (97) (2012) 11853–11855.
[142] J.-H. Choi, M.H.G. Prechtl, Tuneable hydrogenation of nitriles into imines or amines with a ruthenium pincer complex under mild conditions, ChemCatChem 7 (6) (2015) 1023–1028.
[143] S. Chakraborty, D. Milstein, Selective hydrogenation of nitriles to secondary imines catalyzed by an iron pincer complex, ACS Catal. 7 (6) (2017) 3968–3972.
[144] S. Chakraborty, G. Leitus, D. Milstein, Iron-catalyzed mild and selective hydrogenative cross-coupling of nitriles and amines to form secondary aldimines, Angew. Chem. Int. (Ed.) 56 (8) (2017) 2074–2078.
[145] C. Gunanathan, M. Hölscher, W. Leitner, Reduction of nitriles to amines with H2 catalyzed by nonclassical ruthenium hydrides—water-promoted selectivity for primary amines and mechanistic investigations, Eur. J. Inorg. Chem. (22)(2011) 3381–3386.
[146] R. Adam, E. Alberico, W. Baumann, H.J. Drexler, R. Jackstell, H. Junge, et al., NNP-type pincer imidazolylphosphine ruthenium complexes: efficient base-free hydrogenation of aromatic and aliphatic nitriles under mild conditions, Chem. Eur. J. 22 (14) (2016) 4991–5002.
[147] A. Mukherjee, D. Srimani, Y. Ben-David, D. Milstein, Low-pressure hydrogenation of nitriles to primary amines catalyzed by ruthenium pincer complexes. Scope and mechanism, Chem. Cat. Chem. 9 (4) (2017) 559–563.
[148] C. Bornschein, S. Werkmeister, B. Wendt, H. Jiao, E. Alberico, W. Baumann, et al., Mild and selective hydrogenation of aromatic and aliphatic (di)nitriles with a well-defined iron pincer complex, Nat. Commun. 5 (2014) 4111.

[149] A. Mukherjee, D. Srimani, S. Chakraborty, Y. Ben-David, D. Milstein, Selective hydrogenation of nitriles to primary amines catalyzed by a cobalt pincer complex, J. Am. Chem. Soc. 137 (28) (2015) 8888–8891.
[150] S. Elangovan, C. Topf, S. Fischer, H. Jiao, A. Spannenberg, W. Baumann, et al., Selective catalytic hydrogenations of nitriles, ketones, and aldehydes by well-defined manganese pincer complexes, J. Am. Chem. Soc. 138 (28) (2016) 8809–8814.
[151] R.P. Yu, J.M. Darmon, J.M. Hoyt, G.W. Margulieux, Z.R. Turner, P.J. Chirik, High-activity iron catalysts for the hydrogenation of hindered, unfunctionalized alkenes, ACS Catal. 2 (8) (2012) 1760–1764.
[152] D. Srimani, Y. Diskin-Posner, Y. Ben-David, D. Milstein, Iron pincer complex catalyzed, environmentally benign, E-selective semi-hydrogenation of alkynes, Angew. Chem. Int. (Ed.) 52 (52) (2013) 14131–14134.
[153] J. Tsuji, Palladium Reagents and Catalysts. New Perspectives for the 21st Century, Wiley, Chichester, 2004.
[154] E. Negishi, A. de Meijre, Organopalladium Chemistry for Organic Synthesis, Wiley, New York, 2002.
[155] J. Hartwig, Organotransition Metal Chemistry, University Science Books, Sausalito, CA, 2010.
[156] N. Selander, K.J. Szabo, Catalysis by palladium pincer complexes, Chem. Rev. 111 (3) (2011) 2048–2076.
[157] J.T. Singleton, The uses of pincer complexes in organic synthesis, Tetrahedron 59 (11) (2003) 1837–1857.
[158] K.J. Szabo, Palladium-pincer-complex-catalyzed transformations involving organometallic species, Synlett (6) (2006) 811–824.
[159] D. Morales-Morales, C.G.M. Jensen, The Chemistry of Pincer Compounds, Elsevier, Amsterdam, 2007.
[160] D. Benito-Garagorri, K. Kirchner, Modularly designed transition metal PNP and PCP pincer complexes based on aminophosphines: synthesis and catalytic applications, Acc. Chem. Res. 41 (2) (2008) 201–213.
[161] D. Morales-Morales, Recent applications of phosphinite POCOP pincer complexes towards organic transformations, Mini-Rev. Org. Chem. 5 (2) (2008) 141–152.
[162] J.M. Serrano-Becerra, D. Morales-Morales, Applications in catalysis and organic transformations mediated by platinum group PCP and PNP aromatic-based pincer complexes: recent advances, Curr. Org. Synth. 6 (2) (2009) 169–192.
[163] I. Moreno, R. SanMartin, B. Ines, M.T. Herrero, E. Domínguez, Recent advances in the use of unsymmetrical palladium pincer complexes, Curr. Org. Chem. 13 (9) (2009) 878–895.
[164] R.B. Bedford, Palladacyclic catalysts in C–C and C–heteroatom bond-forming reactions, Chem. Commun. (15) (2003) 1787–1796.
[165] N. Selander, K.J. Szabo, Synthesis and transformation of organoboronates and stannanes by pincer-complex catalysts, Dalton Trans. (32) (2009) 6267–6279.
[166] M. Ohff, A. Ohff, M.E. van der Boom, D. Milstein, Highly active Pd(II) PCP-type catalysts for the heck reaction, J. Am. Chem. Soc. 119 (48) (1997) 11687–11688.
[167] D. Morales-Morales, R. Redón, C. Yung, C.M. Jensen, High yield olefination of a wide scope of aryl chlorides catalyzed by the phosphinito palladium PCP pincer complex: [PdCl{$C_6H_3(OPPr^i_2)_2$ -2,6}], Chem. Commun. (17) (2000) 1619–1620.
[168] V. Leigh, W. Ghattas, H. Mueller-Bunz, M. Albrecht, Synthesis of pincer-type N-heterocyclic carbene palladium complexes with a hemilabile ligand and their application in cross-coupling catalysis, J. Organomet. Chem. 771 (2014) 33–39.
[169] Tao Tu, J. Malineni, K.H. Dötz, A. Novel, Pyridine-bridged bis-benzimidazolylidene pincer palladiumcomplex: synthesis and catalytic properties, Adv. Synth. Catal. (350) (2008) 1791–1795.

[170] Z. Wang, X. Feng, W. Fang, T. Tu, Efficient aqueous-phase heck reaction catalyzed by a robust hydrophilic pyridine-bridged bisbenzimidazolylidene-palladium pincer complex, Synlett (7) (2011) 951–954.
[171] N.T.S. Phan, M. Van Der Sluys, C.W. Jones, On the nature of the active species in palladium catalyzed Mizoroki–Heck and Suzuki–Miyaura couplings—homogeneous or heterogeneous catalysis, A Crit. Review, Adv. Synt. Catal. 348 (6) (2006) 609–679.
[172] J. Dupont, C.S. Consorti, J. Spencer, The potential of palladacycles: more than just precatalysts, Chem. Rev. 105 (6) (2005) 2527–2572.
[173] D.E. Bergbreiter, P.L. Osburn, Y.S. Liu, Tridentate SCS palladium(II) complexes: new, highly stable, recyclable catalysts for the heck reaction, J. Am. Chem. Soc. 121 (41) (1999) 9531–9538.
[174] E. Peris, J. Mata, J.A. Loch, R.H. Crabtree, A Pd complex of a tridentate pincer CNC bis-carbene ligand as a robust homogenous Heck catalyst, Chem. Commun. (2) (2001) 201–202.
[175] S. Gründemann, M. Albrecht, J.A. Loch, J.W. Faller, R.H. Crabtree, Tridentate carbene CCC and CNC pincer palladium(II) Complexes: structure, fluxionality, and catalytic activity, Organometallics 20 (25) (2001) 5485–5488.
[176] C.S. Consorti, G. Ebeling, F.R. Flores, R.C. Haddon, J. Dupont, On the use of non-symmetrical mixed PCN and SCN pincer palladacycles as catalyst precursors for the Heck reaction, Adv. Synt. Catal. 346 (6) (2004) 617–624.
[177] N. Ghavale, S.T. Manjare, H.B. Singh, R.J. Butcher, Bis(chalcogenones) as pincer ligands: isolation and Heck activity of the selone-ligated unsymmetrical C,C,Se–Pd pincer complex, Dalton Trans. 44 (26) (2015) 11893–11900.
[178] M.P. Singh, F. Saleem, G.K. Rao, S. Kumar, H. Joshi, A.K. Singh, Palladacycles of unsymmetrical (N,C$^-$,E) (E = S/Se) pincers based on indole: their synthesis, structure and application in the catalysis of Heck coupling and allylation of aldehydes, Dalton Trans. 45 (15) (2016) 6718–6725.
[179] Q. Mahmood, E. Yue, W. Zhang, G.A. Solan, T. Liang, W.H. Sun, Bisiminofunctionalized dibenzo[*a*,*c*]acridines as highly conjugated pincer frameworks for palladium(ii): synthesis, characterization and catalytic performance in Heck coupling, Org. Chem. Front. 3 (12) (2016) 1668–1679.
[180] S. Ramírez-Rave, D. Morales-Morales, J.M. Grévy, Microwave assisted Suzuki-Miyaura and Mizoroki-Heck cross-couplings catalyzed by non-symmetric Pd(II) CNS pincers supported by iminophosphorane ligands, Inorg. Chim. Acta 462 (2017) 249–255.
[181] Rishu, B. Prashanth, D. Bawari, U. Mandal, A. Verma, A.R. Choudhury, et al., Hg(ii) and Pd(ii) complexes with a new selenoether bridged biscarbene ligand: efficient mono- and bis-arylation of methyl acrylate with a pincer biscarbene Pd(ii) precatalyst, Dalton Trans. 46 (19) (2017) 6291–6302.
[182] R.A. Begum, D. Powell, K. Bowman-James, Thioamide pincer ligands with charge versatility, Inorg. Chem. 45 (3) (2006) 964–966.
[183] R.B. Bedford, S.M. Draper, P.N. Scully, S.L. Welch, Palladium bis(phosphinite) 'PCP'-pincer complexes and their application as catalysts in the Suzuki reaction, N. J. Chem. 24 (10) (2000) 745–747.
[184] B. Ines, R. SanMartin, M.J. Moure, E. Domínguez, Insights into the role of new palladium pincer complexes as robust and recyclable precatalysts for Suzuki–Miyaura couplings in neat water, Adv. Synth. Catal. 351 (13) (2009) 2124–2132.
[185] J.L. Bolliger, O. Blacque, C.M. Frech, Short, facile, and high-yielding synthesis of extremely efficient pincer-type Suzuki catalysts bearing aminophosphine substituents, Angew. Chem. Int. (Ed.) 46 (34) (2007) 6514–6517.

[186] F.E. Hahn, M.C. Jahnke, T. Pape, Synthesis of pincer-type bis(benzimidazolin-2-ylidene) palladium complexes and their application in C − C coupling reactions, Organometallics 26 (1) (2007) 150–154.
[187] F. Churruca, R. SanMartin, I. Tellitu, E. Domínguez, N-heterocyclic NCN-pincer palladium complexes: a source for general, highly efficient catalysts in Heck, Suzuki, and Sonogashira coupling reactions, Synlett (20) (2005) 3116–3120.
[188] H.M. Lee, J.Y. Zeng, C.H. Hu, M.T. Lee, A new tridentate pincer phosphine/N-heterocyclic carbene ligand: palladium complexes, their structures, and catalytic activities, Inorg. Chem. 43 (21) (2004) 6822–6829.
[189] J. Kjellgren, J. Aydin, O.A. Wallner, I.V. Saltanova, K.J. Szabo, Palladium pincer complex catalyzed cross-coupling of vinyl epoxides and aziridines with organoboronic acids, Chem. Eur. J. 11 (18) (2005) 5260–5268.
[190] S. Bonnet, M. Lutz, A.L. Spek, G. van Koten, R.J.M. Klein Gebbink, Bimetallic η^6, η^1 SCS- and PCP-pincer ruthenium palladium complexes: synthesis, structure, and catalytic activity, Organometallics 29 (5) (2010) 1157–1167.
[191] S. Bonnet, J.H. van Lenthe, M.A. Siegler, A.L. Spek, G. van Koten, R.J.M. Klein, Gebbink, bimetallic η^6, η^1 NCN-pincer ruthenium palladium complexes with η^6-RuCp coordination: synthesis, X-ray structures, and catalytic properties, Organometallics 28 (7) (2009) 2325–2333.
[192] M.C. Lipke, R.A. Woloszynek, L. Ma, J.D. Protasiewicz, m-Terphenyl anchored palladium diphosphinite pcp-pincer complexes that promote the Suzuki − Miyaura reaction under mild conditions, Organometallics 28 (1) (2009) 188–196.
[193] D. Olsson, O.F. Wendt, Suzuki reaction catalysed by a PCsp3P pincer Pd(II) complex: evidence for a mechanism involving molecular species, J. Organomet. Chem. 694 (19) (2009) 3112–3115.
[194] T. Takemoto, S. Iwasa, H. Hamada, K. Shibatomi, M. Kameyama, Y. Motoyama, et al., Highly efficient Suzuki–Miyaura coupling reactions catalyzed by bis(oxazolinyl)phenyl–Pd(II) complex, Tetrahedron Lett 48 (19) (2007) 3397–3401.
[195] T. Tu, J. Malineni, K.H. Dotz, A. Novel, Pyridine-bridged bis-benzimidazolylidene pincer palladium complex: synthesis and catalytic properties, Adv. Synth. Catal. 350 (11–12) (2008) 1791–1795.
[196] F. Churruca, R. SanMartin, B. Ines, I. Tellitu, E. Domínguez, Hydrophilic CNC-pincer palladium complexes: a source for highly efficient, recyclable homogeneous catalysts in Suzuki–Miyaura cross-coupling, Adv. Synth. Catal. 348 (14) (2006) 1836–1840.
[197] B. Ines, R. SanMartin, F. Churruca, E. Domínguez, M.K. Urtiaga, M.I. Arriortua, et al., Pincer-type palladium catalyst in Suzuki, Sonogashira, and Hiyama couplings in neat water, Organometallics 27 (12) (2008) 2833–2839.
[198] L.Y. Wu, X.Q. Hao, Y.X. Xu, M.Q. Jia, Y.-N. Wang, J.F. Gong, et al., Chiral NCN pincer Pt(II) and Pd(II) complexes with 1,3-Bis(2′-imidazolinyl)benzene: synthesis via direct metalation, characterization, and catalytic activity in the Friedel − Crafts alkylation reaction, Organometallics 28 (12) (2009) 3369–3380.
[199] J. Yorke, J. Sanford, A. Decken, A. Xia, Iminophosphinite pincer palladium complexes: synthesis and application, Inorg. Chim. Acta 363 (5) (2010) 961–966.
[200] B. Ines, I. Moreno, R. SanMartin, E. Domínguez, A nonsymmetric pincer-catalyzed Suzuki − Miyaura arylation of benzyl halides and other nonactivated unusual coupling partners, J. Org. Chem. 73 (21) (2008) 8448–8451.
[201] V.A. Kozlov, D.V. Aleksanyan, Y.V. Nelyubina, K.A. Lyssenko, E.I. Gutsul, L.N. Puntus, et al., Cyclopalladated complexes of 3-thiophosphorylbenzoic acid thioamides: hybrid pincer ligands of a new type: synthesis, catalytic activity, and photophysical properties, Organometallics 27 (16) (2008) 4062–4070.

[202] W. Wei, Y. Qin, M. Luo, P. Xia, M.S. Wong, Synthesis, structure, and catalytic activity of palladium(II) complexes of new cnc pincer-type N-heterocyclic carbene ligands, Organometallics 27 (10) (2008) 2268–2272.
[203] A.M. Sheloumov, P. Tundo, F.M. Dolgushin, A.A. Koridze, Suzuki aryl coupling catalysed by palladium bis(phosphane) pincer complexes based on ferrocene; X-ray structure determination of {PdCl[{2,5-(tBu_2PCH_2)$_2$$C_5H_2$}Fe($C_5H_5$)]}OTf, Eur. J. Inorg. Chem. 2008 (4) (2008) 572–576.
[204] D. Benito-Garagorri, V. Bocokic, K. Mereiter, K. Kirchner, A Modular approach to achiral and chiral nickel(II), palladium(II), and platinum(II) PCP pincer complexes based on diaminobenzenes, Organometallics 25 (16) (2006) 3817–3823.
[205] Q. Luo, S. Eibauer, O. Reiser, Novel bis(oxazole) pincer ligands for catalysis: application in Suzuki-Miyaura cross coupling reactions under aerobic conditions, J. Mol. Catal. 268 (1–2) (2007) 65–69.
[206] C.A. Kruithof, A. Berger, H.P. Dijkstra, F. Soulimani, T. Visser, M. Lutz, et al., Sulfato-bridged ECE-pincer palladium(II) complexes: structures in the solid-state and in solution, and catalytic properties, Dalton Trans. (17) (2009) 3306–3314.
[207] X.Q. Hao, Y.N. Wang, J.R. Liu, K.L. Wang, J.F. Gong, M.P. Song, Unsymmetrical, oxazolinyl-containing achiral and chiral NCN pincer ligand precursors and their complexes with palladium(II), J. Organomet. Chem. 695 (1) (2010) 82–89.
[208] J.L. Bolliger, C.M. Frech, The 1,3-diaminobenzene-derived aminophosphine palladium pincer complex {C_6H_3[NHP(piperidinyl)$_2$]$_2$Pd(Cl)}— a highly active Suzuki–Miyaura catalyst with excellent functional group tolerance, Adv. Synth. Catal. 352 (6) (2010) 1075–1080.
[209] B.S. Zhang, C. Wang, J.F. Gong, M.P. Song, Facile synthesis of achiral and chiral PCN pincer palladium(II) complexes and their application in the Suzuki and copper-free Sonogashira cross-coupling reactions, J. Organomet. Chem. 694 (16) (2009) 2555–2561.
[210] B.S. Zhang, W. Wang, D.D. Shao, X.-Q. Hao, J.F. Gong, M.P. Song, Unsymmetrical chiral PCN pincer palladium(II) and nickel(II) complexes of (imidazolinyl)aryl phosphinite ligands: synthesis via ligand C − H activation, crystal structures, and catalytic studies, Organometallics 29 (11) (2010) 2579–2587.
[211] K. Inamoto, J. Kuroda, K. Hiroya, Y. Noda, Synthesis and catalytic activity of a pincer-type bis(imidazolin-2-ylidene) nickel(II) complex, Organometallics 25 (12) (2006) 3095–3098.
[212] J.-I. Kuroda, K. Inamoto, K. Hiroya, T. Doi, N-heterocyclic carbene derived nickel–pincer complexes: efficient and applicable catalysts for Suzuki–Miyaura coupling reactions of aryl/alkenyl tosylates and mesylates, Eur. J. Org. Chem. 2009 (14) (2009) 2251–2261.
[213] K. Inamoto, J.-I. Kuroda, E. Kwon, K. Hiroya, T. Doi, Pincer-type bis(carbene)-derived complexes of nickel(II): synthesis, structure, and catalytic activity, J. Organomet. Chem. (694) (2009) 389–396.
[214] F. Estudiante-Negrete, S. Hernández-Ortega, D. Morales-Morales, Ni(II)–POCOP pincer compound [NiCl{$C_{10}H_5$-2,10-($OPPh_2$)$_2$}] an efficient and robust nickel catalyst for the Suzuki–Miyaura coupling reactions, Inorg. Chim. Acta 387 (2012) 58–63.
[215] M. Mastalir, B. Stöger, E. Pittenauer, G. Allmaier, K. Kirchner, Air-stable triazine-based Ni(II) PNP pincer complexes as catalysts for the Suzuki–Miyaura cross-coupling, Org. Lett. 18 (14) (2016) 3186–3189.
[216] L.M. Kumar, B.R. Bhat, Cobalt pincer complex catalyzed Suzuki-Miyaura cross coupling—a green approach, J. Organomet. Chem. 827 (2017) 41–48.

[217] J.A. Loch, M. Albrecht, E. Peris, J. Mata, J.W. Faller, R.H. Crabtree, Palladium complexes with tridentate pincer bis-carbene ligands as efficient catalysts for C − C coupling, Organometallics 21 (4) (2002) 700–706.
[218] J.L. Bolliger, C.M. Frech, Highly convenient, clean, fast, and reliable Sonogashira coupling reactions promoted by aminophosphine-based pincer complexes of palladium performed under additive- and amine-free reaction conditions, Adv. Synth. Catal. 351 (6) (2009) 891–902.
[219] G. Xu, X. Li, H. Sun, Nickel-catalyzed cross-coupling of primary alkyl halides with phenylethynyl- and trimethylsilyethynyllithium reagents, J. Organomet. Chem. 696 (18) (2011) 3011–3014.
[220] H. Wang, J.H. Liu, Y. Deng, T. Min, G. Yu, X. Wu, et al., Pincer thioamide and pincer thioimide palladium complexes catalyze highly efficient Negishi coupling of primary and secondary alkyl zinc reagents at room temperature, Chem. Eur. J. 15 (6) (2009) 1499–1507.
[221] J.H. Liu, H. Wang, H. Zhang, X. Wu, H. Zhang, Y. Deng, et al., Identification of a highly efficient alkylated pincer thioimido–palladium(II) complex as the active catalyst in Negishi coupling, Chem. Eur. J. 15 (17) (2009) 4437–4445.
[222] R. Gerber, O. Blacque, C.M. Frech, Negishi cross-coupling reaction catalyzed by an aliphatic, phosphine-based pincer complex of palladium. biaryl formation *via* cationic pincer-type Pd^{IV} intermediates, Dalton Trans. 40 (35) (2011) 8996–9003.
[223] A. Joshi-Pangu, M. Ganesh, M.R. Biscoe, Nickel-catalyzed Negishi cross-coupling reactions of secondary alkylzinc halides and aryl iodides, Org. Lett. 13 (5) (2011) 1218–1221.
[224] M. Mastalir, K. Kirchner, A triazine-based Ni(II) PNP pincer complex as catalyst for Kumada–Corriu and Negishi cross-coupling reactions, Monatsh. Chem. 148 (1) (2017) 105–109.
[225] W.-J. Guo, Z.-X. Wang, Cross-coupling of ArX with ArMgBr catalyzed by N-heterocyclic carbene-based nickel complexes, J. Org. Chem. 78 (3) (2013) 1054–1061.
[226] X.-Q. Zhang, Z.-X. Wang, Amido pincer nickel catalyzed Kumada cross-coupling of aryl, heteroaryl, and vinyl chlorides, Synlett 24 (16) (2013) 2081–2084.
[227] P.M. Perez-Garcia, T. Di-Franco, A. Orsino, P. Ren, X. Hu, Nickel-catalyzed diastereoselective alkyl–alkyl Kumada coupling reactions, Org. Lett. 14 (16) (2012) 4286–4289.
[228] T. Di-Franco, M. Stojanovic, S.C. Keller, R. Scopelliti, X. Hu, A structure–activity study of nickel NNN pincer complexes for alkyl-alkyl Kumada and Suzuki–Miyaura coupling reactions, Helv. Chim. Acta. 99 (11) (2016) 830–847.
[229] D. Olsson, P. Nilsson, M. El Masnaouy, O.F. Wendt, A catalytic and mechanistic investigation of a PCP pincer palladium complex in the Stille reaction, Dalton Trans. (11)(2005) 1924–1929.
[230] C.A. Bessel, P. Aggarwal, A.C. Marschilok, K.J. Takeuchi, Transition-metal complexes containing trans-spanning diphosphine ligands, Chem. Rev. 101 (4) (2001) 1031–1066.
[231] A.H. Norbury, A.I.P. Sinha, The co-ordination of ambidentate ligands, Q. Rev. Chem. Soc. 24 (1) (1970) 69–94.
[232] R. Lindner, B. van den Bosch, M. Lutz, J.N.H. Reek, J.I. van der Vlugt, Tunable hemilabile ligands for adaptive transition metal complexes, Organometallics 30 (3) (2011) 499–510.
[233] D.L.J. Broere, R. Plessius, J.I. van der Vlugt, New avenues for ligand-mediated processes—expanding metal reactivity by the use of redox-active catechol, *o*-aminophenol and *o*-phenylenediamine ligands, Chem. Soc. Rev. 44 (19) (2015) 6886–6915.

[234] P.J. Chirik, K. Wieghardt, Radical ligands confer nobility on base-metal catalysts, Science 327 (5967) (2010) 794–795.
[235] J.I. van der Vlugt, Radical-type reactivity and catalysis by single-electron transfer to or from redox-active ligands, Chem. Eur. J. 25 (11) (2019) 2651–2662.
[236] V. Lyaskovskyy, B. de Bruin, Redox non-innocent ligands: versatile new tools to control catalytic reactions, ACS Catal. 2 (2) (2012) 270–279.
[237] O.R. Luca, R.H. Crabtree, Redox-active ligands in catalysis, Chem. Soc. Rev. 42 (4) (2013) 1440–1459.
[238] V.K. Praneeth, M.R. Ringenberg, T.R. Ward, Redox-active ligands in catalysis, Angew. Chem., Int. (Ed.) 51 (41) (2012) 10228–10234.
[239] J. Stubbe, W.A. van der Donk, Protein radicals in enzyme catalysis, Chem. Rev. 98 (2) (1998) 705–762.
[240] W. Kaim, B. Schwederski, Non-innocent ligands in bioinorganic chemistry—an overview, Coord. Chem. Rev. 254 (13–14) (2010) 1580–1588.
[241] B.L. Small, M. Brookhart, A.M.A. Bennett, Highly active iron and cobalt catalysts for the polymerization of ethylene, J. Am. Chem. Soc. 120 (16) (1998) 4049–4050.
[242] G.J.P. Britovsek, V.C. Gibson, B.S. Kimberley, P.J. Maddox, S.J. McTavish, G.A. Solan, et al., Novel olefin polymerization catalysts based on iron and cobalt, Chem. Commun. (7) (1998) 849–850.
[243] P.H.M. Budzelaar, B. de Bruin, A.W. Gal, K. Wieghardt, J.H. van Lenthe, Metal-to-ligand electron transfer in diiminopyridine complexes of Mn − Zn: a theoretical study, Inorg. Chem. 40 (18) (2001) 4649–4655.
[244] M.W. Bouwkamp, S.C. Bart, E.J. Hawrelak, R.J. Trovitch, E. Lobkovsky, P.J. Chirik, Square planar bis(imino)pyridine iron halide and alkyl complexes, Chem. Commun. (27) (2005) 3406–3408.
[245] M.W. Bouwkamp, E. Lobkovsky, P.J. Chirik, Bis(imino)pyridine iron(II) alkyl cations for olefin polymerization, J. Am. Chem. Soc. 127 (27) (2005) 9660–9661.
[246] M.W. Bouwkamp, A.C. Bowman, E. Lobkovsky, P.J. Chirik, Iron-catalyzed [2π + 2π] cycloaddition of α,ω-dienes: the importance of redox-active supporting ligands, J. Am. Chem. Soc. 128 (41) (2006) 13340–13341.
[247] K.T. Sylvester, P.J. Chirik, Iron-catalyzed, hydrogen-mediated reductive cyclization of 1,6-enynes and diynes: evidence for bis(imino)pyridine ligand participation, J. Am. Chem. Soc. 131 (25) (2009) 8772–8774.
[248] A.M. Tondreau, C.C. Atienza, K.J. Weller, S.A. Nye, K.M. Lewis, J.G. Delis, et al., Iron catalysts for selective anti-markovnikov alkene hydrosilylation using tertiary silanes, Science 335 (6068) (2012) 567–570.
[249] D. Adhikari, S. Mossin, F. Basuli, J.C. Huffman, R.K. Szilagyi, K. Meyer, et al., Structural, spectroscopic, and theoretical elucidation of a redox-active pincer-type ancillary applied in catalysis, J. Am. Chem. Soc. 130 (11) (2008) 3676–3682.
[250] R.A. Zarkesh, J.W. Ziller, A.F. Heyduk, Four-electron oxidative formation of aryl diazenes using a tantalum redox-active ligand complex, Angew. Chem. Int. (Ed.) 47 (25) (2008) 4715–4718.
[251] F. Lu, R.A. Zarkesh, A.F. Heyduk, A redox-active ligand as a reservoir for protons and electrons: O_2 reduction at zirconium(IV), Eur. J. Inorg. Chem. 2012 (3) (2012) 467–470.
[252] A.I. Nguyen, K.J. Blackmore, S.M. Carter, R.A. Zarkesh, A.F. Heyduk, One- and two-electron reactivity of a tantalum(V) complex with a redox-active tris(amido) ligand, J. Am. Chem. Soc. 131 (9) (2009) 3307–3316.
[253] D.M. Spasyuk, D. Zargarian, A. van der Est, New POCN-type pincer complexes of nickel(II) and nickel(III), Organometallics 28 (22) (2009) 6531–6540.
[254] A.I. Nguyen, R.A. Zarkesh, D.C. Lacy, M.K. Thorson, A.F. Heyduk, Catalytic nitrene transfer by a zirconium(IV) redox-active ligand complex, Chem. Sci. 2 (2011) 166–169.

[255] O.R. Luca, S.J. Konezny, J.D. Blakemore, S. Saha, D.M. Colosi, G.W. Brudvig, et al., A tridentate Ni pincer for aqueous electrocatalytic hydrogen production, N. J. Chem. 36 (5) (2012) 1149–1152.
[256] J.L. Wong, R.H. Sanchez, J.G. Logan, R.A. Zarkesh, J.W. Ziller, A.F. Heyduk, Disulfide reductive elimination from an iron(iii) complex, Chem. Sci. 4 (4) (2013) 1906–1910.
[257] D.L.J. Broere, L.L. Metz, B. de Bruin, J.N.H. Reek, M.A. Siegler, J.I. van der Vlugt, Redox-active ligand-induced homolytic bond activation, Angew. Chem. Int. (Ed.) 54 (5) (2014) 1516–1520.
[258] D.L.J. Broere, B. de Bruin, J.N.H. Reek, M. Lutz, S. Dechert, J.I. van der Vlugt, Intramolecular redox-active ligand-to-substrate single-electron transfer: radical reactivity with a palladium(II) complex, J. Am. Chem. Soc. 136 (33) (2014) 11574–11577.
[259] B. Bagh, D.L.J. Broere, V. Sinha, P.F. Kuijpers, N.P. van Leest, B. de Bruin, et al., Catalytic synthesis of n-heterocycles via direct C(sp^3)–H amination using an air-stable iron(III) species with a redox-active ligand, J. Am. Chem. Soc. 139 (14) (2017) 5117–5124.
[260] S. Sinha, S. Das, R. Sikari, S. Parua, P. Brandaõ, S. Demeshko, et al., Redox non-innocent azo-aromatic pincers and their iron complexes. Isolation, characterization, and catalytic alcohol oxidation, Inorg. Chem. 56 (22) (2017) 14084–14100.
[261] S.P. Rath, D. Sengupta, P. Ghosh, R. Bhattacharjee, M. Chakraborty, S. Samanta, et al., Effects of ancillary ligands on redox and chemical properties of ruthenium coordinated azoaromatic pincer, Inorg. Chem. 57 (19) (2018) 11995–12009.
[262] G. Zhang, J. Wu, S. Zheng, M.C. Neary, J. Mao, M. Flores, et al., Redox-noninnocent ligand-supported vanadium catalysts for the chemoselective reduction of C═X (X = O, N) functionalities, J. Am. Chem. Soc. 141 (38) (2019) 15230–15239.
[263] N.I. Regenauer, S. Settele, E. Bill, H. Wadepohl, D.-A. Rosca, Bis(imino)pyrazine-supported iron complexes: ligand-based redox chemistry, dearomatization, and reversible C–C bond formation, Inorg. Chem. 59 (4) (2020) 2604–2612.
[264] P. Daw, A. Kumar, D. Oren, N.A. Espinosa-Jalapa, D. Srimani, Y. Diskin-Posner, et al., Redox noninnocent nature of acridine-based pincer complexes of 3d metals and C-C bond formation, Organometallics 39 (2) (2020) 279–285.

CHAPTER 2

Pincer-group(8) and pincer-group (9) metal complexes for catalytic alkane dehydrogenation reactions

Pran Gobinda Nandi[1], Vinay Arora[1], Eileen Yasmin[1] and Akshai Kumar[1,2,3,*]

[1]Department of Chemistry, Indian Institute of Technology Guwahati, Guwahati, India
[2]Center for Nanotechnology, Indian Institute of Technology Guwahati, Guwahati, India
[3]School of Health Science & Technology, Indian Institute of Technology Guwahati, Guwahati, India
Corresponding author. e-mail address: akshaikumar@iitg.ac.in

2.1 Introduction

Organometallic complexes play a key role in a variety of organic transformations. They are often used in stoichiometric amounts and/or in catalytic amounts either to accomplish reactions that are not possible or to accelerate sluggish reactions. The term "pincer" is derived from the old French word "pincier" which means "to pinch," according to the Oxford Lexico Dictionary, and it usually refers to "one of the pairs of curved claws of an animal like that of a crab," as defined by the Cambridge English Dictionary [1]. On similar lines, a pincer ligand is tridentate in nature and grasps onto a metal center in a meridional geometry [2]. The three binding atoms of the ligand should be coplanar and may be any of N, P, C, S, or O atoms. A pincer ligand attached to a metal center by three nitrogen atoms is referred to as NNN type. Similarly, various types of ligands such as PCP, NCN, PNP, PCN, PNO, and SCS are known in literature. The chelating properties of pincer ligands impart rigidity to the metal ligand complex. On the other hand, the steric and electronic environment of the pincer catalysts controls the selectivity of the catalytic reaction.

The pincer ligand was first reported by Shaw and Moulton who developed tridentate ligand systems with a central anionic carbon attached by two *tert*-butyl phosphine units abbreviated as $^{t}Bu_4PCP$ (Fig. 2.1) [3]. In 1989 van Koten coined the term "pincer" to refer to such tridentate systems [4].

Pincer–Metal Complexes
DOI: https://doi.org/10.1016/B978-0-12-822091-7.00002-6

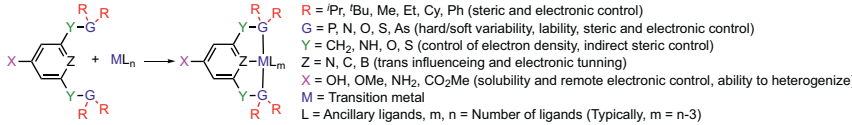

Figure 2.1 General representation of pincer–metal complexes with tailorable properties.

In a pincer complex, while the substituents attached to the binding atoms (G) (Fig. 2.1) that are *trans* to each other control the steric and electronic properties, the central atom (Z) (Fig. 2.1) provides an option to tune the *trans* influence. The aryl backbone in pincers generally imparts rigidity to the system and enhances thermal stability [5–7]. Pincer complexes have been used for several stoichiometric [8,9] and catalytic [10] transformations in order to synthesize fuels, [11,12] fine chemicals [11,12], and commodity chemicals [11,12]. Pincer catalysts are highly active for several reactions such as hydrogenation of alkenes, dehydrogenation of alkanes, and activation of CO_2 [5,10,12–15]. Both homogeneous and heterogeneous pincer catalysts are known for dehydrogenation of alkanes to alkenes. However, the selectivity and yield obtained by heterogeneous catalysts are generally low [16]. The current chapter discusses the state of the art in catalytic alkane dehydrogenation (AD) reactions employing different pincer–metal complexes under homogeneous conditions in addition to the recent attempts to extend their application as heterogeneous catalysts.

2.1.1 Alkane dehydrogenation

Alkanes are saturated hydrocarbons, cyclic or acyclic in nature. Small chain hydrocarbons are the main constituents of petrochemical and natural gas [17,18]. A small portion of these alkanes (C_9–C_{19}) are useful as fuels, but rest of the highly abundant alkanes in nature remain largely unproductive [5]. Small chain alkanes such as propane and butane are the main constituents of LPG (liquefied petroleum gas). The most important sources of alkanes are natural gas and crude oil, whereas synthetically, the Fischer–Tropsch method is widely used for alkane production from CO and H_2 [19]. Alkanes are thus the most abundant organic resources in the world but there are limited methods for the conversion of alkanes to useful chemicals [20]. The corresponding unsaturated hydrocarbons of the highly abundant alkanes are useful as they are the precursors to alcohols,

alkyl halides, and higher alkenes [21–23]. Therefore dehydrogenation of alkanes to alkenes has high commercial and industrial value. Pioneering and independent studies by Crabtree, Felkin, and Goldman have shown that the regioselectivity of dehydrogenation can be controlled by organometallic catalysts.

Crabtree was the first to report AD using a transition metal catalyst in 1979. The Ir(III) complex (**1**) on reaction with cyclopentane or cyclooctane (COA) in the presence of TBE (3,3-dimethyl-1-butene) using 1,2-dicholorethane as solvent under reflux conditions, yielded the corresponding iridium complexes containing cyclopentadienyl (**2**) and cyclooctadiene ligands (**3**) (Scheme 2.1) [24–26].

Due to highly endothermic nature of AD reactions, often a hydrogenation reaction is coupled with it and this is referred to as "transfer dehydrogenation." TBE (3,3-dimethyl-1-butene) has been extensively used as sacrificial acceptor as it does not undergo isomerization and can be easily regenerated from its hydrogenated product [27]. Felkin and coworkers reported the use of rhenium complexes L_2ReH_7 ($L = PPh_3$ and PEt_2Ph), for AD reactions in the presence of TBE [28–30].

The combination of COA and TBE has been extensively studied as a benchmark to determine the efficiency of a dehydrogenation catalyst ever since the report of its first use by Crabtree. This is mainly due to its lower dehydrogenation enthalpy (c. 23 kcal mol^{-1}) as compared to unstrained cycloalkanes or linear alkanes at internal positions (c. 28 kcal mol^{-1}) and at terminal positions (c. 30 kcal mol^{-1}) [13,14]. But the real challenge is the dehydrogenation of acyclic systems and studies done with COA cannot be applied to such systems owing to the strong binding of acyclic olefins with the metal center and higher dehydrogenation enthalpy. Led by the pioneering work of Kaska, Jensen, Goldman, Brookhart, among others, significant advances have been made in the catalytic AD reactions using pincer–metal complexes, in general and pincer–Ir complexes, in particular.

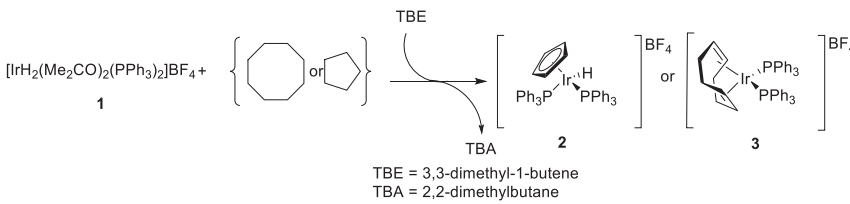

Scheme 2.1 First report on iridium catalyzed alkane dehydrogenation by Crabtree.

2.2 Dehydrogenation reactions of alkane using pincer–Ir complexes

2.2.1 Initial reports based on pincer–Ir catalysts

In 1996 Kaska and Jensen were the first to report the use of a highly stable pincer–Ir catalyst (^{t}Bu4PCP)IrH$_2$ (**5-H$_2$**) (Fig. 2.2) for the AD using TBE as a hydrogen acceptor [31].

The pincer–Ir complex (^{t}Bu4PCP)IrH$_2$ (**5-H$_2$**) is stable at temperatures as high as 200°C [32] and shows high stability and reactivity toward AD. The complex (^{t}Bu4PCP)IrH$_2$ (**5-H$_2$**) was synthesized by the reduction of the corresponding hydrido-chloride complex using LiBEt$_3$H as a reducing agent in tetrahydrofuran (THF) at 25°C under H$_2$ atmosphere with >85% yield [31]. The dehydrogenation reaction was carried out in solutions of TBE [0.38 M] and **5-H$_2$** [1.2 mM] in cyclooctane [8.81 M]. Temperature has a considerable influence on the alkane transfer dehydrogenation, as with increase in temperature from 100°C to 200°C, the initial rate of the COA/TBE [8.81 M/0.38 M] reaction increases from 20.5 to 720 h^{-1}.

The pincer–Ir complex (^{t}Bu4PCP)IrH$_2$ (**5-H$_2$**) is very stable and shows no decomposition even after one week and remains active till the completion of hydrogenation of TBE [31]. The reaction is unaffected by the addition of metallic mercury to the mixture indicating that metallic iridium is not involved in the hydrogen transfer [33]. The higher ratio of both TBE and TBA with respect to catalyst (>300:1) inhibits the catalytic reaction. Kaska and Jensen mitigated this problem by the periodic addition of TBE to the solution and high turnover numbers (up to 1000 TONs) were observed. Notably, the catalytic activity is strongly inhibited in the presence of N$_2$ [31].

Later, in 1997, Jensen, Kaska, and Goldman reported the thermochemical acceptorless AD using **5-H$_2$** as catalyst. This is efficient (several hundred mol product/mol catalyst) for dehydrogenation of alkanes to give the corresponding alkenes and dihydrogen under reflux conditions [34]. Upon refluxing a

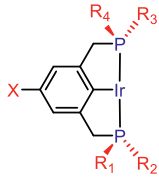

4 X = H, R$_1$ = R$_2$ = R$_3$ = R$_4$ = ^{i}Pr; **5** X = H, R$_1$ = R$_2$ = R$_3$ = R$_4$ = ^{t}Bu;
6 X = H, R$_1$ = R$_2$ = R$_3$ = R$_4$ = Ad; **7** X =H, R$_1$ = R$_2$ = R$_3$ = ^{t}Bu, R$_4$ = Me;
8 X = H, R$_1$ = R$_3$ = ^{t}Bu, R$_2$ = R$_4$ = Me; **9** X = OMe, R$_1$ = R$_2$ = R$_3$ = R$_4$ = ^{i}Pr;
10 X = OMe, R$_1$ = R$_2$ = R$_3$ = R$_4$ = ^{t}Bu; **11** X = NMe$_2$, R$_1$ = R$_2$ = R$_3$ = R$_4$ = ^{t}Bu;
12 X = CO$_2$Me, R$_1$ = R$_2$ = R$_3$ = R$_4$ = ^{t}Bu; **13** X = H, R$_1$ = R$_2$ = R$_3$ = R$_4$ = CF$_3$

Kaska, Jensen, Goldman, Roddick

Figure 2.2 PC(sp^2)P pincer–Ir complexes reported for alkane dehydrogenation.

cyclooctane solution in the presence of (PCP)RhH_2 [10 mM], in a stream of argon gas, negligible cyclooctene formation (<2 mM after 24 h) was observed. But the presence of iridium analog (2 mM **5-H_2**) gave a better result with an initial rate of 11 TOh^{-1} for cyclooctene formation. About 104 and 190 TONs were observed after 44 and 120 h respectively.

In the case of acceptorless cyclodecane (bp = 201°C) dehydrogenation catalyzed by 1 mM **5-H_2**, 170 TONs of cyclodecene (3:1, *cis*:*trans*) is obtained after 4 h, which levels off at 360 TONs after 24 h. [34] The leveling off is attributed to catalyst inhibition by the cycloalkene. The same reaction when carried out in the presence of **4-H_2** resulted in a series of secondary dehydrogenation and isomerization reactions. The reaction gave *trans*, *trans*-1, 5-cyclodecadiene, followed by Cope rearrangement yielding *trans*-1,2-divinylcyclohexane, which accepts dihydrogen and converts cyclodecane to diethylcyclohexane. This isomerization strategy is commonly known as "hydrogen borrowing." [35] (Scheme 2.2).

In 1999 Goldman described the effect of substituents on the catalytic activity and stated that in spite of the "pincer effect" the bulkiness of the tert-butyl groups inhibits H_2 addition; that is, the intermediates of dehydrogenation cycle are sterically disfavored by the tert-butyl groups whereas it is comparatively more favored by isopropyl groups. On the basis of steric hindrance, the dehydrogenation of cyclooctane is more favored by (^{iPr4}PCP)IrH_2 (**4-H_2**) than (^{tBu4}PCP)IrH_2 (**5-H_2**) [20]. The results obtained for cyclooctane dehydrogenation at 150°C using 1 mM **4-H_2** and 1 mM **5-H_2** are summarized in Table 2.1. The rate of acceptorless dehydrogenation of cyclodecane, with a reflux

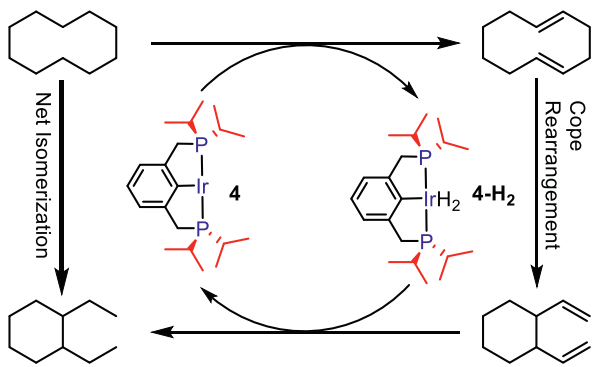

Scheme 2.2 Net isomerization of cyclodecane to deithylcyclohexane, catalyzed by (^{iPr}PCP)Ir (**4**).

Table 2.1 Dehydrogenation of cyclooctane with **4-H$_2$** and **5-H$_2$**.

Entry	Catalyst [1.0 mM]	Time	TONs
1	**4-H$_2$**	30 min	47
2	**4-H$_2$**	1 h	>94
3	**4-H$_2$**	15 h	105
4	**5-H$_2$**	1 h	11

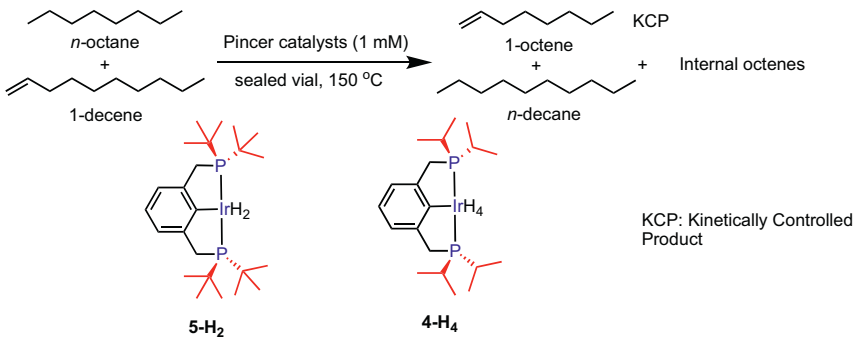

Scheme 2.3 Dehydrogenation of *n*-octane with **4-H$_4$** and **5-H$_2$**.

temperature of 201°C, is much higher than that of cyclooctane (bp = 149°C). In the case of cyclodecane dehydrogenation with **4-H$_2$**, 460 TONs of cyclodecene were observed with a *cis*:*trans* ratio of 4.6:1, after 1 h. However, lower TONs (170 after 4 h) were observed when **5-H$_2$** was used [20].

Goldman was the first to report the acceptorless dehydrogenation of *n*-alkanes using homogenous catalytic system in which mixture of internal isomers were obtained [40]. Compared to cyclodecane, dehydrogenation of *n*-alkanes was less efficient with **4-H$_2$**. In the case of acceptorless dehydrogenation of *n*-alkanes, ($^{t\mathrm{Bu4}}$PCP)IrH$_2$ (**5-H$_2$**) showed a lower efficiency than ($^{i\mathrm{Pr4}}$PCP)IrH$_2$ (**4-H$_2$**). Also, **5-H$_2$** and its isopropyl analog **4-H$_4$** exhibited high kinetic selectivity toward the formation of 1-octene in the *n*-octane/1-decene transfer dehydrogenation at 150°C (Scheme 2.3) [40]. While **5-H$_2$** was more selective than **4-H$_4$** in the catalytic transfer dehydrogenation of *n*-octane/1-decene at 150°C, the latter demonstrated higher catalytic efficiency than the former (Scheme 2.3) [40] The selective dehydrogenation is associated with an iridium catalyzed isomerization of terminal to internal octenes which limits the yield of 1-octene to <100 mM.

2.2.2 Alkane dehydrogenation by PC(sp^2)P-Ir systems

The initial success with **4-H$_4$** and **5-H$_2$** toward AD [31,32] paved way for several PC(sp^2)P-Ir catalysts with varying substituents on the phosphine moiety, different linker atoms on the flanking groups and modifications on the aryl backbone. Goldman and co-workers have systematically studied the steric effect of substituents on catalytic efficiency by sequential substitution of ^{t}Bu groups on the ($^{t\text{Bu4}}$PCP)IrH$_4$ (**5-H$_4$**) by methyl groups as in ($^{t\text{Bu2}}$PCP$^{t\text{BuMe}}$)Ir (**7**) and ($^{t\text{BuMe}}$PCP$^{t\text{BuMe}}$)Ir (**8**) (Fig. 2.2) [41]. In comparison to the second and third ^{t}Bu substitutions, the first Me-for-^{t}Bu substitution was theoretically predicted to have a more favorable effect in lowering the overall barriers of the *n*-alkane transfer dehydrogenation cycle. Experimental studies were in line with these predictions where it is observed that **7** (126 TONs after 10 min) is much more active than **8** (76 TONs after 10 min) for catalytic dehydrogenation of *n*-octane with TBE [0.2 M] at 150°C [41]. Notably, the lower activity of **8** could also be attributed to its tendency to form clusters which would eventually result in its deactivation.

In this context, interesting inferences emerged from the studies carried out by Goldman on the *n*-pentane [4.1 M]/TBE [4.1 M] transfer dehydrogenation that were catalyzed by 1 mM of **8** and **7** at 200°C. While operating at such high concentrations of TBE [4.1 M], the sterically less hindered **8** was observed to be indeed more active than **7** (Table 2.2) [42]. This points to the involvement of cluster formation in the poor activities of **8** at lower acceptor concentrations (say 0.2 M TBE, *vide-supra*) [41], which could be effectively mitigated by operating at very high TBE concentrations [42].

Table 2.2 Dehydrogenation of *n*-pentane/TBE catalyzed by **7-H$_4$** and **8-H$_4$**.

Entry	Catalyst [1 mM]	Time (min)	TBA [mM]	Total olefin [mM]	1-Pentene [mM]	2-Pentene [mM]	1,3-Pentadiene [mM]
1	**7-H$_4$**	0	0	0	0	0	0
		10	125	110	50	60	0
		40	170	150	50	100	0
		180	190	160	45	115	0
2	**8-H$_4$**	0	0	0	0	0	0
		10	495	395	55	270	75
		40	1310	915	75	540	300
		360	2420	1710	100	930	675

Complementary evidence was obtained in the pincer–iridium [1 mM] catalyzed *n*-pentane/propene transfer dehydrogenation in the gas phase at 240°C. At a propene concentration of 1.2 M, better results (340 TONs after 10 min) were obtained with the catalyst **8** in comparison with catalyst **7** (0 TONs after 10 min) (Table 2.3) [43]. In this case, as the reaction occurs in the gas phase, the extent of cluster formation of the solid molecular pincer catalyst **8** is greatly reduced.

The catalytic activity of the (PCP)-Ir catalysts can be modified by introducing groups such as methoxy, ester, and amine at the *para*-position of the aryl backbone [44,45]. The acceptorless dehydrogenation of cyclodecane (CDA) (1.5 mL) with ((*p*-OMe)$^{i\text{Pr4}}$PCP)Ir (**9**) [1 mM] was much more effective than its tert-butyl analog **10** and gave 2120 TONs after 24 h. Very recently, Goldman and co-workers used ($^{t\text{Bu4}}$PCP)Ir (**5**), ($^{t\text{Bu4}}$POCOP)Ir (**22**), and (*p*-OMe-$^{t\text{Bu4}}$POCOP)Ir (**24**) complexes for catalytic dehydrogenation of alkanes using proton and electron acceptors [51]. COA (7.4 M) dehydrogenation was carried out in the presence of Ag[BF_4] [40 mM] and KO^{t}Bu [40 mM at 150°C for 16 h with ($^{t\text{Bu4}}$POCOP)IrH_2 (**22-H$_2$**) [20 mM] to get upto 90% yield with respect to oxidant and base, that translates to about 0.9 catalytic TONs with respect to Ir. The pincer–Ir complexes ($^{t\text{Bu4}}$PCP)IrH_2 (**5-H$_2$**) [4 mM] and (*p*-OMe-$^{t\text{Bu4}}$POCOP)IrH_2 (**24-H$_2$**) [4 mM] demonstrated a better activity for COA [7.4 M] dehydrogenation in the presence of Ag[BF_4] [120 mM] and KO^{t}Bu [120 mM] at 150°C to yield COE [58 mM] with 97% yield (with respect to oxidant and base) and 14.5 TONs (with respect to Ir) after 16 h.

In 2012, Roddick and co-workers carried out the transfer dehydrogenation of COA [3.9 M]/TBE [3.9 M] in the presence of ($^{\text{CF3}}$PCP)Ir(η^4-COD) [**13-COD** [1.3 mM]] at 200°C [49]. The reaction proceeded at a slower rate (40 TOh^{-1}) compared to **5-H$_4$** (1200 TOh^{-1}) [52]. It was observed that on lowering the concentration of TBE (1.3 M from 3.9 M),

Table 2.3 Dehydrogenation of *n*-pentane/propene catalyzed by **7-H$_4$** and **8-H$_4$**.

Entry	Catalyst [1 mM]	Time (min)	Total olefins [mM]	1-Pentene [mM]	% Propene	Dienes [mM]
1	**7-H$_4$**	10	0	0	–	0
		40	59	50	–	0
2	**8-H$_4$**	10	340	105	30	21
		180	950	200	98	150

higher rate (150 TOh^{-1}) of COA dehydrogenation was observed with **13-COD** as catalyst. The reaction of **13-COD** with a mixture of COA/TBE (1:1) produced (^{CF3}PCP)Ir(η^4-isoprene) (**15**). The new isoprene adduct **15** was also obtained independently by the treatment of (^{CF3}PCP)Ir(H)(Cl)(η^2-ethylene) (**14**) with isoprene (Scheme 2.4). It indicated that TBE (95% purity) used in the catalytic dehydrogenation, contained isoprene as a contaminant. The same reaction was repeated with higher purity of TBE [3.9 M] at 200°C and improvement (136 TOh^{-1}) in rate was observed [49]. With high concentration of TBE, the dehydrogenation rate is decreased, which may be due to the impurity (isoprene) present in TBE or partly due to TBE itself, as it can bind with the active catalyst and lead to decrease in the rate of the reaction [52].

The complex (^{CF3}PCP)Ir(η^4-COD) (**13-COD**) was tolerant to dinitrogen and moisture whereas the parent PCP catalyst **5-H_2** was sensitive toward H_2O [53] and N_2 [54,55]. These new types of catalysts offer promise for dehydrogenation of alkanes without the need of complete degassing and drying. The dehydrogenation of COA [3.9 M] in the presence of TBE [3.9 M] catalyzed by (^{CF3}PCP)Ir(η^4-COD) [**13-COD** [1.3 mM]] at 200°C proceeded at a rate of 40 TOh^{-1} before leveling off after 58 h to give 660 TONs [46–50]. In comparison, the parent PCP catalyst **5-H_2** gave only 230 TONs after 20 h. The catalyst activity leveling off occurred due to the leaching out of the ligand (^{CF3}PCP)H owing to decomposition of (^{CF3}PCP)Ir(η^4-COD) (**13-COD**) rather than product

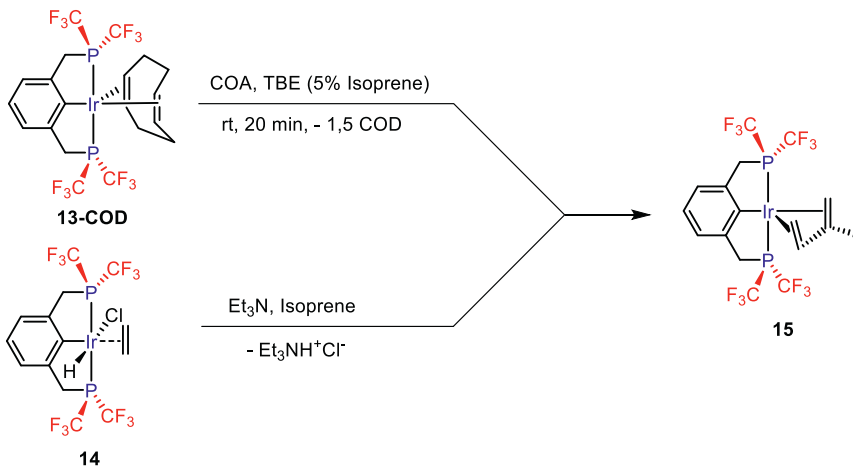

Scheme 2.4 Formation of isoprene adducts upon reaction of **13-COD** with TBE (containing 5% isoprene as impurity).

inhibition as indicated by ^{19}F NMR studies. The catalyst (^{CF3}PCP)Ir(η^4-COD) (**13-COD**) gave 92 TONs in 24 h for the acceptorless dehydrogenation of cyclodecane whereas (*p*-OMe-^{iPr4}PCP)Ir (**9**) gave 2100 TONs under identical conditions [44].

In 2013 Yamamoto reported a 7–6–7 type fused tricyclic pincer–Ir complex (7–6–7^{R4}PCP)Ir (**16**,R = ^{i}Pr; **17**, R = Cy; **18**, R = Ph) for the COA/TBE and *n*-octane/NBE dehydrogenation (Fig. 2.3**)** [56]. The fused nature of the bond imparts thermal stability and rigidity to the iridium metal complex, and due to the flexible backbone, these types of catalysts are highly efficient. The catalytic behavior and activity depends on temperature, which is depicted by the fact that the dehydrogenation rate of COA/TBE (1:1) at low temperature with **18** was higher whereas with **16** it was higher at high temperature. However, at all temperatures, the productivity of COA/TBE dehydrogenation was the highest with complex **18**. The transfer dehydrogenation of COA/TBE (1:1) with **18** occurred with a maximum of 4100 TONs after 24 h at 200°C. The solubility of the metal complex determines its reactivity toward AD. The poor solubility of complex **18** in *n*-octane inhibited its activity for *n*-octane/NBE dehydrogenation and in the case of complex **16**, it showed good catalytic activity for the same at 150°C. The catalyst **16** decomposed over time but was resistant to inhibition by alkenes, whereas **18** was resistant to both.

Similar tricyclic (PCP)–Ir metal complex was developed by Kaska and co-workers. They reported the acceptorless dehydrogenation of alkanes using (^{t}Bu$_4$-Anthraphos)Ir, **20** (Fig. 2.3) [57]. It was observed that aryl backbone imparted rigidity to the overall metal complex and it was

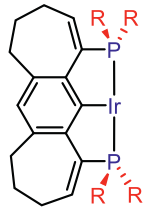

16 R = ^{i}Pr, **17** R = Cy
18 R = Ph

Yamamoto

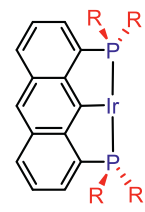

19 R = ^{i}Pr, **20** R = ^{t}Bu

Kaska, Brookhart, Hall, Goldman

Figure 2.3 Fused tricyclic PC(sp^2)P pincer–Ir complexes reported for alkane dehydrogenation.

thermally stable (up to 250°C). Later, Goldman and Brookhart stated that the isopropyl analog ($^{i}Pr_4$-Anthraphos)Ir, **19** was very effective toward AD [58,59]. By using this complex, Brookhart found that the dehydrogenation of *n*-pentane produced 1,3-pentadiene (piperylene) in the presence of propene as an acceptor in good yield (c. 40%) [60]. Dienes are valuable precursors to synthetic rubbers, adhesives and resins. Goldman reported very high yields of piperylene (c. 1.2 M) in the *n*-pentane/TBE [5.1 M] transfer dehydrogenation catalyzed by sterically less hindered ($^{i\text{Pr4}}$PCP)Ir (**4**) [7.0 mM] at 200°C, which is about 100-fold higher than the corresponding yield obtained upon use of ($^{t\text{Bu4}}$PCP)Ir (**5**) [42].

2.2.3 Alkane dehydrogenation by PYC(sp^2)ZP-Ir (Y = O, S, CH_2) systems

The stability and reactivity of the pincer complexes depend greatly on the atom through which phosphine is attached to the aryl ring. To investigate such type of stability, Brookhart and Jensen [52,61–63] independently synthesized ($^{\text{R4}}$POCOP)Ir type pincer complexes and used them for dehydrogenation of alkane (Fig. 2.4**)**. Due to the introduction of heteroatoms (O, S) in place of CH_2 of PCP ligand framework, alteration in reactivity was observed for the catalytic AD. In the case of transfer dehydrogenation of linear alkanes, ($^{t\text{Bu4}}$PCP)Ir (**5**) is a more efficient catalyst compared to ($^{t\text{Bu4}}$POCOP)Ir (**22**) but for COA/TBE dehydrogenation, **22** (1583 TONs after 40 h) is more reactive than **5** (230 TONs after 20 h) [52]. Brookhart and co-workers reported fluoro containing pincer complexes (*p*-F-$^{t\text{Bu4}}$POCOP)Ir (**25**) and (*p*-C_6F_5-$^{t\text{Bu4}}$POCOP)Ir (**26**). They found that the reactivity of (*p*-F-$^{t\text{Bu4}}$POCOP)Ir (**25**) (1530 TONs after 40 h) was comparable to that of ($^{t\text{Bu4}}$POCOP)Ir (**22**) for the COA/TBE (1:1)

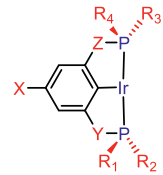

21 X = H, Y = Z = O, $R_1 = R_2 = R_3 = R_4 = {}^{i}Pr$;
22 X = H, Y = Z = O, $R_1 = R_2 = R_3 = R_4 = {}^{t}Bu$;
23 X = OK, Y = Z = O, $R_1 = R_2 = R_3 = R_4 = {}^{t}Bu$;
24 X = OMe, Y = Z = O, $R_1 = R_2 = R_3 = R_4 = {}^{t}Bu$
25 X = F, Y = Z = O, $R_1 = R_2 = R_3 = R_4 = {}^{t}Bu$;
26 X = C_6F_5, Y = Z = O, $R_1 = R_2 = R_3 = R_4 = {}^{t}Bu$;
27 X = H, Y = CH_2, Z = O, $R_1 = R_2 = R_3 = R_4 = {}^{i}Pr$;
28 X = H, Y = CH_2, Z = O, $R_1 = R_2 = R_3 = R_4 = {}^{t}Bu$;
29 X = H, Y = CH_2, Z = O, $R_1 = R_2 = {}^{i}Pr$, $R_3 = R_4 = {}^{t}Bu$;
30 X = H, Y = S, Z = O, $R_1 = R_2 = R_3 = R_4 = {}^{i}Pr$

Brookhart, Jensen, Goldman, Huang

Figure 2.4 PYC(sp^2)ZP pincer–Ir complexes studied for alkane dehydrogenation.

dehydrogenation at 200°C. On the other hand, (p-C_6F_5-^{tBu4}POCOP)Ir (**26**) demonstrated a higher productivity (2041 TONs were obtained after 40 h). Wendt group reported that ((m-$CF_3)_2$-^{tBu4}POCOP)Ir (**32**) efficiently catalyzes the COA/TBE (1:1) transfer dehydrogenation even at 170°C [64]. The activity of (p-((m-$CF_3)_2C_6H_3$)^{tBu4}POCOP)Ir (**31**) was lower (2070 turnovers after 40 h at 200°C) than **32** but comparable to (p-C_6F_5-^{tBu4}POCOP)Ir (**26**) (Fig. 2.5) [52].

Huang and co-workers reported that the COA/TBE (1:1) transfer dehydrogenation [65] with a sulfur variant (^{iPr4}PSCOP)Ir (**30**) (Fig. 2.4) proceeded at a very fast rate (2900 TOh^{-1} at 200°C) whereas the corresponding reaction with (^{tBu4}PCP)Ir (**5**) and (^{tBu4}POCOP)Ir (**22**) proceeded at 1200 TOh^{-1} and 6900, respectively [52]. In the (^{iPr4}PSCOP)Ir (**30**) catalyzed dehydrogenation reactions, complete consumption of TBE occurred after 8 h, but in the case (^{tBu4}POCOP)Ir (**22**) the reaction leveled off after 6 h and gave only 62% conversion. In the case of *n*-octane dehydrogenation using 0.5 M TBE, Huang's catalyst (^{iPr4}PSCOP)Ir (**30**) was more effective (1400 TOh^{-1}) than both (^{tBu4}POCOP)Ir (**22**) (220 TOh^{-1}) and (^{tBu4}PCP)Ir (**5**) (820 TOh^{-1}). Notably, at comparable turnovers (c. 115), both **30** and **5** demonstrated similar regioselectivities (c. 30%).

2.2.4 Mechanism of pincer–Ir-catalyzed alkane dehydrogenation

The generally accepted mechanism for the pincer–Ir-catalyzed AD and the associated isomerization is provided in Scheme 2.5 using butane and TBE as model substrates [66–68]. The first step of the reaction mechanism involves the insertion of TBE into the Ir–H bond in **33** to give **34**.

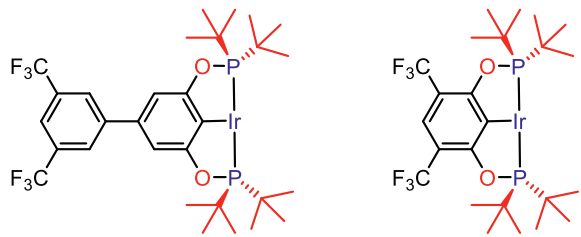

Wendt

Figure 2.5 Fluorine containing POC(sp^2)OP pincer–Ir complexes reported for alkane dehydrogenation.

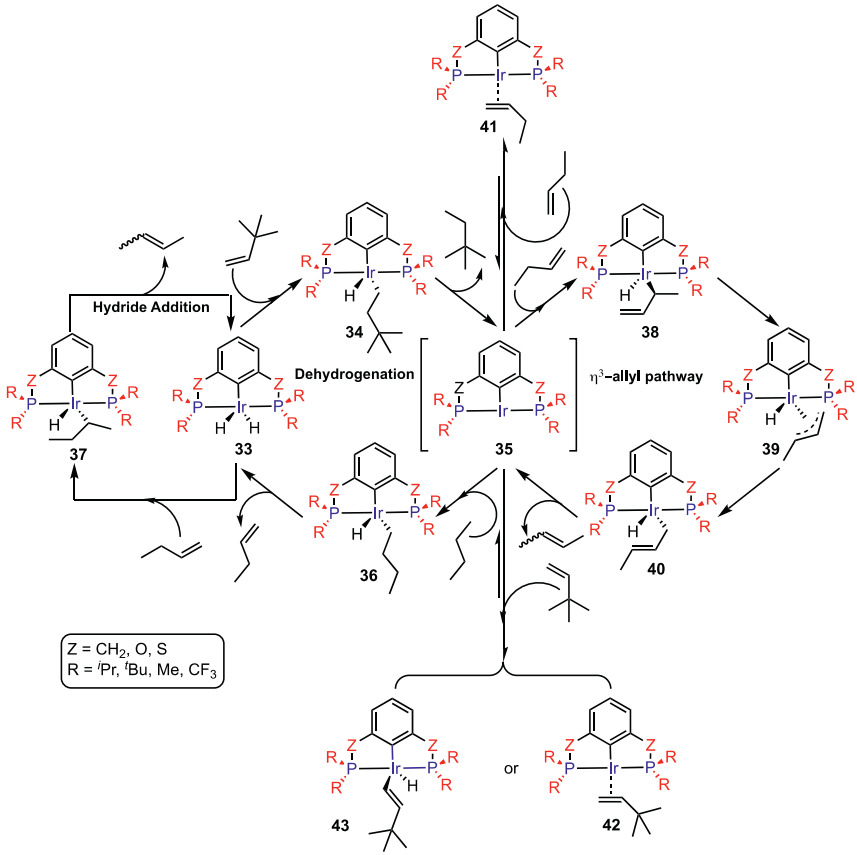

Scheme 2.5 Mechanistic pathway involved in the pincer–Ir-catalyzed *n*-alkane/TBE transfer dehydrogenation and the associated α-olefin isomerization.

A reductive elimination of TBA from **34** generates catalytically active 14-electron species **35**. Oxidative addition of the terminal C-H bond in butane on to the Ir in **35** produces intermediate **36**. The β-hydride elimination from **36** results in the release of the α-olefin along with the regeneration of the active species **33** (Scheme 2.5**)**. Subtle variations in this generalized pathway may be observed depending on the type of pincer–Ir precursor used.

The resting state in a reaction cycle depends on the bulkiness of the attached groups. Sterically crowded pincer–Ir complexes such as (^{tBu4}PCP)Ir (**5**) in the absence of strongly binding olefins favors the formation of dihydride metal complex **33** as the catalyst resting state. In the presence of olefin, the resting state preference shifts to Ir-olefin complexes

41 or **42** or **43**. In presence of α-olefins catalytically active species **35** forms complex **41** in preference to both **42** or **43**. Less bulky pincer–Ir complexes, on reaction with TBE, readily form the π-complex **42**. In contrast, sterically crowded complexes such as ($^{t\text{Bu4}}$PCP)Ir (**5**) reacts with TBE to form a vinyl hydride complex **43**. The preference of the catalyst toward various resting states determines its efficiency as a function of substrate and reaction conditions. Higher acceptor concentrations and sterically less hindered acceptors would accelerate the activity of a catalyst whose resting state is a dihydride complex **33** [13].

The dehydrogenation of *n*-alkanes catalyzed by pincer–Ir complexes mostly give α-olefin as a kinetic product, which subsequently undergoes isomerization in the presence of the catalyst to yield the thermodynamically more stable internal olefin. The isomerization reaction of the olefin occurs through "hydride-addition pathway" or "η^3-allyl pathway" (Scheme 2.5). The dihydride catalyst **33** interacts with the α-olefin and 2,1 addition of the Ir–H bond of **33** to the double bond of α-olefin leads to 2-alkyl hydride **37**. In next step, 3,2-β-hydride elimination from **37** produces the dihydride catalyst **33** and an internal olefin. This isomerization cycle is known as "hydride-addition pathway." Jespersen, Goldman, and Brookhart's experimental studies, well-complemented by DFT calculations, indicated that for sterically bulky complexes such as ($^{t\text{Bu4}}$PCP)Ir (**5**) and ($^{t\text{Bu4}}$POCOP)Ir (**22**), the "η^3-allyl pathway" was more favorable than "hydride-addition pathway" [67]. In the "η^3-allyl pathway," three coordinated 14-electron species **35** undergoes oxidative addition of the internal C–H bond of the α-olefin to form 16-electron η^1-ally hydride complex **38**. To achieve higher stability (18-electron configuration), **38** expands its hapticity from η^1 to η^3 and forms 18-electron η^3-allyl complex **39**. In the next step, isomerization occurs and **39** converts to 16-electron η^1-allyl hydride complex **40**. Reductive elimination of C–H from **40** regenerates the three-coordinate, 14-electron species **35** along with the formation of isomerized internal olefin [67].

The "η^3-allyl pathway" was confirmed experimentally by looking into the ($^{t\text{Bu4}}$PCP)Ir (**5**) and ($^{t\text{Bu4}}$POCOP)Ir (**22**) catalyzed isomerization of 1-octene at 125°C [67]. The analog of **41** was the resting state of ($^{t\text{Bu4}}$PCP)Ir (**5**) and ($^{t\text{Bu4}}$POCOP)Ir (**22**) under the isomerization conditions. Very small concentration of the dihydride **33** could significantly contribute toward catalytic 1-octene isomerization via the "hydride-addition pathway." This tiny steady-state concentration of dihydride **33** would be much greater in *n*-octane as compared to that in *p*-xylene. Goldman and

Brookhart have shown that catalytic isomerization of 1-octene using (^{tBu4}PCP)Ir (**5**) [5 mM] and (^{tBu4}POCOP)Ir (**22**) [5 mM] proceeded at identical rates in both *n*-octane and *p*-xylene [67]. This led to the inference that "η^3-allyl pathway" is the sole contributor in olefin isomerization when (^{tBu4}PCP)Ir (**5**) and (^{tBu4}POCOP)Ir (**22**) are employed as catalysts. However, with less bulky (^{iPr4}PCP)Ir(η^2-C_2H_4)(**4-C_2H_4**) catalysts, the olefin isomerization was found to proceed via both the "hydride-addition" and "η^3-allyl" pathways [43].

To prove "η^3-allyl pathway," low-temperature NMR experiments involving (^{tBu4}POCOP)Ir (**22**) and allene were carried out (Scheme 2.6) [67]. Addition of allene to (^{tBu4}POCOP)Ir(H_2) (**22-H_2**) at −88°C formed (^{tBu4}PCP)Ir(η^3-ally)H (**44**) and (^{tBu4}PCP)Ir(propenyl)H (**45**), both of which were found to isomerize to (^{tBu4}POCOP)Ir(η^2-propene) (**46**) (Scheme 2.6) [67]. CCC pincer−Ir-catalyzed isomerization of alkene through the "η^3-allyl pathway" was reported by Chianese in 2014 [68].

2.2.5 Solid/gas-phase alkane dehydrogenation

Very recently, Goldman reported the molecular solid-phase (^{iPr4}PCP)Ir(η^2-C_2H_4)(**4-C_2H_4**) catalyzed transfer dehydrogenation of gas-phase light alkanes with ethylene and propene as acceptors at 200°C−240°C [43]. The gas-phase dehydrogenation reaction catalyzed by solid-phase catalyst showed higher activity and TONs than the corresponding solution phase

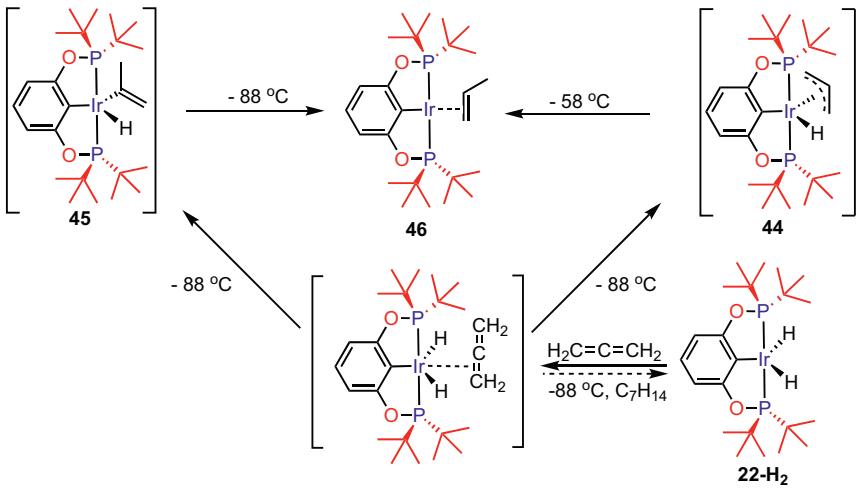

Scheme 2.6 Evidence for η^3-allyl pathway obtained from the reaction of (^{tBu4}POCOP)Ir (**22**) with allene.

experiments [43,69]. In contrast to typical heterogeneous catalysts, these solid-phase catalysts led to higher regioselectivities. The solution-phase kinetics experiments were used as a comparison to explain the high selectivity of solid-phase catalysts.

The alkene isomerization catalyzed by ($^{i\text{Pr4}}$PCP)Ir (**4**) occurs via both "hydride-addition path" and the "η^3-allyl pathway." However, the theoretical calculations indicate that the "η^3-allyl pathway" is much slower than the dehydrogenation of alkane [43]. The higher concentration of dihydride metal Ir complex **33** is disfavored under solid–gas-phase conditions (which operates at a very low concentration of alkane and high concentration of acceptor). These factors ensure a very high yield of α-olefin under the solid–gas-phase conditions where the possibility of isomerization via the "hydride-addition path" is almost absent [43].

It is observed that the catalyst ($^{i\text{Pr4}}$PCP)Ir(η^2-C_2H_4)(**4-C_2H_4**) is more active than ($^{t\text{Bu4}}$PCP)IrH_2 (**5-H_2**) for both the liquid-phase and solid–gas-phase reactions [40]. The dehydrogenation of *n*-octane/ethylene (4 atm) at 200°C catalyzed by **4-C_2H_4** [1 mM] resulted in 1-octene which is about 2.5-folds higher than that obtained with *n*-octane/1-decene [0.5 M] catalyzed by **5-H_2** at 150°C [40]. The dehydrogenation of *n*-pentane/ethylene (4 atm) in the gas phase at 240°C catalyzed by **4-C_2H_4** [1 mM] yielded a maximum of 520 mM of α-olefin [43].

2.2.6 Continuous-flow gas-phase alkane dehydrogenation

Rather than using economical acceptors, industrially, it would be more relevant to use such selective catalysts in an acceptorless and continuous-flow system. Continuous-flow systems allow better control on reaction pressure, temperature, and residence time of the reagents thus providing access to conditions not typically available to batch systems. Unlike batch reactors, the products in continuous-flow reactors are constantly siphoned out, which mitigates the possibility of secondary reactions or catalyst inhibition by-products. To achieve continuous-flow systems with molecular catalysts, the complex has to be immobilized on solid supports.

The AD reaction is well established by homogeneous pincer–Ir catalysts but solid-supported heterogenized molecular catalysts are moderately effective for AD. In 2008, Alt and co-workers reported that silica gel supported heterogenized phosphorus-containing compounds in combination with iridium complex were active for the dehydrogenation reaction [69–71]. The activity of the catalyst was heavily dependent on PPh_3 ligand. The external addition

of PPh_3 to the reaction mixture increased the activation of the alkane (isopentane) [69]. The catalytic activity increased with temperature and it was proposed that at 350°C there was a formation of a new species which were catalytically more active than the initial catalyst.

Pincer complexes having polar groups on the ligand backbone could be heterogenized on a variety of solid surfaces yielding recyclable AD catalysts [42]. A few of such reports include PC(sp^2)P-Ir [45,72], PC(sp^3)P-Ir [73] and POCOP-Ir [45,72] based catalysts that have been anchored on to florisil, alumina, and silica via polar groups (−OK, −OH, −OMe, $-NMe_2$, and $-CO_2H$) [42]. The activity was found to depend on the polarity of anchored groups present on *para*- position [42].

For AD, an Ir(I)/Ir(III) couple is required; in the absence of polar substituents, oxidative addition of the solid-supported hydroxyl groups occurs at the pincer−Ir(I) center to irreversibly generate a pincer−Ir(III) center, which renders it inefficient for AD, due to its inability to generate the required Ir(I)/Ir(III) couple [74−77].

Very recently in 2018, Celik and co-workers reported silica-supported (p-^{t}Bu$_2$PO-$^{t\text{Bu}4}$POCOP)Ir(C_2H_4) (***p*-^{t}Bu$_2$PO-22-C_2H_4**) active model catalyst for continuous-flow gas-phase acceptorless AD system [78]. This solid-supported catalyst is thermally stable at temperatures up to 340°C whereas the analogous homogeneous complexes have been reported to show stable activity at 240°C [31]. Supporting the complex (p-^{t}Bu$_2$PO-$^{t\text{Bu}4}$POCOP)Ir(C_2H_4) resulted in formation of ***p*-SiO$_2$−22-C_2H_4**. Here, the pincer backbone is covalently bound to SiO_2. The interaction of ***p*-^{t}Bu$_2$PO-22-CO** with silica is similar to ***p*-^{t}Bu$_2$PO-22-C_2H_4** [78,79]. On the other hand, the dihydride analog ***p*-^{t}Bu$_2$PO-22-H_2** interacts with silica in a different way. The oxidative addition of surface hydroxyl groups onto the Ir center in ***p*-^{t}Bu$_2$PO-22-H_2** forms **22-H-SiO$_2$**, which was inactive for dehydrogenation of alkane [74−77]. The ***p*-^{t}Bu$_2$PO-22-C_2H_4** catalyzed AD had ***p*-SiO$_2$−22-C_2H_4** as the resting state below 300°C and ***p*-SiO$_2$−22-CO** as the resting state above 300°C. The catalytically active 14-electron species ***p*-SiO$_2$−22** is generated either by the dissociation of CO or C_2H_4 (Scheme 2.7). The catalyst ***p*-SiO$_2$−22-C_2H_4** was active within the temperature range of 200°C−300°C. The activity of catalyst ***p*-SiO$_2$−22-C_2H_4** was found to increase gradually with temperature and a mixture of ***p*-SiO$_2$−22-C_4H_8** and ***p*-SiO$_2$−22-CO** were found to be the resting states. Above 300°C, ^{31}P MAS NMR analysis indicated that ***p*-SiO$_2$−22-CO** was the sole resting state [78].

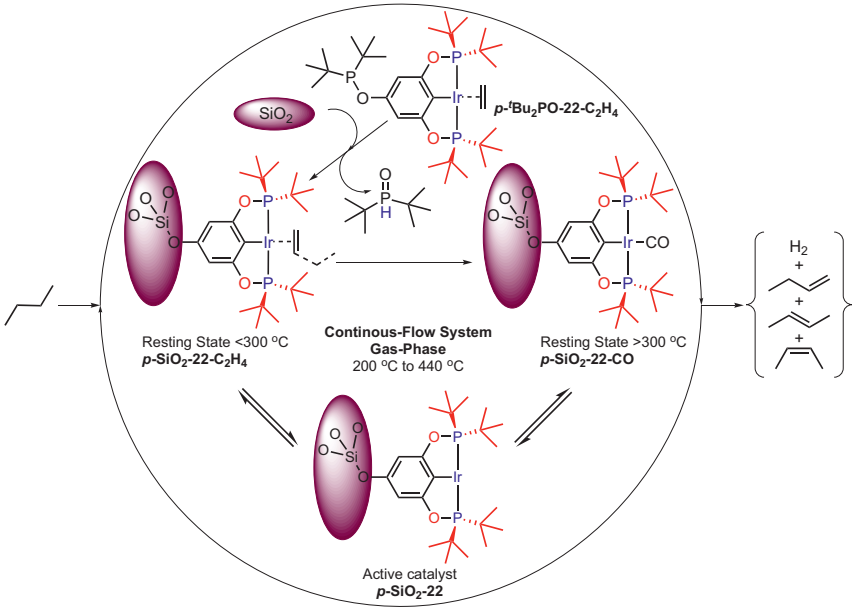

Scheme 2.7 Various intermediates involved in continuous-flow gas-phase alkane dehydrogenation catalyzed by ***p*-^{t}Bu$_2$PO-22-C$_2$H$_4$** supported on silica.

The kinetic profile of the dehydrogenation reaction starting with ***p*-SiO$_2$–22-C$_2$H$_4$** and ***p*-SiO$_2$–22-CO** were identical in the temperature range 340°C to 440°C. Similar deactivation mechanism and kinetics were observed for the reaction starting with ***p*-SiO$_2$–22-C$_2$H$_4$** or ***p*-SiO$_2$–22-CO** at these temperatures [78]. However, below 300°C, the dissociation of C_2H_4 from the Ir center being preferable due to the labile character of ethylene, ***p*-SiO$_2$–22-C$_2$H$_4$** shows a better activity than *p*-**SiO$_2$–22-CO** that has a strongly binding CO ligand.

Celik demonstrated that the dissociation of CO from ***p*-SiO$_2$–22-CO** generates the active 14-electron, three-coordinate species ***p*-SiO$_2$–22** (Scheme 2.7). This dissociation of CO is slow below 300°C and fast above 300°C. Notably, these carbonyl pincer–Ir systems are tolerant toward moisture and air. From XPS analysis, it was observed that above 340°C, loss of pincer ligand and oxidation of Ir(I) to Ir(III) was responsible for the lower activity in the continuous-flow gas-phase AD.

2.2.7 Alkane dehydrogenation by PC(sp^3)P–Ir complexes

Dmitri Gelman and co-workers developed the barrelene-type scaffold, namely, 1,8-*bis*(diisopropylphosphino)triptycene ligand, a new class of

sp^3-carbometalated complexes [80,81]. The C(sp^3) metalated compound **49** exhibited very high thermal and conformational stability even under very harsh and non-inert conditions. The stability of the complex is due to lack of labile R- or β-hydrogens [80]. The transfer dehydrogenation of COA/TBE (1:1) catalyzed by **49** [1.3 mM] resulted in 900 and 2590 TONs after 30 min and 4 h, respectively. The catalyst ($^{t\text{Bu4}}$POCOP)Ir (**22)** under identical conditions gives better initial turnovers (1400 TONs after 30 min) before leveling off at 1800 TONs after 4 h [73]. Wendt reported that among the PC(sp^3)P-Ir complexes **47** and **48** [82,83] (Fig. 2.6), while **48** was inactive for AD, **47** gave only 50 TONs after 20 h in the COA/TBE (1:1) transfer dehydrogenation at 200°C. The low activity can be attributed to low thermal stability as a result of C(sp^3)-H elimination, which is more facile than C(sp^2)-H elimination. Brookhart tested catalysts based on (^{R}triptycenePC(sp^3)P)Ir(η^2-C_2H_4) (**49**, R = ^{i}Pr; **50**, R = Cy; **51**, R = Cp) for the transfer dehydrogenation of alkanes [73]. The transfer dehydrogenation of *n*-octane (with 6 M TBE) at 200°C with complex **49** gives very high initial rates (2400 TOh^{-1}) and unprecedented conversions (6000 TONs in 10 h). The catalyst **49** is very active even at very low temperature (100°C) where a complete conversion was observed for *n*-octane/TBE [0.5 M] dehydrogenation [73]. The analogous complexes **50** (35 TONs after 24 h) and **51** (40 TONs after 24 h) are much less active for AD. The complexes **52** and **53** that were obtained by the introduction of methoxy groups on the triptycene fragment by the Gelman group showed very poor activity in comparison to **49** [84].

Brookhart and co-workers used **52** for the transfer dehydrogenation of alkane in both homogeneous and heterogeneous fashion [73]. Transfer

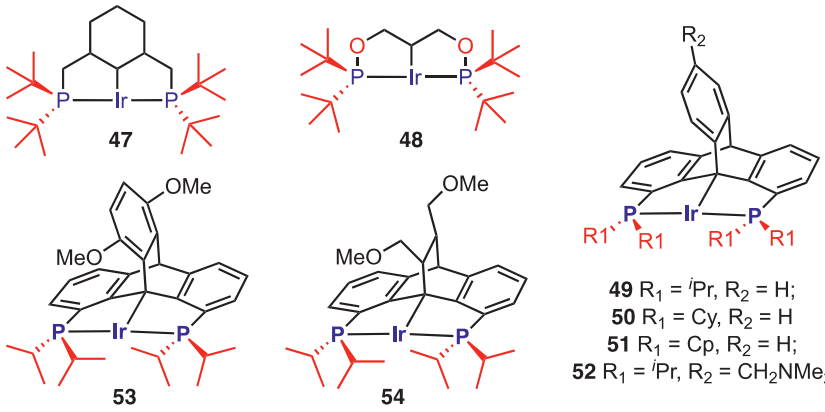

Figure 2.6 PC(sp^3)P pincer–Ir complexes reported for alkane dehydrogenation.

dehydrogenation of COA/TBE (1:1) with **49** (2800 TONs after 20 h) and its derivative **52** (2040 TONs after 20 h) were comparable under homogeneous reaction conditions at 200°C. The complex **49** when attempted to anchor on to alumina (γ or neutral) gave very poor result (20 TONs after 20 h) [73], which shows that the catalysts that lack polar substituents are deactivated by alumina [45,72]. The heterogeneous catalytic systems based on **54** were not recyclable in nature. After 20 h, the transfer dehydrogenation of COA/TBE (1:1) at 200°C with **49** gave 1250, 185, and 70 TONs when anchored on low-soda alumina, γ-alumina, and acidic alumina, respectively.

2.2.8 Alkane dehydrogenation by POCN–Ir, PBP–Ir, PNP–Ir, and PAlP complexes

Alkane dehydrogenation by (POCN)Ir was reported by Huang and coworkers. They synthesized (^{tBu2}NCOP)Ir(H)(Cl) (**55**–**57**) (Fig. 2.7) and carried out COA and *n*-octane transfer dehydrogenation at 150°C in the presence of TBE [0.5 M] [85]. Among **55**, **56**, and **57**, the highest activity

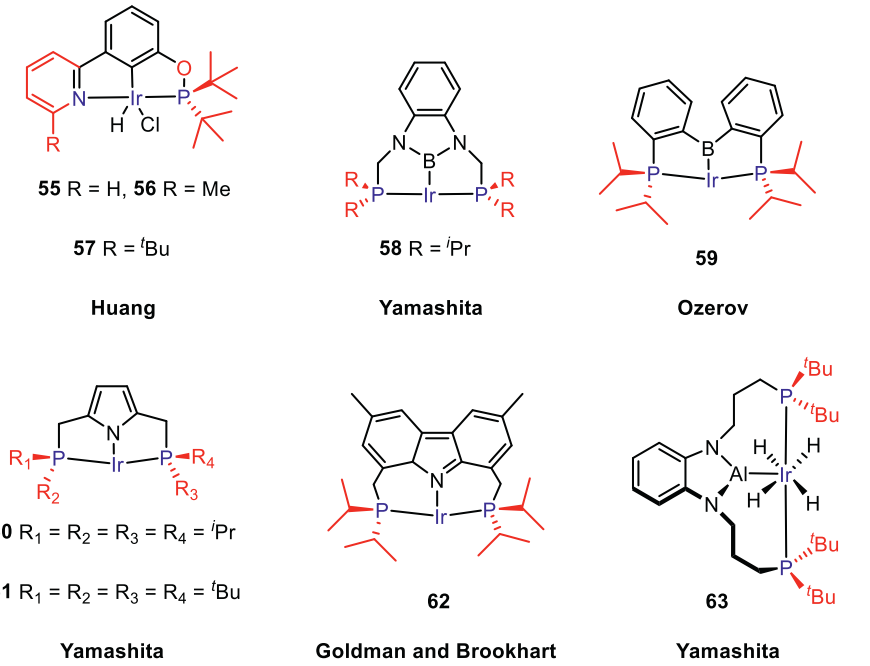

Figure 2.7 POCN–Ir, PBP–Ir, PNP–Ir, and PAlP type pincer complexes that have been studied for alkane dehydrogenation.

(1100 TOh^{-1}) was observed with **55** along with the highest TONs (470) for the COA/TBE dehydrogenation.

In the COA dehydrogenation catalyzed by **55**, the activity (425 TOh^{-1}) was inhibited at higher concentration of TBE [2.5 M]. Notably, the steric hindrance of other catalysts (**56**, **57**) inhibited their activity. In the case of transfer dehydrogenation of *n*-octane with TBE [0.5 M] at 150°C, initial rates of 325, 84, and 60 TOh^{-1} were observed for the catalyst **55**, **56**, and **57**, respectively.

Boron containing PBP pincer ligands and their corresponding iridium complexes (^{iPr4}PBP)Ir(H)(Cl) (**58-HCl**) and (^{iPr4}PBP)Ir(η^2-C_2H_4) (**58-C_2H_4**) complexes were reported by Yamashita and Tanoue [86]. Poor catalytic activity was observed with these complexes for the transfer dehydrogenation of COA [3.9 M]/TBE [3.9 M] at temperatures ranging between 160°C and 220°C. In presence of lithium 2,2,6,6-tetramethylpiperidide [2 mM], 1.3 mM of **58-HCl** gave 43 TONs in the COA [3.9 M]/TBE [3.9 M] transfer dehydrogenation at 220°C. Ozerov and coworkers also observed poor activity in AD catalyzed by (PBP)Ir complex **59** [87].

The pyrrole-based (PNP)Ir complexes (**60**, **61**) were synthesized by Yamashita and co-workers (Fig. 2.7**)** and were used for transfer dehydrogenation of COA in the presence of TBE [88]. The derivative [(^{iPr4}PNP)Ir]$_2$(μ^2-COD) of **60** exhibited poor catalytic activity at 220°C and a maximum of 28 TONs were obtained. The (PNP)Ir complex based on carbazolide ligand **62** was reported by Goldman and Brookhart [89], but was found to be inactive for AD.

In 2019, Yamashita and co-workers reported (PAIP)Ir(H)$_4$ (**63**) complex for AD [90] (Fig. 2.7). The computational studies suggested that the complex was associated with alumanyl-Ir^Vtetrahydride rather than bridging hydride ligands and this was further confirmed by AIM analysis [91]. Very low TONs of 31 were obtained when the transfer dehydrogenation of COA with 1-hexene as a hydrogen acceptor was carried out in the presence of (PAlP)Ir(H)$_4$ (**63**) (COA:**63** = 3000:1) at 180°C [90]. This is the first report of AD with homogeneous pincer−Ir complex based on alumanyl ligand.

2.2.9 Alkane dehydrogenation by PXC(sp^2)NP-Ir-HCl (X = O, S) complexes

Very recently, Zheng and co-workers reported PXC(sp^2)NP-Ir-HCl (X = O, S) complexes (**64-HCl-71-HCl**) for transfer dehydrogenation of

alkane (Fig. 2.8) [92]. The transfer dehydrogenation of COA with TBE was carried out in the presence of **64–71** under varying ratios of COA/TBE/Ir/NaO^{t}Bu (**a**, 3000/3000/1/3; **b**, 3000/1000/1/3; **c**, 15,000/15,000/1/15) at 200°C. The catalytic activity and TONs with the considered catalysts are shown in Table 2.4. The low activity of **65-HCl** and **70-HCl** is attributed to catalysis inhibition by TBE. The productivity of transfer dehydrogenation of COA with TBE in the presence of isopropyl analogous complexes follows the trend: **71**, **68**, **64** > **21** > **30** > **69** > **4** [92].

The transfer dehydrogenation of *n*-octane/TBE was carried out in the presence of activator NaO^{t}Bu at 200°C under ratio of *n*-octane/TBE/Ir/NaO^{t}Bu (3000/3000/1/3) using **30-HCl**, **65-HCl**, **68-HCl**, and **71-HCl** and mixture of alkenes was obtained [92]. The acceptorless dehydrogenation of 1,2,3,4-tetrahydronaphthalene was also carried out in the presence of NaO^{t}Bu [18.6 mM] along with the iridium precatalysts [3.1 mM] (**21-HCl**, **30-HCl**, **64-HCl**, **68-HCl** and **71-HCl**) at 250°C to obtain naphthalene. The TONs steadily increased with time and 3892 TONs were obtained in the case of **64-HCl** after 19 h [92].

2.2.10 Alkane dehydrogenation by non-phosphine-based iridium pincer complexes

Alkane dehydrogenation reactions have been well explored by using phosphine-based iridium complexes. Recently, AD has also been reported with pincer–iridium complexes based on non-phosphine ligands such as CCC [68,88,89,93], AsOCOAs [94], and NCN [95]. In 2010, Chianese and co-workers reported the use of CCC pincer–Ir complexes (**72–77**) based on *bis*(N-heterocyclic carbene) ligands (Fig. 2.9) for the acceptorless dehydrogenation of alkanes [68,88,89,93]. In the case of acceptorless cyclooctane (bp 150°C) dehydrogenation, 103, 84, and 35 TONs were obtained with **74**, **75**, and **77**, respectively after 22 h. On the other hand,

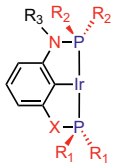

64 X = O, $R_1 = R_2 = {}^i$Pr, R_3 = Me; **65** X = O, $R_1 = R_2 = {}^t$Bu, R_3 = Me;

66 X = O, $R_1 = {}^i$Pr, R_2 = Cy, R_3 = Me; **67** X =O, R_1 = Cy, $R_2 = {}^i$Pr, R_3 = Me;

68 X = O, $R_1 = R_2 = {}^i$Pr, R_3 = Et; **69** X = S, $R_1 = R_2 = {}^i$Pr, R_3 = Me;

70 X = S, $R_1 = R_2 = {}^t$Bu, R_3 = Me

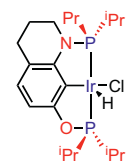

Zheng Huang **71**

Figure 2.8 PXC(sp^2)NP pincer–Ir complexes investigated by Zheng Huang for alkane dehydrogenation.

Table 2.4 Transfer dehydrogenation of COA with TBE with different PXC(sp^2)NP-Ir-HCl (X = O, S) complexes.

Entry	Catalysts	Conditions	Time (h)	TONs
1	**64-HCl**	**a**	1	2980
		c	15	12,690
2	**65-HCl**	**a**	15	212
		b	15	440
3	**66-HCl**	**a**	15	146
		b	15	1000
4	**67-HCl**	**a**	15	420
		b	15	1000
5	**68-HCl**	**a**	1	3000
		c	15	13,870
6	**69-HCl**	**c**	15	2310
7	**70-HCl**	**a**	15	420
		b	15	1000
8	**71-HCl**	**a**	1	3000
		c	15	14720
9	**4-HCl**	**a**	1	1146
		c	15	2100
10	**21-HCl**	**a**	1	2145
		c	15	10,050
11	**30-HCl**	**a**	1	2725
		c	15	6700

the complexes **72**, **73**, and **76** gave poor results under similar conditions. There was hardly any change in activity of **74** upon addition of COE. Use of high-boiling alkane (cyclodecane) did not help to improve the activity of **74**. The activity of **74** was by large mitigated due to decomposition rather than COE inhibition. [68,88,89,93] Both Ar and N_2 atmosphere resulted in comparable reactivity (100 TONs after 22 h). However, in the presence of air, only 5 TONs were observed.

The acceptorless dehydrogenation of *n*-undecane was also reported with **74** and **75** but poor yields (c. 50 TONs) were observed. On the other hand, the catalyst **77** showed 97 TONs in 22 h for the acceptorless dehydrogenation of *n*-undecane [68,88,89,93]. The dehydrogenation of *n*-undecane is associated with the isomerization of terminal olefins to internal olefins and internal undecenes were observed as final products in the presence of **77** and the results were comparable with the (PCP) iridium systems developed by Goldman group [44].

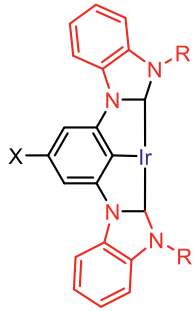

72 X = H, R = ^{t}Bu; **73** X = H, R = Ad;

74 X = H, R = mesityl;

75 X = CF_3, R = mesityl;

76 X = H, R = 2,6-diisopropyl phenyl;

77 X = H, R = 3,5-di-t-butylphenyl

Chianese

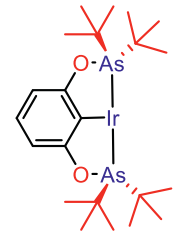

78

Jensen

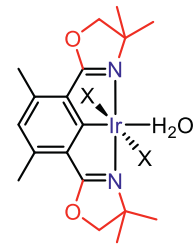

79 X = OAc

Goldberg, Goldman

Figure 2.9 Nonphosphine-based pincer–Ir complexes employed for alkane dehydrogenation.

The transfer dehydrogenation of COA was also reported with arsine oxide-based pincer catalyst (^{tBu4}AsOCOAs)IrH_2 (**78-H_2**) (Fig. 2.9**)** by Jensen and co-workers [94]. The transfer dehydrogenation of COA with TBE in the presence of (^{tBu4}AsOCOAs)IrH_2 (**78-H_2**) [1 mM] carried out at 200°C furnished 300 TONs after 30 min [94], which is very low (three- to fourfold) when compared with that obtained with the phosphine oxide analog **22-H_2** [52,65]. The reaction ultimately leveled off after providing 930 turnovers after 24 h. The catalytic activity was found to increase with increase in temperature (330 TONs at 125°C to 960 TONs at 175°C). Above 175°C, the catalyst **78-H_2** started to decompose and gave lower yields and TONs. A total of 930 TONs were obtained after 24 h when the reaction was carried out at 200°C.

In 2012, Nishiyama and co-workers performed the reaction of *n*-octane with (^{dm}phebox)$Ir(OAc)_2(H_2O)$ (**79**) in the presence of K_2CO_3 at 160°C to produce (^{dm}phebox)Ir(OAc)(*n*-octyl) (**89**) (Scheme 2.9) [95]. Goldberg, in 2013, demonstrated the use of (^{dm}phebox)$Ir(OAc)_2(H_2O)$

(**79**) for the stoichiometric dehydrogenation of *n*-octane at 200°C to give octenes and (^{dm}phebox)Ir(OAc)(H) (**84**) via the intermediacy of (^{dm}phebox)Ir(OAc)(*n*-octyl) (**89**) (Scheme 2.8 and Scheme 2.9) [96].

1-octene was obtained as a major product after 3 h at 30% octane conversion. However, after 120 h, the product contained a mixture of internal octenes. Independent experiments were carried out to confirm that (^{dm}phebox)Ir(OAc)(H) (**84**) catalyzes the isomerization of the initially formed 1-octene. The dehydrogenation was found to proceed via the intermediacy of (^{dm}phebox)Ir(OAc)(*n*-octyl) (**89**). The mechanism of (^{dm}phebox)Ir(OAc)$_2$(H$_2$O) (**79**)-mediated dehydrogenation of *n*-octane involved C−H activation at Ir(III) center in stark contrast to phosphine-based pincer−Ir system where the C−H activation occurred at the Ir(I) center [97]. It was observed that addition of water (120 equiv.) increased the yield (by about 33%) of *n*-octane dehydrogenation mediated by (^{dm}phebox)Ir(OAc)$_2$(H$_2$O) (**79**). In the presence of molecular oxygen, (^{dm}phebox)Ir(OAc)(H) (**84**) led to the formation of (^{dm}phebox)Ir(OAc)$_2$(H$_2$O) (**79**) at room temperature [97]. It is noteworthy that the transformation of **84** → **79** offers immense promise to complete a hypothetical catalytic cycle **79** → **89** → **84** → **79** (Scheme 2.9). Goldman accomplished the (^{dm}phebox)Ir(OAc)(H) (**84**) catalyzed acceptorless dehydrogenation of alkanes at 200°C that proceeded via a cycle involving **84** ↔ **89** cocatalyzed by various Lewis acids (Scheme 2.9) [98].

The acceptorless dehydrogenation of alkanes was further investigated by the Jones group in detail where they have developed (^{dm}phebox)Ir complexes (**80**−**83**) by varying the carboxylate ligands [78]. They noted that the β-H elimination step was dependent on carboxylate ligands but in the case of C−H activation, the carboxylate ligand had no effect [99]. The octane formation with (^{dm}phebox)Ir complexes followed the order **83** > **82** > **81** > **80** > **79**.

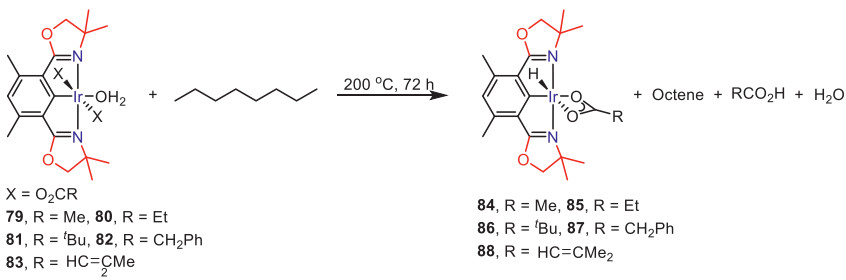

Scheme 2.8 Alkane dehydrogenation by NCN pincer complexes.

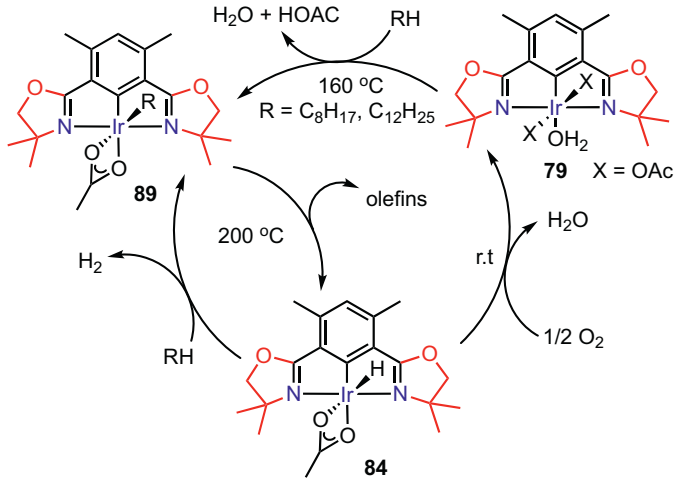

Scheme 2.9 Hypothetical catalytic cycle for alkane dehydrogenation by NCN pincer complex.

2.3 Dehydrogenation of alkanes by pincer–metal complexes other than iridium

2.3.1 Ruthenium pincer complexes for alkane dehydrogenation

Group 8 metal complexes have not much been reported for AD as compared to iridium complexes. Roddick and co-workers were the first to report the (^{CF3}PCP)Ru complexes for AD [100,101]. They have shown that unlike iridium, in which Ir(I) is the active catalytic species, in the case of ruthenium, it is Ru(II) hydride species that takes part in the catalytic cycle (Scheme 2.10). Similar results have been obtained with osmium by the same group [102].

The Roddick group expected to generate (^{CF3}PCP)RuH(H_2)$_2$ by reaction of (^{CF3}PCP)Ru(COD)H (**93**) with H_2 but instead got ruthenium dimeric complex **94** with the loss of COD. On the addition of excess COD, the complex **94** converted back to **93** (Scheme 2.11). The treatment of 12 mM of **93** with COA resulted in only 3 TONs in 10 min and whole of the catalyst got converted to dimeric complex **94**. Upon catalyzing the reaction of equimolar amounts of COA and TBE with lower amounts of catalyst **93** [6 mM], the reactivity increased slightly to 18 TONs with full conversion of **93** to **94**.

In the presence of two equivalents of COD, only 4 TONs of the product were obtained with **93** as the resting state of the catalyst that is

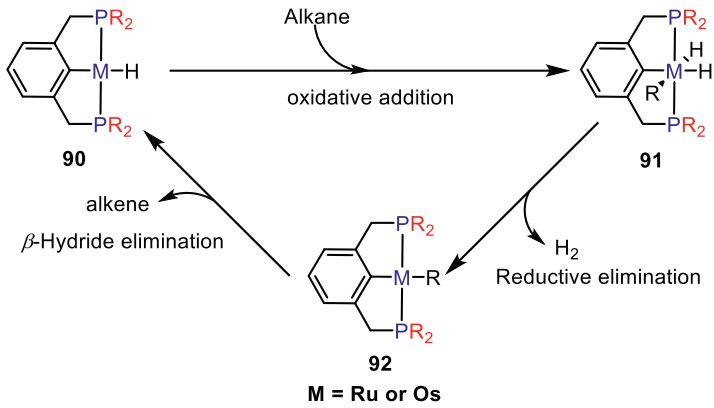

Scheme 2.10 Dehydrogenation of alkane catalyzed by group 8 pincer–metal complexes.

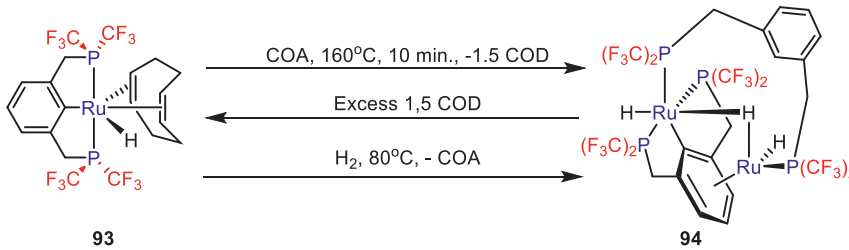

Scheme 2.11 Formation of dimeric Ru complex **94** from **93** on treatment with H_2 and COA.

indicative of inhibition of catalysis by COD. Under similar conditions at lower loading of the catalyst [1.25 mM], reaction proceeded at the rate of 180 TOh^{-1} at 150°C and 1000 TOh^{-1} at 200°C. At 150°C, the reaction stopped after 3 h and 164 TONs were obtained while at 200°C, 180 TONs of the dehydrogenated product were obtained within 30 min. COE was also found to inhibit the activity of the catalyst **93**. One of the most noteworthy observations in the transfer dehydrogenation of COA/TBE catalyzed by **93** was that the reaction was not sensitive to water (100 equiv.), N_2, or O_2 atmosphere.

Transfer dehydrogenation of alkanes (COA/TBE) using pincer–ruthenium complexes (**95**–**99**) have recently been reported by the Huang group (Fig. 2.10) [103]. Initially the complex (^{iPr4}POCOP)Ru(NBD)(H) (**95**; NBD = norbornadiene) was studied for the transfer dehydrogenation of COA/TBE at different concentrations of TBE

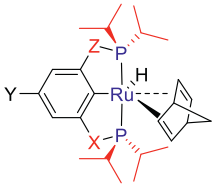

95, X = Z = O, Y = H
96, X = Z = O, Y = C_6F_5
97, X = Z = CH_2, Y = H
98, X = O, Z = S, Y = H

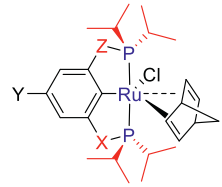

99, X = Z = O, Y = C_6F_5

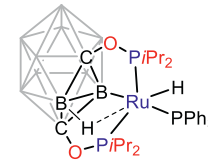

100

Figure 2.10 Ruthenium pincer complexes reported for alkane dehydrogenation.

[0.1–0.8 M]. The reaction was performed at 200°C and complete conversion was observed at lower concentrations of TBE [0.1–0.3 M] [103]. A maximum 306 TONs were obtained with 0.35 M TBE. Higher TBE concentrations [0.4–0.8 M] resulted in inhibition of catalysis.

For the transfer hydrogenation of COA with TBE [0.35 M] at 200°C, the highest catalytic activity was observed with complex **96** (TOFs: 420 h^{-1}; 322 TONs) that was electronically deficient among all the catalysts screened. Initial rate of dehydrogenation was higher (but with lower TONs) for PCP complex **97** (TOFs: 1130 h^{-1}; 260 TONs) as compared to **96** (TOFs: 420 h^{-1}; 322 TONs) and **95** (TOFs: 120 h^{-1}; 306 TONs). Interestingly and contrary to one's expectations, the chloro-substituted complex **99** was also active (TOFs:390 h^{-1}; 240 TONs). Very less TONs were obtained with PSCOP complex **98** (8 TONs after 4 h).

There was no effect on the dehydrogenation rate when complex **96** was treated under an atmosphere of N_2 or air and in the presence of polar additives such as acetone, ethyl acetate, and diethyl ether. The dehydrogenation of *n*-octane with the complexes **95–97** gave poor TONs possibly due to inhibition of the catalysts by α-olefins. Acceptorless dehydrogenation of COA was performed with complex **96** and very low TONs were obtained (39 TONs after 12 h). The same reaction was performed in sealed vessel and surprisingly no decrease in TONs was observed [103].

Later, in 2017, Popov and Peryshkov synthesized pincer–metal complex included in a carborane cage (POBOP)Ru(H)(PPh_3) (**100**) and applied it for the transfer dehydrogenation of COA/TBE system [104]. In the presence of N_2 and air at 170°C, TONs up to 400 and 288 were obtained, respectively. For the dehydrogenation of *n*-octane, the regioselectivity to 1-octene was very low and only 85 TONs were observed. The result was similar to what was obtained with the complex **96** [103].

Very recently, the Goldman group has reported transfer dehydrogenation using PSP ligated ruthenium pincer complexes [105]. They have synthesized ($^{i\text{Pr}}$XanPSP)Ru complexes (**101**−**102**) and studied them for the COA/TBE reaction at lower temperatures (Fig. 2.11). At first, the complex **101-(C_2H_4)$_2$** [1 mM] was investigated for COA [7.43 M]/TBE [300 mM] transfer dehydrogenation reaction at different temperatures. The reaction reached completion within 5 min at 180°C, within 60 min at 150°C, and within 250 min at 120°C. There was no change in catalytic activity when a drop of mercury was added, therefore indicating the absence of any colloidal metal species. This is the first report where such a fast reaction at low temperatures was observed. The results obtained with transfer dehydrogenation of *n*-octane under the same conditions were much lower (17 TONs after 120 min at 150°C). The complex **101-(C_2H_4)$_2$** was found to be ineffective for acceptorless dehydrogenation of COA.

Under the same conditions, the complex **102-(η^3-allyl)(H)** was observed to be far less active than **101-(C_2H_4)$_2$** for the transfer dehydrogenation of COA/TBE largely due to the high stability of allyl hydride complexes. In line with the experimental results, DFT studies show that in the case of linear olefins, stable η^3-allyl hydride complexes are formed and their stability leads to the low activity of ($^{i\text{Pr}}$XanPSP)Ru complexes with linear alkanes.

2.3.2 Osmium pincer complexes for alkane dehydrogenation

Roddick group synthesized the analogous pincer−Os complex (^{CF3}PCP)Os(COD)H (**103**) and studied it for COA/TBE dehydrogenation [102] (Fig. 2.12). Surprisingly, this complex was found to be inactive for COA/

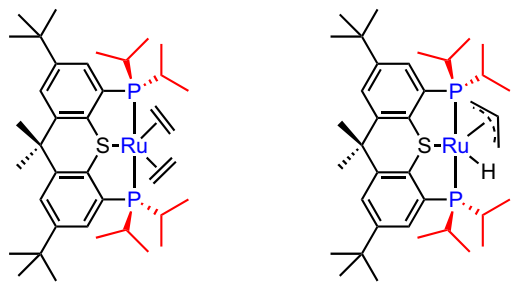

101-(C_2H_4)$_2$ **102-(η^3-allyl)(H)**

Figure 2.11 Ruthenium pincer complexes reported for alkane dehydrogenation by Goldman.

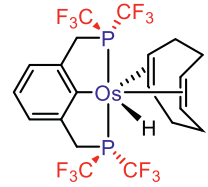

103

Figure 2.12 Osmium pincer complex reported for alkane dehydrogenation by Roddick.

TBE (1:1) transfer dehydrogenation at 150°C unlike its ruthenium analog (^{CF3}PCP)Ru(COD)H (**93**). At 200°C, **103** gave better results for COA/TBE system (1520 TOh^{-1}) as compared to **93** (1000 TOh^{-1}). The thermal stability of **103** is much higher as compared to **93**, which lost its activity after 30 min. The complex **103** gave 610 TONs after 8 h and then decomposed to (^{CF3}PCP)Os(COD)X (**104**), where X = -$CH_2CH_2{}^t$Bu.

The complex **103** was active under N_2, vacuum and water and no decrease in reactivity was observed when the COA/TBE (1:1) dehydrogenation was performed at 200°C. In the presence of 200 Torr O_2 at 200°C, the activity of **103** was affected after 1 h and (^{CF3}PCP)Os$(CO)_2$H (**105**) was formed as observed by ^{19}F NMR analysis. In the above-mentioned reaction conditions, uncatalyzed oxidation of cyclooctane to cyclooctanone was observed in control experiments. Aldehydes were also formed from the trace acyclic hydrocarbons, which further undergo decarbonylation leading to the formation of catalytically inactive species **105**.

No reaction was observed when acceptorless dehydrogenation of COA was performed using **103** at 150°C. On increasing the temperature to 190°C [**103** [1 mM]], acceptorless dehydrogenation of cyclodecane gave 125 TONs after 1 h. The results obtained are similar to that observed with (^{tBu4}PCP)IrH_4 (**5-H$_4$**), which gave 101 TONs after 1 h. TONs further increased to 250 after 6 h for the **103**-catalyzed dehydrogenation and the reaction stopped after 48 h (280 TONs). ^{19}F NMR and ^{31}P NMR studies confirm the formation of dimeric osmium species similar to that observed with (^{CF3}PCP)Ru(COD)H (**93**).

2.3.3 Rhodium pincer complexes for alkane dehydrogenation

Unlike their iridium counterparts, Rh complexes containing PCP pincer ligands are very less catalytically active for AD. One of the examples is of

106-catalyzed transfer dehydrogenation of COA with 0.2 M TBE at 200°C (Fig. 2.13), in which the rate of the reaction is found to be very low, that is, 1.8 TOh^{-1} [31]. The complex **107** (Fig. 2.13) was found to be moderately active for the COA/TBE reaction, giving only 47 mM of the dehydrogenated product after 10 h at 150°C [106]. Goldman had earlier reported the rhodium complexes based on $(PMe_3)_2RhCl$, which were found to be highly active for the dehydrogenation reactions [107,108]. This large difference in reactivity between the PCP–Rh [31,109] and $(PMe_3)_2RhCl$ species was attributed to the strong *trans* influence of the PCP-aryl metal bound carbon as compared to chloride in $(PMe_3)_2RhCl$. The strong *trans* influence of *ipso* C opposes the formation of Rh–C and Rh–H bond via oxidative addition to PCP–Rh, which leads to lower reactivity [110].

To enhance the catalytic activity pincer–Rh complexes, Brookhart and Goldman synthesized carbazolide-based PNP–Ru and -Ir complexes that has a central sp^2 N at the metal center with a weak *trans* influence **(**Fig. 2.13**)**. The sp^2-hybridized N of the PNP ligand is less σ-donating as compared to sp^2-hybridized C of the PCP ligand [111,112].

The complex (carb-PNP)IrH_2 **(62-H_2)** was catalytically inactive toward dehydrogenation. DFT studies revealed that all steps in the catalytic dehydrogenation cycle (Scheme 2.5) are favorable except for the reductive elimination of TBA. The (carb-PNP)Ir(I) state in **62** has much higher energy than (carb-PNP)Ir(III) state in **62-H($C_2H_4{}^tBu$)**. Therefore the formation of **62** (14-electron, 3-coordinate fragment) from **62-H ($C_2H_4{}^tBu$)** via reductive elimination of TBA is not favorable. Due to this, the transfer dehydrogenation does not occur in the presence of complex **62** [111,112].

In comparison, the rhodium analog **(108-H_2)** reacted with ethylene readily to form **108-C_2H_4** and C_2H_6 at room temperature while in the

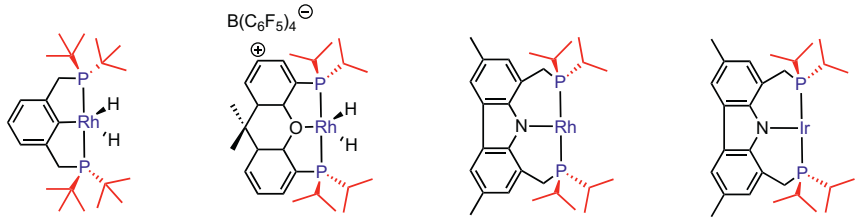

106 107 108 62

Figure 2.13 Rhodium pincer complexes reported for alkane dehydrogenation.

case of **62-H_2**, it occurred only at 70°C. With a more challenging olefin TBE, **108-H_2** was converted to **108-TBE** and TBA at 80°C while **62-H_2** could not hydrogenate TBE even at 100°C in agreement with DFT studies that reveal an unfavorable reductive elimination of TBA from **62-H($C_2H_4{}^tBu$)**. The observations made with these stoichiometric reactions could however not be extrapolated to catalytic reactions. On carrying out the reaction of **108-H_2** and **62-H_2** with TBE in the presence of H_2, different results were obtained. The iridium complex **62-H_2** was able to hydrogenate TBE at room temperature within 1 h, while no reaction was observed with the corresponding rhodium complex **108-H_2** even after 3 h. Computational studies revealed the involvement of Ir(V) species. The complex **62-H_2** on reaction with TBE first forms Ir(III) intermediate **62-H($C_2H_4{}^tBu$)**, which then gets converted to Ir(V) species **62-H_3($C_2H_4{}^tBu$)** in the presence of H_2 and subsequently TBA is released via reductive elimination regenerating **62-H_2**. A corresponding Rh(III)/Rh(V) pathway is not available for the rhodium complex **108-H_2**.

The results obtained for transfer dehydrogenation of COA/TBE (1:1) using 1.3 mM **108-H_2** were satisfactory. A total of 260 TONs were obtained after 3 h at 200°C, and catalyst decomposition was confirmed by ^{31}P NMR studies after 3 h of the reaction. Very low TONs were obtained when the transfer dehydrogenation of *n*-octane/TBE (1:1) was carried out at 200°C (14 TONs after 1 h) using **108-H_2**. The complex (carb-PNP)Rh(1-octene) was not observed, so inhibition due to strong binding of *n*-octene to the metal center was ruled out. Further studies suggested that the olefin isomerization competes with the AD which leads to less TONs. The resting states detected by ^{31}P NMR studies after 5 min of the reaction were (carb-PNP)Rh(TBE) (**108-TBE**) and (carb-PNP)RhH_2 (**108-H_2**) in the ratio 3:1 for both COA and *n*-octane transfer dehydrogenation.

2.4 Applications of alkane dehydrogenation

2.4.1 Alkane metathesis

In order to combat the continual demand for liquid fuel coupled with the rapid declination of natural oil resources, scientists have ventured into nonconventional methods that produce energy sources efficiently, the principle among them being alkane upgradation [113–115]. Low-molecular weight alkanes (C_8–C_{19}), which are essential in this process, are produced mainly by the Fischer–Tropsch process [19,116–119]. They are also obtained from natural gas, coal, or biomass (via reduction or

gasification) [120] or from CO_2 reduction with the use of solar, nuclear, or wind energy [121]. Global reservoirs of light *n*-alkanes can be transformed to liquid fuels via alkane upgradation methods such as alkane metathesis (AM), which will be further elucidated.

AM involves two medium-molecular-weight alkanes reacting to form one alkane of heavy molecular weight and another of light molecular weight. Burnett and Hughes [122] reported the first examples using heterogeneous catalysts, followed by the Basset group [123–126]. But heterogeneous systems yield alkanes with poor molecular weight selectivity [126]. The first homogenous catalyst-based metathesis system was reported by Goldman and Brookhart, who generated a tandem system using pincer–Ir-assisted AD followed by olefin metathesis by Schrock Mo-F12 catalyst **109**, yielding a mixture of high- and low-molecular-weight alkenes [127]. The metathesized alkenes act as hydrogen acceptors and are transformed into the corresponding alkanes by pincer–Ir catalyst (Scheme 2.12).

Apart from the greater selectivity toward linear metathesized heavier alkanes, the milder operating temperatures are the advantages of homogenous tandem AM catalytic systems in comparison to their heterogeneous counterparts [126,127]. For the pincer–Ir system, steric factors determine the yields for *n*-hexane metathesis as shown by the following trend: (^{tBu2}PCP^{tBuMe})IrH$_4$ (**7-H$_4$**) > (^{iPr4}PCP)IrH$_4$(**4-H$_4$**) > (^{tBuMe}PCP^{tBuMe})IrH$_4$(**8-H$_4$**) > (^{tBu4}PCP)IrH$_2$(**5-H$_2$**) [41]. These AM studies have also been extended to cycloalkanes by Scott and co-workers [128]. The formation of *n*-alkanes with intermediate chain lengths in addition to the expected C_{2n-2} *n*-alkanes from C_n alkanes is a drawback of the homogenous systems [36]. The progress of these metathesis studies have been reviewed extensively [6,13–15,23,36–39].

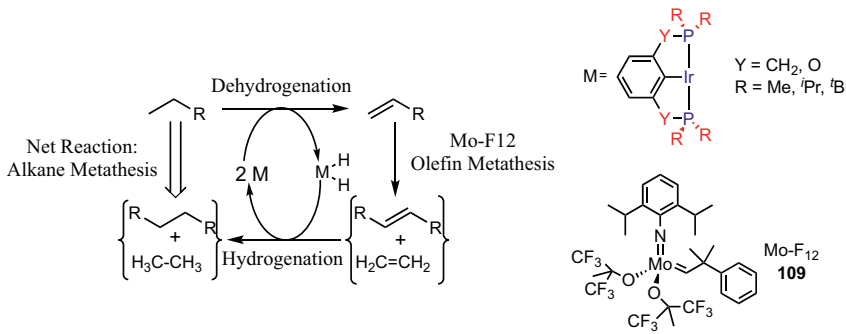

Scheme 2.12 Alkane metathesis catalyzed by pincer–Ir complexes operating in tandem with an olefin metathesis catalyst Mo-F12 (**109**).

The (^{tBu4}PCP)IrH$_2$ (**5-H$_2$**) and (^{tBu4}POCOP)IrH$_2$ (**22-H$_2$**) catalysts for AM gave similar rates, but their corresponding resting states were found to be different [67,129]. The dehydrogenation step catalyzed by (^{tBu4}PCP)IrH$_2$ (**5-H$_2$**) is fast and the rate-determining step is the olefin hydrogenation, with (^{tBu4}PCP)IrH$_2$ (**5-H$_2$**) as the resulting resting state. Whereas in the case of (^{tBu4}POCOP)IrH$_2$ (**22-H$_2$**)-catalyzed reactions, the dehydrogenation is the rate-determining step, (^{tBu4}POCOP)Ir(olefin) (**22-olefin**) being the resting state in this case. To further study the intermediate cases, Goldman and co-workers developed the hybrid PCOP catalysts, whose rate for each step was intermediate between the fast and slow steps of (^{tBu4}PCP)IrH$_2$(**5-H$_2$**) and (^{tBu4}POCOP)IrH$_2$(**22-H$_2$**), which resulted in an overall faster AM rate [129]. The mixed phospine–phosphinite PCOP pincer–Ir catalysts (total TON = 3997) were more active and their corresponding rates were around threefold more than those obtained with either (^{tBu4}PCP)IrH$_2$(**5-H$_2$**) (total TON = 1335) or (^{tBu4}POCOP)IrH$_2$(**22-H$_2$**) (total TON = 1111). The resting state of the mixed catalyst was also found to be a mixture of the other two resting states (i.e., the hydride and olefin complexes).

While poor selectivities were obtained with (^{tBu4}POCOP)IrH$_2$ (**22-H$_2$**) and the PCOP catalysts, the (^{tBu4}PCP)IrH$_2$ (**5-H$_2$**) and the (^{iPr4}PCP)IrH$_4$ (**4-H$_4$**) were better catalysts in generating C_{2n-2} *n*-alkanes via AM. The initial assumption for the low selectivity was rapid olefin isomerization of the C*n* α-alkenes to C*n* internal alkenes [43,67]. While the expected products from AM and consequent hydrogenation are C_{2n-2} *n*-alkane and ethane, the C*n* internal alkenes yield *n*-alkane with intermediate chain lengths [41,67,127,129]. But according to Goldman and Brookhart, this selectivity difference is also attributed to the different regioselectivies of (^{tBu4}POCOP)IrH$_2$ (**22-H$_2$**) and (^{tBu4}PCP)IrH$_2$ (**5-H$_2$**) toward primary dehydrogenation reaction [130]. High selectivity of terminal alkenes was observed using (^{tBu4}PCP)IrH$_2$ (**5-H$_2$**) and (^{iPr4}PCP)IrH$_4$ (**4-H$_4$**), whereas (^{tBu4}POCOP)IrH$_2$ (**22-H$_2$**) and the PCOP catalysts preferably produced internal alkenes.

2.4.2 Alkane coupling

Alkane metathesis is less atom economical as it generates ethane as a by-product, which causes a loss of two units of carbon fragment. In order to be completely efficient, two light C_n *n*-alkanes should combine to form one heavy C_{2n} *n*-alkane. Thus another alkane upgradation method was proposed

by Bercaw and Labinger, which focuses on alkane–alkene coupling [131–133]. Light hydrocarbon feed that typically contains alkene impurities could undergo alkene dimerization in the presence of a suitable catalytic system, followed by alkane transfer hydrogenation. The dimerization catalyst would catalyze the coupling of two C_n alkene fragments to one unit of C_{2n} alkene, and simultaneously the transfer-dehydrogenation catalyst generates C_n alkene from C_n alkane and consequently C_{2n} alkane from C_{2n} alkene. The net reaction is an alkane–alkene coupling to give a higher alkane exclusively, without any by-products (Scheme 2.13) [134,135].

Bercaw and Labinger used Schrock's catalyst $Cp^*Ta(Cl)_2(C_2H_4)$ (**110**) [136] as an alkane dimerization catalyst using a mixture of *n*-heptane and 1-hexene, in tandem with pincer–Ir catalysts (Scheme 2.14) [131–133]. Among (^{iPr4}PCP)IrH_4 (**4-H$_4$**), (^{tBu4}PCP)IrH_2 (**5-H$_2$**), and (^{tBu4}POCOP)IrH_2 (**22-H$_2$**), the latter did not show any activity for the *n*-heptane/1-hexene system. It is probably due to its poor kinetic selectivity that tends to yield only internal alkenes [130] coupled with the fact that the Schrock's catalyst was found to be inert to internal alkenes and sterically hindered terminal alkenes.

On reacting 1-hexene [250 mM] with *n*-heptane (used as solvent) in the presence of (^{tBu4}PCP)IrH_2(**5-H$_2$**) [10 mM] and **110** [16 mM], C_{13} (from hexane/heptane coupling) and C_{14} alkenes were generated with 35% cooperativity. Cooperativity is defined as the amount of *n*-heptene that is incorporated into the C_{13} and C_{14} alkenes. No C_{13} and C_{14} alkanes are found, however, which is attributed to the poor hydrogen-accepting ability of 1,1-substituted alkenes due to which the catalytic cycle remains incomplete.

(^{iPr4}PCP)IrH_4 (**4-H$_4$**) gave better total turnovers compared to (^{tBu4}PCP)IrH_2 (**5-H$_2$**), despite having identical cooperativity. On adding 1-hexene slowly via a syringe pump to a refluxing *n*-heptane solution at 100°C with low catalyst loading ([**4-H$_4$**] = 5 mM and [110] = 8 mM), in a high dilution

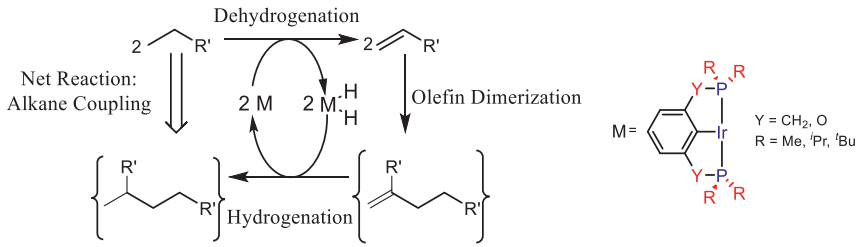

Scheme 2.13 Alkane coupling catalyzed by pincer–Ir complexes.

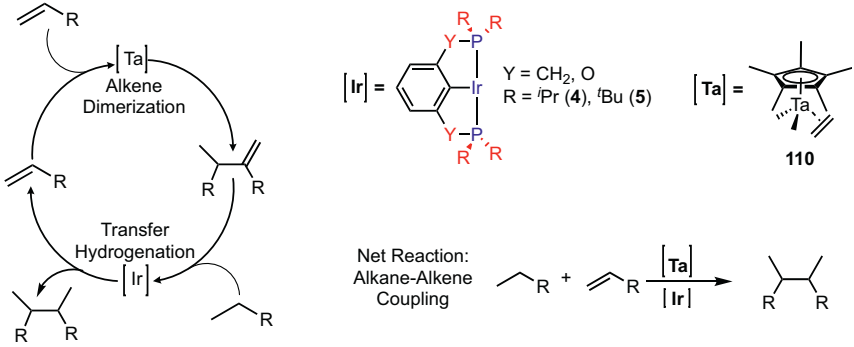

Scheme 2.14 Alkane–alkene coupling catalyzed by pincer–Ir complexes operating in tandem with tantalum catalyst **110**.

technique, there was significant improvement in the yields (40%) of the preferred alkene dimers along with high cooperativity (91%). Higher yields of C_{14} alkenes were also obtained using TBE (which is inert to dimerization) as an acceptor for the catalytic dimerization of *n*-heptane.

2.4.3 Synthesis of aromatics

There is a continual rise in the worldwide demand for the petroleum refinery aromatics: benzene, toluene, and xylene, commonly referred together as "BTX" chemicals [137]. The limited natural gas resources coupled with the omnipresent demand for fine chemicals have opened alternative ways to generate these BTX chemicals quickly and efficiently. Linear alkylbenzenes (LABs) are also high in demand due to their usefulness as precursors to surfactants with high detersive powers [138,139]. Synthesizing these can be challenging via anti-Markovnikov's arylation of alkenes [140–142]. The more common method in use is the Friedel–Craft's alkylation [143]. An efficient way to achieve the transformation of *n*-alkanes to aromatics (BTX and/or LABs) is by using a robust catalytic system like that of the pincer–Ir catalyst via the following routes.

2.4.3.1 Dehydroaromatization

Goldman and Brookhart have used pincer–Ir catalysts for dehydroaromatization of alkanes in order to generate *n*-alkyl arenes. Goldman had reported that the (*p*-OMe-^{iPr4}PCP)IrH_4 (**9-H$_4$**) catalyzed the dehydrogenation of *n*-hexane to give trace amounts of benzene. [44] On carrying out further studies, Goldman and Brookhart found that (^{tBu4}PCP)IrH_2 (**5-H$_2$**) and (^{tBu4}POCOP)IrH_2 (**22-H$_2$**) were inefficient for this reaction.

However, better yields of benzene from *n*-hexane were obtained by using the catalysts ($^{i\text{Pr4}}$Anthraphos)IrH_4 (**19-H$_4$**), ($^{i\text{Pr4}}$PCP)IrH_4 (**4-H$_4$**), and ($^{i\text{Pr4}}$PCOP)IrH_2 (**27-H$_2$**), perhaps due to their lesser steric bulkiness, and among these, **27-H$_2$** gave the highest benzene yield (0.67 M c. 44%) (Scheme 2.15) [58,144].

These complexes were thus said to catalyze dehydrogenation of alkanes ($\geq C_6$) sequentially to conjugated trienes, which upon ring closure gave cyclohexadienes and their corresponding aromatic compound following further dehydrogenation [58,144]. Higher alkanes gave substituted benzenes, mainly, *ortho*-alkyl toluenes. In presence of ($^{i\text{Pr4}}$PCOP)IrH_2(**27-H$_2$**) [5 mM], *n*-octane [1.4 M] coupled with TBE [5.6 M] as an acceptor to give *o*-xylene as major product and ethylbenzene as minor, with a total conversion of 86% after 118 h. Likewise, *n*-dodacane gave *o*-pentyl toluene as the major product (c. 21%) (Scheme 2.16) [58,144].

TBE has been traditionally used as a reliable hydrogen acceptor [27]. However, it is not economically sustainable to use it industrially, which gave rise to the need of cheaper alternatives. The foremost among them are the readily available and abundant ethylene and propene, the latter proving to be better acceptor alternative to TBE [58,144].

2.4.3.2 Cyclodimerization

Ethylene has gained prominence in the role of an acceptor due to the recent abundance of ethane owing to the shale gas boom in North America in 2010 [145]. It has been used as an acceptor and a dienophile by the Brookhart group to synthesize piperylene, toluene, and *p*-xylene from *n*-alkanes [59,60]. Ethylene could be used to generate 1-hexene by

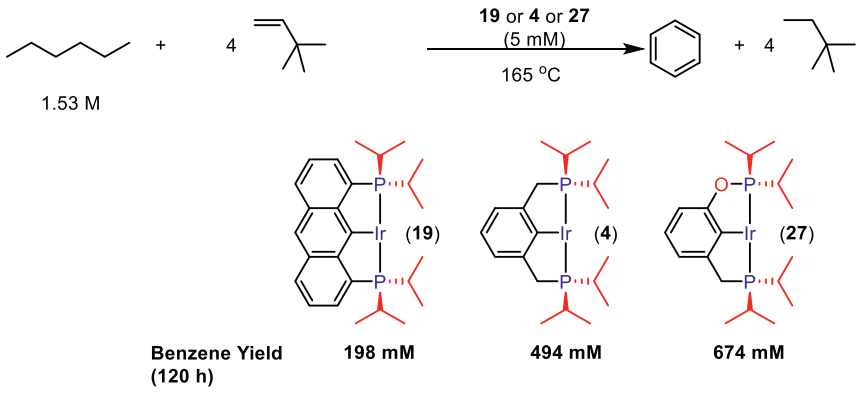

Scheme 2.15 Dehydroaromatization of alkanes catalyzed by pincer–Ir complexes.

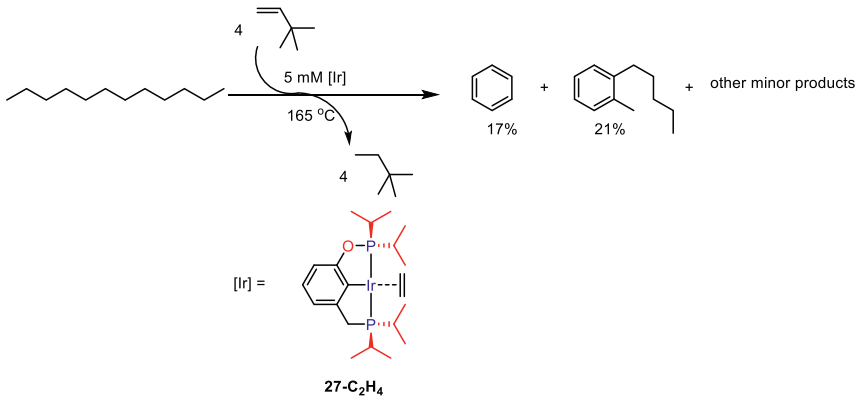

Scheme 2.16 Dehydroaromatization of *n*-dodecane.

trimerization, which would disproportionate to form *n*-hexane and 1,3-hexadiene in a reaction catalyzed by pincer–Ir catalysts such as (^{iPr4}Anthraphos)(C_2H_4) (**19-C_2H_4**), (^{iPr4}PCOP) (C_2H_4) (**27-C_2H_4**), (^{tBu4}PCP)(C_2H_4) (**5-C_2H_4**), and (^{tBu4}POCOP)(C_2H_4) (**22-C_2H_4**). The compound 1,3-hexadiene then isomerizes to thermodynamically favorable 2,4-hexadiene (Scheme 2.17) [59]. 2,4-hexadiene undergoes Diels–Alder reaction with ethylene at 250°C to give an 8:1 mixture of 3,6-dimethyl-cyclohexene and 3-ethylcyclohexene. This is dehydrogenated in the presence of Pt/Al_2O_3 at 400°C to give 8.5:1 mixture of *p*-xylene (93%) and ethylbenzene (88%) [59]. In a similar way, pentene with ethylene has led to the synthesis of piperylene and toluene [60].

2.4.3.3 Alkyl group cross metathesis

Upgradation of *n*-alkyl benzenes from shorter to longer alkyl chains has been carried out by Goldman and Schrock [127,146] using pincer–Ir catalysts. The alkyl group cross metathesis (AGCM) proceeds without the requirement of any additional acceptor, via the dehydrogenation of a mixture of *n*-alkanes and *n*-alkyl benzenes yielding a mixture of alkenes, which in turn undergoes metathesis (Scheme 2.18). These metathesized olefins are hydrogenated to give the final products, which are exclusively mono-*n*-alkylbenzenes. The POCOP-Ir and PCOP-Ir catalysts have already been deemed as having poor selectivity toward terminal olefins [34]. As a result of this, a wide distribution of cross metathesized products having varying chain lengths were observed, which was attributed to the metathesis of styrene with internal alkenes. Using (^{tBu4}PCP)IrH_2 (**5-H_2**)

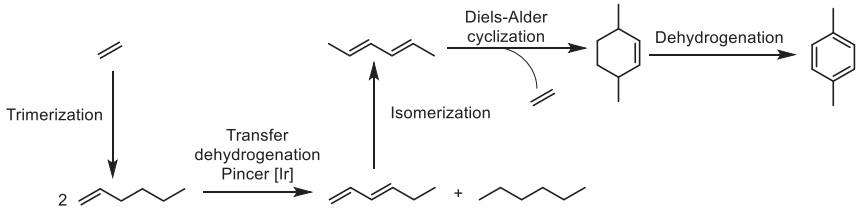

Scheme 2.17 Trimerization of ethylene followed by Diels–Alder cyclization.

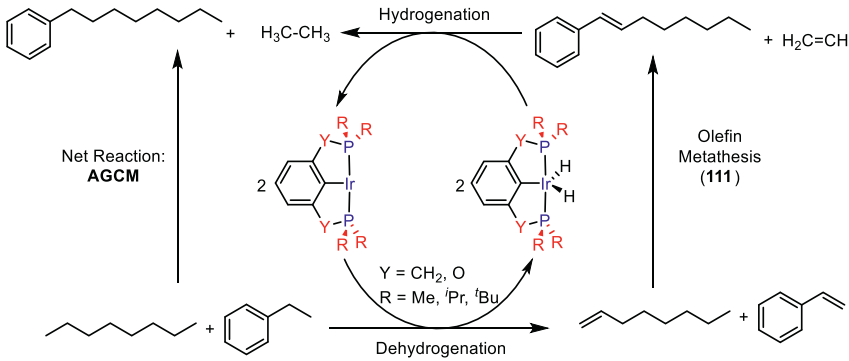

Scheme 2.18 Cross metathesis of *n*-octane with ethyl benzene.

[7 mM] (which has been employed to achieve excellent selectivity toward terminal dehydrogenation) enhanced the yields of 1-phenyl octane [350 mM] when the reaction of *n*-octane and ethyl benzene was carried out at 180°C with W(NAr)(C_3H_6)(Pyr)(OHIPT) (**111**) [11 mM] [Ar = 2,6-$Me_2C_6H_3$, OHIPT = 2,6-(2,4,6-*i*-$Pr_3C_6H_2)_2C_6H_3O$] as the cocatalyst. In comparison to the AM product tetradecane, AGCM showed exceptional selectivity toward 1-phenyl octane (17:1) [146].

2.4.3.4 Alkyl–aryl coupling

The AD reaction has been applied to carry out intermolecular alkyl–aryl coupling reactions in association with zeolite catalysts. The pincer–Ir catalysts designed by Goldman and co-workers were successfully used for this reaction. *N*-pentyl benzene solutions were refluxed in the presence of both pincer–Ir catalysts and zeolites, which worked in tandem, and with a loss of H_2 molecule, 1-methyl-1,2,3,4-tetrahydronaphthalene is produced [147,148]. This product was then dehydrogenated to form 1-methylnaphthalene or isomerized to 2-methyl-1,2,3,4-tetrahydronaphthalene, the latter being further dehydrogenated to 2-methylnaphthalene

(Scheme 2.19) [147,148]. The reaction was carried out with 5.8 M *n*-pentylbenzene in the presence of (^{t}Bu4PCP)IrH$_2$ (**5-H$_2$**) [2 mM] and H-SSZ-25 zeolite (0.3 g/2.7 mL) at 250°C and 4.8 M of cyclized product was obtained (78% yield). In the absence of (^{t}Bu4PCP)IrH$_2$ (**5-H$_2$**), only 1.2 M of product was formed, and in the absence of zeolite, only the alkenyl benzenes were formed. These experiments are a proof of the assumption that the pincer–Ir and the zeolite catalysts work in tandem and complement each other [147,148].

2.4.4 Functionalization of alkanes

Alkanes have been proved to function as abundant and reliable starting materials to several value-added chemicals via dehydrogenation and C–H activation. In the recent years, there has been a steady development in exploiting the vast scope that dehydrogenation of alkanes provides, especially combining it with secondary reactions. Although initially, it was limited to reactions involving only hydrocarbon substrates [58–60,127,147,148] (primarily due to the low tolerance of polar groups by pincer–Ir complexes), recent studies have been carried out regarding reactions with heteroatom-containing reagents, which are one-pot synthesis carried out in two successive steps [149,150]. The first step involving pincer–Ir-catalyzed dehydrogenation proceeds smoothly as there is no cocatalyst or other substrates present during that time [149,150]. Reagents of the secondary reactions are introduced into the same vessel after the dehydrogenative step has been performed. Thus, as the second step is performed without purification of the first product, the cocatalyst is required to be in

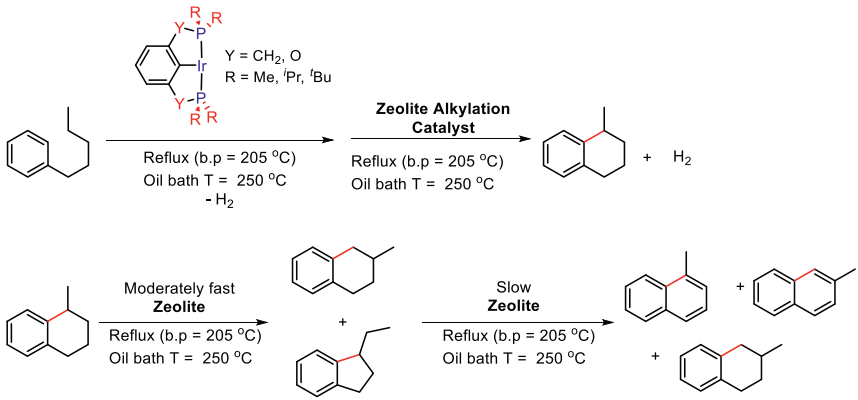

Scheme 2.19 Pincer–Ir/zeolite catalyzed tandem intramolecular coupling of *n*-pentyl benzene.

cohesion with the dehydrogenation catalyst. Also, the substrates of the second step need to be unreactive to the initial pincer—Ir catalyst used under the particular reaction conditions.

2.4.4.1 Silylation and borylation

Huang and co-workers were the first to report the catalytic conversion of alkanes to linear chain silanes [149]. The pincer—Ir PSCOP complex catalyzes the dehydrogenation of *n*-alkanes to a mixture of terminal and internal alkenes, while the pincer—Fe catalyst **112** or **113** not only isomerizes the internal alkenes to terminal ones but also accomplished their hydrosilylation to finally give the linear alkyl silanes (Scheme 2.20) [149].

In an experiment, *n*-hexane was treated with *trans*-3-octene and *bis* (trimethylsilyloxy)methyl silane, catalyzed by **30-HCl** (0.5 mol%) and $NaHBEt_3$ (1 mol%) at room temperature. The product formed was only 6% of branched alkylsilane, which indicated that the catalyst **30-HCl** was not only ineffective for the isomerization of internal alkenes to terminal

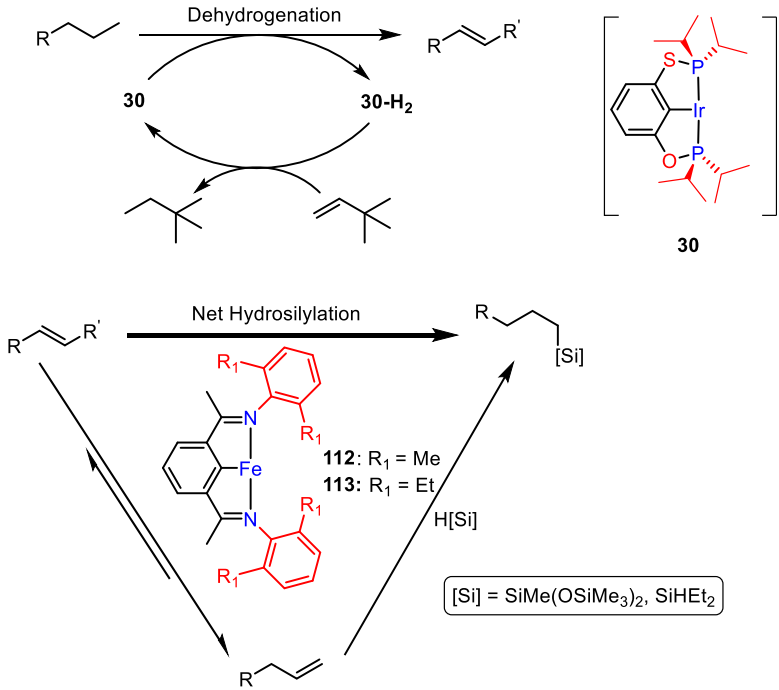

Scheme 2.20 Silylation of alkanes catalyzed by pincer—Ir in tandem with pincer—Fe catalysts **112** and **113**.

alkenes but also was inactive toward hydrosilylation reaction [149]. Replacing the pincer–Ir catalyst with the pincer–Fe catalysts **112-Cl_2** or **113-Cl_2** (all other factors remaining constant), the reaction yielded 86% of the linear alkylsilane. The yields of **112-Cl_2** or **113-Cl_2** catalyzed hydrosilylation reaction hardly changed in the presence of **30-HCl** [149]. This is indicative of the compatible nature of the pincer–iron complexes with their pincer–iridium counterparts during the hydrosilylation segment of the tandem reaction, which formed the basis of the pincer–Ir/pincer–Fe-catalyzed net silylation of alkanes.

A mixture of *n*-octane and TBE [0.25 M] was heated with **30-HCl** [2.5 mM] and NaO^{t}Bu [2.5 mM] at 200°C for 10 min. This is followed by addition of silane [0.25 M], pincer–Fe catalyst [25 mM], and $NaHBEt_3$ [25 mM] at room temperature. The silylation reaction gave high yields (up to 83%) for the reaction of *n*-octane with diethylsilane. It was observed that longer reaction time lowered the yields of silanes due to the inhibition of pincer–Fe complexes by dienes, as suggested by control experiments carried out using deca-1,3-diene [149].

Similar type of strategy has been applied to synthesize linear alkylboronate esters by the same group (Scheme 2.21). Mixture of *n*-octane and TBE [0.25 M] was first dehydrogenated at 200°C to give octenes catalyzed by **30-HCl**. A further isomerization–hydroboration catalyzed by **114** was carried out at room temperature to yield alkyl-boronic ester (95%) [149].

2.4.4.2 Formylation and aminomethylation

Application of AD has been extended to the synthesis of alkyl aldehydes and alkyl amines, both having profound industrial utility [151]. Linear

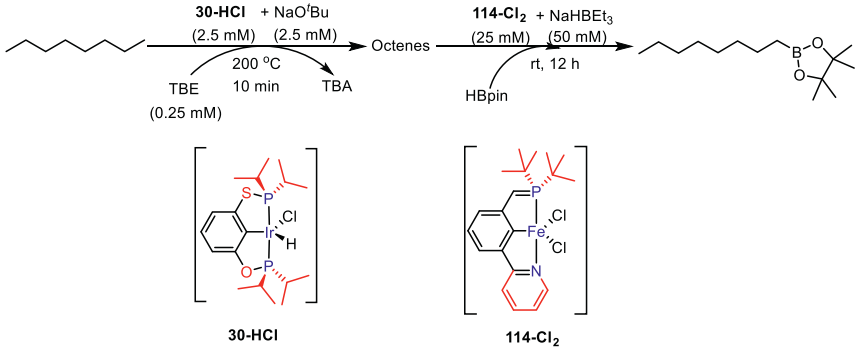

Scheme 2.21 Borylation of alkanes catalyzed by pincer–Ir in tandem with pincer–Fe catalyst **114**.

aldehydes from even number α-olefins are produced via hydroformylation industrially, which certainly poses some limitation to the chain length of the aldehydes [152]. Direct formylation from alkanes mitigates this problem to a great extent, providing versatile aldehydes with varying chain lengths. The well-known Rh hydroformylation catalysts are known to work in tandem with a handful of heterogenous catalysts for the direct formylation from alkanes but with unimpressive results [153,154]. The yield of alkane formylation is low and a variety of undesired side-products are formed in the process.

The Huang group has, of late, made use of the pincer−Ir catalysts in association with the Rh hydroformylation catalysts to give much improved results. The former catalyzes AD and the latter accomplished the combined isomerization−hydroformylation (ISO−HF) of the resulting product with CO and H_2, leading to a one-pot two-step synthesis. The net reaction is the transformation of alkanes to linear aldehydes with one unit increase in the carbon chain [150].

Aminomethylation of α-olefins lead to the formation of alkyl amines [150]. The product of the hydroformylation reaction is reacted with a suitable amine followed by hydrogenation to yield the desired alkyl amine. After the AD−ISO−HF step, the amine introduced in the medium reacts with the carbonylated product, giving rise to a linear alkyl amine (Scheme 2.22) [150].

Huang and co-workers had used the same catalyst they had employed in the silylation-borylation reactions [149] for the AD step. $Rh(acac)(CO)_2$ was found to be a suitable catalyst, and in combination with biphephos ligand, gave the best results when used in the ratio 1:4 of Rh:ligand. The reaction catalyzed by **30** (1 mol%)/ **115** (1 mol%) and **116** (4 mol%) gave the best yields (81%) on using *n*-octane as starting material under 5 bar pressure of CO and H_2, the *n:i* regioselectivity being 13.1 (Scheme 2.22) [150].

The *n:i* regioselectivity was observed to decrease with the increase in chain length. It was highest when *n*-pentane was used (c. 48.9) and lowest in the case of *n*-dodecane (c. 8.5) [150]. This data is a reflection of the fact that internal to terminal isomerization of alkenes is much faster in the case of shorter chain lengths than longer ones [150]. Ethylene has again been used as a cheaper alternative hydrogen acceptor in the transfer dehydrogenation step of *n*-octane AD−ISO−HF [150], to give pretty high turnover numbers of 577 and 1110 with respect to Ir ([**30**] = 2.5 mM) and Rh ([**115**] = 1.3 mM), respectively with a *n:i* ratio 11.1. Thus linear

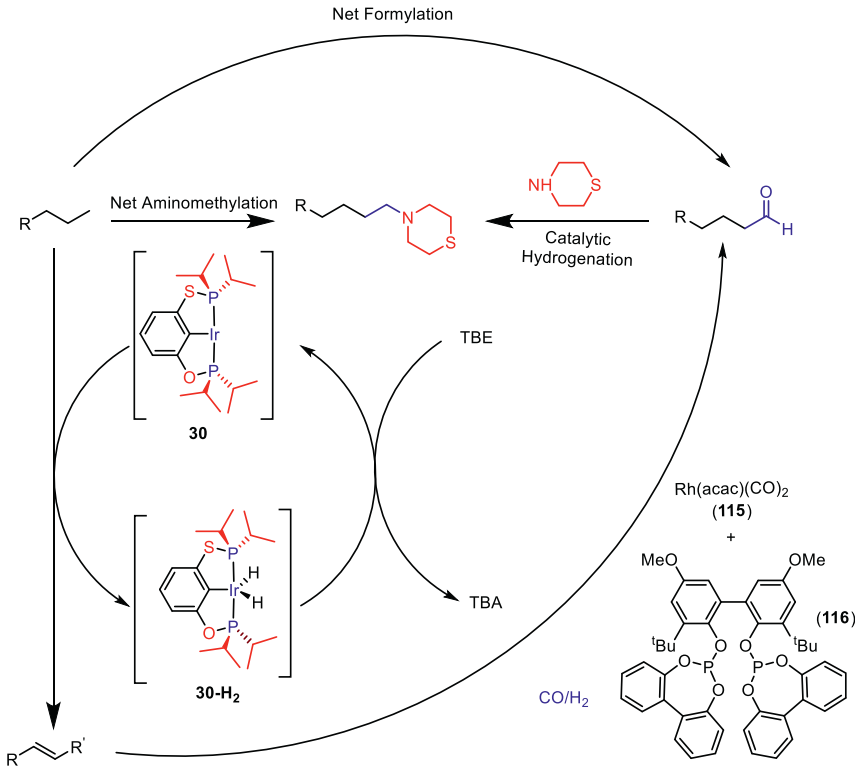

Scheme 2.22 Aminomethylation and formylation of alkanes using pincer–Ir in tandem with Rh catalysts.

alkyl amines were synthesized for the first time using this novel strategy [149,150].

2.5 Summary and outlook

Significant advances have been made in enhancing the applications of the pincer–Ir catalyst to the productive field of AD by systematic mechanistic studies. Complexes ligated with PCP, POCOP, PCOP, and others are highly stable and have been favorably tuned to accomplish excellent reactivity. Though the homogenous pincer–Ir catalysts offer high selectivity toward formation of terminal olefins, the pincer–Ir-catalyzed double bond isomerization continues to be a challenge. The studies have been extended to the use acceptors such as ethylene and propene that are economical, easily recyclable, and readily available. However, the efficiency

seems to be limited to transfer dehydrogenation reactions and better results with acceptorless dehydrogenation are yet to be achieved with these catalysts. Immobilization of pincer–iridium catalysts on to solid supports appears to be straightforward and effective that has led to formulation of effective solid–gas-phase continuous-flow dehydrogenation systems.

The AD reaction has found a plethora of applications when coupled with other reactions such as olefin metathesis, dimerization, Diels–Alder reaction, hydroformylation, and aminomethylation among many others. Many of these reactions occur in a tandem fashion, that is, the pincer complex carries out the dehydrogenation, and a second catalyst completes the consequent step, both catalysts functioning parallelly without hindering each other. Industrially valuable products such as BTX chemicals, linear *n*-alkyl arenes, alkyl silanes, alkyl-boronate esters, and linear alkyl aldehydes have been efficiently produced by these coupling reactions. The pincer-catalyzed AD reaction is a contemporary field of research that is being continuously explored and there is further scope to utilize this reaction toward various applications.

Non-PCP–pincer complexes are the alternatives newly explored for AD. In comparison with their phosphine counterparts, these complexes offer great promise as they are air and moisture stable, and, thus, are easy to handle. Of particular interest are the pincer–Ir complexes based on Phebox and on ^{CF3}PCP ligands owing to their favorable thermodynamics toward alkane to dioxygen transfer dehydrogenation and C–H oxygenation reaction. The dehydrogenation reaction of noniridium-based pincer complexes based on Ru and Os are also well-tolerant toward N_2 and H_2O. The fact that the dehydrogenation chemistry using pincer catalysts based on Ru and Os are still in their infancy certainly presents exciting avenues.

References

[1] C. Dictionary, Recuperado de. <https://dictionary.cambridge. org/es/diccionario/ingles/blended-learning>, 2008.
[2] J. Dupont, C.S. Consorti, J. Spencer, Organometallic pincer-type complexes: recent applications in synthesis and catalysis, in: D. Morales-Morales, C.M. Jensen (Eds.), The Chemistry of Pincer Compounds, Elsevier Science B.V., Amsterdam, 2007, pp. 1–24.
[3] C.J. Moulton, B.L. Shaw, Complexes of nickel, palladium, platinum, rhodium and iridium with the tridentate ligand 2,6-bis[(di-t-butylphosphino)methyl]phenyl, J. Chem. Soc., Dalton Trans. (11) (1976) 1020–1024.

[4] G.V. Koten, Tuning the reactivity of metals held in a rigid ligand environment, Pure Appl. Chem. 61 (10) (1989) 1681–1694.
[5] K. Das, A. Kumar, in: P.J. Pérez (Ed.), Advances in Organometallic Chemistry, vol. 72, Academic Press, 2019, Chapter 1, pp. 1–57.
[6] E. Peris, R.H. Crabtree, Key factors in pincer ligand design, Chem. Soc. Rev. 47 (6) (2018) 1959–1968.
[7] M.A.W. Lawrence, K.-A. Green, P.N. Nelson, S.C. Lorraine, Review: pincer ligands-tunable, versatile and applicable, Polyhedron 143 (2018) 11–27.
[8] G. Bauer, X. Hu, Recent developments of iron pincer complexes for catalytic applications, Inorg. Chem. Front. 3 (6) (2016) 741–765.
[9] C.A. Rettenmeier, J. Wenz, H. Wadepohl, L.H. Gade, Activation of aryl halides by nickel(I) pincer complexes: reaction pathways of stoichiometric and catalytic dehalogenations, Inorg. Chem. 55 (16) (2016) 8214–8224.
[10] H. Valdés, M.A. García-Eleno, D. Canseco-Gonzalez, D. Morales-Morales, Recent advances in catalysis with transition-metal pincer compounds, ChemCatChem. 10 (15) (2018) 3136–3172.
[11] D. Morales-Morales, Pincer Compounds: Chemistry and Applications, Elsevier, 2018.
[12] L. Piccirilli, D. Lobo Justo Pinheiro, M. Nielsen, Recent progress with pincer transition metal catalysts for sustainability, Catalysts 10 (7) (2020) 773.
[13] A. Kumar, T.M. Bhatti, A.S. Goldman, Dehydrogenation of alkanes and aliphatic groups by pincer-ligated metal complexes, Chem. Rev. 117 (19) (2017) 12357–12384.
[14] H. Fang, G. Liu, Z. Huang, Chapter 18 - pincer iridium and ruthenium complexes for alkane dehydrogenation, in: D. Morales-Morales (Ed.), Pincer Compounds, Elsevier, 2018, pp. 383–399.
[15] A. Kumar, A.S. Goldman, Recent advances in alkane dehydrogenation catalyzed by pincer complexes, in: G. van Koten, R.A. Gossage (Eds.), The Privileged Pincer-Metal Platform: Coordination Chemistry & Applications, Springer International Publishing, Cham, 2016, pp. 307–334.
[16] A. Peters, United States, Ullmann's Encyclopedia of Industrial Chemistry. Vol. A2. VCH Verlagsgesellschaft, Weinheim, FRG, 1985. Xii +, Elsevier, 1986, p. 553. ISBN 3–527-20102-5.
[17] J.J.H.B. Sattler, J. Ruiz-Martinez, E. Santillan-Jimenez, B.M. Weckhuysen, Catalytic dehydrogenation of light alkanes on metals and metal oxides, Chem. Rev. 114 (20) (2014) 10613–10653.
[18] S. Faramawy, T. Zaki, A.A.E. Sakr, Natural gas origin, composition, and processing: A review, J. Nat. Gas Sci. Eng. 34 (2016) 34–54.
[19] M.E. Dry, The Fischer–Tropsch process: 1950–2000, Catal. Today 71 (3) (2002) 227–241.
[20] F. Liu, A.S. Goldman, Efficient thermochemical alkane dehydrogenation and isomerization catalyzed by an iridium pincer complex, Chem. Commun. (7)(1999) 655–656.
[21] D. Konya, K.Q. Almeida Leñero, E. Drent, Highly selective halide anion-promoted palladium-catalyzed hydroformylation of internal alkenes to linear alcohols, Organometallics 25 (13) (2006) 3166–3174.
[22] R. Lin, A.P. Amrute, J. Pérez-Ramírez, Halogen-mediated conversion of hydrocarbons to commodities, Chem. Rev. 117 (5) (2017) 4182–4247.
[23] X. Tang, X. Jia, Z. Huang, Challenges and opportunities for alkane functionalisation using molecular catalysts, Chem. Sci. 9 (2) (2018) 288–299.
[24] R.H. Crabtree, J.M. Mihelcic, J.M. Quirk, Iridium complexes in alkane dehydrogenation, J. Am. Chem. Soc. 101 (26) (1979) 7738–7740.

[25] R.H. Crabtree, P.C. Demou, D. Eden, J.M. Mihelcic, C.A. Parnell, J.M. Quirk, et al., Dihydrido olefin and solvento complexes of iridium and the mechanisms of olefin hydrogenation and alkane dehydrogenation, J. Am. Chem. Soc. 104 (25) (1982) 6994–7001.
[26] R.H. Crabtree, M.F. Mellea, J.M. Mihelcic, J.M. Quirk, Alkane dehydrogenation by iridium complexes, J. Am. Chem. Soc. 104 (1) (1982) 107–113.
[27] S.B. Kogan, M. Herskowitz, Dehydrogenation of neohexane to neohexene on platinum polymetallic catalysts, Industr. Eng. Chem. Res. 41 (24) (2002) 5949–5951.
[28] D. Baudry, M. Ephritikhine, H. Felkin, The activation of C–H bonds in cyclopentane by bis(phosphine)rhenium heptahydrides, J. Chem. Soc., Chem. Commun. (24) (1980) 1243–1244.
[29] D. Baudry, M. Ephritikhine, H. Felkin, The activation of C–H bonds in cycloalkanes by rhenium complexes, J. Chem. Soc., Chem. Commun. (11) (1982) 606–607.
[30] D. Baudry, M. Ephritikhine, H. Felkin, J. Zakrzewski, The selective conversion of n-pentane into pent-1-ene via trihydrido(trans-penta-1,3-diene)bis(triarylphosphine) rhenium, J. Chem. Soc., Chem. Commun. (21) (1982) 1235–1236.
[31] M. Gupta, C. Hagen, R.J. Flesher, W.C. Kaska, C.M. Jensen, A highly active alkane dehydrogenation catalyst: stabilization of dihydrido rhodium and iridium complexes by a P–C–P pincer ligand, Chem. Commun. (17) (1996) 2083–2084.
[32] M.A. McLoughlin, R.J. Flesher, W.C. Kaska, H.A. Mayer, Synthesis and reactivity of [IrH2(tBu2P)CH2CH2CHCH2CH2P(tBu2)], a dynamic iridium polyhydride complex, Organometallics 13 (10) (1994) 3816–3822.
[33] D.R. Anton, R.H. Crabtree, Dibenzo [a, e] cyclooctatetraene in a proposed test for heterogeneity in catalysts formed from soluble platinum-group metal complexes, Organometallics 2 (7) (1983) 855–859.
[34] W.-w Xu, G.P. Rosini, K. Krogh-Jespersen, A.S. Goldman, M. Gupta, C.M. Jensen, et al., Thermochemical alkane dehydrogenation catalyzed in solution without the use of a hydrogen acceptor, Chem. Commun. (23) (1997) 2273–2274.
[35] M.G. Edwards, R.F.R. Jazzar, B.M. Paine, D.J. Shermer, M.K. Whittlesey, J.M.J. Williams, et al., Borrowing hydrogen: a catalytic route to C–C bond formation from alcohols, Chem. Commun. (1) (2004) 90–91.
[36] M.C. Haibach, S. Kundu, M. Brookhart, A.S. Goldman, Acc. Chem. Res. 45 (2012) 947.
[37] M. Findlater, J. Choi, A.S. Goldman, M. Brookhart, Alkane dehydrogenation, in: P. J. Pérez (Ed.), Alkane C-H Activation by Single-Site Metal Catalysis, Springer:, Netherlands, Dordrecht, 2012, pp. 113–141.
[38] J. Choi, A.H.R. MacArthur, M. Brookhart, A.S. Goldman, Dehydrogenation and related reactions catalyzed by iridium pincer complexes, Chem. Rev. 111 (3) (2011) 1761–1779.
[39] J. Choi, A.S. Goldman, Ir-catalyzed functionalization of C–H bonds, in: P.G. Andersson (Ed.), Iridium Catalysis, Springer Berlin Heidelberg, Berlin, Heidelberg, 2011, pp. 139–167.
[40] F. Liu, E.B. Pak, B. Singh, C.M. Jensen, A.S. Goldman, Dehydrogenation of n-alkanes catalyzed by iridium "Pincer" complexes: Regioselective formation of α-olefins, J. Am. Chem. Soc. 121 (16) (1999) 4086–4087.
[41] S. Kundu, Y. Choliy, G. Zhuo, R. Ahuja, T.J. Emge, R. Warmuth, et al., Rational design and synthesis of highly active pincer-iridium catalysts for alkane dehydrogenation, Organometallics 28 (18) (2009) 5432–5444.
[42] A. Kumar, J.D. Hackenberg, G. Zhuo, A.M. Steffens, O. Mironov, R.J. Saxton, et al., High yields of piperylene in the transfer dehydrogenation of pentane catalyzed by pincer-ligated iridium complexes, J. Mol. Catal. A: Chem. 426 (2017) 368–375.

[43] A. Kumar, T. Zhou, T.J. Emge, O. Mironov, R.J. Saxton, K. Krogh-Jespersen, et al., Dehydrogenation of n-alkanes by solid-phase molecular pincer-iridium catalysts. High yields of α-olefin product, J. Am. Chem. Soc. 137 (31) (2015) 9894–9911.
[44] K. Zhu, P.D. Achord, X. Zhang, K. Krogh-Jespersen, A.S. Goldman, Highly effective pincer-ligated iridium catalysts for alkane dehydrogenation. DFT calculations of relevant thermodynamic, kinetic, and spectroscopic properties, J. Am. Chem. Soc. 126 (40) (2004) 13044–13053.
[45] Z. Huang, M. Brookhart, A.S. Goldman, S. Kundu, A. Ray, S.L. Scott, et al., Highly active and recyclable heterogeneous iridium pincer catalysts for transfer dehydrogenation of alkanes, Adv. Synth. Catal. 351 (1–2) (2009) 188–206.
[46] J.J. Adams, N. Arulsamy, D.M. Roddick, Acceptor PCP pincer iridium(I) chemistry: stabilization of nonmeridional PCP coordination geometries, Organometallics 30 (4) (2011) 697–711.
[47] J.J. Adams, A. Lau, N. Arulsamy, D.M. Roddick, Acceptor PCP pincer iridium chemistry: (CF3PCP)IrIII coordination properties, Organometallics 30 (4) (2011) 689–696.
[48] J.J. Adams, N. Arulsamy, D.M. Roddick, Acceptor CF3PCPH pincer reactivity with (PPh3)3Ir(CO)H, Dalton Trans. 40 (39) (2011) 10014–10019.
[49] J.J. Adams, N. Arulsamy, D.M. Roddick, Investigation of iridium CF3PCP pincer catalytic dehydrogenation and decarbonylation chemistry, Organometallics 31 (4) (2012) 1439–1447.
[50] D.M. Roddick, Tuning of PCP pincer ligand electronic and steric properties, in: G. van Koten, D. Milstein (Eds.), Organometallic Pincer Chemistry, Springer Berlin Heidelberg, Berlin, Heidelberg, 2013, pp. 49–88.
[51] A.D.R. Shada, A.J.M. Miller, T.J. Emge, A.S. Goldman, Catalytic dehydrogenation of alkanes by PCP–pincer iridium complexes using proton and electron acceptors, ACS Catal. 11 (5) (2021) 3009–3016.
[52] I. Göttker-Schnetmann, P. White, M. Brookhart, Iridium bis(phosphinite) p-XPCP pincer complexes: highly active catalysts for the transfer dehydrogenation of alkanes, J. Am. Chem. Soc. 126 (6) (2004) 1804–1811.
[53] D. Morales-Morales, D.W. Lee, Z. Wang, C.M. Jensen, Oxidative addition of water by an iridium PCP pincer complex: catalytic dehydrogenation of alkanes by IrH(OH){C6H3-2,6-(CH2PBut2)2}, Organometallics 20 (2001) 1144.
[54] D.W. Lee, W.C. Kaska, C.M. Jensen, Mechanistic features of iridium pincer complex catalyzed hydrocarbon dehydrogenation reactions: inhibition upon formation of a μ-dinitrogen complex, Organometallics 17 (1) (1998) 1–3.
[55] R. Ghosh, M. Kanzelberger, T.J. Emge, G.S. Hall, A.S. Goldman, Dinitrogen complexes of pincer-ligated iridium, Organometallics 25 (23) (2006) 5668–5671.
[56] Y. Shi, T. Suguri, C. Dohi, H. Yamada, S. Kojima, Y. Yamamoto, Highly active catalysts for the transfer dehydrogenation of alkanes: synthesis and application of Novel 7–6–7 ring-based pincer iridium complexes, Chem.—Euro. J. 19 (32) (2013) 10672–10689.
[57] M.W. Haenel, S. Oevers, K. Angermund, W.C. Kaska, H.-J. Fan, M.B. Hall, Thermally stable homogeneous catalysts for alkane dehydrogenation, Angew. Chem. Int. Ed. 40 (19) (2001) 3596–3600.
[58] R. Ahuja, B. Punji, M. Findlater, C. Supplee, W. Schinski, M. Brookhart, et al., Catalytic dehydroaromatization of n-alkanes by pincer-ligated iridium complexes, Nat. Chem. 3 (2) (2011) 167–171.
[59] T.W. Lyons, D. Guironnet, M. Findlater, M. Brookhart, Synthesis of p-xylene from ethylene, J. Am. Chem. Soc. 134 (38) (2012) 15708–15711.

[60] S. Kundu, T.W. Lyons, M. Brookhart, Synthesis of piperylene and toluene via transfer dehydrogenation of pentane and pentene, ACS Catal. 3 (8) (2013) 1768–1773.
[61] I. Göttker-Schnetmann, P.S. White, M. Brookhart, Synthesis and properties of iridium bis(phosphinite) pincer complexes (p-XPCP)IrH2, (p-XPCP)Ir(CO), (p-XPCP)Ir(H)(aryl), and {(p-XPCP)Ir}2{μ-N2} and their relevance in alkane transfer dehydrogenation, Organometallics 23 (8) (2004) 1766–1776.
[62] D. Morales-Morales, R. o Redón, C. Yung, C.M. Jensen, Dehydrogenation of alkanes catalyzed by an iridium phosphinito PCP pincer complex, Inorg. Chim. Acta 357 (10) (2004) 2953–2956.
[63] I. Göttker-Schnetmann, M. Brookhart, Mechanistic studies of the transfer dehydrogenation of cyclooctane catalyzed by iridium bis(phosphinite) p-XPCP pincer complexes, J. Am. Chem. Soc. 126 (30) (2004) 9330–9338.
[64] O.O. Kovalenko, O.F. Wendt, An electron poor iridium pincer complex for catalytic alkane dehydrogenation, Dalton Trans. 45 (40) (2016) 15963–15969.
[65] W. Yao, Y. Zhang, X. Jia, Z. Huang, Selective catalytic transfer dehydrogenation of alkanes and heterocycles by an iridium pincer complex, Angew. Chem. Int. Ed. 53 (5) (2014) 1390–1394.
[66] K.B. Renkema, Y.V. Kissin, A.S. Goldman, Mechanism of alkane transfer-dehydrogenation catalyzed by a pincer-ligated iridium complex, J. Am. Chem. Soc. 125 (26) (2003) 7770–7771.
[67] S. Biswas, Z. Huang, Y. Choliy, D.Y. Wang, M. Brookhart, K. Krogh-Jespersen, et al., Olefin isomerization by iridium pincer catalysts. Experimental evidence for an η3-allyl pathway and an unconventional mechanism predicted by DFT calculations, J. Am. Chem. Soc. 134 (32) (2012) 13276–13295.
[68] S.M.M. Knapp, S.E. Shaner, D. Kim, D.Y. Shopov, J.A. Tendler, D.M. Pudalov, et al., Mechanistic studies of alkene isomerization catalyzed by CCC-pincer complexes of iridium, Organometallics 33 (2) (2014) 473–484.
[69] H.G. Alt, I.K. Böhmer, Catalytic dehydrogenation of isopentane with iridium catalysts, Angew. Chem. Int. Ed. 47 (14) (2008) 2619–2621.
[70] S. Taubmann, H.G. Alt, Heterogeneous catalysts for the dehydrogenation of saturated hydrocarbons, J. Mol. Catal. A: Chem. 287 (1) (2008) 102–109.
[71] I.K. Böhmer, H.G. Alt, Influence of triphenylphosphine on the activity of heterogeneous iridium, rhodium and platinum containing catalysts for the dehydrogenation of saturated hydrocarbons, J. Organomet. Chem. 694 (7) (2009) 1001–1010.
[72] Z. Huang, E. Rolfe, E.C. Carson, M. Brookhart, A.S. Goldman, S.H. El-Khalafy, et al., Efficient heterogeneous dual catalyst systems for alkane metathesis, Adv. Synth. Catal. 352 (1) (2010) 125–135.
[73] D. Bézier, M. Brookhart, Applications of PC(sp3)P iridium complexes in transfer dehydrogenation of alkanes, ACS Catal. 4 (10) (2014) 3411–3420.
[74] M. Rimoldi, D. Fodor, J.A. van Bokhoven, A. Mezzetti, Catalytic hydrogenation of liquid alkenes with a silica-grafted hydride pincer iridium(iii) complex: support for a heterogeneous mechanism, Catal. Sci. Technol. 5 (9) (2015) 4575–4586.
[75] M. Rimoldi, A. Mezzetti, Batch and continuous flow hydrogenation of liquid and gaseous alkenes catalyzed by a silica-grafted iridium(III) hydride, Helvet. Chim. Acta 99 (12) (2016) 908–915.
[76] M. Rimoldi, A. Mezzetti, Silica-grafted 16-electron hydride pincer complexes of iridium(III) and their soluble analogues: synthesis and reactivity with CO, Inorg. Chem. 53 (22) (2014) 11974–11984.
[77] M. Rimoldi, D. Fodor, J.A. van Bokhoven, A. Mezzetti, A stable 16-electron iridium(iii) hydride complex grafted on SBA-15: a single-site catalyst for alkene hydrogenation, Chem. Commun. 49 (96) (2013) 11314–11316.

[78] B. Sheludko, M.T. Cunningham, A.S. Goldman, F.E. Celik, Continuous-flow alkane dehydrogenation by supported pincer-ligated iridium catalysts at elevated temperatures, ACS Catal. 8 (9) (2018) 7828—7841.
[79] B. Sheludko, C.F. Castro, A.S. Goldman, F.E. Celik, Poison or promoter? Investigating the dual-role of carbon monoxide in pincer-iridium-based alkane dehydrogenation systems via operando diffuse reflectance infrared Fourier transform spectroscopy, ACS Catal. 10 (21) (2020) 12425—12436.
[80] C. Azerraf, D. Gelman, New shapes of PC(sp3)P pincer complexes, Organometallics 28 (22) (2009) 6578—6584.
[81] C. Azerraf, D. Gelman, Exploring the reactivity of C(sp3)-cyclometalated IrIII compounds in hydrogen transfer reactions, Chem. Euro. J. 14 (33) (2008) 10364—10368.
[82] A.V. Polukeev, R. Gritcenko, K.J. Jonasson, O.F. Wendt, Catalytic dehydrogenation of cyclooctane and triethylamine using aliphatic iridium pincer complexes, Polyhedron 84 (2014) 63—66.
[83] K.J. Jonasson, N. Ahlsten, O.F. Wendt, Aliphatic pincer-type POCOP ligands and their complexation behaviour with iridium: crystal structure of an iridium(III) phosphinite complex, Inorg. Chim. Acta 379 (1) (2011) 76—80.
[84] S. De-Botton, S. Cohen, D. Gelman, Iridium PC(sp3)P pincer complexes with Hemilabile Pendant Arms: synthesis, characterization, and catalytic activity, Organometallics 37 (8) (2018) 1324—1330.
[85] X. Jia, L. Zhang, C. Qin, X. Leng, Z. Huang, Iridium complexes of new NCP pincer ligands: catalytic alkane dehydrogenation and alkene isomerization, Chem. Commun. 50 (75) (2014) 11056—11059.
[86] K. Tanoue, M. Yamashita, Synthesis of pincer iridium complexes bearing a boron atom and iPr-substituted phosphorus atoms: application to catalytic transfer dehydrogenation of alkanes, Organometallics 34 (16) (2015) 4011—4017.
[87] W.-C. Shih, O.V. Ozerov, Synthesis and characterization of PBP pincer iridium complexes and their application in alkane transfer dehydrogenation, Organometallics 36 (1) (2017) 228—233.
[88] A.R. Chianese, A. Mo, N.L. Lampland, R.L. Swartz, P.T. Bremer, Iridium complexes of CCC-pincer N-heterocyclic carbene ligands: synthesis and catalytic C − H functionalization, Organometallics 29 (13) (2010) 3019—3026.
[89] A.R. Chianese, S.E. Shaner, J.A. Tendler, D.M. Pudalov, D.Y. Shopov, D. Kim, et al., Iridium complexes of bulky CCC-pincer N-heterocyclic carbene ligands: steric control of coordination number and catalytic alkene isomerization, Organometallics 31 (21) (2012) 7359—7367.
[90] S. Morisako, S. Watanabe, S. Ikemoto, S. Muratsugu, M. Tada, M. Yamashita, Synthesis of A pincer-IrV complex with a base-free alumanyl ligand and its application toward the dehydrogenation of alkanes, Angew. Chem. Int. Ed. 58 (42) (2019) 15031—15035.
[91] R.F.W. Bader, Atoms in Molecules: A Quantum Theory, Clarendon Press, 1994.
[92] X. Zhang, S.-B. Wu, X. Leng, L.W. Chung, G. Liu, Z. Huang, N-Bridged pincer iridium complexes for highly efficient alkane dehydrogenation and the relevant linker effects, ACS Catal. 10 (11) (2020) 6475—6487.
[93] A.R. Chianese, M.J. Drance, K.H. Jensen, S.P. McCollom, N. Yusufova, S.E. Shaner, et al., Acceptorless alkane dehydrogenation catalyzed by iridium CCC-pincer complexes, Organometallics 33 (2) (2014) 457—464.
[94] D.F. Brayton, P.R. Beaumont, E.Y. Fukushima, H.T. Sartain, D. Morales-Morales, C.M. Jensen, Synthesis, characterization, and dehydrogenation activity of an iridium arsenic based pincer catalyst, Organometallics 33 (19) (2014) 5198—5202.

[95] J.-i Ito, T. Kaneda, H. Nishiyama, Intermolecular C−H bond activation of alkanes and arenes by NCN pincer iridium (III) acetate complexes containing bis (oxazolinyl) phenyl ligands, Organometallics 31 (12) (2012) 4442−4449.
[96] K.E. Allen, D.M. Heinekey, A.S. Goldman, K.I. Goldberg, Alkane dehydrogenation by C−H activation at iridium(III), Organometallics 32 (6) (2013) 1579−1582.
[97] K.E. Allen, D.M. Heinekey, A.S. Goldman, K.I. Goldberg, Regeneration of an iridium(III) complex active for alkane dehydrogenation using molecular oxygen, Organometallics 33 (6) (2014) 1337−1340.
[98] Y. Gao, C. Guan, M. Zhou, A. Kumar, T.J. Emge, A.M. Wright, et al., β-Hydride elimination and C−H activation by an iridium acetate complex, catalyzed by Lewis acids. Alkane dehydrogenation cocatalyzed by Lewis acids and [2,6-bis(4,4-dimethyloxazolinyl)-3,5-dimethylphenyl]iridium, J. Am. Chem. Soc. 139 (18) (2017) 6338−6350.
[99] H. Yuan, W.W. Brennessel, W.D. Jones, Effect of carboxylate ligands on alkane dehydrogenation with (dmPhebox)Ir complexes, ACS Catal. 8 (3) (2018) 2326−2329.
[100] B.C. Gruver, J.J. Adams, S.J. Warner, N. Arulsamy, D.M. Roddick, Acceptor pincer chemistry of ruthenium: catalytic alkane dehydrogenation by (CF3PCP)Ru (cod)(H), Organometallics 30 (19) (2011) 5133−5140.
[101] J.J. Adams, B.C. Gruver, R. Donohoue, N. Arulsamy, D.M. Roddick, Acceptor pincer Ru(ii) chemistry, Dalton Trans. 41 (40) (2012) 12601−12611.
[102] B.C. Gruver, J.J. Adams, N. Arulsamy, D.M. Roddick, Acceptor pincer chemistry of osmium: catalytic alkane dehydrogenation by (CF3PCP)Os(cod)(H), Organometallics 32 (21) (2013) 6468−6475.
[103] Y. Zhang, H. Fang, W. Yao, X. Leng, Z. Huang, Synthesis of pincer hydrido ruthenium olefin complexes for catalytic alkane dehydrogenation, Organometallics 35 (2) (2016) 181−188.
[104] B.J. Eleazer, M.D. Smith, A.A. Popov, D.V. Peryshkov, Rapid reversible borane to boryl hydride exchange by metal shuttling on the carborane cluster surface, Chem. Sci. 8 (8) (2017) 5399−5407.
[105] X. Zhou, S. Malakar, T. Zhou, S. Murugesan, C. Huang, T.J. Emge, et al., Catalytic alkane transfer dehydrogenation by PSP-pincer-ligated ruthenium. Deactivation of an extremely reactive fragment by formation of allyl hydride complexes, ACS Catal. 9 (5) (2019) 4072−4083.
[106] M.C. Haibach, D.Y. Wang, T.J. Emge, K. Krogh-Jespersen, A.S. Goldman, (POP) Rh pincer hydride complexes: unusual reactivity and selectivity in oxidative addition and olefin insertion reactions, Chem. Sci. 4 (9) (2013) 3683−3692.
[107] J.A. Maguire, A. Petrillo, A.S. Goldman, Efficient transfer-dehydrogenation of alkanes catalyzed by rhodium trimethylphosphine complexes under dihydrogen atmosphere, J. Am. Chem. Soc. 114 (24) (1992) 9492−9498.
[108] J.A. Maguire, A.S. Goldman, Efficient low-temperature thermal functionalization of alkanes. Transfer dehydrogenation catalyzed by Rh(PMe3)2Cl(CO) in solution under a high-pressure hydrogen atmosphere, J. Am. Chem. Soc. 113 (17) (1991) 6706−6708.
[109] K. Wang, M.E. Goldman, T.J. Emge, A.S. Goldman, Transfer-dehydrogenation of alkanes catalyzed by rhodium(I) phosphine complexes, J. Organomet. Chem. 518 (1) (1996) 55−68.
[110] D.Y. Wang, Y. Choliy, M.C. Haibach, J.F. Hartwig, K. Krogh-Jespersen, A.S. Goldman, Assessment of the electronic factors determining the thermodynamics of "Oxidative Addition" of C−H and N−H bonds to Ir(I) complexes, J. Am. Chem. Soc. 138 (1) (2016) 149−163.

[111] D. Bézier, C. Guan, K. Krogh-Jespersen, A.S. Goldman, M. Brookhart, Experimental and computational study of alkane dehydrogenation catalyzed by a carbazolide-based rhodium PNP pincer complex, Chem. Sci. 7 (4) (2016) 2579–2586.
[112] C. Cheng, B.G. Kim, D. Guironnet, M. Brookhart, C. Guan, D.Y. Wang, et al., Synthesis and characterization of carbazolide-based iridium PNP pincer complexes. Mechanistic and computational investigation of alkene hydrogenation: evidence for an Ir(III)/Ir(V)/Ir(III) catalytic cycle, J. Am. Chem. Soc. 136 (18) (2014) 6672–6683.
[113] J. Murray, D. King, Oil's tipping point has passed, Nature 481 (7382) (2012) 433–435.
[114] A.R. Brandt, A. Millard-Ball, M. Ganser, S.M. Gorelick, Peak oil demand: the role of fuel efficiency and alternative fuels in a global oil production decline, Environ. Sci. Technol. 47 (14) (2013) 8031–8041.
[115] R.A. Kerr, Peak oil production may already be here, Science 331 (6024) (2011) 1510–1511.
[116] M.E. Dry, High quality diesel via the Fischer–Tropsch process – a review, J. Chem. Technol. Biotechnol. 77 (1) (2002) 43–50.
[117] D. Leckel, Diesel production from Fischer – Tropsch: the past, the present, and new concepts, Energy Fuels 23 (5) (2009) 2342–2358.
[118] D. Hildebrandt, D. Glasser, B. Hausberger, B. Patel, B.J. Glasser, Producing transportation fuels with less work, Science 323 (5922) (2009) 1680–1681.
[119] M.E. Dry, Present and future applications of the Fischer–Tropsch process, Appl. Catal. A: Gen. 276 (1) (2004) 1–3.
[120] G.W. Huber, S. Iborra, A. Corma, Synthesis of transportation fuels from biomass: chemistry, catalysts, and engineering, Chem. Rev. 106 (9) (2006) 4044–4098.
[121] C. Graves, S.D. Ebbesen, M. Mogensen, K.S. Lackner, Sustainable hydrocarbon fuels by recycling CO2 and H2O with renewable or nuclear energy, Renewab. Sustain. Energy Rev. 15 (1) (2011) 1–23.
[122] R.L. Burnett, T.R. Hughes, Mechanism and poisoning of the molecular redistribution reaction of alkanes with a dual-functional catalyst system, J. Catal. 31 (1) (1973) 55–64.
[123] J.M. Basset, C. Copéret, L. Lefort, B.M. Maunders, O. Maury, E. Le Roux, et al., Primary products and mechanistic considerations in alkane metathesis, J. Am. Chem. Soc. 127 (24) (2005) 8604–8605.
[124] C. Copéret, O. Maury, J. Thivolle-Cazat, J.-M. Basset, σ-bond metathesis of alkanes on a silica-supported tantalum(v) alkyl alkylidene complex: first evidence for alkane cross-metathesis, Angew. Chemie Int. Ed. 40 (12) (2001) 2331–2334.
[125] V. Vidal, A. Théolier, J. Thivolle-Cazat, J.-M. Basset, Metathesis of alkanes catalyzed by silica-supported transition metal hydrides, Science 276 (5309) (1997) 99–102.
[126] J.-M. Basset, C. Coperet, D. Soulivong, M. Taoufik, J.T. Cazat, Metathesis of alkanes and related reactions, Acc. Chem. Res. 43 (2) (2010) 323–334.
[127] A.S. Goldman, A.H. Roy, Z. Huang, R. Ahuja, W. Schinski, M. Brookhart, Catalytic alkane metathesis by tandem alkane dehydrogenation-olefin metathesis, Science 312 (5771) (2006) 257–261.
[128] R. Ahuja, S. Kundu, A.S. Goldman, M. Brookhart, B.C. Vicente, S.L. Scott, Catalytic ring expansion, contraction, and metathesis-polymerization of cycloalkanes, Chem. Commun. (2) (2008) 253–255.
[129] A.J. Nawara-Hultzsch, J.D. Hackenberg, B. Punji, C. Supplee, T.J. Emge, B.C. Bailey, et al., Rational design of highly active "Hybrid" phosphine–phosphinite pincer iridium catalysts for alkane metathesis, ACS Catal. 3 (11) (2013) 2505–2514.

[130] S. Biswas, T. Zhou, D.Y. Wang, J. Hackenberg, A. Nawara-Hultzsch, R.R. Schrock, et al., Abstracts of Papers, 245th ACS National Meeting & Exposition, New Orleans, LA, April 7_11, 2013; Washington DC: American Chemical Society, 2013; INOR-681.
[131] J.A. Labinger, D.C. Leitch, J.E. Bercaw, M.A. Deimund, M.E. Davis, Upgrading light hydrocarbons: a tandem catalytic system for alkane/alkene coupling, Topics Catal. 58 (7) (2015) 494–501.
[132] D.C. Leitch, J.A. Labinger, J.E. Bercaw, Scope and mechanism of homogeneous tantalum/iridium tandem catalytic alkane/alkene upgrading using sacrificial hydrogen acceptors, Organometallics 33 (13) (2014) 3353–3365.
[133] D.C. Leitch, Y.C. Lam, J.A. Labinger, J.E. Bercaw, Upgrading light hydrocarbons via tandem catalysis: a dual homogeneous Ta/Ir system for alkane/alkene coupling, J. Am. Chem. Soc. 135 (2013) 10302.
[134] A.S. Goldman, R.T. Stibrany, W.L. Schinski, Chevron U.S.A. Inc. Rutgers, The State University of New Jersey, US patent US20130090503A12013 (n.d.).
[135] O. Mironov, R.J. Saxton, A.S. Goldman, A. Kumar. Chevron U.S.A. Inc. Rutgers, The State University of New Jersey, 2018. US Patent US10017430B2.
[136] S.J. McLain, C.D. Wood, R.R. Schrock, Preparation and characterization of tantalum(III) olefin complexes and tantalum(V) metallacyclopentane complexes made from acyclic. alpha. olefins, J. Am. Chem. Soc. 101 (16) (1979) 4558–4570.
[137] M. Schulze, Industrial organic chemicals, Chem. Ingen. Tech. 86 (8) (2014) 1304.
[138] J.A. Kocal, B.V. Vora, T. Imai, Production of linear alkylbenzenes, Appl. Catal. A: Gen. 221 (1) (2001) 295–301.
[139] J. Yang, W. Qiao, Z. Li, L. Cheng, Effects of branching in hexadecylbenzene sulfonate isomers on interfacial tension behavior in oil/alkali systems, Fuel 84 (12) (2005) 1607–1611.
[140] G. Bhalla, S.M. Bischof, S.K. Ganesh, X.Y. Liu, C.J. Jones, A. Borzenko, et al., Mechanism of efficient anti-Markovnikov olefin hydroarylation catalyzed by homogeneous Ir(iii) complexes, Green Chem. 13 (1) (2011) 69–81.
[141] J. Oxgaard, R.P. Muller, W.A. Goddard, R.A. Periana, Mechanism of homogeneous Ir(III) catalyzed regioselective arylation of olefins, J. Am. Chem. Soc. 126 (1) (2004) 352–363.
[142] N.A. Foley, J.P. Lee, Z. Ke, T.B. Gunnoe, T.R. Cundari, Ru(II) catalysts supported by hydridotris(pyrazolyl)borate for the hydroarylation of olefins: reaction scope, mechanistic studies, and guides for the development of improved catalysts, Acc. Chem. Res. 42 (5) (2009) 585–597.
[143] N.O. Calloway, The Friedel-Crafts syntheses, Chem. Rev. 17 (3) (1935) 327–392.
[144] A. Goldman, R. Ahuja, W. Schinski. Rutgers, The State University of New Jersey, 2013. US patent US20130123552A12013.
[145] B. Franco, E. Mahieu, L. Emmons, Z. Tzompa-Sosa, E. Fischer, K. Sudo, et al., Evaluating ethane and methane emissions associated with the development of oil and natural gas extraction in North America, Environ. Res. Lett. 11 (4) (2016) 044010.
[146] G.E. Dobereiner, J. Yuan, R.R. Schrock, A.S. Goldman, J.D. Hackenberg, Catalytic synthesis of n-alkyl arenes through alkyl group cross-metathesis, J. Am. Chem. Soc. 135 (34) (2013) 12572–12575.
[147] L.V. Dinh, B. Li, A. Kumar, W. Schinski, K.D. Field, A. Kuperman, et al., Alkyl–aryl coupling catalyzed by tandem systems of pincer-ligated iridium complexes and zeolites, ACS Catal. 6 (5) (2016) 2836–2841.
[148] A.S. Goldman, L.V. Dinh, W.L. Schinski. Rutgers, The State University of New Jersey, Chevron U.S.A. Inc., 2013. US patent WO2013070316A12013.

[149] X. Jia, Z. Huang, Conversion of alkanes to linear alkylsilanes using an iridium–iron-catalysed tandem dehydrogenation–isomerization–hydrosilylation, Nat. Chem. 8 (2) (2016) 157–161.
[150] X. Tang, X. Jia, Z. Huang, Catalytic conversion of alkanes to linear aldehydes and linear amines, J. Am. Chem. Soc. 140 (11) (2018) 4157–4163.
[151] R. Franke, D. Selent, A. Börner, Applied hydroformylation, Chem. Rev. 112 (11) (2012) 5675–5732.
[152] P.W. Van Leeuwen, C. Claver, Rhodium Catalyzed Hydroformylation, , 22, Springer Science & Business Media, 2002.
[153] S. Walter, M. Haumann, P. Wasserscheid, H. Hahn, R. Franke, n-Butane carbonylation to n-pentanal using a cascade reaction of dehydrogenation and SILP-catalyzed hydroformylation, AIChE J. 61 (3) (2015) 893–897.
[154] S. Fritschi, W. Korth, J. Julis, D. Kruse, H. Hahn, R. Franke, et al., Synthese von aliphatischen Aldehyden aus Alkanen und Kohlendioxid: Valeraldehyd aus Butan und CO2 – Machbarkeit und Grenzen, Chem. Ingen. Tech. 87 (10) (2015) 1313–1326.

CHAPTER 3

Transition metal-catalyzed dehydrogenation of methanol and related transformations

Sujan Shee[1], Bhaskar Paul[1,2] and Sabuj Kundu[1,*]
[1]Department of Chemistry, Indian Institute of Technology Kanpur, Kanpur, India
[2]University of California at Riverside, Riverside, CA, United States
Corresponding author. e-mail address: sabuj@iitk.ac.in

3.1 Introduction

Methanol is a highly abundant (produced ~70 million tons/year), biodegradable, simplest aliphatic alcohol, and is one of the essential components in chemical laboratory and industry [1,2]. Methanol was first produced as a by-product from the distillation of wood [3]. Currently, natural gas, coal, and biomass are the common sources for methanol production [4]. Industrially, methanol is mainly produced from syngas (CO/H_2) in the presence of CuO/ZnO catalyst at elevated temperature (200 °C−300 °C) and pressure (50−100 atm.) [5,6]. Lately, transition metal-catalyzed few pioneering reports were immersed for the production of methanol from more sustainable resources such as CO_2 and methane [7−10]. Methanol is mostly used to produce various fine chemicals (~40% of methanol used for the synthesis of formaldehyde) and as the solvent [11]. Recently, the utilization of methanol was explored as a liquid organic hydrogen carrier, as it is an excellent hydrogen reservoir (up to $3H_2$/MeOH) [12,13]. Interestingly, methanol is also used in the fuel cell for the production of electricity [14].

Methylated molecules are extremely significant in the chemical and pharmaceutical industries; approximately 67% of drug molecules contain at least one methyl group [15]. The presence of a methyl group is highly important in biological systems. It alters many stereoelectronic functions such as receptor selectivity, membrane permeability, gene modification, protection against enzyme metabolism, and many more [16−18]. Several important natural steroid products also contain the methyl group that displayed the pharmacological activity [15]. Owing to the importance of

Pincer−Metal Complexes
DOI: https://doi.org/10.1016/B978-0-12-822091-7.00001-4

methyl group, several conventional reagents such as methyl iodide, methyl sulfate, diazomethane etc., have been used for the methylation reactions [19,20]. However, most of these reagents are carcinogenic and generate waste chemicals. In this context, methanol is one of the greener alternatives to overcome these limitations. Nevertheless, compared to the other long-chain alcohols, dehydrogenation of methanol require much higher energy ($\Delta H = 84\ \text{kJ mol}^{-1}$), which makes the utilization of methanol relatively more challenging [21]. Therefore a more efficient catalytic system is essential to overcome the energy barrier.

In the last decade, transition metal-catalyzed utilization of alcohols as alkyl sources in various organic transformations was explored, following the "Borrowing Hydrogen (BH)" and "Acceptorless Dehydrogenative Coupling (ADC)" strategies. According to these principles, alcohol gets dehydrogenated to a carbonyl species in the presence of transition metal catalyst, which then reacts with nucleophile to form an unsaturated molecule with the elimination of water. For ADC strategy, this unsaturated molecule is the final product with the release of water and H_2 as by-products. For the BH principle, the same H_2 (as M − H) is utilized for the hydrogenation of unsaturated species to get the saturated alkylated molecule (Scheme 3.1) [22–25].

Applying these protocols, in the last decade, transition metal-catalyzed various C-, N- and O-methylation or formylation reactions have been published utilizing methanol. This chapter highlights mainly most of the reports related to the production of hydrogen from methanol and its application as a C1 source for the construction of various C − C and C − N bonds.

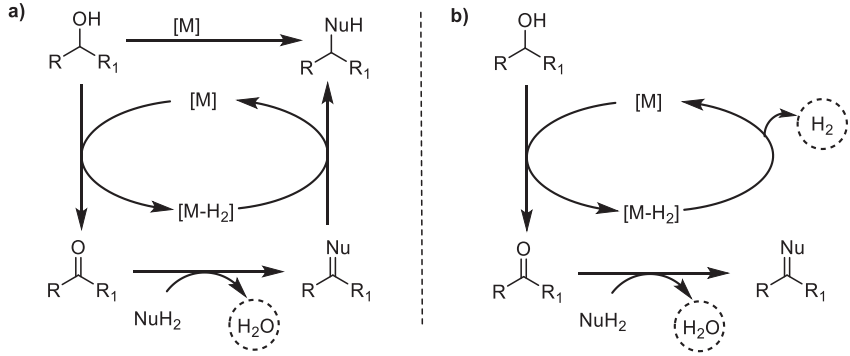

Scheme 3.1 (a) "Borrowing Hydrogen (BH)" and (b) "Acceptorless Dehydrogenative Coupling (ADC)" strategies.

3.2 Hydrogen production

Nowadays, worldwide energy consumption mostly depends on fossil fuel (>80%) [26]. In this context, hydrogen is considered an efficient and cleaner energy carrier for the future [12,27]. The reaction of hydrogen gas with the combination of oxygen release the chemical energy stored in the H–H bond, yielding only water as a product. However, due to the safety issues of hydrogen gas regarding the handling and transportation, recently methanol-based fuel cell has taken increasing attention [27]. Hydrogen molecules can be chemically stored in methanol with a very high gravimetric hydrogen content of 12.6% [27]. The conversion of the methanol–water mixture to H_2 and CO_2 gas is known as methanol steam reforming, which typically requires high temperature (200 °C–300 °C) in the presence of heterogeneous catalyst [27,28]. It is noteworthy to mention that the first step of the following sequence is endothermic and the second step is exothermic [Eqs. (3.1) and (3.2)]. This causes the overall process endothermic of ΔH_r = 38.8 kJ mol^{-1} [28].

$$CH_3OH + H_2O \rightarrow HCOOH + 2H_2 \quad \Delta H_r = 53.3 \text{ kJ mol}^{-1} \tag{3.1}$$

$$HCOOH \rightarrow CO_2 + H_2 \quad \Delta H_r = -14.5 \text{ kJ mol}^{-1} \tag{3.2}$$

In this process, the partial hydrogenation of CO_2 with the H_2 furnishes poisonous CO(g) as a side product, which contaminates the produced H_2(g). As CO is harmful to the fuel cell, the generation of pure hydrogen is crucial [12,29]. In the last decade, several catalytic systems were developed for the synthesis of pure hydrogen from methanol (Scheme 3.2) [27–36].

In 1988 Cole-Hamilton and co-workers developed a [$RuH_2(N_2)(PPh_3)_3$]-catalyzed hydrogen production from methanol [37]. After that, Bowker and co-workers reported a similar transformation using an Au/TiO_2 photocatalytic system [38]. Later, tremendous progress has been made in this field by Beller, Grützmacher, Milstein, and many other groups (Scheme 3.3) [27–36]. Grützmacher and co-workers developed Ru(II)-catalyzed hydrogen

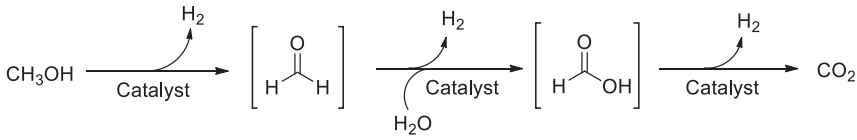

Scheme 3.2 Pathway for hydrogen production from methanol–water mixtures.

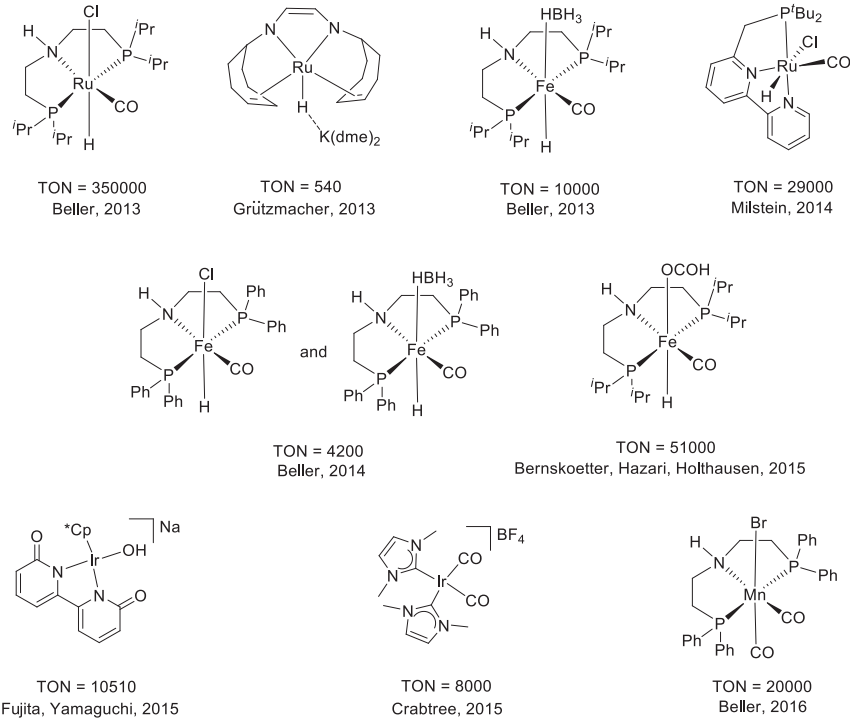

Scheme 3.3 Selected catalytic systems and turnover numbers (TONs) for hydrogen production from methanol.

production from methanol in 2013. In this process, the evolved CO_2 was converted to MCO_3 in the presence of $M(OH)_2$, which avoids the formation of by-product CO, as a result pure H_2 gas was generated [28]. Later, Beller and co-workers reported a (PNP)Ru(II)-catalyzed low-temperature (65 °C–95 °C) dehydrogenation of the methanol–water mixture (4:1) to hydrogen and CO_2. This catalytic system exhibited considerably high turnover number (TON) (TON >350,000; TOF 4700/h), and the methanol dehydrogenation process followed an *outer-sphere* mechanism [27]. In 2013 the same group developed a well-defined (PNP)Fe(II) complex for a similar transformation (2013) [30]. Subsequently, several Ru [29,31,34,39,40], Ir [33,41], Rh [36], Fe [32], Mn [35], etc. complexes as well as photocatalytic system [42,43] were developed for the reforming of methanol to hydrogen. Furthermore, Shi, Wen, Ma, and co-workers introduced a Pt/α-MoC heterogeneous catalyst, which exposed the outstanding hydrogen production activity with an average turnover frequency of 18,046 h^{-1} [44].

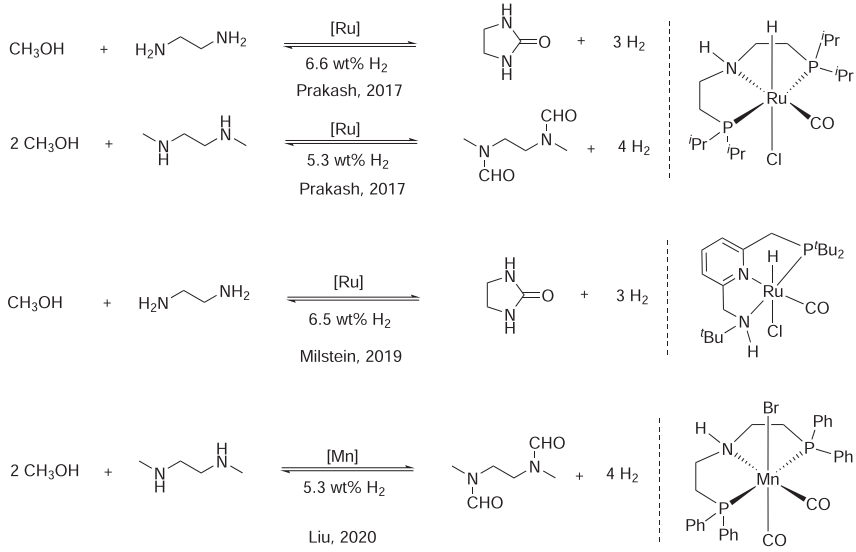

Scheme 3.4 Reversible hydrogen storage systems using amine and methanol.

Recently, several reversible liquid organic hydrogen carrier systems using methanol were developed (Scheme 3.4). In 2017 Prakash and co-workers disclosed a reversible hydrogen carrier system based on amine reforming of methanol where they employed both primary and secondary diamine [45]. Milstein and co-workers described a Ru(II)-catalyzed similar transformation based on methanol/ethylene diamine system in 2019 [46]. Recently Liu and co-workers developed an Mn(I) catalytic system for amine reforming of methanol where they employed *N,N*-dimethylethylenediamine/methanol system [47].

3.3 *N*-Methylation reactions

3.3.1 *N*-Methylation of amines

N-Methylation of amine using methanol was explored in the past few decades by several groups. In 1981 Grigg and co-workers first reported $RhH(PPh_3)_4$-catalyzed *N*-methylation of amines using methanol; however, substrate scope was limited for this transformation [48]. In the same year, Watanabe and co-workers described $RuCl_2(PPh_3)_3$-catalyzed similar *N*-methylation of aniline at 180 °C, although the yield was relatively low (13%) [49]. Employing the same $RuCl_2(PPh_3)_3$ catalyst, Arcelli and co-workers reported the selective *N,N*-dimethylated amines, or dialkylmethyl

amines from alkyl amine substrates [50]. Later, the Watanabe group again described the same reaction using $RuCl_3.H_2O/P(OBu)_3$ catalytic system, which provided up to 86% yield of *N*,*N*-dimethylated amine products [51].

The *N*-methylation process with methanol has got significant momentum, particularly from 2004. Del Zotto and co-workers demonstrated a half-sandwich cyclopentadienyl Ru(II) complex-catalyzed *N*-methylation of secondary/tertiary amines in the absence of base at relatively lower temperature (100 °C) in 2004 [52]. Interestingly, under standard reaction conditions, various aliphatic amines delivered the desired product; however, aromatic substrates including simple aniline did not work. Then in 2007, the Bhattacharjee group conveyed *N*-alkylation of amines with various alcohols including methanol using $[RuCl(PPh_3)_2(CH_3CN)_3][BPh_4]$ catalyst [53]. Later, Li and co-workers described an efficient and general method for the *N*-monomethylation of various aromatic amines and sulphonamides by using $[Cp^*IrCl_2]_2$ (0.1–0.4 mol%) at relatively higher temperature (150 °C) [54]. Crabtree and co-workers reported bis(*N*-heterocyclic carbene) containing Ir(III) complex-catalyzed *N*-methylation of aromatic amines with methanol under microwave conditions at 120 °C [41].

In 2015 Seayad et al. developed a simple and efficient method for the *N*-methylation of various aromatic, hetero-aromatic, and aliphatic amines under relatively mild reaction conditions [55]. By employing a $[Cp^*RuCl_2]_2$/dpePhos catalytic system, they synthesized various *N*-methylated amines and sulphonamides in 65%–98% yields at 40 °C–100 °C. Notably, they synthesized an antifungal agent "Naftifine" by applying this protocol. In recent years, this process was rapidly explored by Beller, Kundu, Liu, Sortais, and many other groups (Scheme 3.5) [56–67]. In 2016 Beller and co-workers reported Mn(I)-catalyzed *N*-alkylation of amines with methanol and other long-chain alcohols for the first time [58]. After that, Sortais and Beller independently described *N*-methylation of amines using a well-defined Mn(I)–pincer complex and synthesized a wide range of methylated products efficiently [59,60]. Next, a $Co(acac)_2$-catalyzed similar transformation was developed by Liu and co-workers in the presence of a tetradentate phosphine ligand $P(CH_2CH_2PPh_2)_3$ at 140 °C [61]. Additionally, various *N*-methylated products were synthesized in >99% yields. They performed several control experiments and deuterium labeling studies to supports the mechanism of this process. In 2018 a (PNP)Re(I)–pincer complex was introduced for the same reaction by Sortais et al. [63]. Various kinetic studies, control experiments, and detailed density functional theory (DFT) calculations were performed to

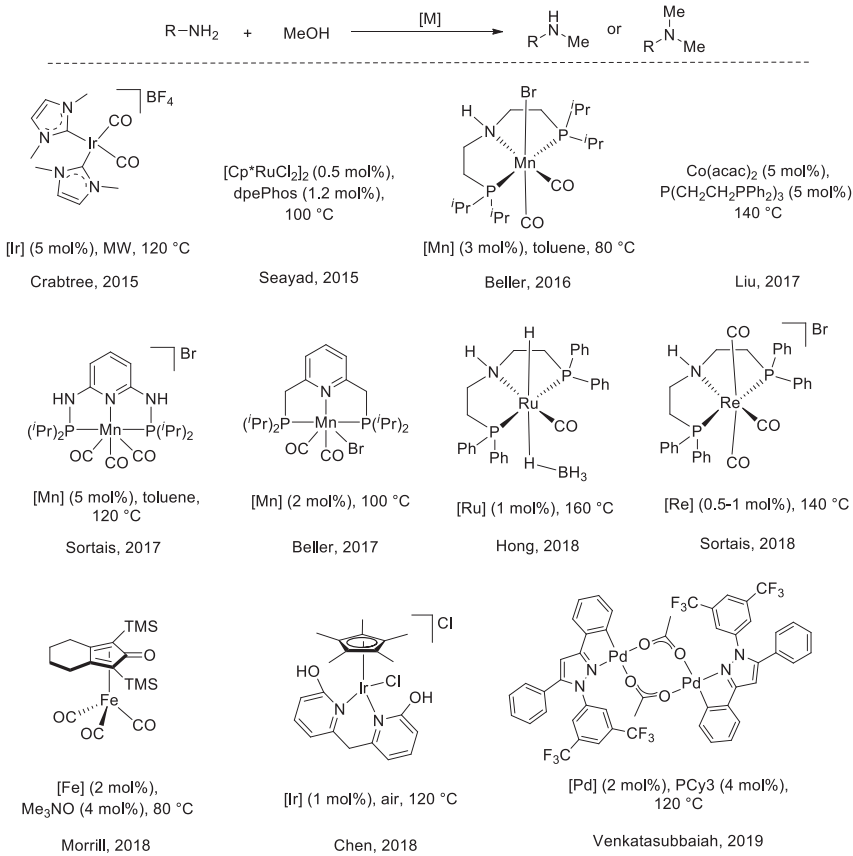

Scheme 3.5 Selective homogeneous catalytic systems for the *N*-methylation of amines.

realize the reaction mechanism of this Re(I) catalyst. In the same year, Morrill and co-workers reported a Fe(II)-catalyzed *N*-monomethylation of amines and sulphonamides. In this transformation, they employed a Knölker-type (cyclopentadienone)iron carbonyl complex in the presence of Me_3NO as a cocatalyst at 80 °C [65]. Chen and co-workers described the same *N*-methylation of amines in the presence of 2-hydroxypyridine based Ir(III)−complex under air [66]. Palladacycle with a combination of PCy_3 ligand also provided good yields of *N*-methylated amines as reported by the Venkatasubbaiah group in 2019 [67]. Recently, Siddiki and Shimizu et al. performed the same reaction under heterogeneous conditions [68]. Different *N*-methylated amines were synthesized with this

Pt/C catalyst at 150 °C. They also tested the reusability of the catalyst, and notably, it did not lose its catalytic activity significantly even after the 5th cycle. The author performed several kinetic studies, which suggested that the moderate metal–hydrogen bond strength of platinum was the main reason for its high reactivity over other carbon supported metal catalysts.

3.3.2 *N*-Methylation of nitro, nitrile, and azide compounds

N-Methylated amines are also accessed directly from nitro compounds, nitriles, and azides using methanol (Scheme 3.6). As an early work, Li and co-worker reported a Raney Ni-based catalytic system for the reductive *N*-methylation of nitro compound with methanol [69]. However, in this process, high temperature (170 °C) and high pressure (3 MPa) of nitrogen gas were required and scope was limited to the only nitrobenzene. A similar photocatalytic transformation was described by Shi and co-workers in 2015 [57]. By employing Pd/TiO_2 catalyst, they synthesized few *N*-methylated amines directly from the nitro compounds under UV radiation/irradiation (365 nm LED (light emitting diode)). Later, Ru(II)- and Pd(II)-catalyzed similar transformation was reported in tandem fashion by Kundu and Beller et al., respectively. In 2017 Kundu and co-workers developed air- and moisture-stable (NNN)Ru(II) complex to synthesize various *N*-methylated amines from diverse nitro compounds [70]. The reductive *N*-methylation of nitroarenes, α,β-unsaturated nitro compounds, and nitroalkanes provided

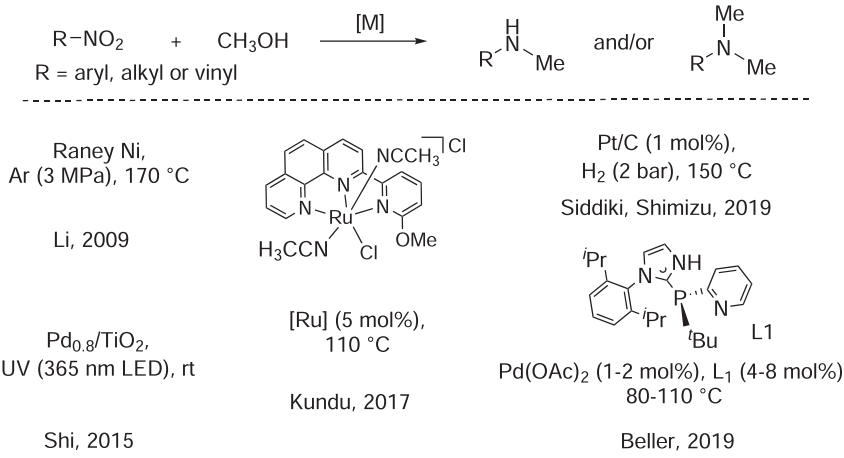

Scheme 3.6 Conversion of nitro compounds to *N*-methylated amines.

selectively *N*-monomethylated and *N,N*-dimethylated amines up to 98% yields. A similar transformation was accomplished by Beller and co-workers using $Pd(OAc)_2$/phosphine system in 2019. This system catalyzed the direct conversion of aromatic nitro compounds to the corresponding *N*-monomethylated products up to 85% yields. Although this catalytic system provided a large substrates scope (30 examples), it was limited to only aromatic substrates [71]. Additionally, heterogeneous catalyst Pt/C was also capable of accomplishing this reaction utilizing methanol [68]. Siddiki, Shimizu, and co-workers obtained several *N*-methylated amines in the presence of 1.0 mol% Pt/C catalyst and 1 equivalent of KO^{t}Bu under 2 bar of additional H_2 pressure at 150 °C (Scheme 3.6).

Recently, Kundu and co-workers established a protocol for the tandem transformation of nitriles and azides to the corresponding *N*-methylated amines using (NNN)Ru(II)−pincer complexes (Scheme 3.7) [72,73]. Various nitriles were smoothly transformed to the *N,N*-dimethylated amines under the standard catalytic conditions [72]. To demonstrate the practical relevance of this protocol, preparative scale synthesis of various methylated products and synthesis of antiallergic drug pheneramine were also performed. The same group also demonstrated the tandem transformation of azides, which are readily accessed from halide in the presence

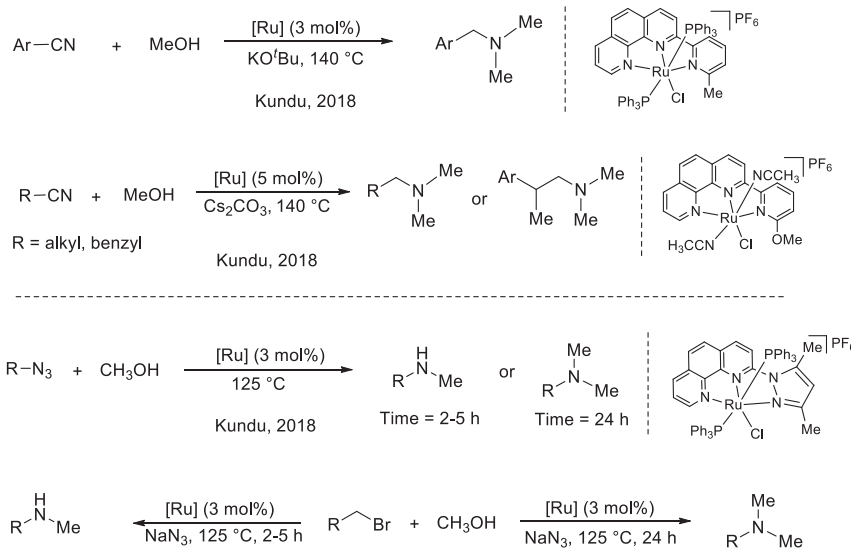

Scheme 3.7 Direct synthesis of *N*-methylated amines from nitriles and azides.

of NaN_3 to *N*-methylated amines using methanol. Notably, various *N*-monomethylated and *N,N*-dimethylated amines were selectively synthesized by the alteration of reaction time [73]. Interestingly, one-pot conversion of various alkyl and aryl bromide to the methylated products were also performed with methanol in the presence of NaN_3.

3.3.3 *N*-Methylation of amides and oximes

Only few reports are known on transition metal-catalyzed *N*-methylation of amides using methanol. For such conversion, a considerable contribution was made by Kundu and co-workers [74–76]. In 2019 this group described the *N*-methylation of various amide molecules with methanol in the presence of a well-defined (NNN)Ru(II)–pincer complex [74]. The authors clarified that under basic condition, the nucleophilic attack of methoxide to the carbonyl center of amide produced methyl ester when methanol was used as sole solvent. Notably, the formation of *N*-methylated ester was minimized by using a mixture of methanol and nonpolar solvent toluene in a 1:5 volumetric ratio (Scheme 3.8). Under the optimized conditions, this Ru(II) system provided several *N*-methylated amides as well as C- and *N*-methylated amides in excellent yields. The control experiments and kinetic studies suggested that the C- and *N*-methylation were much faster compared to the amide *N*-methylation. They also performed detailed DFT studies for a better understanding of the reaction mechanism.

Aldoximes, which are easily synthesized from aldehyde and hydroxylamines, could be used as the surrogate for amide [77,78]. Keeping this in mind, Ru(II)–complex-mediated rearrangement of aldoximes, followed by *N*-methylation of amides using methanol/toluene mixture (1:3.5, v/v), was described by Kundu and co-workers (Scheme 3.9) [75]. This Ru(II) system provided several *N*-methylated amides in good to excellent yields. A possible reaction mechanism for this catalytic process is shown in Scheme 3.9. Initially, ruthenium coordination to aldoxime generated the ruthenium bounded nitrile species after elimination of water. Then, the nucleophilic attack of another

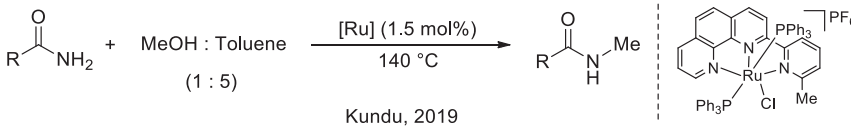

Scheme 3.8 *N*-Methylation of amides with methanol.

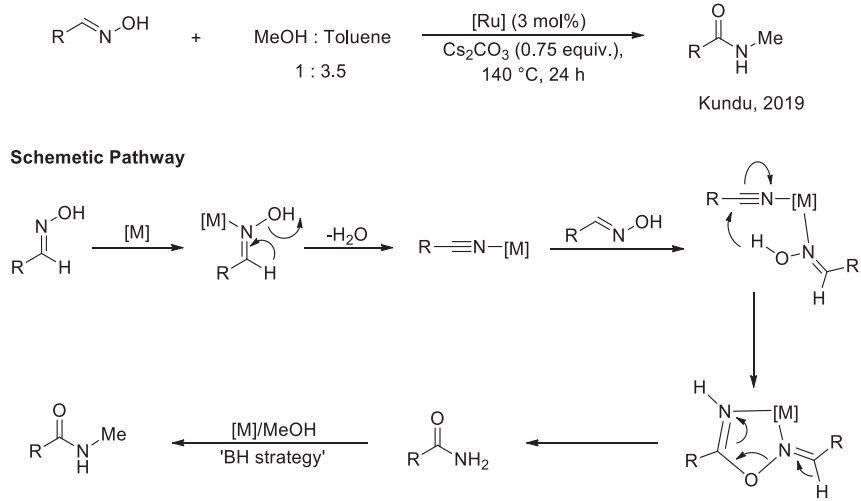

Scheme 3.9 Synthesis of *N*-methylated amides from aldoximes and probable reaction mechanism.

aldoxime molecule to the metal-bounded nitrile followed by rearrangement produced amide molecule, which reacted with formaldehyde to generate imine intermediate. Finally, insertion of this imine molecule to the Ru(II)-H followed by methanolysis produced the *N*-methylamide. In this proposed mechanism, aldoxime acted as the nucleophile, not the water, which was confirmed by the H_2O^{18} labeling study.

Recently, the same group reported the synthesis of various *N*-methylated amides from nitriles in the presence of $CoBr_2/P(CH_2CH_2PPh_2)_3$ system using methanol–water mixture following a hydration/methylation sequence [76]. Initially, the authors observed the formation of a considerable amount of benzyl alcohol as a side product during the optimization of reaction parameters. To minimize the benzyl alcohol formation and to make hydration of nitrile faster than the hydrogenation steps, small amount of water and a mixture of the bases (0.5 equivalent of KO^{t}Bu and 1 equivalent of Cs_2CO_3) were utilized (Scheme 3.10). The authors mentioned that KO^{t}Bu was superior for hydration of nitrile, and Cs_2CO_3 was the most effective for *N*-methylation of amide step. They performed extensive work on experimental studies as well as DFT calculations to get information about the mechanism and reactivity differences of the substrates. Controlled experiments using H_2O^{18} and CD_3OD confirmed the source of the oxygen atom and the methyl group in *N*-methyl amides.

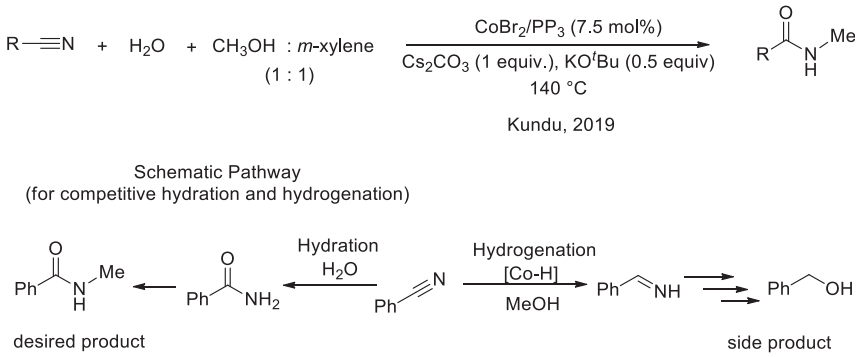

Scheme 3.10 Synthesis of *N*-methylated amides from nitriles.

3.4 *N*-Formylation reactions

Glorius and co-workers developed a Ru(II)–NHC complex-catalyzed *N*-formylation of amines in 2013. Ru(II) complex was synthesized from [Ru(COD)(2-methylallyl)$_2$] and ICy.HCl at 70 °C in toluene. Then, they performed the same pot reaction using different amines in the presence of 3.3 equivalents of methanol and 3 equivalents of styrene as a hydrogen acceptor, which provided excellent yields of *N*-formamide products [79]. Later, in 2015 Hong and co-workers reported the same transformation from both nitriles and amines using a Ru(II)–NHC system [80]. In this work, they synthesized various *N*-formylated compounds up to 99% yields without base or hydrogen acceptor. Base metal-catalyzed similar transformation was conveyed by Milstein and co-workers in 2017 [81]. A benzo-fused (PNP)Mn(I) bifunctional complex provided up to 86% yields of the desired products. In the same year, the Bernskoetter group disclosed synthesis of several *N*-formylated products in THF at 80 °C using methanol as formylating agent using a well-defined (PNP)Fe(II) catalyst (0.1 mol%) [82]. In 2018 remarkably a tuneable *N*-formylation, *N*,*N*-formylmethylation, and *N*,*N*-dimethylation reaction was demonstrated with a single Ru(II)–MACHO–BH complex by Hong and co-workers (Scheme 3.11) [64]. Mechanistic studies revealed that reaction temperature and hydrogen (generated from methanol) played a pivotal role in controlling the selectivity to form the different classes of products.

3.5 C-Methylation reactions

3.5.1 α-Methylation of ketones

Metal complex-catalyzed α-methylation of carbonyl compounds with methanol was explored in the last decades by various groups (Scheme 3.12). In

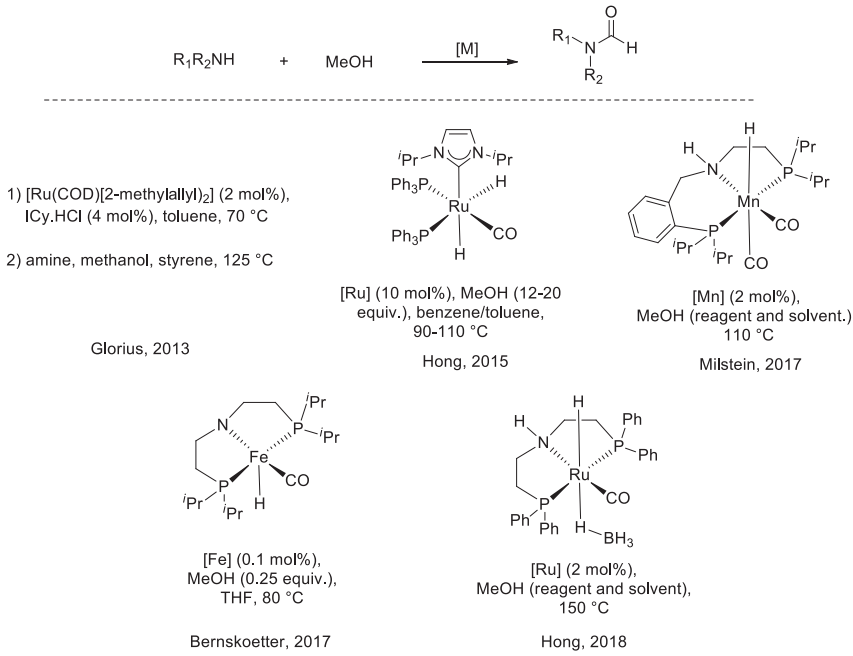

Scheme 3.11 *N*-Formylation of amines using methanol.

2014 Donohoe and co-workers reported an Rh(III)-catalyzed α-methylation of ketones using methanol under aerobic conditions [83]. This catalytic system was applicable to a broad range of aromatic and aliphatic ketones. Interestingly, consecutive one-pot double methylation of simple methyl ketones was also explored. By using a combination of Ir (2 mol%) and Rh (10 mol%) catalysts, they also performed a tandem one-pot three-component coupling reaction. Later, Obora and co-workers demonstrated a Ir(III) complex-catalyzed α-methylation of various multisubstituted ketones [84]. Moreover, they extended this protocol to synthesize tandem three-component α-methylation using ketone, methanol, and primary alcohol, although relatively higher catalyst loading (10 mol%) was required. In the presence of Ir(III) catalysts, α-methylation of ketones was later executed by Li and Anderson groups [85,86]. Li and co-workers performed the reaction in aerobic conditions to regenerate the catalyst in active form during the reaction. They defined the role of functional bipyridonate ligand of Ir(III) complex in both dehydrogenation of methanol and hydrogenation of α,β-unsaturated ketone intermediate [85]. Whereas Anderson group demonstrated an NHC-phosphine ligand-based Ir(III) catalyst, which performed the

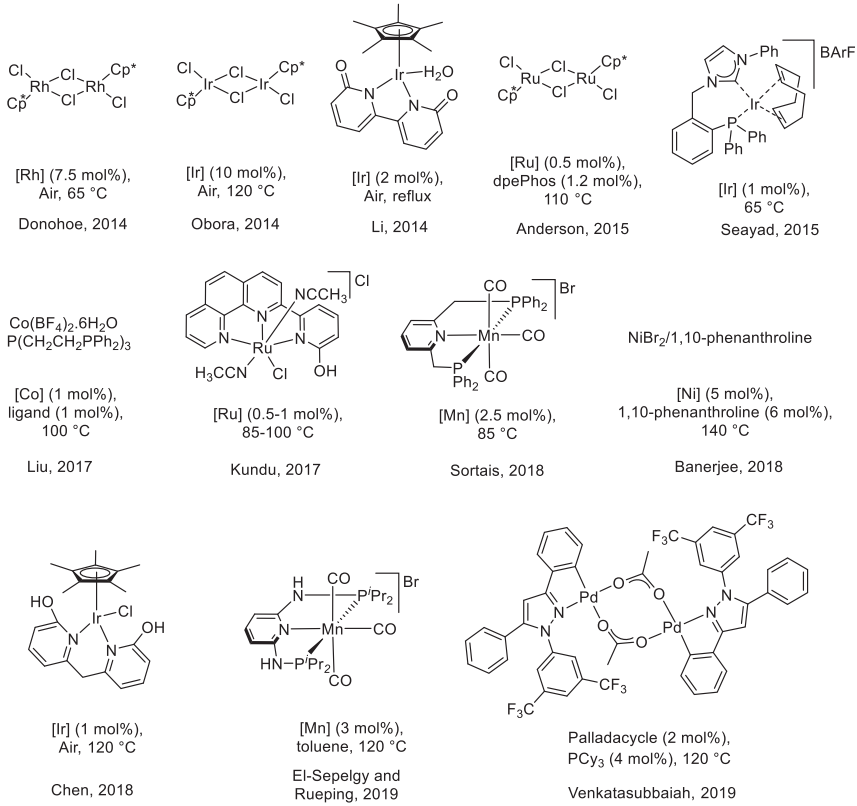

Scheme 3.12 Some examples of homogeneous complexes used in C-methylation of ketones.

reaction at mild reaction conditions and required lower catalyst loading compared to commercially available $[Cp^*IrCl_2]_2$ catalyst [86].

In 2016 Ru(II) catalyst was introduced for C-methylation of both ketones and esters by Seayad and co-workers (Scheme 3.12) [87]. Interestingly, a TON up to 710 for the α-methylation of ketones was achieved by this phosphine-based Ru(II) catalyst. The author also synthesized the antiinflammatory agent ketoprofen in consecutive two catalytic steps. Methylation of the readily available starting material ester by this Ru(II) system, followed by palladium(II)-catalyzed carbonylative coupling with phenylboronic acid generated the ester derivative of ketoprofen, which finally provided the ketoprofen after hydrolysis of the ester with aq. NaOH (Scheme 3.13).

Kundu and co-workers established a nonphosphine-based bifunctional NNN–Ru(II) complex for the similar α-methylation reaction in 2017 [70].

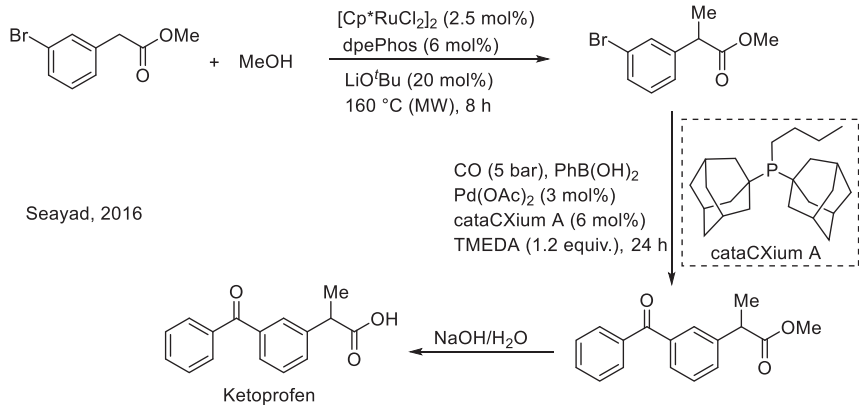

Scheme 3.13 Synthesis of ketoprofen.

Similar yields of the products were obtained in the presence of only 0.1 mol% Ru(II) catalyst at 120 °C. Notably, the tandem three-component coupling of various ketones with methanol and different primary alcohols was also achieved in excellent yields in the presence of 1.0 mol% catalyst. Several kinetic studies and DFT calculations were performed to acquire the plausible pathway for this conversion. In 2018 Chen group reported the synthesis of 2-hydroxy-6-((6-hydroxypridin-2-yl)methyl)pyridine ligand and its Ir(III) complex, which provided C-methylated ketones in high yield under air [66]. Venkatasubbaiah and co-workers demonstrated the same methylation reaction by employing a palladacycle and PCy_3 in methanol [67]. This catalytic system also furnished excellent yields of the desired methylated products.

Notably, first-row metal-based catalysis has drawn significant attention in the last few years for the C-methylation of ketones. In 2017 Liu and co-workers reported cobalt-catalyzed methylation of different substituted ketones, arylacetonitriles, and indoles derivatives [88]. The Co $(BF_4)_2 \cdot 6H_2O/P(CH_2CH_2PPh_2)_3$ catalytic system showed good to excellent yields of methylated products at 100 °C (Scheme 3.12). In the next year, a Knölker-type (cyclopentadienone)iron carbonyl complex was introduced as catalyst by Morill and co-workers [89]. This Fe(0) system provided a broad substrate scope for the methylation of various ketones, indoles, oxindoles, amines, and sulphonamides. After that, Mn(I) complex-catalyzed methylation reaction using methanol was described separately by Sortais and Rueping groups (Scheme 3.12) [90,91]. Sortais group reported a (PNP)Mn(I) complex (3.0 mol%) for the C-methylation of ketones and ester derivatives at 120 °C. Whereas Rueping and

co-workers described the methylation of various ketone derivatives by using methanol and deuterated methanol (Scheme 3.12). In 2018 a $NiBr_2$/1,10-phenanthroline catalytic system was introduced by Banerjee and co-workers; however, the scope was limited, and moderate yields were observed for such transformation (only three examples) [92].

Not only the homogeneous but some heterogeneous catalysts were also explored for a similar transformation. In 2017 Das and co-workers developed polymer-stabilized palladium nanoparticles for C-methylation of ketones using methanol and other long-chain aromatic and aliphatic alcohols (Scheme 3.14) [93]. This system required a trace amount of air, for the activation of the catalyst, which by alcohol dehydrogenation, followed by condensation between ketone and aldehyde and subsequent hydrogenation of resultant alkene completed the cycle as shown in Scheme 3.15.

In the same year, an efficient Pd heterogeneous catalyst for α-methylation of various substituted ketones with methanol was described by Hou and co-workers (Scheme 3.14) [94]. The highly robust and chemical-resistant Pd nanoparticles immobilized in syndiotactic poly(*para*-*N,N*-dimethylaminostyrene) polymer (Pd@sPS-N) exhibited superior catalytic activity, and this system maintained its activity even after the 5th run. In 2018 a carbon-stabilized Pt nanoparticle (Pt/C)-catalyzed C-methylation reactions with methanol was demonstrated by Shimizu and co-workers (Scheme 3.14) [95]. Easy separation of both catalyst and products, catalytic recyclability (at least five runs), and excellent TON (>3000) were the advantages for this catalytic system. Further, a heterogeneous nonnoble metal catalyst Ni/SiO_2-Al_2O_3 furnished several methylated ketones at relatively higher temperature (185 °C) (Scheme 3.14) [96].

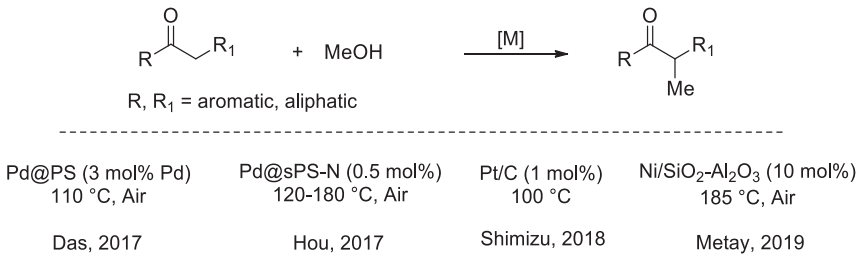

Scheme 3.14 α-Methylation of ketones in the presence of heterogeneous catalysts.

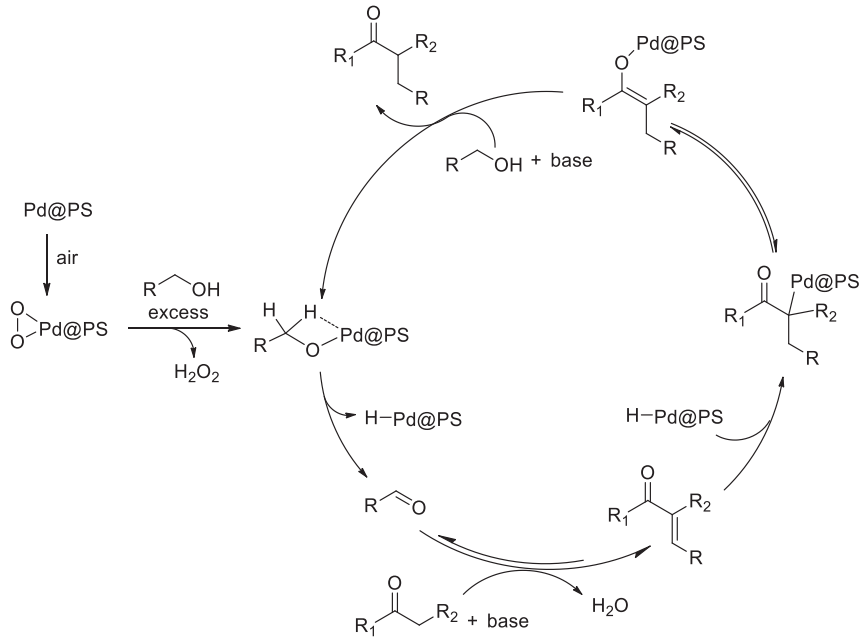

Scheme 3.15 Mechanism of the α-alkylation of ketones with palladium catalyst.

3.5.2 C-Methylation of alcohols

Carlini and co-workers described the synthesis of isobutanol from a mixture of MeOH and n-PrOH by employing a heterogeneous Cu cromite catalyst [95]. Later, the same group performed a similar transformation from the combination of MeOH/^{i}PrOH/EtOH in harsh reaction conditions [97,98]. They described that the reaction parameters and the amount of reagent were the key for getting a higher yield of ^{i}BuOH. This group further extended this work by using Ni, Ru, and Rh catalysts for the selective production of isobutanol by modulating the reaction parameters. In 2003 Marchionna and co-workers reported a Guerbet-type condensation reaction of MeOH and ^{i}PrOH in the presence of homogeneous Pd catalyst ($Pd(PPh_3)_4$, $Pd(dba)_2$, and $Pd(dppe)Cl_2$) [99]. In this study, they conveyed that both homogeneous and heterogeneous activities of Pd catalyst were observed. The authors proposed that during the reaction, generated solid Pd^0 metal was in equilibrium with the Pd−OMe complex in an alcoholic medium (Scheme 3.16). However, for all these above-mentioned reports, a significantly higher reaction temperature (~200 °C) was required to achieve sufficient conversion.

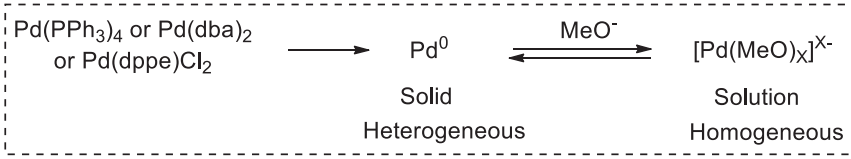

Scheme 3.16 Equilibrium of palladium catalyst between homogeneous and heterogeneous phases.

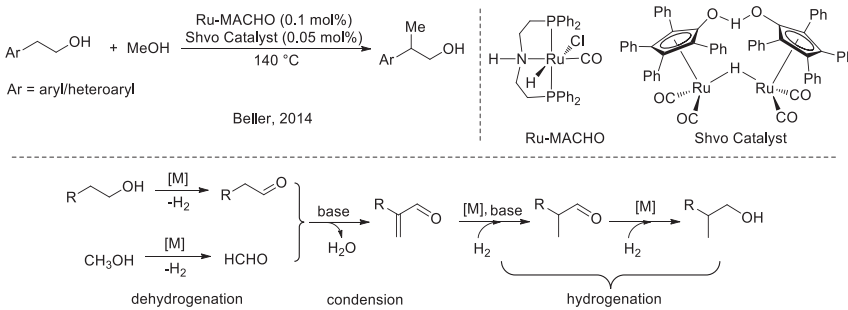

Scheme 3.17 Synthesis of β-methylated alcohols using Ru(II)–MACHO and Shvo's catalyst.

Beller and co-workers in 2014 described β-methylation of 2-arylethanols with methanol in the presence of a bimetallic Ru(II)-MACHO and Shvo catalysts (Scheme 3.17) [100]. Kinetic experiments suggested that dehydrogenation of both alcohols was the critical step to obtain a high yield of the desired products. The author described Ru(II)-MACHO catalyst favored the dehydrogenation of methanol, but not 2-arylethanol. Thus Shvo's catalyst was required to enhance the dehydrogenation of 2-arylethanol, which synergistically increased the yield of final products. To improve the final product yield, the stepwise release of reaction pressure (release of H_2 gas) was necessary, which shifted the equilibrium toward the aldol products. Initially, dehydrogenation of both aryl ethanol and methanol was occurred by the transition metal catalyst. Then, the resultant ketone and formaldehyde underwent base-catalyzed aldol condensation to generate double unsaturated molecules. Finally, the unsaturated intermediate was hydrogenated in a stepwise manner by the transition metal catalyst to furnish the desired product (Scheme 3.17).

Later, Obora and co-workers developed DMF-stabilized Ir–NCs heterogeneous material for the β-methylation of alcohols (Scheme 3.18) [101]. The TEM and DLS studies showed that the particles were

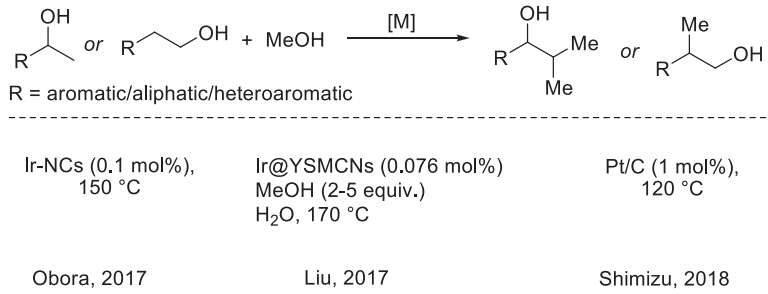

Scheme 3.18 Heterogeneous catalysts used in the β-methylation reaction.

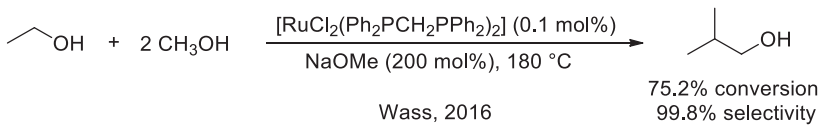

Scheme 3.19 Production of isobutanol from ethanol–methanol mixture using Ru(II) catalyst.

1.0–1.5 nm scale, whereas ^{1}H NMR, TG-DTA, and FT-IR analysis indicated the presence of DMF as a surface coating on Ir–NCs particles. This Ir–NCs catalyst (0.1 mol%) methylated several aromatic and semi-aromatic alcohols in the presence of 1 equivalent of KOH at 150 °C. Interestingly, a high TON of 48,000 was achieved for this transformation. In 2016 Wass and co-workers reported a Guerbet-type production of isobutanol from methanol using homogeneous phosphine-based Ru(II) catalyst (Scheme 3.19) [102]. The author revealed that phosphine with a small bite angle provided greater productivity and selectivity toward the formation of isobutanol from a methanol–ethanol mixture. In this study, the excess amount of methanol was required to prevent the homo-coupling of ethanol (methanol:ethanol = 14.4:1).

Later, Xu, Mu, and co-workers introduced Ir-encapsulated yolk–shell-structured mesoporous carbon nanospheres (Ir@YSMCNs) for the C-methylation of alcohols (Scheme 3.18) [103]. The reaction was performed in a water medium using 2–5 equivalents of methanol (with respect to alcohol) in the presence of 1 equivalent of KOH at 170 °C. A broad range of substrate provided excellent yields of β-methylated alcohols. Furthermore, methylation of 1,2-diol derivatives was achieved in good yields. In 2018 carbon-supported Pt (Pt/C) catalyst was reported by Shimizu group, which furnished various β-methylated aryl, aliphatic, and heterocyclic alcohols in good to excellent yields (Scheme 3.18) [95].

Leitner and co-workers described a phosphine-based Ru(II)–dihydrido complex (Ru–MACHO–BH) for the conversion of a variety of aromatic and aliphatic alcohols to the desired β-methylated products (Scheme 3.20) [104]. In this study, the authors stated that the prolonged heating drastically decreases the product formation due to the increase of hydrogen pressure in the reaction vessel, which simultaneously hydrogenated the resultant ketone to the starting alcohol back. They achieved a high turnover number (18,000) for such transformation. The same group performed detailed DFT calculations with this Ru(II) catalyst, which advocated that the de- and re-hydrogenation required the energy in the range of ca. 10–15 kcal mol^{-1}. A moderate energy barrier of 13.6 kcal mol^{-1} was required for the base-catalyzed C – C bond formation but comprises the highest transition state with energy at 26.9 kcal mol^{-1} relative to the reference point [105].

Recently, replacing the noble metals with earth-abundant, relatively cheap 3d metal-based homogeneous catalysis has been studied for a similar transformation (Scheme 3.20). Morill and co-workers reported selective β-methylation of alcohols using well-defined bench-stable (cyclopentadienone)iron(0) carbonyl complex and efficiently synthesized various β-methylated alcohols (Scheme 3.20) [65]. Initially, decarbonylation of [Fe] precatalyst by either Me_3NO or base in the presence of methanol generated the active iron complex, which after dehydrogenated methanol and 2-phenylethanol produced formaldehyde and 2-phenylacetaldehyde, respectively. After that, base-catalyzed aldol condensation followed by the hydrogenation with the [Fe] – H species finally produced the desired β-methylated alcohol product (Scheme 3.21).

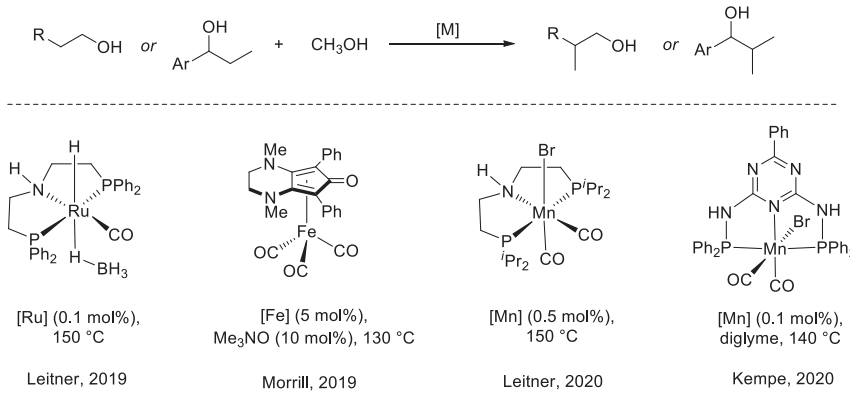

Scheme 3.20 Homogeneous catalysts used in β-methylation of alcohols.

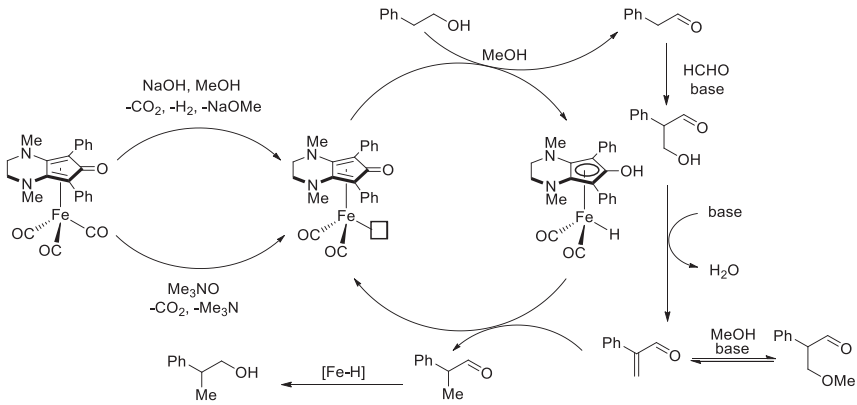

Scheme 3.21 Proposed mechanism of β-methylation of alcohols with Fe(II) catalyst.

In 2020 Leitner and co-workers introduced another earth-abundant and environmentally benign 3d metal, manganese, as a form of Mn(I)−MACHO complex for such conversion (Scheme 3.20) [106]. Interestingly, a large variety of β-methylated secondary, primary, and cyclic alcohols was obtained by this catalytic system. The stoichiometric reaction of the Mn(I)−MACHO complex with NaO^{t}Bu generated an unsaturated Mn−amide complex, which produced intermediate alcoholate complexes after the addition of 2-phenylethanol or methanol (Scheme 3.22). In the case of methanol, a hydride complex with formaldehyde and hydrogen was produced, suggesting the dehydrogenation activity of the active Mn−amide complex. These experiments advocated that the reactions followed the ligand-assisted *outer-sphere* mechanism. Recently, Kempe and co-workers described the same transformation using a bimetallic Mn(I)-K catalyst [107]. This catalytic system was highly effective; a low catalyst loading of 0.1 mol% was capable of producing a wide range of β-methylated alcohols within a short reaction time (3 h).

3.5.3 C3-Methylation of indoles

Transition metal-mediated C3-methylation of indoles with methanol were developed by several groups (Scheme 3.23). In 2012 Cai and co-workers demonstrated the C-methylation of indoles and pyrroles using $[Cp^*IrCl_2]_2$ and KO^{t}Bu at 140 °C under aerobic conditions (Scheme 3.23) [108]. Interestingly, simple pyrrole was transformed into the tetramethylated pyrroles under catalytic conditions. For indole substrates, various methylated products were synthesized up to 91% yields, and during

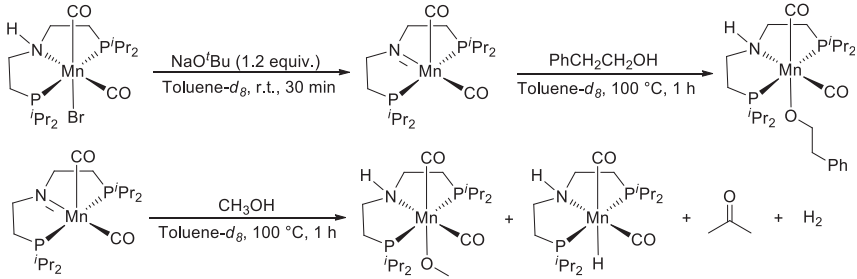

Scheme 3.22 Spectroscopically identified Mn(I) intermediates.

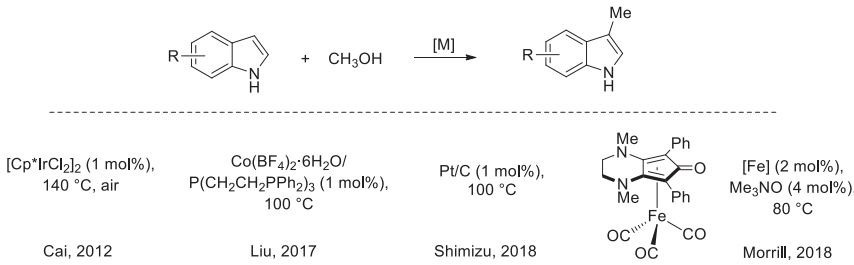

Scheme 3.23 C3-Methylation of indoles with methanol.

this transformation, reducible groups such as nitro, nitrile, and ester were well tolerated. No C3-methylated product was observed for *N*-methyl indole, which supports the mechanism of the base-mediated tautomerization. In 2017 Liu and co-workers described the C-methylation of indoles in the presence of $Co(BF_4)_2 \cdot 6H_2O/P(CH_2CH_2PPh_2)_3$ at 100 °C (Scheme 3.23) [88]. A broad scope of this transformation furnished various methylated products in 88%–95% yields. Later, Fe(0)-catalyzed similar transformation was performed at 80 °C by Morrill and co-workers (Scheme 3.23) [89]. In the same year, Shimizu and co-workers developed a heterogeneous carbon-supported platinum (Pt/C) catalyst for this C3-methylation of indoles (Scheme 3.23) [95]. They synthesized the methylated products up to 95% yields and tested the reusability of this catalytic system, which was well tolerable for up to five cycles.

3.5.4 α-Methylation of arylacetonitriles

Several reports on alkylation at the α-position of arylacetonitrile were also described with methanol following BH methodology (Scheme 3.24).

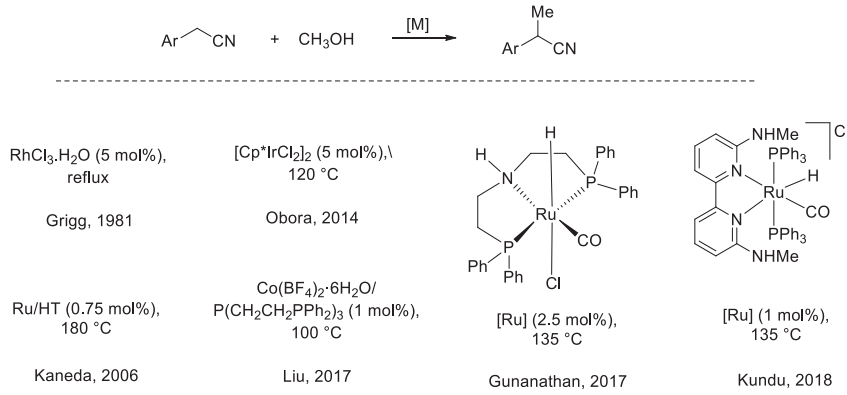

Scheme 3.24 α-Methylation of arylacetonitriles.

Grigg and co-workers first (1981) reported this reaction in 1981 with methanol and other alcohols in the presence of $RhCl_3.6H_2O$ at refluxing conditions (Scheme 3.24) [109]. However, the scope was limited, and a very low yield of the methylated products was observed. A ruthenium-grafted hydrotalcite (Ru/HT)-catalyzed similar conversion was described in 2006 by Kaneda and co-workers with methanol and other long-chain alcohols at 180 °C (Scheme 3.24) [110]. Later, Obora and co-workers conveyed the α-methylation of arylacetonitriles with methanol by employing a $[Cp^*IrCl_2]_2$ catalyst (Scheme 3.24) [84]. Differently substituted arylacetonitriles were methylated at 120 °C and furnished the desired product in 75%–87% yields. After that, a cobalt-catalyzed α-methylation of arylacetonitriles with methanol was described by Liu and co-workers in 2017 [88]. In this transformation, they used a commercially available $Co(BF_4)_2 \cdot 6H_2O$ and a tetradentate phosphine ligand P$(CH_2CH_2PPh_2)_3$ (PP_3) system, which provided various methylated products in 81%–94% yields. In the same year, Gunanathan and co-workers reported this similar transformation by using a metal ligand cooperative (PNP)Ru(II)–pincer complex (Scheme 3.24) [111]. The scope of this transformation was broad, and they employed methanol, ethanol, and other long-chain alcohols α-alkylation of aryl acetonitrile at 135 °C, although a prolonged heating (40 h) was required for this C-methylation reaction. In 2018 Kundu and co-workers introduced an ortho-amino group functionalized 2,2′-bipyridine-based Ru(II) complex for this similar transformation (Scheme 3.24) [112]. They explored this reaction's scope by using methanol (at 135 °C) and other long-chain alcohols (at 115 °C).

3.5.5 Aminomethylations

Hong and co-workers described a Ru(II)–MACHO–BH-complex catalyzed aminomethylation of several phenol derivatives in 2017 (Scheme 3.25) [113]. Interestingly, for naphthol derivatives, $Ru(acac)_3$/triphos system produced α-methylated naphthols as major products instead of aminomethylated one. Based on various mechanistic studies, the authors proposed a catalytic pathway for this aminomethylation reaction (Scheme 3.25). At first, Ru(II)-catalyzed dehydrogenation of MeOH lead to the formation of formaldehyde, which then reacted with amine to generate the hemiaminal intermediate. Then, the phenolate anion reacted with iminium cation (generated after dehydration) to produce the final product. Whereas formamide intermediate barely participates in the reaction. But, in the case of naphthol, the reaction between iminium cation with naphtholate anion, followed by deamination via an E1cB mechanism produce enal intermediate, which finally furnished the α-methyl naphthol.

Later, (PNP)Mn(I) complex-catalyzed three-component aminomethylation of various aromatic compounds was reported by Kirchner and co-workers in 2017 [114]. Differently substituted naphthols, phenols, pyridines, carbazoles, indoles, and thiophenes with a combination of amines and MeOH provided the corresponding aminomethylated products

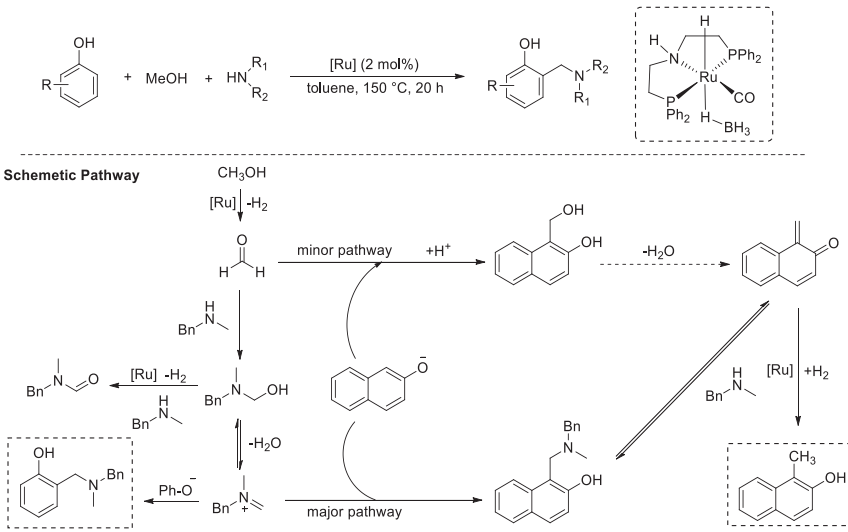

Scheme 3.25 Ru(II)-catalyzed aminomethylation and methylation of phenol derivatives.

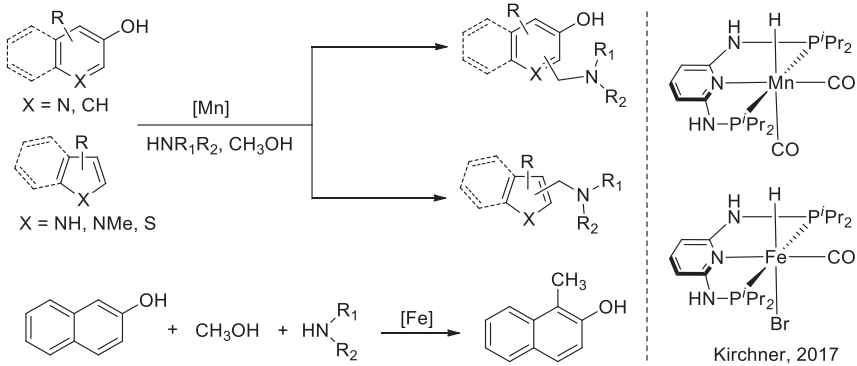

Scheme 3.26 Aminomethylation of aromatic compounds using Mn(I) catalyst.

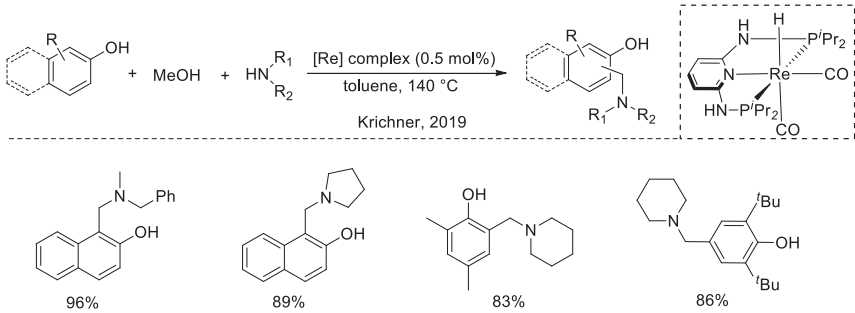

Scheme 3.27 Re(I)-catalyzed aminomethylation of aromatic compounds.

efficiently. Notably, (PNP)Fe(II) complex predominantly delivered α-methylated naphthols rather than the aminomethylated products (Scheme 3.26).

In 2019 Kirchner group performed the same transformation using a rhenium complex bearing the same (PNP) ligand fragment [115]. Methanol, secondary amines, and phenols/naphthols provided the corresponding aminomethylated products with high isolated yields in the presence of 0.5 mol% of Re(I) complex at 140 °C (Scheme 3.27).

3.6 *N*-Heterocycles synthesis

$N-$Heterocyclic compounds are widely known as biologically active compounds and used in various fields, including medicinal chemistry. In 2016 Li and co-workers demonstrated a novel methodology for the synthesis of a series of substituted quinazolinones by the reaction between

o-aminobenzamides and methanol following the acceptorless dehydrogenation coupling strategy [116]. They performed this reaction in the presence of bifunctional [Cp*Ir(2,2′-bpyo)(H_2O)] complex under microwave irradiation and synthesized a range of various substituted desired products in excellent yields. Importantly, biologically active molecule erlotinib, an anticancer drug, and receptor tyrosine kinase initiator was produced under the standard conditions (Scheme 3.28). A plausible mechanism for this acceptorless dehydrogenation reaction is shown in Scheme 3.28. At first, dissociation of H_2O molecule, followed by protonation of one pyridonate system generated $Ir-OMe$ complex, which then underwent $\beta-$hydride elimination to form $Ir-H$ species and formaldehyde molecule. Subsequently, the condensation between *o*-aminobenzamide with formaldehyde produced 2,3-dihydroquinazolinone, which furnished the final product after dehydrogenation.

Recently, the same transformation was described by using inexpensive commercially available $Cu(OAc)_2.4H_2O$ and Cs_2CO_3, under an O_2 atmosphere (Scheme 3.29) [117]. At the beginning of the reaction, Cu^{II} catalyst oxidized methanol to formaldehyde and itself got reduced to Cu^{I} system. Next, the condensation between formaldehyde and *o*-aminobenzamide generated the imine intermediate, which after cyclization, afforded 2,3-dihydroquinazolinone molecule. Finally, Cu^{I} system oxidized to Cu^{II}

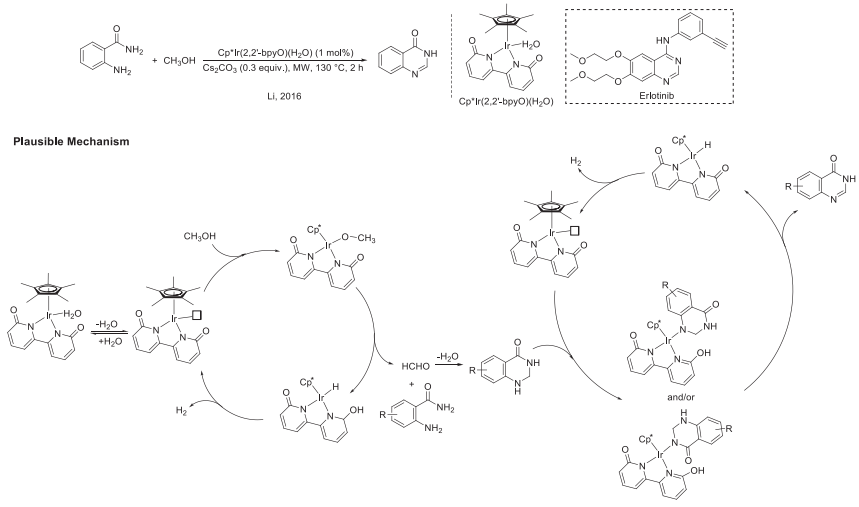

Scheme 3.28 Proposed mechanism for synthesis of quinazolinones by Ir(III) catalyst.

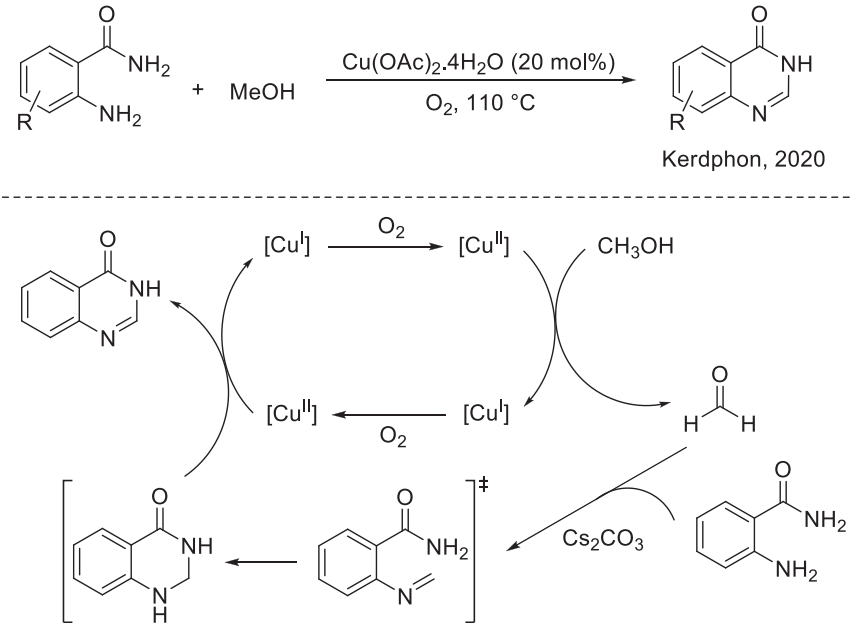

Scheme 3.29 Cu(II)-catalyzed synthesis of quinazolinones.

species, which dehydrogenated the 2,3-dihydroquinazolinone species to produce the quinazolinone (Scheme 3.29).

The direct synthesis of quinazolinones from 2-aminobenzonitriles would be an attractive protocol in a one-pot manner. In this context, Kundu and co-workers developed a suitable protocol to obtain these molecules from 2-aminobenzonitriles using a methanol–water mixture [118]. The authors utilized a bipyridine-based Ru(II) complex, which was stable enough in water under the standard reaction conditions. The kinetic experiments advocated that methanol and H_2O were the sources of C1 and O1, respectively, in the final product (Scheme 3.30).

In 2019 Ilangovan and co-workers reported a $CuCl_2.2H_2O$-catalyzed cyclization reaction for the synthesis of quinazolines in the presence of tert-butylhydroperoxide (TBHP) as an oxidant (Scheme 3.31) [119]. In this work, they used methanol and ammonium acetate as carbon and nitrogen sources, respectively. Moreover, using this protocol, a muscle-relaxing drug quazodine was synthesized in good yield. Another important class of *N*-heterocycles benzimidazoles was successfully synthesized by Barta and co-workers in 2012 (Scheme 3.31) [120]. Copper-doped porous metal oxide (Cu-PMO) was utilized for the coupling of readily available

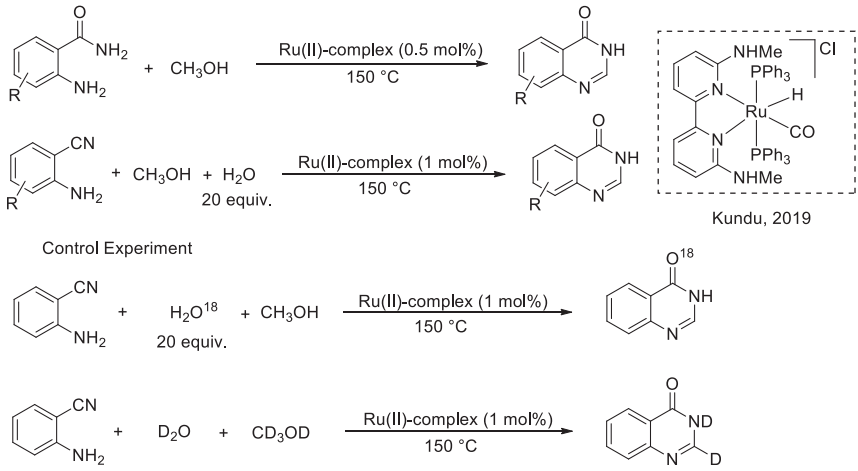

Scheme 3.30 Synthesis of quinazolinones by using Ru(II) catalyst.

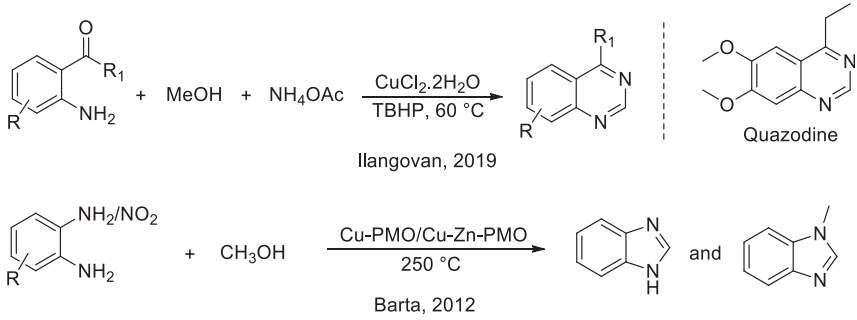

Scheme 3.31 Synthesis of quinazoline and benzimidazole derivatives.

2-nitroanilines and aniline derivatives with methanol. In this study, supercritical methanol acted as both the C1 source and solvent. However, this reaction was not selective, both benzimidazole and *N*-methyl benzimidazole were formed at high reaction temperature (250 °C).

3.7 Miscellaneous transformations

Methanol is also employed in some other transformations as a C1 source, for example, in transfer hydrogenations, synthesis of urea, C − C coupling with allenes, and many others. In this section, we describe some of the representative examples of them. Ir(III) complex-catalyzed transfer hydrogenation with methanol was reported by Tani and Sundararaju groups

(Scheme 3.32) [121,122]. In 1999 Tani and co-workers described transfer hydrogenation of alkenes and alkynes by using an Ir(III) complex at 80 °C (Scheme 3.32) [121]. However, in these transformations, the scope was limited, and moderate yields of the products were observed. Recently, Sundararaju and co-workers demonstrated the transfer hydrogenation of ketones in the presence of $[Cp^*IrCl_2]_2$/2,2′-bipyridine-6,6′-diol (Scheme 3.32) [122]. They also screened $[Cp^*CoI_2]_2$ and $[Cp^*RhCl_2]_2$ in this transformation, [Rh] complex yielded 29% product, whereas [Co] complex was ineffective. Notably, various functional groups such as nitro, nitrile, alkene, alkyne, and ester were well tolerated under catalytic conditions.

Urea derivatives could be synthesized from amines and methanol in the presence of transition metal catalysts following the BH strategy instead of using toxic reagents such as phosgene, isocyanates, etc. (Scheme 3.33) [123,124]. In 2016 Hong and co-workers developed this remarkable transformation using a (PNP)Ru(II)−pincer complex (Scheme 3.33) [125]. They synthesized both symmetrical and unsymmetrical urea molecules in the absence of any base, oxidant, or hydrogen acceptor. Symmetric urea molecules were synthesized in a single step, whereas sequential addition of reactants was essential for the synthesis of unsymmetrical molecules. Bernskoetter and co-workers described a similar transformation using a (PNP)Fe(II) complex. They revealed a broad substrate scope for the synthesis of symmetrical urea derivatives (Scheme 3.33) [126].

Ir(III)-catalyzed direct coupling of allenes with methanol was reported by Krische and co-workers in 2011. This catalytic system provided various branched alcohols in high yield (Scheme 3.34) [21]. The Cole-Hamilton

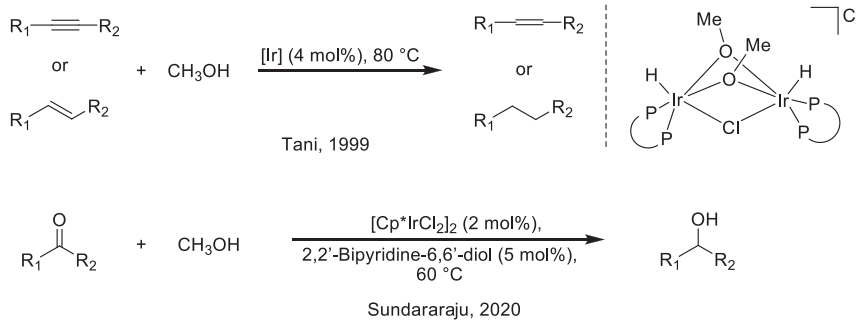

Scheme 3.32 TH of alkynes, alkenes, and ketones with methanol.

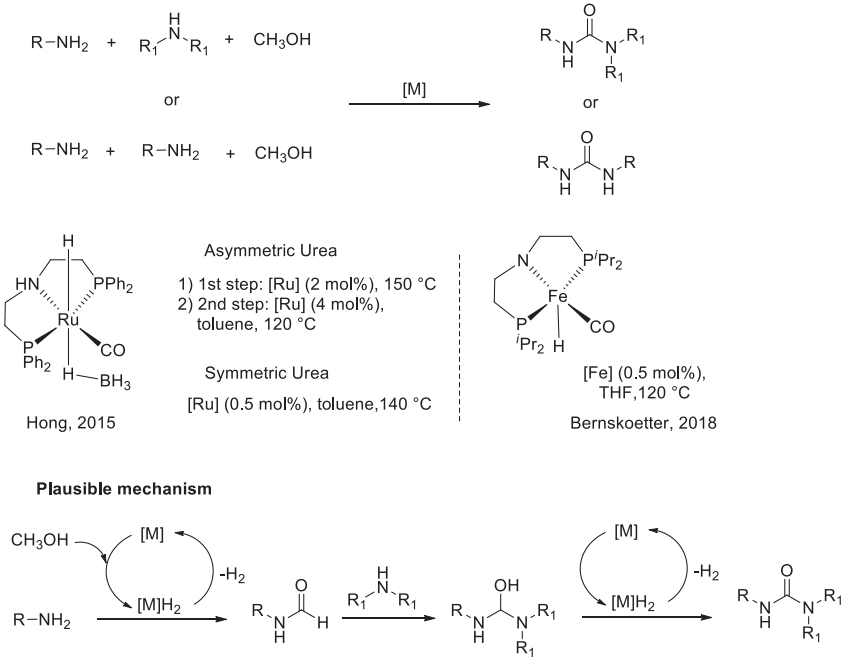

Scheme 3.33 Synthesis of urea derivatives using methanol and plausible mechanism.

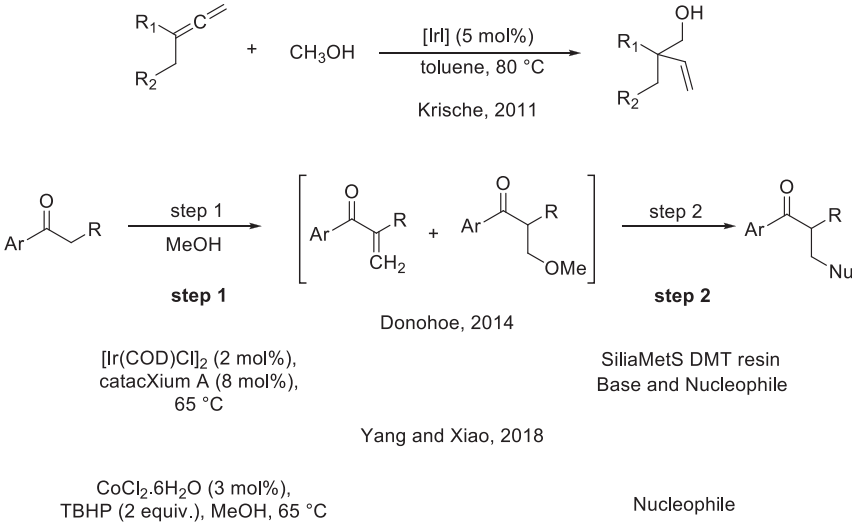

Scheme 3.34 Synthesis of branch alcohols and ketones.

group reported a Ru(II) complex-catalyzed α-methylenation of methyl propanoate following the methanol dehydrogenation strategy [127]. Following BH and interrupted BH methodology, Donohoe and co-workers developed a one-pot methylenation and conjugate addition of aryl ketones in the presence of $[Ir(COD)Cl]_2$ (Scheme 3.34) [128]. Following this one-pot, two-step process, they synthesized various α-branched ketones by employing different nucleophiles. Then, a cobalt-catalyzed α-methoxylation and amino methylation were described in 2018 by Yang, Xiao, and co-workers utilizing $CoCl_2.6H_2O$ in the presence of TBHP as oxidant (Scheme 3.34) [129]. Several control experiments were also performed; notably, the formation of formaldehyde by the oxidation of methanol was confirmed by the silver mirror test.

In 2008 Jun and co-workers demonstrated a protocol for the synthesis of *di*-alkyl ketones using an $Rh(Cl)(PPh_3)_3$ catalyst (Scheme 3.35) [130]. In this protocol, they also utilized a catalytic amount of 2-amino-4-picoline and benzoic acid. The C3-coupling between two substituted indole molecules using $[Cp^*Ir(Cl)_2]_2$ catalyst at 150 °C employing methanol was developed by Li and co-workers (Scheme 3.35) [131]. In this transformation, the scope was good, and up to 91% yields were observed. However, in other metal catalysts like $[Cp^*Rh(Cl)_2]_2$ or $[Ru(p\text{-cymene})(Cl)_2]_2$, only 6%–45% yields were observed. In 2018 Morrill and co-workers described a Fe(0)-catalyzed C-methylation of oxindoles with

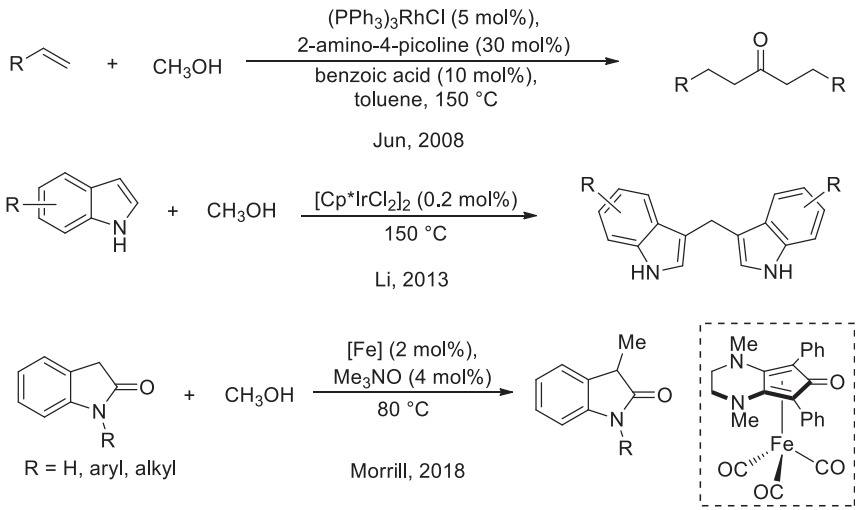

Scheme 3.35 Synthesis of dialkyl ketones, *bis*-indoles, and methyl oxindoles.

methanol at 80 °C (Scheme 3.35) [89]. For this transformation, they employed a Knölker-type (cyclopentadienone)iron carbonyl complex as a catalyst in the presence of Me_3NO as cocatalyst and synthesized some methylated oxindoles up to 86% yields.

3.8 Conclusion

Methanol is a potential H_2 reservoir, and thus recently, various promising catalytic protocols are developed for the production of hydrogen from methanol. Additionally, methanol can also be utilized as a C1 source in the numerous transformations based on the "BH" and "ADC" strategies. Following these protocols, methanol is employed as a green reagent, which provides a high atom economy. The overview of this chapter is described as the development of different approaches toward the achievement of cost-effective and more viable processes for *N*-methylation, C-methylation, *N*-formylation reactions, etc. We discussed the reactions of amines, nitriles, amides, nitro compounds, ketones, esters, etc., with methanol to synthesize various valuable C-methylated, *N*-methylated, *N*-formylated, and *N*-heterocycles products. Although methanol is mostly used as a building block in the industry to produce various bulk chemicals, many other potential applications are still possible using methanol as a reagent. This green alcohol has a promising future for utilization as a carbon source for C- and *N*-methylation reactions replacing the toxic reagents; however, for the large-scale synthesis, more efficient catalytic system is required. Additionally, there are enormous scopes in the asymmetric synthesis using methanol and photocatalyzed methanol activation under mild conditions.

References

[1] G.A. Olah, Beyond oil and gas: the methanol economy, Angew. Chem. Int. (Ed.) 44 (18) (2005) 2636–2639.
[2] D. Prat, A. Wells, J. Hayler, H. Sneddon, C.R. McElroy, S. Abou-Shehada, et al., CHEM21 selection guide of classical- and less classical-solvents, Green. Chem. 18 (1) (2016) 288–296.
[3] E. Farber, Evolution of Chemistry, 2nd (ed.), Ronald Press, New York, 1969.
[4] D.R. Palo, R.A. Dagle, J.D. Holladay, Methanol steam reforming for hydrogen production, Chem. Rev 107 (10) (2007) 3992–4021.
[5] J.-P. Lange, Methanol synthesis: a short review of technology improvements, Catal. Today 64 (1) (2001) 3–8.
[6] W.L. Luyben, Design and control of a methanol reactor/column process, Ind. Eng. Chem. Res 49 (13) (2010) 6150–6163.

[7] C.A. Huff, M.S. Sanford, Cascade catalysis for the homogeneous hydrogenation of CO_2 to methanol, J. Am. Chem. Soc. 133 (45) (2011) 18122–18125.
[8] S. Wesselbaum, T. vom Stein, J. Klankermayer, W. Leitner, Hydrogenation of carbon dioxide to methanol by using a homogeneous ruthenium–phosphine catalyst, Angew. Chem. Int. (Ed.) 51 (30) (2012) 7499–7502.
[9] V.L. Sushkevich, D. Palagin, M. Ranocchiari, J.A. van Bokhoven, Selective anaerobic oxidation of methane enables direct synthesis of methanol, Science. 356 (6337) (2017) 523.
[10] J. Xie, R. Jin, A. Li, Y. Bi, Q. Ruan, Y. Deng, et al., Highly selective oxidation of methane to methanol at ambient conditions by titanium dioxide-supported iron species, Nat. Catal. 1 (11) (2018) 889–896.
[11] F. Dalena, A. Senatore, A. Marino, A. Gordano, M. Basile, A. Basile, Chapter 1—methanol production and applications: an overview, in: A. Basile, F. Dalena (Eds.), Methanol, Elsevier, 2018, pp. 3–28.
[12] R.M. Navarro, M.A. Peña, J.L.G. Fierro, Hydrogen production reactions from carbon feedstocks: fossil fuels and biomass, Chem. Rev. 107 (10) (2007) 3952–3991.
[13] A.F. Dalebrook, W. Gan, M. Grasemann, S. Moret, G. Laurenczy, Hydrogen storage: beyond conventional methods, Chem. Commun. 49 (78) (2013) 8735–8751.
[14] A. Sartbaeva, V.L. Kuznetsov, S.A. Wells, P.P. Edwards, Hydrogen nexus in a sustainable energy future, Energy Env. Sci. 1 (1) (2008) 79–85.
[15] E.J. Barreiro, A.E. Kümmerle, C.A.M. Fraga, The methylation effect in medicinal chemistry, Chem. Rev. 111 (9) (2011) 5215–5246.
[16] P.B.C.G. Wermuth, The Practice of Medicinal Chemistry, Accademic Press;, San Diego, 2008.
[17] K.C. Chu, The Basis of Medicinal Chemistry/Burger's Medicinal Chemistry, John Wiley, New York, 1980.
[18] H. Schönherr, T. Cernak, profound methyl effects in drug discovery and a call for new C-H methylation reactions, Angew. Chem. Int. (Ed.) 52 (47) (2013) 12256–12267.
[19] G.L.C. Agüero, A comparison of several modern alkylating agents, ARKIVOC. (2009) 251–264.
[20] Y. Chen, Recent advances in methylation: a guide for selecting methylation reagents, Chem. Eur. J. 25 (14) (2019) 3405–3439.
[21] J. Moran, A. Preetz, R.A. Mesch, M.J. Krische, Iridium-catalysed direct C–C coupling of methanol and allenes, Nat. Chem. 3 (4) (2011) 287–290.
[22] M.H.S.A. Hamid, P.A. Slatford, J.M.J. Williams, Borrowing hydrogen in the activation of alcohols, Adv. Synth. Catal. 349 (10) (2007) 1555–1575.
[23] G.E. Dobereiner, R.H. Crabtree, Dehydrogenation as a substrate-activating strategy in homogeneous transition-metal catalysis, Chem. Rev. 110 (2) (2010) 681–703.
[24] C. Gunanathan, D. Milstein, Applications of acceptorless dehydrogenation and related transformations in chemical synthesis, Science. 341 (6143) (2013) 1229712.
[25] A. Corma, J. Navas, M.J. Sabater, Advances in one-pot synthesis through borrowing hydrogen catalysis, Chem. Rev. 118 (4) (2018) 1410–1459.
[26] N. Armaroli, V. Balzani, The legacy of fossil fuels, Chem. Asian J. 6 (3) (2011) 768–784.
[27] M. Nielsen, E. Alberico, W. Baumann, H.-J. Drexler, H. Junge, S. Gladiali, et al., Low-temperature aqueous-phase methanol dehydrogenation to hydrogen and carbon dioxide, Nature. 495 (7439) (2013) 85–89.
[28] R.E. Rodríguez-Lugo, M. Trincado, M. Vogt, F. Tewes, G. Santiso-Quinones, H. Grützmacher, A homogeneous transition metal complex for clean hydrogen production from methanol–water mixtures, Nat. Chem. 5 (4) (2013) 342–347.
[29] P. Hu, Y. Diskin-Posner, Y. Ben-David, D. Milstein, Reusable homogeneous catalytic system for hydrogen production from methanol and water, ACS Catal. 4 (8) (2014) 2649–2652.

[30] E. Alberico, P. Sponholz, C. Cordes, M. Nielsen, H.-J. Drexler, W. Baumann, et al., Selective hydrogen production from methanol with a defined iron pincer catalyst under mild conditions, Angew. Chem. Int. (Ed.) 52 (52) (2013) 14162—14166.
[31] A. Monney, E. Barsch, P. Sponholz, H. Junge, R. Ludwig, M. Beller, Base-free hydrogen generation from methanol using a bi-catalytic system, Chem. Commun. 50 (6) (2014) 707—709.
[32] E.A. Bielinski, M. Förster, Y. Zhang, W.H. Bernskoetter, N. Hazari, M.C. Holthausen, Base-free methanol dehydrogenation using a pincer-supported iron compound and Lewis acid Co-catalyst, ACS Catal. 5 (4) (2015) 2404—2415.
[33] K.-I. Fujita, R. Kawahara, T. Aikawa, R. Yamaguchi, Hydrogen production from a methanol—water solution catalyzed by an anionic iridium complex bearing a functional bipyridonate ligand under weakly basic conditions, Angew. Chem. Int. (Ed.) 54 (31) (2015) 9057—9060.
[34] M. Lei, Y. Pan, X. Ma, The nature of hydrogen production from aqueous-phase methanol dehydrogenation with ruthenium pincer complexes under mild conditions, Eur. J. Inorg. Chem. 2015 (5) (2015) 794—803.
[35] M. Andérez-Fernández, L.K. Vogt, S. Fischer, W. Zhou, H. Jiao, M. Garbe, et al., A stable manganese pincer catalyst for the selective dehydrogenation of methanol, Angew. Chem. Int. (Ed.) 56 (2) (2017) 559—562.
[36] Y.-L. Zhan, Y.-B. Shen, S.-P. Li, B.-H. Yue, X.-C. Zhou, Hydrogen generation from methanol reforming under unprecedented mild conditions, Chin. Chem. Lett. 28 (7) (2017) 1353—1357.
[37] D. Morton, D.J. Cole-Hamilton, Molecular hydrogen complexes in catalysis: highly efficient hydrogen production from alcoholic substrates catalysed by ruthenium complexes, J. Chem. Soc., Chem. Commun. 17 (1988) 1154—1156.
[38] J. Greaves, L. Al-Mazroai, A. Nuhu, P. Davies, M. Bowker, Photocatalytic methanol reforming on Au/TiO_2 for hydrogen production, Gold. Bull. 39 (4) (2006) 216—219.
[39] V. Sinha, N. Govindarajan, B. de Bruin, E.J. Meijer, How solvent affects C—H activation and hydrogen production pathways in homogeneous Ru-catalyzed methanol dehydrogenation reactions, ACS Catal. 8 (8) (2018) 6908—6913.
[40] N. Govindarajan, V. Sinha, M. Trincado, H. Grützmacher, E.J. Meijer, B. de Bruin, An in-depth mechanistic study of Ru-catalysed aqueous methanol dehydrogenation and prospects for future catalyst design, ChemCatChem. 12 (9) (2020) 2610—2621.
[41] J. Campos, L.S. Sharninghausen, M.G. Manas, R.H. Crabtree, Methanol dehydrogenation by iridium N-heterocyclic carbene complexes, Inorg. Chem. 54 (11) (2015) 5079—5084.
[42] Z. Liu, Z. Yin, C. Cox, M. Bosman, X. Qian, N. Li, et al., Room temperature stable CO_X production from methanol with magnesium oxide nanophotocatalysts, Sci. Adv. 2 (9) (2016) e1501425.
[43] M. Wakizaka, T. Matsumoto, R. Tanaka, H.-C. Chang, Dehydrogenation of anhydrous methanol at room temperature by o-aminophenol-based photocatalysts, Nat. Commun. 7 (1) (2016) 12333.
[44] L. Lin, W. Zhou, R. Gao, S. Yao, X. Zhang, W. Xu, et al., Low-temperature hydrogen production from water and methanol using Pt/α-MoC catalysts, Nature. 544 (7648) (2017) 80—83.
[45] J. Kothandaraman, S. Kar, R. Sen, A. Goeppert, G.A. Olah, G.K.S. Prakash, Efficient reversible hydrogen carrier system based on amine reforming of methanol, J. Am. Chem. Soc. 139 (7) (2017) 2549—2552.
[46] Y. Xie, P. Hu, Y. Ben-David, D. Milstein, A reversible liquid organic hydrogen carrier system based on methanol-ethylenediamine and ethylene urea, Angew. Chem. Int. (Ed.) 58 (15) (2019) 5105—5109.

[47] Z. Shao, Y. Li, C. Liu, W. Ai, S.-P. Luo, Q. Liu, Reversible interconversion between methanol-diamine and diamide for hydrogen storage based on manganese catalyzed (de)hydrogenation, Nat. Commun. 11 (1) (2020) 591.
[48] R. Grigg, T.R.B. Mitchell, S. Sutthivaiyakit, N. Tongpenyai, Transition metal-catalysed N-alkylation of amines by alcohols, J. Chem. Soc, Chem Commun. 12 (1981) 611–612.
[49] Y. Watanabe, Y. Tsuji, Y. Ohsugi, The ruthenium catalyzed N-alkylation and N-heterocyclization of aniline using alcohols and aldehydes, Tetrahedron Lett. 22 (28) (1981) 2667–2670.
[50] A. Arcelli, K. Bui The, G. Porzi, Selective conversion of primary amines into N,N-dimethylalkyl- or N,N-dialkylmethyl-amines with methanol and $RuCl_2(Ph_3P)_3$, J. Organomet. Chem. 235 (1) (1982) 93–96.
[51] H. Keun-Tae, T. Yasushi, K. Masanobu, O. Fumio, W. Yoshihisa, Ruthenium catalyzed N-methylation of aminoaranes using methanol, Chem. Lett. 17 (3) (1988) 449–452.
[52] A. Del Zotto, W. Baratta, M. Sandri, G. Verardo, P. Rigo, Cyclopentadienyl RuII complexes as highly efficient catalysts for the N-methylation of alkylamines by methanol, Eur. J. Inorg. Chem. 2004 (3) (2004) 524–529.
[53] S. Naskar, M. Bhattacharjee, Selective N-monoalkylation of anilines catalyzed by a cationic ruthenium(II) compound, Tetrahedron Lett. 48 (19) (2007) 3367–3370.
[54] F. Li, J. Xie, H. Shan, C. Sun, L. Chen, General and efficient method for direct N-monomethylation of aromatic primary amines with methanol, RSC Adv. 2 (23) (2012) 8645–8652.
[55] T.T. Dang, B. Ramalingam, A.M. Seayad, Efficient ruthenium-catalyzed N-methylation of amines using methanol, ACS Catal. 5 (7) (2015) 4082–4088.
[56] V.N. Tsarev, Y. Morioka, J. Caner, Q. Wang, R. Ushimaru, A. Kudo, et al., N-Methylation of amines with methanol at room temperature, Org. Lett. 17 (10) (2015) 2530–2533.
[57] L. Zhang, Y. Zhang, Y. Deng, F., Shi, N. Light-promoted, N-dimethylation of amine and nitro compound with methanol catalyzed by Pd/TiO2 at room temperature, RSC Adv. 5 (19) (2015) 14514–14521.
[58] S. Elangovan, J. Neumann, J.-B. Sortais, K. Junge, C. Darcel, M. Beller, Efficient and selective N-alkylation of amines with alcohols catalysed by manganese pincer complexes, Nat. Commun. 7 (1) (2016) 12641.
[59] A. Bruneau-Voisine, D. Wang, V. Dorcet, T. Roisnel, C. Darcel, J.-B. Sortais, Mono-N-methylation of anilines with methanol catalyzed by a manganese pincer-complex, J. Catal. 347 (2017) 57–62.
[60] J. Neumann, S. Elangovan, A. Spannenberg, K. Junge, M. Beller, Improved and general manganese-catalyzed N-methylation of aromatic amines using methanol, Chem. Eur. J. 23 (23) (2017) 5410–5413.
[61] Z. Liu, Z. Yang, X. Yu, H. Zhang, B. Yu, Y. Zhao, et al., Efficient cobalt-catalyzed methylation of amines using methanol, Adv. Synth. Catal. 359 (24) (2017) 4278–4283.
[62] B. Paul, S. Shee, K. Chakrabarti, S. Kundu, Tandem transformation of nitro compounds into N-methylated amines: greener strategy for the utilization of methanol as a methylating agent, ChemSusChem. 10 (11) (2017) 2370–2374.
[63] D. Wei, O. Sadek, V. Dorcet, T. Roisnel, C. Darcel, E. Gras, et al., Selective mono N-methylation of anilines with methanol catalyzed by rhenium complexes: an experimental and theoretical study, J. Catal. 366 (2018) 300–309.
[64] G. Choi, S.H. Hong, Selective N-formylation and N-methylation of amines using methanol as a sustainable C1 source, ACS Sustain. Chem. Eng. 7 (1) (2019) 716–723.

[65] K. Polidano, J.M.J. Williams, L.C. Morrill, Iron-catalyzed borrowing hydrogen β-C (sp3)-methylation of alcohols, ACS Catal. 9 (9) (2019) 8575–8580.
[66] D. Deng, B. Hu, M. Yang, D. Chen, Methylation of amines and ketones with methanol catalyzed by an iridium complex bearing a 2-hydroxypyridylmethylene fragment, Organometallics. 37 (19) (2018) 3353–3359.
[67] R. Mamidala, P. Biswal, M.S. Subramani, S. Samser, K. Venkatasubbaiah, Palladacycle-phosphine catalyzed methylation of amines and ketones using methanol, J. Org. Chem. 84 (16) (2019) 10472–10480.
[68] M.A.R. Jamil, A.S. Touchy, M.N. Rashed, K.W. Ting, S.M.A.H. Siddiki, T. Toyao, et al., N-Methylation of amines and nitroarenes with methanol using heterogeneous platinum catalysts, J. Catal. 371 (2019) 47–56.
[69] L. Xu, X. Li, Y. Zhu, Y. Xiang, One-pot synthesis of N,N-dimethylaniline from nitrobenzene and methanol, N. J. Chem. 33 (10) (2009) 2051–2054.
[70] K. Chakrabarti, M. Maji, D. Panja, B. Paul, S. Shee, G.K. Das, et al., Utilization of MeOH as a C1 building block in tandem three-component coupling reaction, Org. Lett. 19 (18) (2017) 4750–4753.
[71] L. Wang, H. Neumann, M. Beller, Palladium-catalyzed methylation of nitroarenes with methanol, Angew. Chem. Int. (Ed.) 58 (16) (2019) 5417–5421.
[72] B. Paul, S. Shee, D. Panja, K. Chakrabarti, S. Kundu, Direct synthesis of N,N-dimethylated and β-methyl N,N-dimethylated amines from nitriles using methanol: experimental and computational studies, ACS Catal. 8 (4) (2018) 2890–2896.
[73] K. Chakrabarti, A. Mishra, D. Panja, B. Paul, S. Kundu, Selective synthesis of mono- and di-methylated amines using methanol and sodium azide as C1 and N1 sources, Green. Chem. 20 (14) (2018) 3339–3345.
[74] B. Paul, D. Panja, S. Kundu, Ruthenium-catalyzed synthesis of N-methylated amides using methanol, Org. Lett. 21 (15) (2019) 5843–5847.
[75] B. Paul, M. Maji, D. Panja, S. Kundu, Tandem transformation of aldoximes to N-methylated amides using methanol, Adv. Synth. Catal. 361 (23) (2019) 5357–5362.
[76] B. Paul, M. Maji, S. Kundu, Atom-economical and tandem conversion of nitriles to N-methylated amides using methanol and water, ACS Catal. 9 (11) (2019) 10469–10476.
[77] S. Park, Y.-A. Choi, H. Han, S. Ha Yang, S. Chang, Rh-catalyzed one-pot and practical transformation of aldoximes to amides, Chem. Commun. (15) (2003) 1936–1937.
[78] C.L. Allen, R. Lawrence, L. Emmett, J.M.J. Williams, Mechanistic studies into metal-catalyzed aldoxime to amide rearrangements, Adv. Synth. Catal. 353 (18) (2011) 3262–3268.
[79] N. Ortega, C. Richter, F. Glorius, N-formylation of amines by methanol activation, Org. Lett. 15 (7) (2013) 1776–1779.
[80] B. Kang, S.H. Hong, Hydrogen acceptor- and base-free N-formylation of nitriles and amines using methanol as C1 source, Adv. Synth. Catal. 357 (4) (2015) 834–840.
[81] S. Chakraborty, U. Gellrich, Y. Diskin-Posner, G. Leitus, L. Avram, D. Milstein, Manganese-catalyzed N-formylation of amines by methanol liberating H_2: a catalytic and mechanistic study, Angew. Chem. Int. (Ed.) 56 (15) (2017) 4229–4233.
[82] E.M. Lane, K.B. Uttley, N. Hazari, W. Bernskoetter, Iron-catalyzed amide formation from the dehydrogenative coupling of alcohols and secondary amines, Organometallics. 36 (10) (2017) 2020–2025.
[83] L.K.M. Chan, D.L. Poole, D. Shen, M.P. Healy, T.J. Donohoe, Rhodium-catalyzed ketone methylation using methanol under mild conditions: formation of α-branched products, Angew. Chem. Int. (Ed.) 53 (3) (2014) 761–765.
[84] S. Ogawa, Y. Obora, Iridium-catalyzed selective α-methylation of ketones with methanol, Chem. Commun. 50 (19) (2014) 2491–2493.

[85] F. Li, J. Ma, N. Wang, α-Alkylation of ketones with primary alcohols catalyzed by a Cp*Ir complex bearing a functional bipyridonate ligand, J. Org. Chem. 79 (21) (2014) 10447–10455.
[86] X. Quan, S. Kerdphon, P.G. Andersson, C-C coupling of ketones with methanol catalyzed by a N-heterocyclic carbene–phosphine iridium complex, Chem. Eur. J. 21 (9) (2015) 3576–3579.
[87] T.T. Dang, A.M. Seayad, A convenient ruthenium-catalysed α-methylation of carbonyl compounds using methanol, Adv. Synth. Catal. 358 (21) (2016) 3373–3380.
[88] Z. Liu, Z. Yang, X. Yu, H. Zhang, B. Yu, Y. Zhao, et al., Methylation of C (sp3)–H/C(sp2)–H bonds with methanol catalyzed by cobalt system, Org. Lett. 19 (19) (2017) 5228–5231.
[89] K. Polidano, B.D.W. Allen, J.M.J. Williams, L.C. Morrill, Iron-catalyzed methylation using the borrowing hydrogen approach, ACS Catal. 8 (7) (2018) 6440–6445.
[90] A. Bruneau-Voisine, L. Pallova, S. Bastin, V. César, J.-B. Sortais, Manganese catalyzed α-methylation of ketones with methanol as a C1 source, Chem. Commun. 55 (3) (2019) 314–317.
[91] J. Sklyaruk, J.C. Borghs, O. El-Sepelgy, M. Rueping, Catalytic C1 alkylation with methanol and isotope-labeled methanol, Angew. Chem. Int. (Ed.) 58 (3) (2019) 775–779.
[92] J. Das, K. Singh, M. Vellakkaran, D. Banerjee, Nickel-catalyzed hydrogen-borrowing strategy for α-alkylation of ketones with alcohols: a new route to branched gem-bis(alkyl) ketones, Org. Lett. 20 (18) (2018) 5587–5591.
[93] C.B. Reddy, R. Bharti, S. Kumar, P. Das, Supported palladium nanoparticle catalyzed α-alkylation of ketones using alcohols as alkylating agents, ACS Sustain. Chem. Eng. 5 (11) (2017) 9683–9691.
[94] L. Jiang, F. Guo, Z. Shi, Y. Li, Z. Hou, Syndiotactic poly(aminostyrene)-supported palladium catalyst for ketone methylation with methanol, ChemCatChem. 9 (20) (2017) 3827–3832.
[95] S.M.A.H. Siddiki, A.S. Touchy, M.A.R. Jamil, T. Toyao, K.-I. Shimizu, C-Methylation of alcohols, ketones, and indoles with methanol using heterogeneous platinum catalysts, ACS Catal. 8 (4) (2018) 3091–3103.
[96] A. Charvieux, N. Duguet, E. Métay, α-Methylation of ketones with methanol catalyzed by Ni/SiO_2-Al_2O_3, Eur. J. Org. Chem. 2019 (22) (2019) 3694–3698.
[97] C. Carlini, A. Macinai, M. Marchionna, M. Noviello, A.M.R. Galletti, G. Sbrana, Selective synthesis of isobutanol by means of the Guerbet reaction: Part 3: Methanol/n-propanol condensation by using bifunctional catalytic systems based on nickel, rhodium and ruthenium species with basic components, J. Mol. Catal. A: Chem. 206 (1) (2003) 409–418.
[98] C. Carlini, M. Di Girolamo, A. Macinai, M. Marchionna, M. Noviello, A.M. Raspolli Galletti, et al., Selective synthesis of isobutanol by means of the Guerbet reaction: Part 2. Reaction of methanol/ethanol and methanol/ethanol/n-propanol mixtures over copper based/MeONa catalytic systems, J. Mol. Catal. A: Chem. 200 (1) (2003) 137–146.
[99] C. Carlini, M.D. Girolamo, A. Macinai, M. Marchionna, M. Noviello, A.M.R. Galletti, et al., Synthesis of isobutanol by the Guerbet condensation of methanol with n-propanol in the presence of heterogeneous and homogeneous palladium-based catalytic systems, J. Mol. Catal. A: Chem. 204–205 (2003) 721–728.
[100] Y. Li, H. Li, H. Junge, M. Beller, Selective ruthenium-catalyzed methylation of 2-arylethanols using methanol as C1 feedstock, Chem. Commun. 50 (95) (2014) 14991–14994.
[101] K. Oikawa, S. Itoh, H. Yano, H. Kawasaki, Y. Obora, Preparation and use of DMF-stabilized iridium nanoclusters as methylation catalysts using methanol as the C1 source, Chem. Commun. 53 (6) (2017) 1080–1083.

[102] R.L. Wingad, E.J.E. Bergström, M. Everett, K.J. Pellow, D.F. Wass, Catalytic conversion of methanol/ethanol to isobutanol—a highly selective route to an advanced biofuel, Chem. Commun. 52 (29) (2016) 5202–5204.
[103] Q. Liu, G. Xu, Z. Wang, X. Liu, X. Wang, L. Dong, et al., Iridium clusters encapsulated in carbon nanospheres as nanocatalysts for methylation of (bio)alcohols, ChemSusChem. 10 (23) (2017) 4748–4755.
[104] A. Kaithal, M. Schmitz, M. Hölscher, W. Leitner, Ruthenium(II)-catalyzed β-methylation of alcohols using methanol as C1 source, ChemCatChem. 11 (21) (2019) 5287–5291.
[105] A. Kaithal, M. Schmitz, M. Hölscher, W. Leitner, On the mechanism of the ruthenium-catalyzed β-methylation of alcohols with methanol, ChemCatChem. 12 (3) (2020) 781–787.
[106] A. Kaithal, P. van Bonn, M. Hölscher, W. Leitner, Manganese(I)-catalyzed β-methylation of alcohols using methanol as C1 source, Angew. Chem. Int. (Ed.) 59 (1) (2020) 215–220.
[107] M. Schlagbauer, F. Kallmeier, T. Irrgang, R. Kempe, Manganese-catalyzed β-methylation of alcohols by methanol, Angew. Chem. Int. (Ed.) 59 (4) (2020) 1485–1490.
[108] S.-J. Chen, G.-P. Lu, C. Cai, Iridium-catalyzed methylation of indoles and pyrroles using methanol as feedstock, RSC Adv. 5 (86) (2015) 70329–70332.
[109] R. Grigg, T.R.B. Mitchell, S. Sutthivaiyakit, N. Tongpenyai, Oxidation of alcohols by transition metal complexes part V. Selective catalytic monoalkylation of arylacetonitriles by alcohols, Tetrahedron Lett. 22 (41) (1981) 4107–4110.
[110] K. Motokura, N. Fujita, K. Mori, T. Mizugaki, K. Ebitani, K. Jitsukawa, et al., Environmentally friendly one-pot synthesis of α-alkylated nitriles using hydrotalcite-supported metal species as multifunctional solid catalysts, Chem. Eur. J. 12 (32) (2006) 8228–8239.
[111] S. Thiyagarajan, C. Gunanathan, Facile ruthenium(II)-catalyzed α-alkylation of arylmethyl nitriles using alcohols enabled by metal–ligand cooperation, ACS Catal. 7 (8) (2017) 5483–5490.
[112] B.C., Roy, S. Debnath, K. Chakrabarti, B. Paul, M. Maji, S. Kundu, Ortho-amino group functionalized 2,2′-bipyridine based Ru(ii) complex catalysed alkylation of secondary alcohols, nitriles and amines using alcohols, Org. Chem. Front. 5 (6) (2018) 1008–1018.
[113] S. Kim, S.H. Hong, Ruthenium-catalyzed aminomethylation and methylation of phenol derivatives utilizing methanol as the C1 source, Adv. Synth. Catal. 359 (5) (2017) 798–810.
[114] M. Mastalir, E. Pittenauer, G. Allmaier, K. Kirchner, Manganese-catalyzed aminomethylation of aromatic compounds with methanol as a sustainable C1 building block, J. Am. Chem. Soc. 139 (26) (2017) 8812–8815.
[115] M. Mastalir, M. Glatz, E. Pittenauer, G. Allmaier, K. Kirchner, Rhenium-catalyzed dehydrogenative coupling of alcohols and amines to afford nitrogen-containing aromatics and more, Org. Lett. 21 (4) (2019) 1116–1120.
[116] F. Li, L. Lu, P. Liu, Acceptorless dehydrogenative coupling of o-aminobenzamides with the activation of methanol as a C1 source for the construction of quinazolinones, Org. Lett. 18 (11) (2016) 2580–2583.
[117] S. Kerdphon, P. Sanghong, J. Chatwichien, V. Choommongkol, P. Rithchumpon, T. Singh, et al., Commercial copper-catalyzed aerobic oxidative synthesis of quinazolinones from 2-aminobenzamide and methanol, Eur. J. Org. Chem. 2020 (18) (2020) 2730–2734.
[118] B.C., Roy, S.A. Samim, D. Panja, S. Kundu, Tandem synthesis of quinazolinone scaffolds from 2-aminobenzonitriles using aliphatic alcohol–water system, Catal. Sci. Technol. 9 (21) (2019) 6002–6006.

[119] G. Satish, A. Polu, L. Kota, A. Ilangovan, Copper-catalyzed oxidative amination of methanol to access quinazolines, Org. Biomol. Chem. 17 (19) (2019) 4774–4782.
[120] Z. Sun, G. Bottari, K. Barta, Supercritical methanol as solvent and carbon source in the catalytic conversion of 1,2-diaminobenzenes and 2-nitroanilines to benzimidazoles, Green. Chem. 17 (12) (2015) 5172–5181.
[121] K. Tani, A. Iseki, T. Yamagata, Efficient transfer hydrogenation of alkynes and alkenes with methanol catalysed by hydrido(methoxo)iridium(III) complexes, Chem. Commun. (18)(1999) 1821–1822.
[122] N. Garg, S. Paira, B. Sundararaju, Efficient transfer hydrogenation of ketones using methanol as liquid organic hydrogen carrier, ChemCatChem. 12 (13) (2020) 3472–3476.
[123] F. Bigi, R. Maggi, G. Sartori, Selected syntheses of ureas through phosgene substitutes, Green. Chem. 2 (4) (2000) 140–148.
[124] L. Tiwari, V. Kumar, B. Kumar, D. Mahajan, A practically simple, catalyst free and scalable synthesis of N-substituted ureas in water, RSC Adv. 8 (38) (2018) 21585–21595.
[125] S.H. Kim, S.H. Hong, Ruthenium-catalyzed urea synthesis using methanol as the C1 source, Org. Lett. 18 (2) (2016) 212–215.
[126] M. Lane Elizabeth, N. Hazari, W.H. Bernskoetter, Iron-catalyzed urea synthesis: dehydrogenative coupling of methanol and amines, Chem. Sci. 9 (16) (2018) 4003–4008.
[127] P. Lorusso, J. Coetzee, G.R. Eastham, D.J. Cole-Hamilton, α-Methylenation of methyl propanoate by the catalytic dehydrogenation of methanol, ChemCatChem. 8 (1) (2016) 222–227.
[128] D. Shen, D.L. Poole, C.C. Shotton, A.F. Kornahrens, M.P. Healy, T.J. Donohoe, Hydrogen-borrowing and interrupted-hydrogen-borrowing reactions of ketones and methanol catalyzed by iridium, Angew. Chem. Int. (Ed.) 54 (5) (2015) 1642–1645.
[129] J. Yang, S. Chen, H. Zhou, C. Wu, B. Ma, J. Xiao, Cobalt-catalyzed α-methoxymethylation and aminomethylation of ketones with methanol as a C1 source, Org. Lett. 20 (21) (2018) 6774–6779.
[130] E.-A. Jo, J.-H. Lee, C.-H. Jun, Rhodium(i)-catalyzed one-pot synthesis of dialkyl ketones from methanol and alkenes through directed sp3 C–H bond activation of N-methylamine, Chem. Commun. 44 (2008) 5779–5781.
[131] C. Sun, X. Zou, F. Li, Direct use of methanol as an alternative to formaldehyde for the synthesis of 3,3′-bisindolylmethanes (3,3′-BIMs), Chem. Eur. J. 19 (42) (2013) 14030–14033.

CHAPTER 4

Transition metal pincer complexes in acceptorless dehydrogenation reactions

Vinita Yadav[1,2], Ganesan Sivakumar[3] and Ekambaram Balaraman[3,*]
[1]Organic Chemistry Division, CSIR—National Chemical Laboratory (CSIR—NCL), Pune, India
[2]Academy of Scientific and Innovative Research (AcSIR), Ghaziabad, India
[3]Department of Chemistry, Indian Institute of Science Education and Research (IISER), Tirupati, India
Corresponding author. e-mail address: eb.raman@iisertirupati.ac.in

4.1 Introduction

In the mid-1970s Moulton and Shaw published their first report on the family of meridional tridentate ligands currently referred to as pincer ligands [1]. These pincer ligands and their complexes have long been an overly neglected topic and only recently it became the subject of intense investigations from many different research groups. Careful examination of these compounds indicated their extraordinary thermal stability and high melting points. These complexes can be used for homogenous catalysis applications as active catalytic species to perform a variety of organic transformations.

The development of the sustainable, mild, and efficient synthetic protocol is at the forefront of chemical research. In this context, catalysis represents an alternative to the so-called conventional methods that require a stoichiometric amount of activating reagents and producing wasteful by-products. The catalytic acceptorless dehydrogenation of organic compounds such as alcohols, amines, and N-heterocycles, using transition metal-based homogenous catalysts is one of the most essential organic transformations, with applications in the field of energy storage as well as in the synthesis of a wide variety of other substrates when dehydrogenative coupling of intermediates resulting from initial dehydrogenation process undergoes further reactions [2]. In terms of green and sustainable chemistry, catalytic acceptorless dehydrogenation—as one of the most promising synthetic approach—represents a highly atom-efficient and clean process [3]. In general, dehydrogenation reactions are thermodynamically unfavorable and can be driven by removing hydrogen gas

Pincer–Metal Complexes
DOI: https://doi.org/10.1016/B978-0-12-822091-7.00004-X

from the system. In the acceptorless dehydrogenation reactions, the removal of hydrogen gas from various substrates occurs without any hydrogen acceptors. In the last two decades, there has been tremendous growth in the field of homogenous catalysis; in particular, transition metal pincer complex-catalyzed acceptorless dehydrogenation reactions are emerging as a powerful approach. This chapter will focus on the applications of transition metal pincer complexes for the acceptorless dehydrogenation of a wide variety of substrates such as alcohols, amines, partially saturated aromatics, and heteroaromatics.

Based on the advances in the field of homogenous catalysis using pincer metal complexes, as described in the other chapters of this book, options for designing and developing new catalysts and new or modified synthetic transformations employing these catalysts will continue to expand. In this chapter, we have chosen to focus on the application of pincer metal complexes in acceptorless dehydrogenation (AD) reactions, in which hydrogen is liberated with the formation of dehydrogenated products.

4.2 Acceptorless dehydrogenation

4.2.1 Acceptorless alcohol dehydrogenation

Over the past decades, the development of a sustainable, atom-economical, and selective approach is one of the major goals in catalysis and organometallic chemistry. In this regard, acceptorless alcohol dehydrogenation (AAD) represents an alternative to the conventional methods which often require a stoichiometric amount of oxidants such as peroxides, metal oxides, or sacrificial hydrogen acceptors. Although alcohols are unreactive and less susceptible toward nucleophilic substitution reactions because of the poor leaving group ability of the hydroxyl (OH) group, it is still among the common precursors required in organic synthesis and pharmaceutical industries. With the liberation of molecular hydrogen as the only by-product, AAD provide a straightforward route to access a wide range of carbonyl compounds such as aldehydes, ketones, and esters or, in some cases, carboxylic acids. The molecular hydrogen in itself is very useful for hydrogen storage applications, or it can be utilized in situ in the dehydrogenative coupling reactions of intermediate carbonyl compounds with other substrates such as alcohols, amines, etc. The early investigations in the field of AAD require precious metal (Ru, Ir, and Rh)-based complexes of bulky, electron-rich pincer ligands, which

facilitate the oxidation reactivity by enhancing the electron density at the metal center as well as stabilize the coordinatively unsaturated complexes.

The research group of Milstein first reported a pincer ligand pertaining transition metal catalysts for AAD. Several electron-rich, bulky tridentate PNN and PNP type ruthenium complexes were developed for the dehydrogenation of secondary alcohols to ketones and primary alcohols to esters by the same research group. Upon activation with a strong base such as sodium isopropoxide, the complex **Ru1** was moderately active for the dehydrogenation of secondary alcohols; however, it failed to yield the dehydrogenated product with primary alcohols (Fig. 4.1) [4]. A catalytic cycle involving Ru dihydride [$RuIIH_2$] and Ru(0) intermediates was proposed. Further, modification of the pyridine−pincer ligand resulted in the highly selective AD of primary alcohols to esters by **Ru2** and **Ru3** complexes [5]. With an equimolar amount of KOH, complex **Ru3** exhibited greater activity and selectivity than **Ru2** in the self-dehydrogenative coupling of primary alcohols to esters. The amido complex **Ru4** derived by benzylic deprotonation with KOtBu from **Ru3** complex showed excellent activity, and the formation of ester was observed around 90% yield (TON > 900) in relatively short reaction time under base-free conditions (Fig. 4.1). Based on low-temperature Nuclear Magnetic Resonance (NMR) studies, it was found that complex **Ru3** can easily activate primary alcohols at −80°C to give the corresponding alkoxy complex, and thereafter, the aldehydes obtained were efficiently trapped by **Ru3** complex through unusual C−C coupling with the PNN pincer ligand [6]. Moreover, they also reported an N_2 bridged binuclear complex **Ru5** which, upon the addition of base, effectively catalyzed the reaction of secondary alcohols to ketones and primary alcohols to esters, with the liberation of molecular hydrogen [7]. The reaction of secondary alcohols requires almost 70−100 h to obtain the desired ketone products, while in the case of primary alcohols, over 90% of the resultant esters were formed after 24 h with excellent turnover numbers. In closely related work, Milstein and co-workers used this N_2 bridged binuclear complex **Ru5** with an excess of $NaBH_4$ in 2-propanol to synthesize ruthenium(II) hydrido borohydride complex **Ru6**, which effectively catalyzed the dehydrogenation of primary alcohols under mild and neutral conditions and provided the desired esters in good yields (up to 98%) with excellent turnover numbers (TON ~ 1000) (Fig. 4.1) [8]. The catalyst **Ru6** was also active for dehydrogenation of secondary alcohols to the corresponding ketones and dehydrogenative cyclization of diols to lactones. Besides,

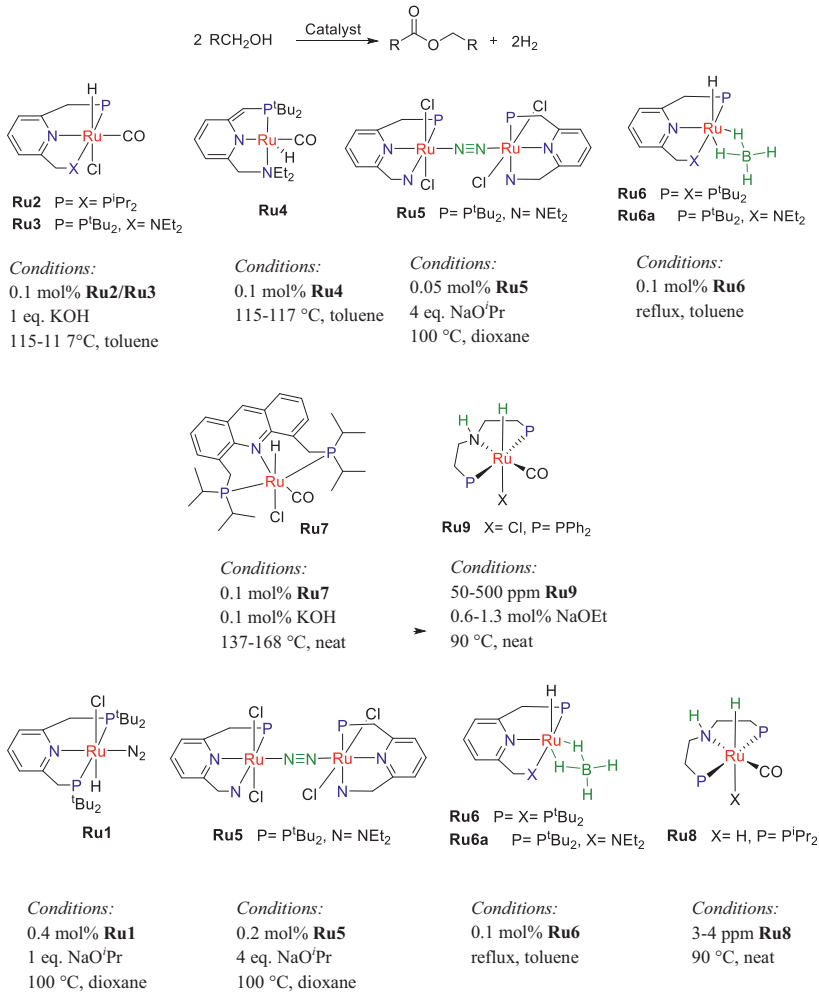

Figure 4.1 Ruthenium pincer complexes for the dehydrogenation of (A) primary alcohols to esters and (B) secondary alcohols to ketones.

Milstein and co-workers reported a new acridine-based pincer complex **Ru7**-catalyzed (in the presence of catalytic amount of base) dehydrogenation of primary alcohols to esters with a trace amount of acetals as the side product [9]. The catalyst showed reversed selectivity in the absence of base and provided acetals in high yield.

In related chemistry, Beller and co-workers showed that complexe **Ru8** containing HPNP$^{\mathbf{iPr}}$ ligand with an aliphatic NH moiety were active for hydrogen production from alcohols under mild, neutral, and

base-free conditions [10]. Complex **Ru8** is active at low temperature (<100°C) and catalyzed the dehydrogenation of isopropyl alcohol and ethanol with excellent yields and high turnover frequencies. In the case of ethanol, both acetaldehyde and ethyl acetate were formed in considerable amounts. Further, they modified the ligand system in complex **Ru9** for the bulk-scale synthesis of ethyl acetate from ethanol [11]. With catalyst loadings in the ppm range, complex **Ru9** catalyzed the dehydrogenation of ethanol to ethyl acetate in high yield and high turnover number (>15,000) (Fig. 4.1). Moreover, the catalyst was also applied to other alcohols to provide the corresponding ester products.

Inspired by the development of ruthenium-based pincer complexes for the acceptorless dehydrogenation of alcohols, Gelman and co-workers reported a new bifunctional dibenzobarrelene-based $PC_{sp^3}P$ pincer ligand and its iridium complex **Ir1**, which is 3d unlike other pincer complexes [12]. Employing 0.1 mol% of **Ir1** and a catalytic amount of base, a range of alcohols including aliphatic and aromatic secondary alcohols, aromatic primary alcohols, and diol 1,4-butanediol were successfully converted to the corresponding ketones, esters, and lactone, respectively (Fig. 4.2). Further, Gelman et al. reported that a modified version of **Ir1** in which

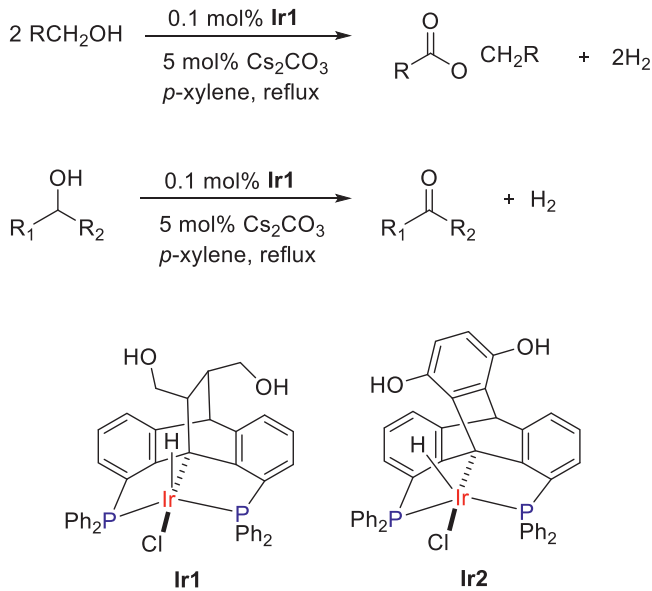

Figure 4.2 $PC_{sp^3}P$ pincer iridium catalysts for the dehydrogenation of (A) primary alcohols to esters and (B) secondary alcohols to ketones.

the pendant side arm containing butane-1,4-diol group on the $PC_{sp^3}P$ ligand was replaced with p-hydroquinone moiety, **Ir2**, results in a catalytic system that was also found to be active for the acceptorless dehydrogenation of alcohols to ketones or esters [13].

The coordination flexibility of these $PC_{sp^3}P$ ligands allowing for metal–hydroxyl/alkoxide coordination switch is crucial for catalyzing acceptorless dehydrogenation of alcohols by **Ir1** and **Ir2** complexes through outer sphere hydrogen transfer mechanism (Fig. 4.3).

Later, Szymczak and co-workers reported a new amide-derived NNN pincer ruthenium complex containing the bmpi (1,3-bis(6′ -methyl-2′-pyridylimino)-isoindoline) ligand that efficiently catalyzed the chemoselective dehydrogenation of alcohols under base-free conditions [14]. Using low catalyst loadings and moderate (<120°C) conditions, complex **Ru10** catalyzed the acceptorless dehydrogenation and dehydrogenative coupling of secondary and primary alcohols/diols to the corresponding ketones and esters/lactones, respectively (Fig. 4.4). Also, it is quite noteworthy that complex **Ru10** promotes the chemoselective dehydrogenation of secondary alcohols in the presence of primary alcohols without any base or hydrogen acceptors. The same catalyst was also used for chemoselective dehydrogenation of amines as illustrated in Section 4.2.3.

A new family of unsymmetrical pyridyl-based NNN ruthenium pincer complexes, **Ru11** and **Ru12**, for the acceptorless dehydrogenation of secondary alcohols were reported by Yu et al. [15,16]. The dimeric complex **Ru11** with an unsymmetrical pyrazolyl-pyridylamino-pyridine ligand catalyzed the dehydrogenation of secondary alcohols in the presence of a

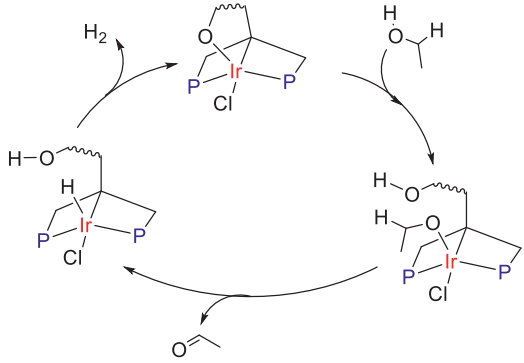

Figure 4.3 Proposed pathway for **Ir1-** and **Ir2**-catalyzed dehydrogenation of alcohols.

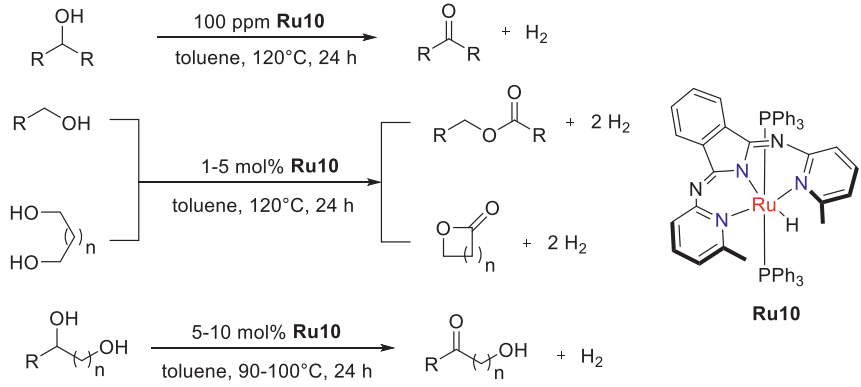

Figure 4.4 Complex **Ru10** for the acceptorless dehydrogenation of (A) secondary alcohols to ketones, (B) primary alcohols/diols to esters/lactones, and (C) Ru-catalyzed chemoselective dehydrogenation of secondary alcohols.

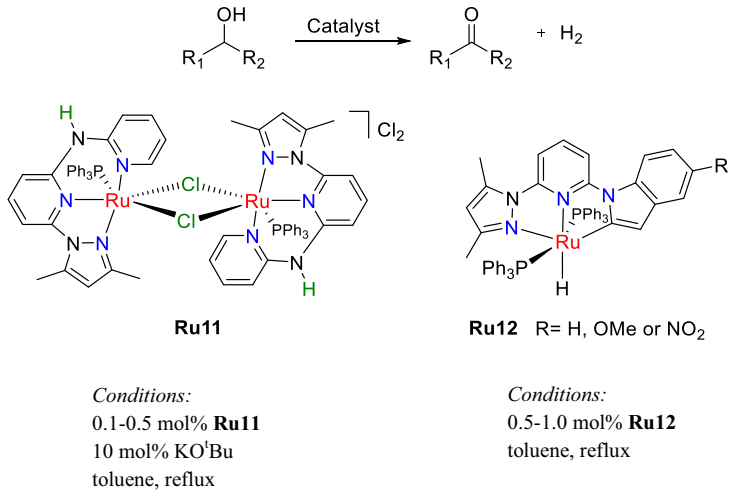

Figure 4.5 Ruthenium pincer complexes for the acceptorless dehydrogenation of secondary alcohols to ketones.

catalytic amount of base. In contrast, no base was required with complex **Ru12** bearing a pyrazolyl-(2-indolyl)-pyridine ligand (Fig. 4.5). Both the complexes showed comparable activity, and a wide variety of substrates including substituted aromatic secondary alcohols, aliphatic cyclic and acyclic secondary alcohols and sterically hindered alcohols such as diphenylmethanol and 2-naphthylmethanol, etc. were successfully converted to

the corresponding ketones in excellent yields (82%–99%). Complex **Ru12** was also used for the acceptorless dehydrogenation of N-heterocycles as demonstrated in Section 4.2.4.

Given the above examples, it can be concluded that catalysts based on precious metals (Ru, Ir, etc.) have contributed significantly in the field of AAD reactions. In many cases, the catalytic systems exhibited high activity and selectivity for the dehydrogenation of alcohols. In contrast to precious metals, which are rare and expensive, first-row transition metals (Co, Fe, etc.) are abundant, relatively nontoxic, and economical. Therefore, first-row transition metals offer more sustainable systems compared with precious metal-based catalysts. Zhang and Hanson reported the first nonprecious metal-based system for the acceptorless dehydrogenation of alcohols [17]. The active cobalt complex **Co1** was generated in situ from its precatalyst **1** and $H[BAr^F{}_4].(Et_2O)_2$ in refluxing toluene solvent, which catalyzes the dehydrogenation of a variety of secondary alcohols to the corresponding ketones in good to excellent yields (Fig. 4.6). The catalyst was relatively less active for the dehydrogenation of aliphatic alcohols and 4-methoxybenzyl alcohol.

Further, Zhang and co-workers investigated the mechanism of this cobalt-catalyzed dehydrogenation reaction [18]. When the reaction of 1-phenyl ethanol using 10 mol% of **Co1** was monitored by NMR spectroscopy, the formation of diamagnetic cobalt intermediate with a coordinated acetophenone molecule was detected. The isolated cobalt(III) acetyl phenyl hydride complex **2** was found to be active for the acceptorless dehydrogenation of alcohols, implicating its involvement in the catalytic cycle (Fig. 4.7). In addition, the replacement of the N–H group with the N–Me group does not affect the catalytic activity of **Co1**, which indicates the involvement of metal–ligand cooperativity is unlikely. Based on

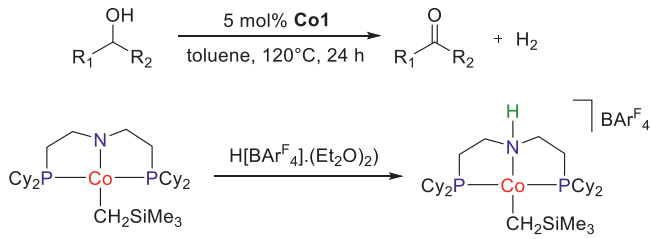

1 **Co1**

Figure 4.6 Cobalt pincer complex-catalyzed acceptorless dehydrogenation of secondary alcohol.

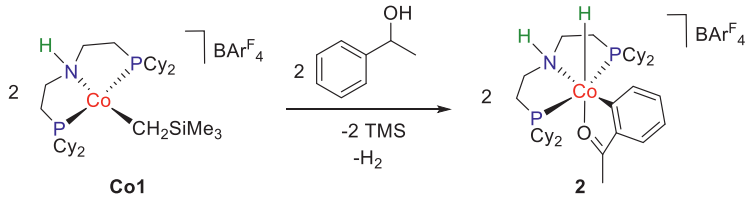

Figure 4.7 The formation of Co(III) complex **2**.

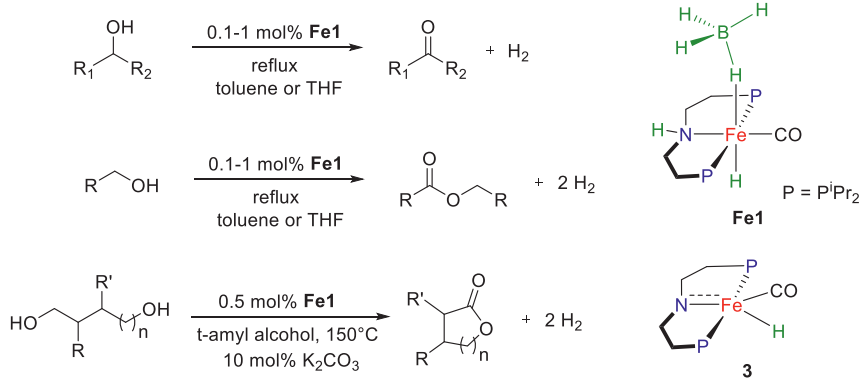

Figure 4.8 Iron–pincer complexes for the dehydrogenation of secondary alcohols to ketones, primary alcohols to esters and diols to lactones.

these findings, the authors proposed a CoI/CoIII cycle for the acceptorless dehydrogenation of alcohols. Later, based on density functional theory (DFT) calculations, Yang et al. proposed a similar mechanism for the acceptorless dehydrogenation of alcohols [19].

Subsequently, the acceptorless dehydrogenation of primary and secondary alcohols using iron–pincer complex **Fe1** was demonstrated by Jones, Schneider et al. (Fig. 4.8) [20]. Using catalyst loadings as low as 0.1–1 mol%, secondary alcohols including aromatic and aliphatic substrates were dehydrogenated to the corresponding ketones in moderate to good isolated yields. Besides secondary alcohols, primary alcohols and diols were also successfully dehydrogenated to the corresponding esters and lactones. In the case of mixed primary/secondary diols, the catalyst showed good chemoselectivity with dehydrogenation at the secondary alcohol moiety, leaving the primary alcohol unaffected. Based on experiments and DFT calculations, the pentacoordinate iron amido hydride species **3** was found to be the active catalyst in the dehydrogenation reaction.

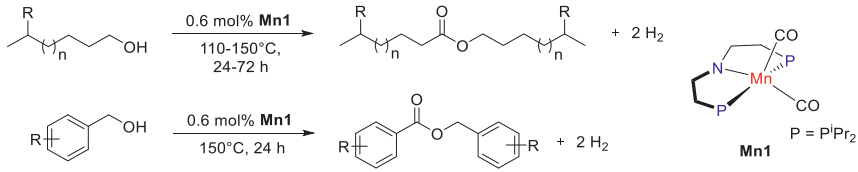

Figure 4.9 **Mn1**-catalyzed dehydrogenation of primary alcohols to esters.

In closely related work, Gauvin and co-workers reported the manganese (I) dicarbonyl complexes supported by similar aliphatic PNP ligands for the acceptorless dehydrogenative coupling of alcohols to esters under base-free conditions (Fig. 4.9) [21]. A wide variety of alcohols such as long, linear aliphatic chain (C_8–C_{18}) alcohols, lighter alcohols, and aromatic alcohols were transformed into the corresponding esters in good to excellent yields with a trace amount of aldehydes. As mentioned earlier with the iron–PNP catalytic system, the dehydrogenative coupling of primary alcohols to the corresponding ester derivatives by **Mn1** catalyst also results from cycling between amido and amino-hydride forms of the PNP–$Mn(CO)_2$ scaffold. These two complexes (**Mn1** and **Fe1**) were also used for the acceptorless dehydrogenation of primary alcohols to carboxylic acids under basic conditions as described in Section 4.2.2.

4.2.2 Dehydrogenation of alcohols to carboxylic acids

Apart from the acceptorless dehydrogenation of alcohols to esters, catalytic dehydrogenation of alcohols can also lead to the formation of corresponding carboxylic acids in the presence of water as an oxygen source. Traditionally, the oxidation of alcohols to carboxylic acid requires chlorinated solvents and stoichiometric amounts of strong and toxic oxidants such as iodates or chlorite with catalytic ruthenium and chromium oxides, which generates copious waste. However, recent reports present catalytic systems that require sacrificial hydrogen acceptors or the use of molecular oxygen, limiting the applicability of the protocol for large-scale synthesis. Acceptorless dehydrogenation has been one of the most attractive approaches for the oxidation of alcohols to acid salts in the presence of water as the oxygen donor with concomitant release of dihydrogen gas. There are several reports of catalysts for the acceptorless dehydrogenation of alcohols to acid salts and most of these systems are based on precious metals.

In 2013 Milstein and co-workers reported the first bipyridine-based ruthenium complex **Ru13** for the dehydrogenation of alcohols to carboxylic acid salts [22]. Using catalyst loadings as low as 0.2 mol% in basic aqueous solution, a wide variety of aliphatic, nonactivated alcohols, and activated benzylic alcohols were converted to the corresponding carboxylic acid salts in good yields, which upon acid treatment give the desired carboxylic acids (Fig. 4.10). Diols were also converted to the corresponding dicarboxylic acids with lactones as side products. The mechanism of the reaction was proposed based on DFT studies, which showed that the hydrogen transfer from the methylene arm of the ligand to the hydride located on the metal center is one of the most endergonic steps of the

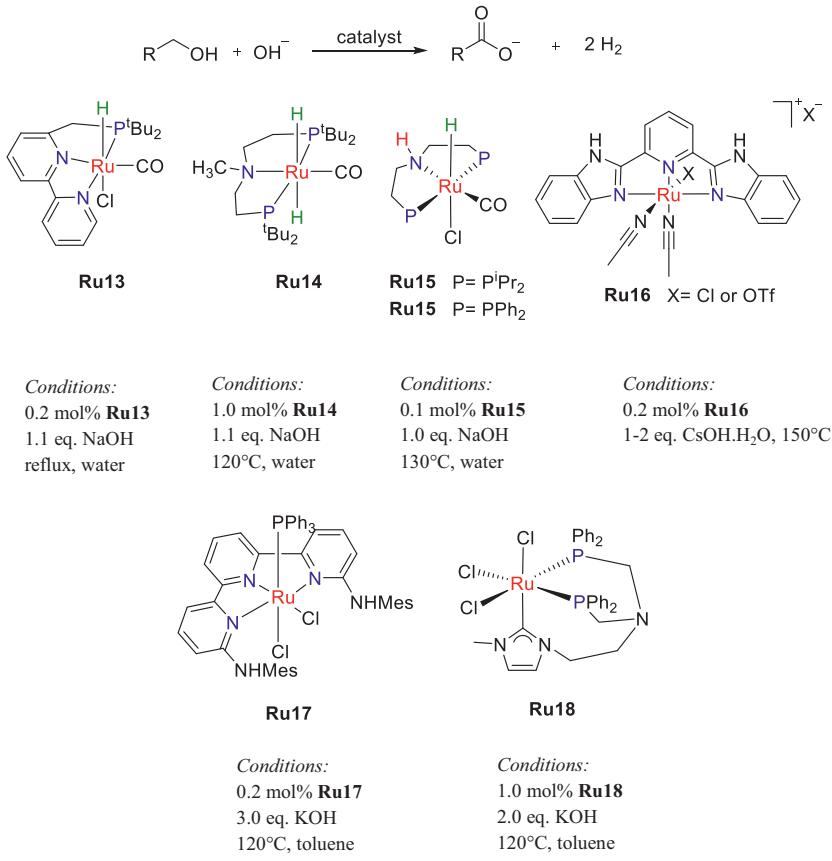

Figure 4.10 Ruthenium pincer complexes for the acceptorless dehydrogenation of primary alcohols to carboxylic acids.

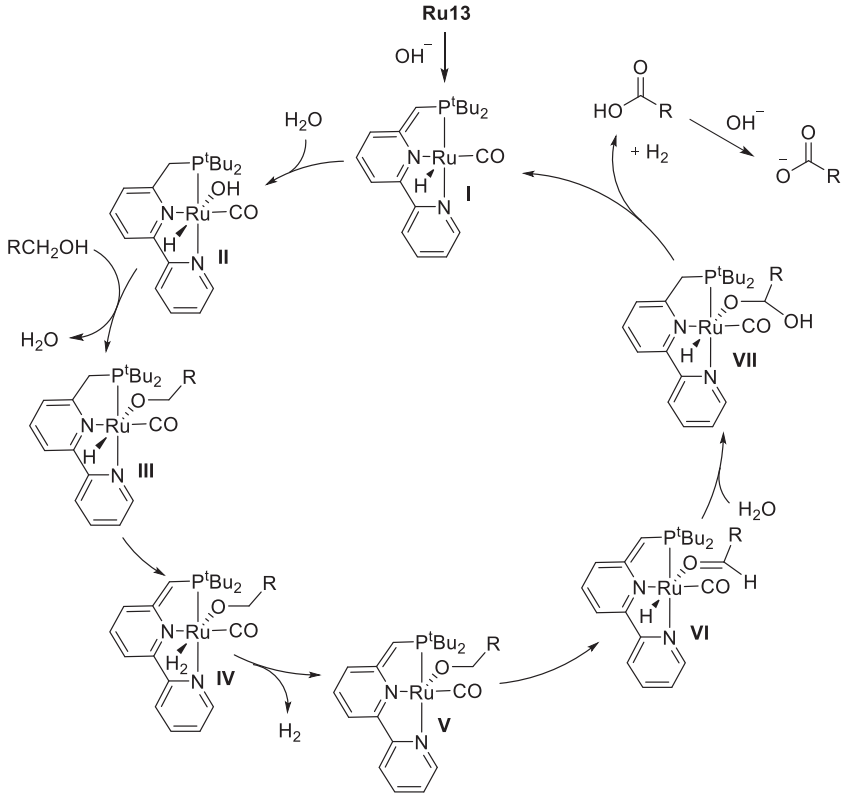

Figure 4.11 Proposed reaction mechanism for **Ru13**-catalyzed acceptorless dehydrogenation of primary alcohols to carboxylic acids.

reaction (Fig. 4.11). Moreover, **Ru13** was also reported to promote the dehydrogenative synthesis of amino acid salts from amino alcohols and basic water [23]. Using low catalyst loadings with a stoichiometric amount of NaOH (required to avoid the catalyst deactivation by acid), a wide variety of useful natural and unnatural amino acid salts were formed in excellent yields. The subsequent three reports, from Prechtl and co-workers, Beller and co-workers, and Gauvin, Dumeignil and co-workers, all reported aliphatic PNP ligand-supported ruthenium catalysts Ru14, Ru15PiPr$_2$, and Ru15PPh$_2$ for the acceptorless dehydrogenation of alcohols to carboxylic acid salts [24–26]. The ruthenium complex **Ru15PiPr$_2$** was shown to be highly active for hydrogen release from aqueous ethanol and bioethanol with high catalyst turnover numbers and acetic acid yields up to 70% [25]. Furthermore, bioethanol obtained from

fermentation processes can be used directly in this protocol for the benign production of acetic acid, representing an alternative to the known high-temperature processes based on fossil feedstocks.

In 2017 two reports describing ruthenium pincer complexes for efficient dehydrogenation of primary alcohols to carboxylic acids were independently published in short succession. The first report from Peng, Zhang, and co-workers described the application of a new class of ruthenium complexes **Ru16** (X = Cl, OTf) in the dehydrogenation of a number of primary alcohols to carboxylic acids in good yields (72%–98%) and high selectivity in an alcohol/CsOH (1:1) system [27]. Further, it was shown that higher yields (up to 100%) and turnover numbers (~10,000) were obtained by using an excess amount of alcohol to CsOH with lower catalyst loading. The subsequent report from Szymczak and co-workers demonstrated that a slight modification in the secondary sphere of classical terpyridine pincer ligand, with pendent NHR (R = mesityl) groups, enhanced the catalytic lifetime and activity of ruthenium complex in dehydrogenation catalysis [28]. Thus, catalyst **Ru17** showed good activity in the acceptorless dehydrogenation of primary alcohols to carboxylic acids (Fig. 4.10). Recently, a new-type facial ruthenium complex **Ru18**, generated in situ from $[Ru(COD)Cl_2]_n$ and a hybrid N-heterocyclic carbene (NHC) − phosphine − phosphine ligand (CPP), was reported by Li et al. [29]. The catalyst exhibited high catalytic activity and stability, and a high turnover number (up to 20,000) with the catalyst loading as low as 0.002 mol% (Fig. 4.10). Moreover, the catalyst **Ru18** worked well for sterically hindered alcohols, *ortho*-substituted benzylic alcohols, and bulky adamantanyl methanol as well as for cholesterol. The exceptionally high catalyst stability was tentatively ascribed to both the anchoring role of NHC and the hemilability of phosphines.

Beller and co-workers explored the dehydrogenation of glycerol, a valuable feedstock chemical produced on a bulk scale as a byproduct in biodiesel refining [30]. Using 2.5 ppm of **Ru9** as the precatalyst and 1.1 eq. of NaOH, glycerol was selectively dehydrogenated to lactic acid in 67% yield with a remarkably high TON of 265,326 (Fig. 4.12). Further, industrial glycerol, containing only 86%–88% glycerol, also showed a similar reactivity. In closely related work, Crabtree and co-workers explored the dehydrogenation of glycerol to lactic acid using a first-row transition metal catalyst [31]. Under lowering catalyst loading (0.02 mol% **Fe2**), glycerol was dehydrogenated to lactic acid with high selectivity

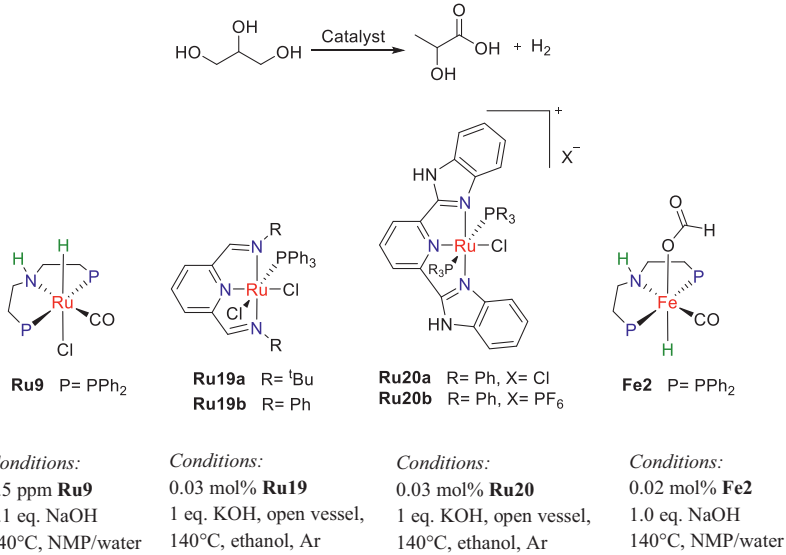

Figure 4.12 Ruthenium and iron–pincer complexes for the acceptorless dehydrogenation of glycerol to lactic acid.

(83%) and TON of 880 after 3 h (Fig. 4.12). Further, a maximum TON of 1050 was obtained when catalyst loading decreased to 0.004 mol%, which is the highest for a base-metal catalyst but considerably smaller than the best TONs obtained with nonprecious metal systems [32].

Dutta et al. reported the selective conversion of glycerol to lactic acid in high yields (up to 90%) by NNN–Ru pincer catalysts **Ru19–Ru20** [33]. With 0.03 mol% **Ru19a** or **Ru19b**, glycerol was converted to lactic acid in low to moderate yields (Fig. 4.12). While the catalysts **Ru20a** or **Ru20b** based on 2,6-bis(benzimidazole-2yl) pyridine ligand exhibited good activity toward the selective dehydrogenation of glycerol, and the product was obtained with 98% selectivity with a TON of 3000 after 48 h. The free-energy profile study of the **Ru19–Ru20**-catalyzed glycerol dehydrogenation indicated that the catalysts based on 2,6-bis(benzimidazole-2yl) pyridine ligands (**Ru20**) have the optimal Ru–P bond energy. This assists in the easy generation of an active catalyst with less steric crowding around the Ru center, making **Ru20** as efficient catalysts compared to **Ru19**. The mechanism of NNN–Ru pincer complex-catalyzed dehydrogenation of glycerol to lactic acid is depicted in Fig. 4.13.

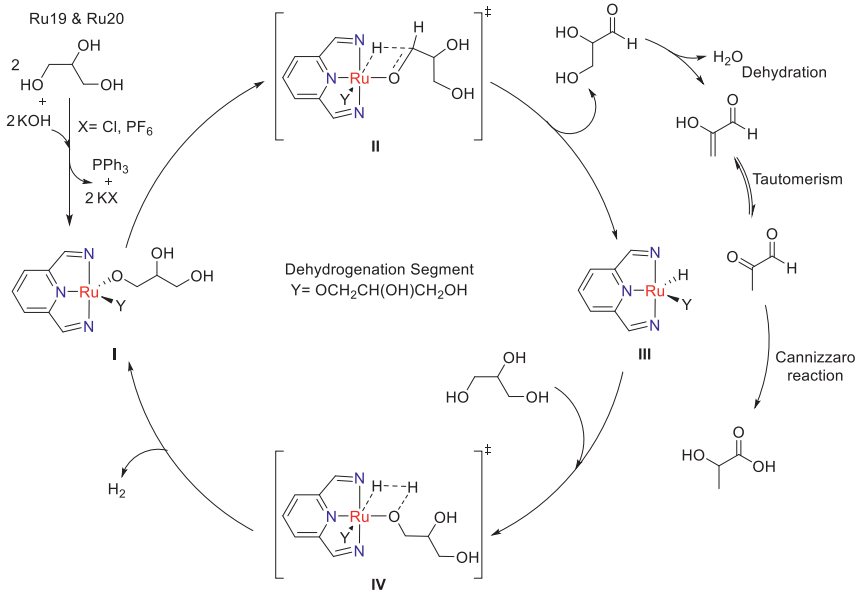

Figure 4.13 Proposed reaction mechanism for **Ru19** and **Ru20** catalyzed AD of glycerol to lactic acid.

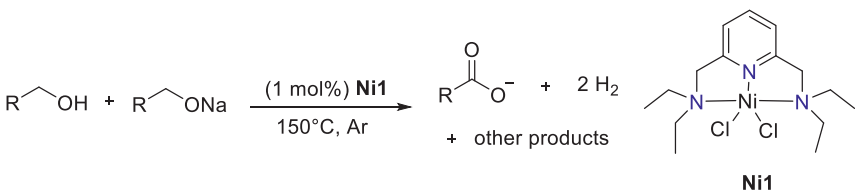

Figure 4.14 Nickel pincer complex **Ni1**-catalyzed acceptorless dehydrogenation of primary alcohols to carboxylic acids.

Traditionally, precious metal systems have been used for the acceptorless dehydrogenation of primary alcohols to carboxylic acid salts, and it was only in the last decade that catalysts based on earth-abundant metals such as Mn, Fe, and Co have been reported. Peng, Zhang, and co-workers reported the first pyridine-based N′NN′ pincer nickel complex **Ni1**, which catalyzed the acceptorless dehydrogenation of a series of aromatic and few primary aliphatic alcohols to carboxylic acids in good yields (40%–90%) under anhydrous conditions (Fig. 4.14) [34]. Based on the preliminary mechanistic experiments, it was found that the desired carboxylate salt was accompanied by the formation of corresponding ethers

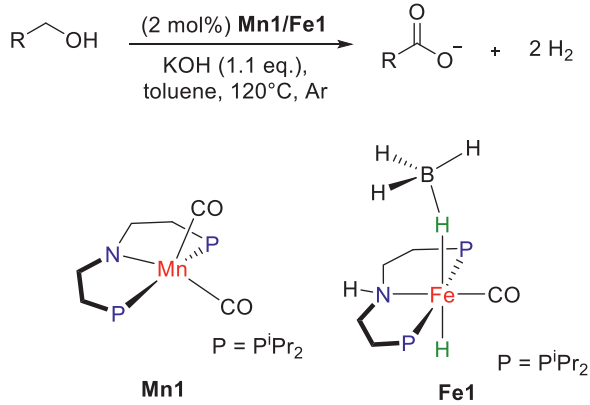

Figure 4.15 Iron (**Fe1**)- and manganese (**Mn1**)-catalyzed acceptorless dehydrogenation of primary alcohols to carboxylic acids.

and aldehydes, and the water produced by the etherification of alcohols provided the second oxygen of the carboxylate.

In addition, at this stage, there are three more reports of well-defined catalysts using earth-abundant metals, with iron and manganese pincer complexes comprising two of those examples [35–37]. The first contribution from Gauvin, Dumeignil, and co-workers described aliphatic PNP pincer-supported iron and manganese complexes for the catalytic acceptorless dehydrogenation of biomass-derived alcohols into carboxylic acid salts in good to excellent yields under basic conditions (Fig. 4.15) [35]. Interestingly, these Mn and Fe complexes required no water condition to achieve high yields as compared to their parent Ru catalysts. Further, it was found that the manganese-based pincer catalyst **Mn1** was catalytically more efficient as compared to their Fe counterpart **Fe1**.

The subsequent report by Liu et al. described a well-defined manganese complex-catalyzed acceptorless dehydrogenative coupling of alcohols with alkaline water to form carboxylate salts [36]. A wide range of carboxylic acid derivatives was synthesized with high yields and excellent functional group tolerance (Fig. 4.16). Further, in the case of aliphatic alcohols, anisole was used as a cosolvent to increase the homogeneity of the reaction mixture for better efficiency. In addition, the protocol was applied for the direct synthesis of carboxylic acid-based pharmaceutical molecules. Mechanistic studies including control experiments, X-ray crystallography, and NMR studies indicated the possibility of an aldehyde

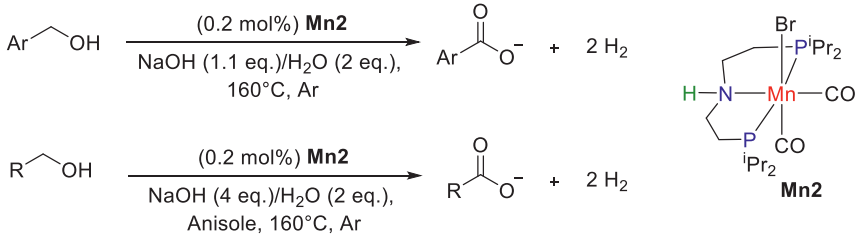

Figure 4.16 Manganese pincer complex (**Mn2**)-catalyzed acceptorless dehydrogenation of primary alcohols to carboxylic acids.

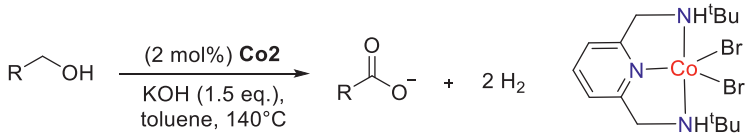

Figure 4.17 Cobalt-catalyzed acceptorless dehydrogenation of primary alcohols to carboxylic acids.

intermediate, as the case with other earth-abundant metal-based catalysts for the dehydrogenation of alcohols to carboxylic acids.

Very recently, Gunanathan and co-workers developed a highly efficient and simple cobalt catalyst **Co2** for the acceptorless dehydrogenative oxidation of alcohols to carboxylate salts under basic conditions (Fig. 4.17) [37]. This protocol was applied to a wide variety of alcohols including aromatic, aliphatic, and heteroaromatic alcohols. This reaction showed a broad substrate scope and wide functional group tolerance including pyridyl and nitro, and olefinic motifs. Moreover, diols were successfully converted to the corresponding dicarboxylic acids, and ethanol was also dehydrogenated to potassium acetate in moderate yield. The mechanistic investigation indicated that the reaction follows the Cannizzaro-type pathway with KOH acting as the source of second oxygen of the carboxylate salt.

4.2.3 Dehydrogenation of amines

Catalytic dehydrogenation of amines can lead to a variety of products such as imines, secondary amines, nitriles, and N-heterocycles. These unsaturated compounds having C−N multiple bonds are of significant importance as reactive intermediates for synthetic applications, (organo) catalysts, in dyes, and pharmaceutically active compounds [38]. While

there are several robust and well-developed methods for the dehydrogenation of amines, still these methods suffer from various limitations such as the use of an excess of base, hydrogen acceptors, and high temperatures (160°C–200°C) [39]. Although the acceptorless dehydrogenation of alcohols is well established, the dehydrogenation of amines is much less studied. This might be due to the slower β-hydrogen elimination from amido complexes as compared to the alkoxides [40]. Furthermore, the dehydrogenation of amines is very much challenging because the reversible nature of these reactions results in a mixture of products (Fig. 4.18). There are only a few reports on pincer-supported transition metal catalysts for the acceptorless dehydrogenation of amines.

Huang and co-workers described the application of a class of novel pincer ruthenium complexes (**Ru21**–**Ru23**) in the dehydrogenative homocoupling of amines to imines [41]. The reactivity of these ruthenium complexes was significantly enhanced by replacing the CH (as shown in Milstein's catalyst **Ru4**) with the N-group in the phosphine arm. Using these complexes under base- and oxidant-free conditions, a variety of different benzyl amines were selectively coupled to provide the desired imine products in high conversion and yields (Fig. 4.19). Complex **Ru21** was slightly more active while Milstein's catalyst exhibited lower activity than other catalysts **Ru21**–**Ru23**. A slight decrease in the yield of imine products was observed with electron-donating substituents resulting from additional amine dehydrogenation to give nitrile products. The formation of these nitriles could be minimized when the reactions were performed under neat conditions.

Afterward, Szymczak and co-workers demonstrated the chemoselective acceptorless dehydrogenation of primary amines to nitriles and secondary amines to imines using an amide-derived NNN–Ru(II) hydride complex **Ru10** [42]. With low catalyst loadings, a diverse range of

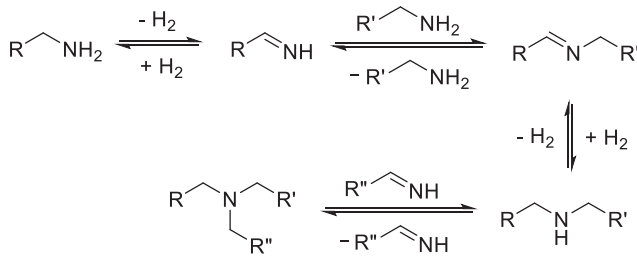

Figure 4.18 Acceptorless dehydrogenation of amines.

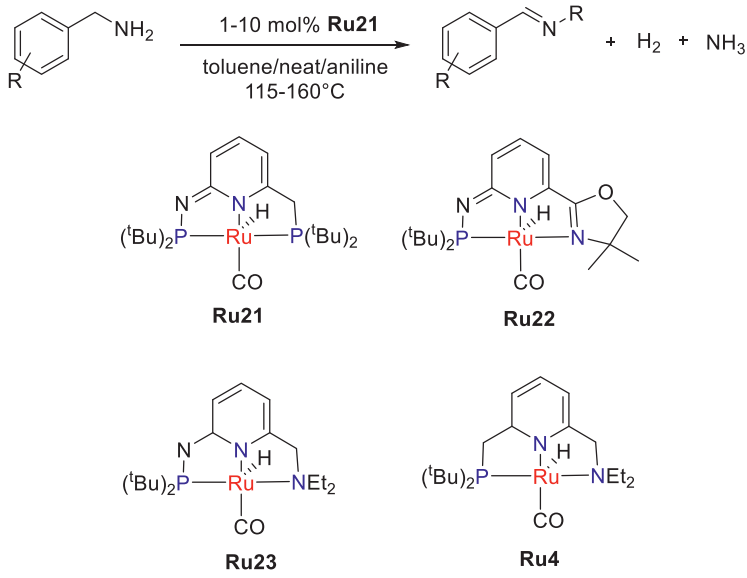

Figure 4.19 Dehydrogenative imine formation by ruthenium pincer complexes.

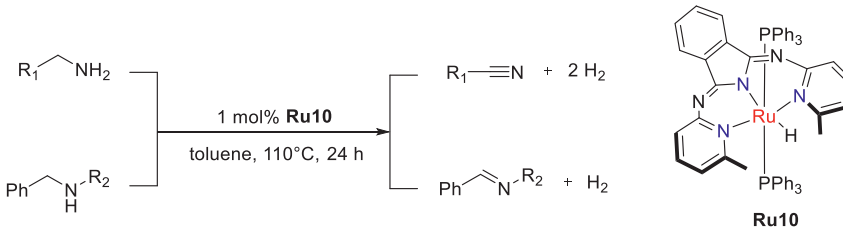

Figure 4.20 Dehydrogenation of amines catalyzed by **Ru10**.

primary amines and secondary amines was selectively dehydrogenated to the corresponding nitriles and imines in good to moderate yields (Fig. 4.20). The catalytic system is selective for primary amines ($-CH_2NH_2$) in presence of primary amines without α-CH hydrogens.

Later, they reported the detailed mechanism of the acceptorless double dehydrogenation of amines using this complex [43]. Based on combined experimental (ligand substitutions, kinetics, and steric catalyst modification) and computational studies, an inner sphere mechanism was supported. The high binding affinity for imine intermediates and the lower activation barrier for the second dehydrogenation prevent amine dissociation and further transamination reactions, making the reaction highly

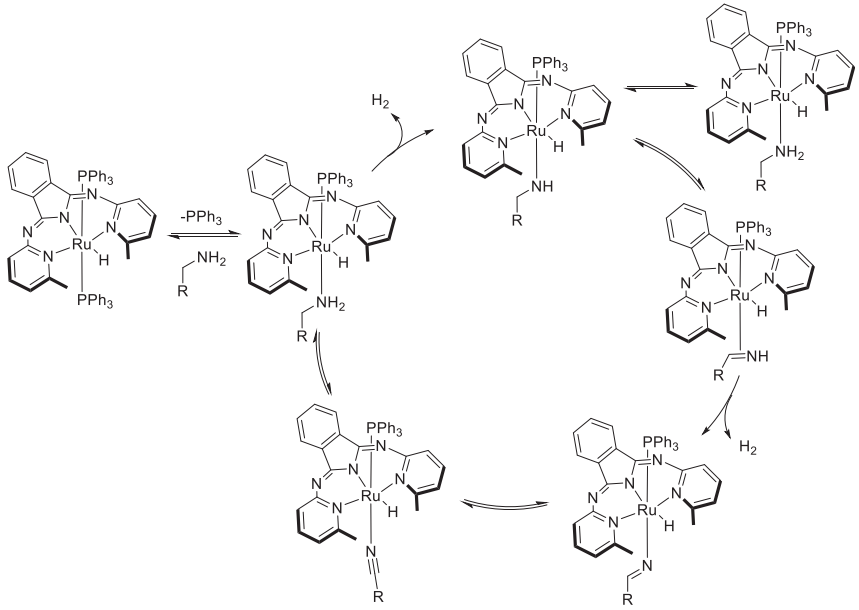

Figure 4.21 Proposed mechanism for the double dehydrogenation of primary amines to nitriles.

selective toward nitriles. The mechanistic cycle for the double dehydrogenation of primary amines is depicted in Fig. 4.21.

4.2.4 Dehydrogenation of N-heterocycles

Dehydrogenation of N-heterocycles is an important class of reactions because of its application in the synthesis of numerous pharmaceuticals and bioactive molecules. Mostly the acceptorless dehydrogenations of N-heterocycles are the microscopic reverse of the hydrogenation reactions. Owing to these reversible dehydrogenation properties, saturated and unsaturated heterocycles are also considered as potential liquid organic hydrogen carriers (LOHCs).

Since the dehydrogenation of N-heterocycles is an endothermic process, it requires the removal of H_2 from the reaction system. Besides, computational and experimental studies showed that the presence of one or more N-atoms decreases the endothermicity of the reaction when compared to cycloalkanes [44]. In spite of the numerous examples of dehydrogenation of N-heterocycles based on heterogeneous catalytic systems or homogenous Ir-based catalysts, there are only few reports based on pincer complexes for the dehydrogenation of these nitrogenous substrates.

Jones and co-workers reported for the first time a well-defined homogeneous iron catalyst **Fe1**, supported by a bis(phosphino)amine (PNP) pincer ligand, for the acceptorless dehydrogenation of N-heterocycles under mild conditions [45]. Several substrates including tetrahydroquinoline derivatives, 2,6-dimethylpiperidine, and 2-methylindoline underwent successful dehydrogenation to their corresponding N-heterocycles in reasonable isolated yields (Fig. 4.22). Mechanistic studies suggest that the presence of N-atom in cycloalkanes is crucial for catalysis and the reaction follows a sequential amine isomerization−dehydrogenation process. Simultaneously, Sawatlon and Surawatanawong established the mechanism of dehydrogenation of N-heterocycles using **Fe1** based on the density functional studies, which also showed the involvement of a pentacoordinate Fe-hydride species as an intermediate and dehydrogenation only occurs at C−N bond with followed by isomerization [46].

Subsequently, a cobalt pincer complex-catalyzed reversible acceptorless dehydrogenation and hydrogenation of N-heterocycles were reported by the research group of Jones [47]. The aminobis(phosphine) [PN(H)P] pincer ligand-supported cobalt catalyst **Co1** worked well for the dehydrogenation of a variety of saturated N-heterocycles and provided high yield of the products (Fig. 4.23). The same catalyst was also discussed earlier in Section 4.2.1 for dehydrogenation of alcohols to ketones.

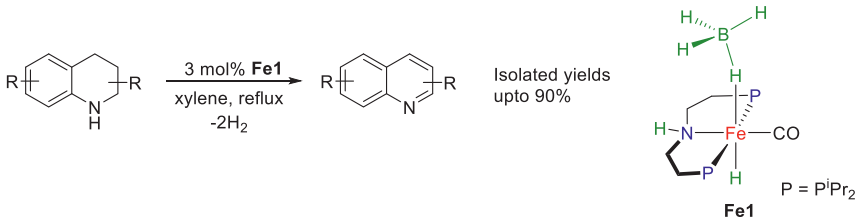

Figure 4.22 **Fe1**-catalyzed dehydrogenation of partially saturated N-heterocycles.

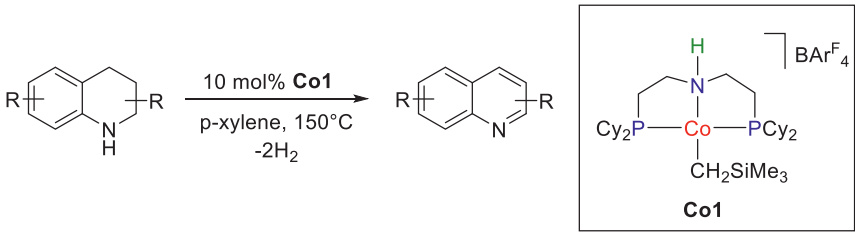

Figure 4.23 **Co1**-catalyzed dehydrogenation of partially saturated N-heterocycles.

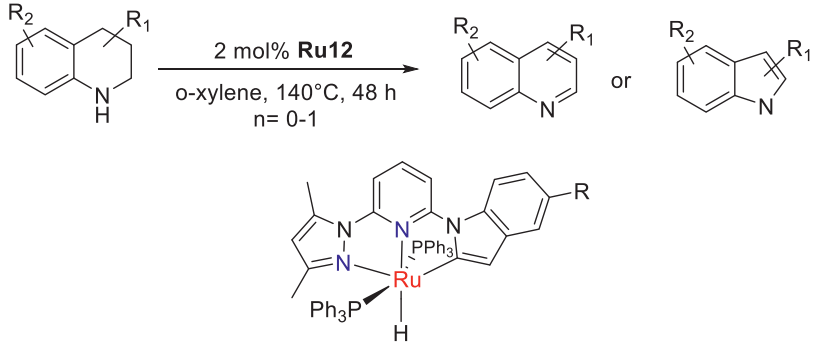

Ru12 R= H, OMe or NO_2

Figure 4.24 Ru12-catalyzed dehydrogenation of N-heterocycles.

Wang and co-workers reported the acceptorless dehydrogenation of N-heterocyclic compounds using complex **Ru12**, which also efficiently catalyzed the dehydrogenation of secondary alcohols to ketones (see Section 4.2.1) [16]. Using 2 mol% of **Ru12**, a wide variety of substituted tetrahydroquinolines and indolines were dehydrogenated to give the corresponding unsaturated N-heterocycles in moderate to good yields under base-free conditions (Fig. 4.24).

More recently, Rueping and co-workers described that a manganese complex supported by a PNP ligand, **Mn3**, was active for the dehydrogenation of N-containing heterocycles [48]. In the presence of a catalytic amount of base, **Mn3** was able to dehydrogenate a variety of indolines as well as 1,2,3,4-tetrahydroquinoxalines derivatives (Fig. 4.25). Mechanistic experiments suggest metal–ligand cooperative catalysis.

4.3 Conclusion and future perspective

Acceptorless dehydrogenation is a sustainable, atom-economical, and selective approach that affords a wide variety of unsaturated compounds without the need of an oxidant or hydrogen acceptors. In the last 20 years there has been tremendous advancement in this area using pincer-supported transition metal complexes. In this chapter, we described the development of well-defined transition metal-based pincer catalysts that are active in the acceptorless dehydrogenation reactions of various substrates such as alcohols, amines, and N-heterocycles. A great amount of progress has been made in the selective dehydrogenation of alcohols while

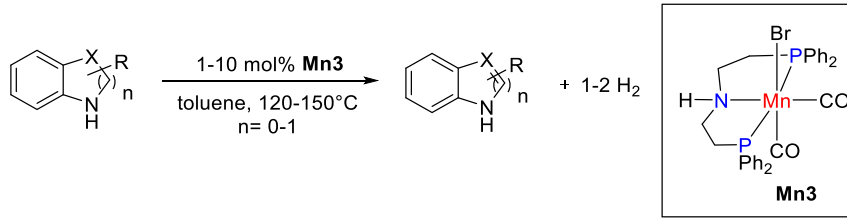

Figure 4.25 Manganese-catalyzed dehydrogenation of N-containing heterocycles.

the dehydrogenation of amines and N-heterocycles is still somewhat challenging due to the many side reactions in amines and high-temperature conditions for the dehydrogenation of N-heterocycles. However, it is possible to achieve high selectivity by careful design of catalysts through ligand design. Further, there has been a significant effort toward using catalyst systems based on base-metal catalysts; still, precious metal catalysts currently outperform pincer-supported nonprecious metal systems for most other homogenous dehydrogenation reactions. This may be because of the significant difference in the maturity of the respected fields, and greater advancements in this area will emerge in the coming years.

In summary, pincer ligand-supported transition metal catalysts have demonstrated tremendous potential in catalytic acceptorless dehydrogenation reactions of alcohols, amines, and N-heterocycles. Given the many benefits of earth-abundant metal-based pincer catalysts, it is clear that the future development in this area will produce more catalysts based on earth-abundant metals, which can surpass the activity and selectivity of their precious metal analogs.

Acknowledgments

This work is supported by the SERB, India (No. CRG/2018/002480) and IISER-Tirupati. E. B. acknowledges SwarnaJayanti Fellowship grant (DST/SJF/CSA-04/2019-2020 and SERB/F/5892/2020-2021). G.S. thanks IISER-Tirupati for fellowship. V.Y. acknowledges the UGC, India for her fellowship.

References

[1] C.J. Moulton, B.L. Shaw, Transition metal–carbon bonds. Part XLII. Complexes of nickel, palladium, platinum, rhodium and iridium with the tridentate ligand 2,6-bis[(di-t-butylphosphino)methyl]phenyl, J. Chem. Soc. Dalton Trans. (1976) 1020–1024.

[2] C. Gunanathan, D. Milstein, Applications of acceptorless dehydrogenation and related transformations in chemical synthesis, Science 341 (2013) 1229712.

[3] R.A. Sheldon, Green chemistry and resource efficiency: towards a green economy, Green. Chem. 18 (2016) 3180—3183.
[4] J. Zhang, M. Gandelman, L.J.W. Shimon, H. Rozenberg, D. Milstein, Electron-rich, bulky ruthenium PNP-type complexes. Acceptorless catalytic alcohol dehydrogenation, Organometallics 23 (2004) 4026—4033.
[5] J. Zhang, G. Leitus, Y. Ben-David, D. Milstein, Facile conversion of alcohols into esters and dihydrogen catalyzed by new ruthenium complexes, J. Am. Chem. Soc. 127 (2005) 10840—10841.
[6] M. Montag, J. Zhang, D. Milstein, Aldehyde binding through reversible C − C coupling with the pincer ligand upon alcohol dehydrogenation by a PNP − ruthenium catalyst, J. Am. Chem. Soc. 134 (2012) 10325—10328.
[7] J. Zhang, M. Gandelman, L.J.W. Shimonb, D. Milstein, Electron-rich, bulky PNN-type ruthenium complexes: synthesis, characterization and catalysis of alcohol dehydrogenation, Dalton Trans. (2007) 107—113.
[8] J. Zhang, E. Balaraman, G. Leitus, D. Milstein, Electron-rich PNP- and PNN-type ruthenium(II) hydrido borohydride pincer complexes. Synthesis, structure, and catalytic dehydrogenation of alcohols and hydrogenation of esters, Organometallics 30 (2011) 5716—5724.
[9] C. Gunanathan, L.J.W. Shimon, D. Milstein, Direct conversion of alcohols to acetals and H_2 catalyzed by an acridine-based ruthenium pincer complex, J. Am. Chem. Soc. 131 (2009) 3146—3147.
[10] M. Nielsen, A. Kammer, D. Cozzula, H. Junge, S. Gladiali, M. Beller, Efficient hydrogen production from alcohols under mild reaction conditions, Angew. Chem. Int. (Ed.) 50 (2011) 9593—9597.
[11] M. Nielsen, H. Junge, A. Kammer, M. Beller, Towards a green process for bulk-scale synthesis of ethyl acetate: efficient acceptorless dehydrogenation of ethanol, Angew. Chem. Int. (Ed.) 51 (2012) 1—4.
[12] S. Musa, I. Shaposhnikov, S. Cohen, D. Gelman, Ligand—metal cooperation in PCP pincer complexes: rational design and catalytic activity in acceptorless dehydrogenation of alcohols, Angew. Chem. Int. (Ed.) 50 (2011) 3533—3537.
[13] S.D. Botton, R. Romm, G. Bensoussan, M. Hitrik, S. Musa, D. Gelman, Coordination versatility of p-hydroquinone-functionalized dibenzobarrelene-based PC(sp3)P pincer ligands, Dalton Trans. 45 (2016) 16040—16046.
[14] K.-N.T. Tseng, J.W. Kampf, N.K. Szymczak, Base-free, acceptorless, and chemoselective alcohol dehydrogenation catalyzed by an amide-derived NNN-ruthenium(II) hydride complex, Organometallics 32 (2013) 2046—2049.
[15] Q. Wang, H. Chai, Z. Yu, Dimeric ruthenium(II)-NNN complex catalysts bearing a pyrazolyl-pyridylamino-pyridine ligand for transfer hydrogenation of ketones and acceptorless dehydrogenation of alcohols, Organometallics 36 (2017) 3638—3644.
[16] Q. Wang, H. Chai, Z. Yu, Acceptorless dehydrogenation of N-heterocycles and secondary alcohols by Ru(II)-NNC complexes bearing a pyrazoyl-indolylpyridine ligand, Organometallics 37 (2018) 584—591.
[17] G. Zhang, S.K. Hanson, Cobalt-catalyzed acceptorless alcohol dehydrogenation: synthesis of imines from alcohols and amines, Org. Lett. 15 (2013) 650—653.
[18] G. Zhang, K.V. Vasudevan, B.L. Scott, S.K. Hanson, Understanding the mechanisms of cobalt-catalyzed hydrogenation and dehydrogenation reactions, J. Am. Chem. Soc. 135 (2013) 8668—8681.
[19] Y. Jing, X. Chen, X. Yang, Computational mechanistic study of the hydrogenation and dehydrogenation reactions catalyzed by cobalt pincer complexes, Organometallics 34 (2015) 5716—5722.
[20] (a) S. Chakraborty, P.O. Lagaditis, M. Forster, E.A. Bielinski, N. Hazari, M.C. Holthausen, et al., Well-defined iron catalysts for the acceptorless reversible

dehydrogenation-hydrogenation of alcohols and ketones, ACS Catal 4 (2014) 3994–4003.
(b) P.J. Bonitatibus Jr., S. Chakraborty, M.D. Doherty, O. Siclovan, W.D. Jones, G. L. Soloveichik, Reversible catalytic dehydrogenation of alcohols for energy storage, Proc. Natl. Acad. Sci. United States A. 112 (2015) 1687–1692.
[21] D.H. Nguyen, X. Trivelli, F. Capet, J.-F. Paul, F. Dumeignil, R.M. Gauvin, Manganese pincer complexes for the base-free, acceptorless dehydrogenative coupling of alcohols to esters: development, scope, and understanding, ACS Catal. 7 (2017) 2022–2032.
[22] E. Balaraman, E. Khaskin, G. Leitus, D. Milstein, Catalytic transformation of alcohols to carboxylic acid salts and H_2 using water as the oxygen atom source, Nat. Chem. 5 (2013) 122–125.
[23] P. Hu, Y.B. David, D. Milstein, General synthesis of amino acid salts from amino alcohols and basic water liberating H_2, J. Am. Chem. Soc. 138 (2016) 6143–6146.
[24] J.-H. Choi, L.E. Heim, M. Ahrens, M.H.G. Prechtl, Selective conversion of alcohols in water to carboxylic acids by in situ generated ruthenium trans dihydrido carbonyl PNP complexes, Dalton Trans. 43 (2014) 17248–17254.
[25] P. Sponholz, D. Mellmann, C. Cordes, P.G. Alsabeh, B. Li, Y. Li, et al., Efficient and selective hydrogen generation from bioethanol using ruthenium pincer-type complexes, ChemSusChem 7 (2014) 2419–2422.
[26] L. Zhang, D.H. Nguyen, G. Raffa, X. Trivelli, F. Capet, S. Desset, et al., Catalytic conversion of alcohols into carboxylic acid salts in water: scope, recycling, and mechanistic insights, ChemSusChem 9 (2016) 1413–1423.
[27] Z. Dai, Q. Luo, X. Meng, R. Li, J. Zhang, T. Peng, Ru(II) complexes bearing 2,6-bis(benzimidazole-2-yl)pyridine ligands: a new class of catalysts for efficient dehydrogenation of primary alcohols to carboxylic acids and H_2 in the alcohol/CsOH system, J. Organomet. Chem. 830 (2017) 11–18.
[28] E.W. Dahl, T.L.- Goff, N.K. Szymczak, Second sphere ligand modifications enable a recyclable catalyst for oxidant-free alcohol oxidation to carboxylates, Chem. Commun. 53 (2017) 2287–2289.
[29] H.-M. Liu, L. Jian, C. Li, C.-C. Zhang, H.-Y. Fu, X.-L. Zheng, et al., Dehydrogenation of alcohols to carboxylic acid catalyzed by in situ-generated facial ruthenium-CPP complex, J. Org. Chem. 84 (2019) 9151–9160.
[30] Y. Li, M. Nielsen, B. Li, P.H. Dixneuf, H. Junge, M. Beller, Ruthenium-catalyzed hydrogen generation from glycerol and selective synthesis of lactic acid, Green. Chem. 17 (2015) 193–198.
[31] L.S. Sharninghausen, B.Q. Mercado, R.H. Crabtree, N. Hazari, Selective conversion of glycerol to lactic acid with iron pincer precatalysts, Chem. Commun. 51 (2015) 16201–16204.
[32] Z. Lu, I. Demianets, R. Hamze, N.J. Terrile, T.J. Williams, A prolific catalyst for selective conversion of neat glycerol to lactic acid, ACS Catal. 6 (2016) 2014–2017.
[33] M. Dutta, K. Das, S.J. Prathapa, H.K. Srivastava, A. Kumar, Selective and high yield transformation of glycerol to lactic acid using NNN pincer ruthenium catalysts, Chem. Commun. 56 (2020) 9886–9889.
[34] Z. Dai, Q. Luo, H. Jiang, Q. Luo, H. Li, J. Zhang, et al., Ni(II)–N′NN′ pincer complexes catalyzed dehydrogenation of primary alcohols to carboxylic acids and H_2 accompanied by alcohol etherification, Catal. Sci. Technol. 7 (2017) 2506–2511.
[35] D.H. Nguyen, Y. Morin, L. Zhang, X. Trivelli, F. Capet, S. Paul, et al., Oxidative transformations of biosourced alcohols catalyzed by earth-abundant transition metals, ChemCatChem 9 (2017) 2652–2660.

[36] Z. Shao, Y. Wang, Y. Liu, Q. Wang, X. Fub, Q. Liu, A general and efficient Mn-catalyzed acceptorless dehydrogenative coupling of alcohols with hydroxides into carboxylates, Org. Chem. Front. 5 (2018) 1248–1256.
[37] D.R. Pradhan, S. Pattanaik, J. Kishore, C. Gunanathan, Cobalt-catalyzed acceptorless dehydrogenation of alcohols to carboxylate salts and hydrogen, Org. Lett. 22 (2020) 1852–1857.
[38] (a) A. Erkkilä, I. Majander, P.M. Pihko, Iminium catalysis, Chem Rev 107 (2007) 5416–5470.
(b) S. Mukherjee, J.W. Yang, S. Hoffmann, B. List, Asymmetric enamine catalysis, Chem Rev 107 (2007) 5471–5569.
(c) Z.Y. Liu, Y.M. Wang, Z.R. Li, J.D. Jiang, D.W. Boykin, Synthesis and anticancer activity of novel 3,4-diarylthiazol-2(3H)-ones (imines), Bioorg Med Chem Lett 19 (2009) 5661–5664.
(d) F.F. Fleming, L. Yao, P.C. Ravikumar, L. Funk, B.C. Shook, Nitrile-containing pharmaceuticals: efficacious roles of the nitrile pharmacophore, J Med Chem 53 (2010) 7902–7917.
(e) S. Luo, E. Zhang, Y. Su, T. Cheng, C. Shi, A review of NIR dyes in cancer targeting and imaging, Biomaterials 32 (2011) 7127–7138.
(f) S. Kobayashi, Y. Mori, J.S. Fossey, M.M. Salter, Catalytic enantioselective addition to imines, Chem Rev 111 (2011) 2626–2704.
[39] (a) X.-Q. Gu, W. Chen, D. Morales-Morales, C.M. Jensen, Dehydrogenation of secondary amines to imines catalyzed by an iridium PCP pincer complex: initial aliphatic or direct amino dehydrogenation? J. Mol. Catal. A: Chem. 189 (2002) 119–124.
(b) W.H. Bernskoetter, M. Brookhart, Kinetics and mechanism of iridium-catalyzed dehydrogenation of primary amines to nitriles, Organometallics 27 (2008) 2036–2045.
(c) Z. Wang, J. Bellib, C.M. Jensen, Homogeneous dehydrogenation of liquid organic hydrogen carriers catalyzed by an iridium PCP complex, Faraday Discuss 151 (2011) 297–305.
[40] G.E. Dobereiner, R.H. Crabtree, Dehydrogenation as a substrate-activating strategy in homogeneous transition-metal catalysis, Chem. Rev. 110 (2010) 681–703.
[41] L.-P. He, T. Chen, D. Gong, Z. Lai, K.-W. Huang, Enhanced reactivities toward amines by introducing an imine arm to the pincer ligand: direct coupling of two amines to form an imine without oxidant, Organometallics 31 (2012) 5208–5211.
[42] K.-N.T. Tseng, A.M. Rizzi, N.K. Szymczak, Oxidant-free conversion of primary amines to nitriles, J. Am. Chem. Soc. 135 (2013) 16352–16355.
[43] L.V. Hale, T. Malakar, K.N. Tseng, P.M. Zimmerman, A. Paul, N.K. Szymczak, The mechanism of acceptorless amine double dehydrogenation by N,N,N-amide ruthenium(II) hydrides: a combined experimental and computational study, ACS Catal. 6 (2016) 4799–4813.
[44] E. Clot, O. Eisenstein, R.H. Crabtree, Computational structure–activity relationships in H_2 storage: how placement of N atoms affects release temperatures in organic liquid storage materials, Chem. Commun. (2007) 2231–2233.
[45] S. Chakraborty, W.W. Brennessel, W.D. Jones, A molecular iron catalyst for the acceptorless dehydrogenation and hydrogenation of N-heterocycles, J. Am. Chem. Soc. 136 (2014) 8564–8567.
[46] B. Sawatlon, P. Surawatanawong, Mechanisms for dehydrogenation and hydrogenation of N-heterocycles using PNP-pincer-supported iron catalysts: a density functional study, Dalton Trans. 45 (2016) 14965–14978.

[47] R. Xu, S. Chakraborty, H. Yuan, W.D. Jones, Acceptorless, reversible dehydrogenation and hydrogenation of N-heterocycles with a cobalt pincer catalyst, ACS Catal. 5 (2015) 6350–6354.
[48] V. Zubar, J.C. Borghs, M. Rueping, Hydrogenation or dehydrogenation of N-containing heterocycles catalyzed by a single manganese complex, Org. Lett. 22 (2020) 3974–3978.

CHAPTER 5

An outlook on the applications of pincer-metal complexes in catalytic dehydrogenation chemistry

Eileen Yasmin[1], Vinay Arora[1] and Akshai Kumar[1,2,3,*]
[1]Department of Chemistry, Indian Institute of Technology Guwahati, Guwahati, India
[2]Center for Nanotechnology, Indian Institute of Technology Guwahati, Guwahati, India
[3]School of Health Science & Technology, Indian Institute of Technology Guwahati, Guwahati, India
Corresponding author. e-mail address: akshaikumar@iitg.ac.in

Homogenous catalysts are used in organometallic chemistry for a vast number of organic transformations due to their ease of handling, moderate reaction conditions, and the selectivity of the products that they offer. Among them, complexes based on tridentate pincer ligands have gained immense popularity due to their optimum balance between stability and reactivity [1]. Their various features like tunability of the ligand framework [2], metal-ligand cooperation [3], hemilability of side arms [4], and redox-active nature [5] render them suitable for a range of reactions like C−C, C−H, and C−O bond activation, hydrogenation, and dehydrogenation reactions of organic molecules and as building blocks for the synthesis of self-assembled supramolecular structures [6−14]. The study on pincer complexes originated in late 1970s by Shaw [15], although they were classified into a separate class of catalysts much later in 1989, when G. Van Koten first coined the term "Pincer" [16].

As the natural reserves of fossil fuels are fast depleting, one of the most promising alternatives of energy sources is hydrogen, and rightly, scientists have been trying to address the challenges regarding its storage. Chemically, hydrogen can be stored by some organic compounds with high hydrogen density, such as HCOOH, CH_3OH, and organic heterocycles [17−22]. Apart from the general catalytic applications of pincer metal complexes, Chapter 1 by Daw, Application of Pincer Metal Complexes in Catalytic Transformations, discusses about how ammonia

Pincer−Metal Complexes
DOI: https://doi.org/10.1016/B978-0-12-822091-7.00005-1

borane can be used as an efficient hydrogen storage medium, due to its high hydrogen content (up to 19.6%) [23]. Various catalysts have been employed to dehydrogenate ammonia borane ($H_3B.NH_3$) and convert it to poly(aminoborane) $[H_2BNH_2]_n$, borazine $[HBNH]_3$, or polyborazylene (hydrogen storage capacity 6.8–12.96 wt.%) [24,25]. Several groups have successfully used pincer complexes in an attempt to maximize the hydrogen yield and to get a clear understanding of the mechanistic aspects of the reaction. In her pioneering work, Goldberg reported ammonia borane dehydrogenation catalyzed by the $(POCOP)Ir(H)_2(Cl)$ pincer complex [26]. The same catalyst was later used by Manners for similar reactions [27]. These initial success stories were soon followed by valuable contributions from Schneider (with their Ru–amido complex), Yamashita (pincer–iridium catalyst with boron backbone), Velez, Weller, and others [28–32]. A range of inexpensive pincer–metal complexes based on earth-abundant 3d metal such as Fe and Co have also been studied for catalytic ammonia borane dehydrogenation [33–38].

The chemical inertness, high bond dissociation energy (945 kJ mol^{-1}), low proton affinity, non-polar character, and large HOMO-LUMO gap make the transformation of dinitrogen into value-added chemicals like ammonia or hydrazine a very challenging reaction [1,39]. Ammonia, which is industrially produced by the Haber–Bosch process from nitrogen typically under harsh conditions, finds invaluable applications [40–42]. Very few examples involving homogenous catalysts deal with catalytic dinitrogen transformation under ambient conditions [43–57]. Pioneering work in this field came from the Schrock group, who demonstrated that homogenous Mo-based catalysts could effectively reduce dinitrogen into ammonia under ambient conditions [58]. Nishibayashi and co-workers demonstrated the excellent activity of a series of Mo-based pincer complexes toward ammonia formation, yielding high turnovers [59]. In an alternative approach, water oxidation was coupled with nitrogen fixation using visible light as initiator in the presence of SmI_2 as a reductant source [60]. Ammonia synthesis starting from nitrogen was studied by Tuczek group using a PN^3P-Mo pincer catalyst [61]. There are a few reports of first row transition metal-catalyzed nitrogen to ammonia transformation, based on pincer–Fe, pincer–Co, and pincer–Cr complexes, with the former two being carried out by Nishibayashi [62–64]. Dinitrogen fixation with pincer–V [65], pincer–Ti, and pincer–Zr were also reported [66–67].

Nitride functionalization was reported by Schneider and co-workers who used pincer metal-nitride complexes to carry out C–N bond formation and generate a range of compounds like acetonitrile, benzonitrile,

and benzamide. These reactions often involved the intermediacy of bridging dinitrogen and nitrido complexes [68–70].

Silylation of dinitrogen to yield silyl amines was also attempted successfully by Mézailles and co-workers by employing PPP pincer–Mo and pincer–Fe dinitrogen complexes [71,72]. Notably, the silyl amines could be further hydrolyzed to ammonia. PSiP pincer catalysts based on Fe, Co, and Rh were also effective [73].

Pincer catalysts have also been largely used for the hydrogenation of a number of organic compounds like esters, amides, nitriles, and alkynes, a great part of this work being investigated by Milstein [74] and Beller [75]. The pincer–Ir, pincer–Fe [76–77], and pincer–Mn [78] catalysts based on the MACHO ligand were found to be exceptionally active for ester hydrogenation. Milstein reported the first example of ester hydrogenation to alcohol using a PNNH pincer–Co catalyst [79]. The same group also reported amide hydrogenation to amines and alcohols using pincer–Ru [80–82], pincer–Fe [83], and pincer–Mn [84] complexes. The amide hydrogenation reported by Beller and co-workers were highly active and selective [85]. Urea [86], carbonate [87–88], and carbamate [89] derivatives were hydrogenated to methanol and the corresponding amines by pincer–Ru and pincer–Mn catalysts. The hydrogenation of cyclic imides to diols and amines using a pincer–Ru catalyst was demonstrated by the Milstein group [90]. Similarly, pincer–metal complexes find application in the hydrogenation of nitriles to imines as well as amines [91]. In particular, much success has been attained with pincer–Ru catalyst based on imidazolylphosphine PNN ligand [92]. Pincer complexes bearing nonprecious metals were also efficient in the hydrogenation of a wide range of aliphatic, aromatic, and heterocyclic nitriles [93–96]. Though there are several reports on the hydrogenation of esters, amides, and nitriles, the corresponding reports on hydrogenation of alkynes are limited. For instance, alkyne hydrogenation was reported by the Chirik group using electron-rich *bis*(arylimidazol-2-ylidene) pincer–Fe complex [97].

Coupling reactions involving C–C bond formation are of paramount value, both from an industrial and pharmaceutical point of view. A variety of coupling reactions like Heck-Mizoroki [98], Negishi [99–100], Suzuki-Miyaura [101–107], Kumada [108–109], Stille [110], and Sonogashira [111–112] have been successfully catalyzed mainly by pincer–Pd [113–120] and pincer–Ni [121] complexes.

Pincers can be fine-tuned at their various sites to vary the steric and electronic properties, which renders them an extremely versatile set of

ligands. Among the various subclassifications based on ligand motifs, the "non-innocent" type ligands [122], such as the pincers, display excellent reactivity and selectivity over a wide range of reactions. Non-innocent ligands are redox-active, which have energetically favorable levels, that allows them to reduce or oxidize and act as electron reservoirs [123]. These ligands can often transform themselves into radicals when being bound to a metal. Redox non-innocent ligand motif has gained much importance due to its effective strategy in catalysis [124]. A subclassification of noninnocence involves a "spectator ligand," which modifies the Lewis acidity of the metal by its redox reaction, thereby influencing the substrate affinity for subsequent reactions [125–126]. In recent past, much success has been attained in finding alternative lower barrier pathway for various organic transformations via multielectron processes mediated by redox-active/non-innocent pincer complexes based on relatively abundant and non-toxic 3d transition metals [127] such as Fe [128–132]and Ni [133–134] apart from their precious counterparts like Ta [135–136], Zr [137–138], Pd [139–140], and Ru [141].

Chapter 2 on alkane dehydrogenation deals with the transformation of abundant and readily available starting materials like alkanes into a myriad of chemically relevant intermediates [11–13]. Dehydrogenation of alkanes also finds great applications on coupling with other reactions [11–13,142]. The field has been largely dominated by homogenous pincer–Ir catalysts, most of which are phosphine-based, as these have exhibited the most promising results. These catalysts offer high α-olefin selectivity in alkane dehydrogenation as compared to their heterogeneous counterparts [143]. Complexes ligated with PCP, POCOP, PCOP, and others have been reported by Kaska [144–149], Jensen [150], Goldman [151], Brookhart [152–153], Goldberg [154–156], Roddick [157–159], Chianese [160–162], Zheng [163–166], and Yamamoto [167] to be highly stable, which could be favorably tuned to accomplish excellent reactivity. Scientists have been devoted to decipher its detailed mechanistic pathways and extend the reaction toward other applications. The dehydrogenation is typically catalyzed by an Ir(I) species, and the dehydrogenation cycle is accompanied by either of the two isomerization pathways, the "hydride addition pathway" or the "η^3-allyl pathway," which yields the more stable internal olefins [168–170]. These catalysts have been employed toward both transfer and acceptorless dehydrogenation, and moderate to good results have been obtained with both. The drawback of phosphine-based pincer–Ir complexes are that they are not air- and moisture-stable

and do not offer easy handling. Also, the high-energy requirement of dehydrogenation (23–30 kcal mol^{-1}) [13,171] requires operation at high reaction temperatures, which may cause the catalysts to decompose. Another major problem encountered is that the secondary dehydrogenation at internal positions of primary dehydrogenation products is easier and that the terminal-to-internal isomerizations are faster, both of which contribute to hinder the selective dehydrogenation at terminal positions leading to low α-olefin yields apart from poor product selectivity in tandem reactions.

In recent years, deviation from the original scheme of complexes has given rise to solid-supported pincer–iridium heterogeneous catalysts, which are highly robust and exhibited high initial rates of dehydrogenation [172–173]. Ir complexes based on ^{CF3}PCP ligand moiety, developed by the Roddick group, show moderately good activity toward alkane transfer dehydrogenation even in presence of molecular oxygen [157,159,174]. Non-PCP–pincer complexes like NCN–Ir complexes are the alternatives newly explored for alkane dehydrogenation. Some of these complexes are better than their phosphine counterparts as they are air and moisture stable and thus, are easy to handle. Nishiyama and Goldberg independently developed an NCN-based catalyst with phebox backbone in which they found that the active species was an Ir(III) one, rather than an Ir(I) species, as is observed in the case of phosphine-based complexes [175]. Not only was this complex stable in the presence of water, O_2, and α-olefins, the yield of *n*-octane dehydrogenation product was found to increase significantly while using this complex in presence of added water.

Other than pincer–Ir, pincer complexes based on Ru, Rh, and Os have also been synthesized and employed for alkane dehydrogenation. In case of the Group 8 metals, the catalytically active species was found to be M(II) (M = Ru, Os). The Roddick group developed a pincer–Ru complex, which was tolerant to water, O_2, and N_2 atmospheres [176–178]. Apart from that, Goldman [179], Peryshkov [180], and Huang Zheng [181] have also contributed toward pincer–Ru-catalyzed alkane dehydrogenation. Pincer–Os [182] complexes by Roddick and pincer–Rh [145,183–185] complexes developed by Goldman and Brookhart have shown meager activity toward such reactions. While strong *trans*- influencing *ipso* carbon resulted in favorable energetics in the case of PCP–Ir, the corresponding energetics were strongly disfavored with pincer–Rh. Replacing the *ipso* carbon with a weak *trans*- influencing N lead to slight improvement in reactivity of the resulting PNP–Rh complex.

The alkane dehydrogenation reaction has found a plethora of applications when coupled with other reactions such as olefin metathesis [186–187], coupling reactions [188], Diels–Alder reaction [189] among others. Many of these reactions occur in a tandem fashion, that is, the pincer complex catalyzes the dehydrogenation, and a second catalyst completes the consequent step, both catalysts functioning in conjunction without hindering each other. Industrially valuable products like BTX chemicals [190], linear *n*-alkyl arenes [191], alkyl silanes [192], alkyl boronate-esters [192], and linear alkyl aldehydes [193] have been efficiently produced by these coupling reactions. One of the major drawbacks of the best catalysts reported for alkane dehydrogenation is their susceptibility to be poisoned by common chemicals containing polar groups such as nitrogen, carbon dioxide, carbon monoxide, and hydrocarbon derivatives (alcohols, amines, and esters). It is noteworthy that pincer complexes that are based either on non-Ir metals or on non-innocent ligands have performed well both in terms of tolerance toward polar functional groups and good reactivity toward dehydrogenation of hydrocarbon derivatives (Chapters 1, 3, and 4). However, for alkane dehydrogenation, clearly, these non-Ir-based pincer complexes are below par in comparison to their Ir counterparts. This diverse nature of reactivity makes the pincer-catalyzed alkane dehydrogenation reaction a contemporary field of research that is being continuously explored, and there is further scope to utilize this reaction toward various applications.

In Chapter 3, Transition Metal Catalyzed Dehydrogenation of Methanol and Related Transformations, Kundu and co-workers discuss various synthetic procedures that can be carried out using methanol as a starting material. The versatility of methanol as a source of single carbon and hydrogen and how it can be explored in several useful transformations have been described. Methanol is an abundant (annual production: 70 million tons) and essential chemical both from the laboratory and an industrial point of view [194–195]. It can be produced from coal, natural gas, and biomass [196], from syngas (CO/H_2) [197], and also, lately, from CO_2 and methane [198–200]. Its multitude of uses include, but are not limited to, production of fine chemicals like formaldehyde, as a hydrogen gas reservoir, formation of fuel cells, and as an essential pharmaceutical unit [201–205]. One such use involves its application as a methylating agent to obtain pharmaceutically important chemicals. In order to utilize it effectively for various C-, N- and O-methylation or formylation reactions, it has become increasingly necessary to use transition metal catalysts to overcome its high energy of

dehydrogenation ($\Delta H = 84\ \text{kJ mol}^{-1}$) [206]. The two strategies commonly followed are "Hydrogen Borrowing" and "Acceptorless Dehydrogenative Coupling (ADC)" [7,207–209].

One of the most important reactions of methanol is its conversion to H_2 and CO_2, which is endothermic by about $38.8\ \text{kJ mol}^{-1}$ [210]. The high-temperature conditions and partial oxidation (leading to harmful CO formation) can be mitigated by switching from heterogeneous to homogenous catalysts based on Ru, Rh, Ir, Fe, and Mn, that has been extensively studied by several groups like Beller, Grutzmacher, Milstein, and Liu [210–218].

N-methylation of amines utilizes the Hydrogen Borrowing strategy to generate a plethora of secondary and tertiary amines assisted by homogenous catalysts. After the first report by Grigg in 1981 who used $RhH(PPh_3)_4$ [219], several other groups have continued the work using catalytic systems like $RuCl_2(PPh_3)_3$, $RuCl_3 \cdot H_2O/P(OBu)_3$, and other Ru-, Re-, Ir-, Mn-, Fe-, and Pd-based systems [220–233].

N-methylation of nitrile, nitride, and azide groups have been successfully executed by groups of Shi, Kundu, Beller, and Shimizu. Reactions could be carried out under UV radiation [225], or be catalyzed by a tandem Ru(II)/Pd(II) system [234], and give high yields of products (up to 98%), though mainly of aromatic substrates. Its practical application is exhibited by the synthesis of antiallergic drug pheneramine [235], among other medically relevant methylated products. A similar reaction with amides was efficiently carried out by Kundu and co-workers using their (NNN)Ru(II)-based catalysts, which yielded good results, also supported by DFT studies [236–238]. They extended this work using aldoximes as substrates and also designed a protocol to effectively synthesize amides from the corresponding nitriles [239,240].

N-Formylation of amines to generate a variety of *N*-formamide reagents were carried out by Glorius, Hong, Milstein, and Bernskoetter groups who showed that Ru, pincer–Mn, and pincer–Fe catalysts turned out to be the most efficient for such transformations [241–244].

A vast field where methanol transformations is applied is C-methylation of various substrates like ketones, alcohols, and some heterocycles. Most of the significant work considering ketones as substrates has been accomplished by using Ir and Ru phosphine-based complexes; a few non-phosphine-based complexes like (NNN)Ru(II), however, have shown great promise toward using environment-friendly catalysts for such reactions [245–250]. For β-methylation of alcohols, it was observed that both homogenous and

heterogeneous Pt species, homogenous Ru complexes and Ir-based nanoparticles gave good yields [251–255]. Homogenous complexes like $[Cp^*IrCl_2]_2$ and heterogeneous ones like Pt/C catalysts were found to be effective when heterocyclic substrates like indole and pyrrole were considered [256,257]. Recently, scientists have been increasingly attentive toward much cheaper and abundant first row transition metal catalysts, based on Co, Fe, Mn, and Ni, which has shown promising results [258–262]. This work was also extended to α-methylation of acetonitrile and aminomethylation of phenols by various groups using similar types of catalysts [263–267].

Methanol is also utilized to generate a number of *N*-heterocyclic compounds, which have great medicinal value, such as erlotinib, quinazolinones, and benzimidazoles [268–272]. Apart from all the reactions mentioned above, methanol also finds use in catalytic transfer hydrogenation of alkynes, alkenes, and ketones [273,274], synthesis of urea derivatives [275–278], and branched alcohols and ketones [279–282]. Overall, there are a plethora of highly applicative reactions in which an abundant and low-cost starting material like methanol can be utilized effectively.

The transition metal-mediated acceptorless dehydrogenation of alcohols, amines, and *N*-heterocycles has emerged as one of the most essential organic transformations owing to its high atom efficiency and environmental friendly approach [283,284], with applications in field of energy storage and synthetic processes [209]. Chapter 4 by Balaraman, Transition Metal Pincer Complexes in Acceptorless Dehydrogenation Reactions, focuses on the utilization of pincer-based transition metal complexes for the catalytic acceptorless dehydrogenation of numerous substrates such as alcohols, amines, partially saturated aromatics, and heteroaromatics.

Acceptorless alcohol dehydrogenation is a simple and greener route to access a variety of carbonyl compounds, esters, and carboxylic acids. Milstein was the first to report pincer–Ru-catalyzed dehydrogenation of secondary alcohols in the presence of strong base such as sodium isopropoxide [285]. Later, the group reported several PNN and PNP pincer–Ru complexes for the dehydrogenation of secondary and primary alcohols to ketones and esters, respectively [285–290]. The proposed mechanism consisted of pincer–Ru dihydride and pincer–Ru(0) species. The Beller group also reported the pincer–ruthenium complexes based on $HPNP^{iPr}$ for the hydrogen production from alcohols under mild base-free conditions [291,292]. Gelman and co-workers also described the acceptorless dehydrogenation of alcohols to ketones and esters using bifunctional

dibenzobarrelene-based PC^{sp3}P−Ir complexes [293,294]. Amine-based NNN pincer−Ru-catalyzed chemoselective alcohol dehydrogenation under base-free conditions was reported by Szymczak, and the same catalyst was found to be active for the chemoselective dehydrogenation of amines [295]. The Yu group employed two unsymmetrical pyridyl-based NNN pincer−Ru complexes for the acceptorless dehydrogenation of secondary alcohols, and wide substrate scope including substituted aromatic secondary alcohols, aliphatic cyclic, and acyclic secondary alcohols was reported [296,297]. Zhang and Hanson employed a pincer−cobalt complex, which was generated *in-situ*, for the alcohol dehydrogenation to ketones exhibiting good to excellent yields [298,299], which was the first report on 3d metal-based systems. The proposed mechanism involved Co(I)/Co(III) pathway that was later proved by DFT studies carried out by Yang *et al.* [300]. Jones and Schneider reported the alcohol dehydrogenation using an pincer−iron complex giving good to moderate yields of the corresponding ketones [301,302]. Similar to this report, Gauvin group reported Mn(I) dicarbonyl complexes consisting of aliphatic PNP ligands for the acceptorless coupling of alcohols with esters under base-free conditions [303]. Both pincer−Mn and pincer−Fe complexes were also active for the acceptorless dehydrogenation of primary alcohols to carboxylic acids.

Acceptorless dehydrogenation for the oxidation of alcohols to acid salts in the presence of water as oxygen donor and liberation of dihydrogen is one of the most significant approaches for obtaining carboxylic acids [209,304]. Milstein and co-workers used bipyrdine-based pincer−Ru complex and converted a variety of aliphatic, non-activated alcohols, and activated benzylic alcohols in the presence of 0.2 mol% catalyst loading in basic aqueous solution [305]. The complex also exhibited the dehydrogenative synthesis of amino acid salts from amino alcohols and basic water [306]. Numerous aliphatic PNP−ruthenium complexes were employed for the alcohol oxidation to carboxylic acid salts, from Prechtl group [307], Beller group [308], and Gauivin, Dumeignila, and co-workers [309]. Good yields and high selectivity were obtained using alcohol/CsOH system by Peng and Zhang [310]. Szymczak slightly modified the secondary sphere of terpyridine ligand with pendant NHR (R = mesityl) groups and observed enhanced reactivity of Ru complex in dehydrogenation catalysis [311]. Very recently, Li and co-workers reported a new type of facial ruthenium complex generated in situ from $[Ru(COD)Cl_2]_n$ and hybrid NHC−CPP ligand, for the catalytic dehydrogenation of alcohol resulting in very high TONs (up to 20,000) with very low catalyst loading (0.0002 mol%) [312].

Dehydrogenation of glycerol, a valuable chemical produced in large scale as a by-product from biodiesel refining was carried out by Beller using a PNP ruthenium complex to obtain lactic acid in 67% yield and high TONs (up to 265,326) [313]. Good selectivity and TON were also obtained by Crabtree (880 TON) [314] and Kumar (15000 TON) [315].

Among the earth-abundant metals used for the dehydrogenation of alcohols to acids, Peng, Zhang, and co-workers were the first to report pyridine-based N'N'N' pincer–nickel complex for acceptorless dehydrogenation of aromatic and aliphatic alcohols to carboxylic acids in good yields (40%–90%) under anhydrous conditions [316]. Aliphatic PNP pincer-supported iron and manganese complexes for the catalytic dehydrogenation of alcohols under basic conditions and in absence of water were reported by Gauivin, Dumeignila, and co-workers [317]. The subsequent report by Liu group employed a well-defined Mn pincer complex for ADC of alcohols with alkaline water to form carboxylate salts [318]. Mechanistic studies pointed toward the involvement of aldehyde intermediate, similar to observations made with other earth-abundant catalysts. Very recently, a highly efficient pincer–cobalt complex-catalyzed acceptorless oxidation of alcohols was reported by Gunanathan group [319]. Apart from broad substrate scope and wide functional group tolerance, diols were successfully converted to dicarboxylic acids and ethanol to potassium acetate. The mechanistic studies indicate the Cannizaro-type pathway with KOH acting as the source of second oxygen of carboxylate salt.

The compounds consisting of unsaturated C–N bonds are of great industrial value and are found in various dyes and pharmaceutically active compounds [320–325]. Due to the slower β-hydride elimination from amido complexes as compared to alkoxides, dehydrogenation of amines is not well established [207,326–328]. Huang and co-workers described a wide range of pincer–ruthenium complexes for dehydrogenative coupling of amines to form imines under base- and oxidant-free conditions [329]. Szymczak reported the chemoselective acceptorless dehydrogenation of amines using amide-derived NNN–Ru(II) hydride complex, which was selective for primary amines [330].

Dehydrogenation of *N*-heterocycles finds application in synthesis of various pharamaceuticals and bioactive molecules. Jones reported well-defined PNP pincer–iron complex for the acceptorless dehydrogenation of *N*-heterocycles under mild conditions [331]. Sawatlon and Surawatanawong reported the mechanism of dehydrogenation of *N*-heterocycles using pincer–iron catalyst reported by Jones, and DFT studies proved the

involvement of pentacoordinated Fe–hydride species [332]. Jones later reported the dehydrogenation of *N*-heterocycles using a pincer–cobalt complex affording the product in good yields [333]. Pincer–ruthenium complex reported by Wang for dehydrogenation of alcohols was also efficient for the acceptorless dehydrogenation of *N*-heterocycles and converted wide range of substituted tetrahydroquinolines and indolines to give unsaturated *N*-heterocycles [297]. Very recently, Rueping group demonstrated the dehydrogenation of *N*-heterocycles such as indolines and 1,2,3,4-tetrahydroquinoxalines derivatives, using PNP pincer–Mn complex in the presence of catalytic amounts of base [334].

Thus it is clear that pincer-based transition metal complexes have shown great potential in catalytic acceptorless dehydrogenation of alcohols, amines, and *N*-heterocycles. Apart from the reports based on precious metals, earth-abundant metal pincer systems are also active for such transformations.

To conclude, this book elucidates in detail the several hydrogenation and dehydrogenation reactions that can be carried out effectively, with selective product yields with the assistance of pincer–metal complexes leading to a range of value-added products. The non-innocent nature of the pincer ligand leads to efficient catalysis in the case of redox reactions, reactions occurring via radical intermediates and (de)hydrogenation reactions of substituted hydrocarbons. On the other hand, purely organometallic mechanisms are operative in pincer–metal-catalyzed dehydrogenation of alkanes. Apparently, pincer–metal-catalyzed dehydrogenation reactions carried out over the course of the last four decades could be broadly classified as those of unactivated hydrocarbons, hydrocarbon derivatives, and ammonia-boranes. The fact that pincer–metal catalysts that are active for the latter two are also tolerant toward polar functionalities and small molecules such as N_2, CO_2, and CO offers promising avenues for functionalization of the former. Collective efforts of the scientific community are necessary to understand the subtle variations that exist in these two reactions that possess strikingly similar but yet distinctively diverse mechanistic pathways. The knowledge that is churned out of this exercise could help in exploiting these complexes to the best of their ability. Considering the rapidly expanding landscape of pincer ligands coupled with the large library of transition metals that are at one's disposal, exciting opportunities lie ahead for pincer–metal complexes in addressing traditionally difficult reactions involving dehydrogenation and tandem functionalization of hydrocarbons.

References

[1] G. Bauer, X. Hu, Recent developments of iron pincer complexes for catalytic applications, Inorg. Chem. Front. 3 (6) (2016) 741—765.
[2] E. Peris, R.H. Crabtree, Key factors in pincer ligand design, Chem. Soc. Rev. 47 (6) (2018) 1959—1968.
[3] J.R. Khusnutdinova, D. Milstein, Metal—ligand cooperation, Angew. Chem. Int. (Ed.) 54 (42) (2015) 12236—12273.
[4] C.S. Slone, D.A. Weinberger, C.A. Mirkin, The transition metal coordination chemistry of hemilabile ligands, Prog. Inorg. Chem. 48 (1999) 233—350.
[5] C.K. Jørgensen, Differences between the four halide ligands, and discussion remarks on trigonal-bipyramidal complexes, on oxidation states, and on diagonal elements of one-electron energy, Coord. Chem. Rev. 1 (1—2) (1966) 164—178.
[6] J. Choi, A.H.R. MacArthur, M. Brookhart, A.S. Goldman, Dehydrogenation and related reactions catalyzed by iridium pincer complexes, Chem. Rev. 111 (3) (2011) 1761—1779.
[7] A. Corma, J. Navas, M.J. Sabater, Advances in one-pot synthesis through borrowing hydrogen catalysis, Chem. Rev. 118 (4) (2018) 1410—1459.
[8] S. Waiba, B. Maji, Manganese catalyzed acceptorless dehydrogenative coupling reactions, ChemCatChem 12 (7) (2020) 1891—1902.
[9] J. Ito, H. Nishiyama, Recent topics of transfer hydrogenation, Tetrahedron Lett. 55 (20) (2014) 3133—3146.
[10] M.E. Van Der Boom, D. Milstein, Cyclometalated phosphine-based pincer complexes: mechanistic insight in catalysis, coordination, and bond activation, Chem. Rev. 103 (5) (2003) 1759—1792.
[11] A. Kumar, A.S. Goldman, Recent advances in alkane dehydrogenation catalyzed by pincer complexes, in: G. van Koten, R.A. Gossage (Eds.), The Privileged Pincer-Metal Platform: Coordination Chemistry & Applications, Springer International Publishing, Cham, 2016, pp. 307—334.
[12] K. Das, A. Kumar, Chapter One—alkane dehydrogenation reactions catalyzed by pincer-metal complexes, in: P.J. Pérez (Ed.), Advances in Organometallic Chemistry, Vol. 72, Academic Press, 2019, pp. 1—57.
[13] A. Kumar, T.M. Bhatti, A.S. Goldman, Dehydrogenation of alkanes and aliphatic groups by pincer-ligated metal complexes, Chem. Rev. 117 (19) (2017) 12357—12384.
[14] C. Gunanathan, D. Milstein, Bond activation and catalysis by ruthenium pincer complexes, Chem. Rev. 114 (24) (2014) 12024—12087.
[15] C.J. Moulton, B.L. Shaw, Transition metal—carbon bonds. Part XLII. Complexes of nickel, palladium, platinum, rhodium and iridium with the tridentate ligand 2,6-bis [(di-t-butylphosphino)methyl]phenyl, J. Chem. Society, Dalton Trans. (11)(1976) 1020—1024.
[16] G. v Koten, Tuning the reactivity of metals held in a rigid ligand environment, Pure Appl. Chem. 61 (10) (1989) 1681.
[17] F. Uhrig, J. Kadar, K. Müller, Reliability of liquid organic hydrogen carrier-based energy storage in a mobility application, Energy Sci. Eng. 8 (6) (2020) 2044—2053.
[18] E. Gianotti, M. l Taillades-Jacquin, J. Rozière, D.J. Jones, High-purity hydrogen generation via dehydrogenation of organic carriers: a review on the catalytic process, ACS Catal. 8 (5) (2018) 4660—4680.
[19] R.H. Crabtree, Nitrogen-Containing Liquid Organic Hydrogen Carriers: Progress and Prospects, ACS Publications, 2017.
[20] K. Müller, K. Brooks, T. Autrey, Hydrogen storage in formic acid: a comparison of process options, Energy Fuels 31 (11) (2017) 12603—12611.

[21] J. Andersson, S. Grönkvist, Large-scale storage of hydrogen, Int. J. Hydrog. Energy 44 (23) (2019) 11901–11919.
[22] J. Eppinger, K.-W. Huang, Formic acid as a hydrogen energy carrier, ACS Energy Lett. 2 (1) (2017) 188–195.
[23] S. Akbayrak, S. Özkar, Ammonia borane as hydrogen storage materials, Int. J. Hydrog. Energy 43 (40) (2018) 18592–18606.
[24] C. Salameh, G. Moussa, A. Bruma, G. Fantozzi, S. Malo, P. Miele, et al., Robust 3D boron nitride nanoscaffolds for remarkable hydrogen storage capacity from ammonia borane, Energy Technol. 6 (3) (2018) 570–577.
[25] A.R. Ploszajski, M. Billing, A.S. Nathanson, M. Vickers, S.M. Bennington, Freeze-dried ammonia borane-polyethylene oxide composites: phase behaviour and hydrogen release, Int. J. Hydrog. Energy 43 (11) (2018) 5645–5656.
[26] M.C. Denney, V. Pons, T.J. Hebden, D.M. Heinekey, K.I. Goldberg, Efficient catalysis of ammonia borane dehydrogenation, J. Am. Chem. Soc. 128 (37) (2006) 12048–12049.
[27] A. Staubitz, M.E. Sloan, A.P. Robertson, A. Friedrich, S. Schneider, P.J. Gates, et al., Catalytic dehydrocoupling/dehydrogenation of N-methylamine-borane and ammonia-borane: synthesis and characterization of high molecular weight polyaminoboranes, J. Am. Chem. Soc. 132 (38) (2010) 13332–13345.
[28] E.A.K. Spearing-Ewyn, N.A. Beattie, A.L. Colebatch, A.J. Martinez-Martinez, A. Docker, T.M. Boyd, et al., The role of neutral Rh (PONOP) H, free NMe 2 H, boronium and ammonium salts in the dehydrocoupling of dimethylamine-borane using the cationic pincer [Rh (PONOP)(η 2-H 2)] + catalyst, Dalton Trans. 48 (39) (2019) 14724–14736.
[29] M.A. Esteruelas, P. Nolis, M. Oliván, E. Oñate, A. Vallribera, A. Vélez, Ammonia borane dehydrogenation promoted by a pincer-square-planar rhodium (I) monohydride: a stepwise hydrogen transfer from the substrate to the catalyst, Inorg. Chem. 55 (14) (2016) 7176–7181.
[30] E.H. Kwan, H. Ogawa, M. Yamashita, A highly active PBP–iridium catalyst for the dehydrogenation of dimethylamine–borane: catalytic performance and mechanism, ChemCatChem 9 (13) (2017) 2457–2462.
[31] A.N. Marziale, A. Friedrich, I. Klopsch, M. Drees, V.R. Celinski, J.R. Schmedt auf der Günne, et al., The mechanism of borane–amine dehydrocoupling with bifunctional ruthenium catalysts, J. Am. Chem. Soc. 135 (36) (2013) 13342–13355.
[32] M. Käß, A. Friedrich, M. Drees, S. Schneider, Ruthenium complexes with cooperative PNP ligands: bifunctional catalysts for the dehydrogenation of ammonia–borane, Angew. Chem. Int. (Ed.) 48 (5) (2009) 905–907.
[33] J.W. Nugent, M. García-Melchor, A.R. Fout, Cobalt-catalyzed ammonia borane dehydrogenation: mechanistic insight and isolation of a cobalt hydride-amidoborane complex, Organometallics 39 (15) (2020) 2917–2927.
[34] T.M. Boyd, K.A. Andrea, K. Baston, A. Johnson, D.E. Ryan, A.S. Weller, A simple cobalt-based catalyst system for the controlled dehydropolymerisation of H 3 B· NMeH 2 on the gram-scale, Chem. Commun. 56 (3) (2020) 482–485.
[35] T.-P. Lin, J.C. Peters, Boryl-mediated reversible H2 activation at cobalt: Catalytic hydrogenation, dehydrogenation, and transfer hydrogenation, J. Am. Chem. Soc. 135 (41) (2013) 15310–15313.
[36] M.R. Elsby, K. Ghostine, U.K. Das, B.M. Gabidullin, R.T. Baker, Iron-SNS and-CNS complexes: selective caryl–S bond cleavage and amine-borane dehydrogenation catalysis, Organometallics 38 (19) (2019) 3844–3851.
[37] P. Bhattacharya, J.A. Krause, H. Guan, Mechanistic studies of ammonia borane dehydrogenation catalyzed by iron pincer complexes, J. Am. Chem. Soc. 136 (31) (2014) 11153–11161.

[38] A. Glüer, M. Förster, V.R. Celinski, Jr Schmedt auf der Günne, M.C. Holthausen, S. Schneider, Highly active iron catalyst for ammonia borane dehydrocoupling at room temperature, ACS Catal. 5 (12) (2015) 7214–7217.
[39] A. Shilov, Catalytic reduction of molecular nitrogen in solutions, Russ. Chem. Bull. 52 (12) (2003) 2555–2562.
[40] J.N. Galloway, A.R. Townsend, J.W. Erisman, M. Bekunda, Z. Cai, J.R. Freney, et al., Transformation of the nitrogen cycle: recent trends, questions, and potential solutions, Science 320 (5878) (2008) 889–892.
[41] D. Fowler, M. Coyle, U. Skiba, M.A. Sutton, J.N. Cape, S. Reis, et al., The global nitrogen cycle in the twenty-first century, Philos. Trans. R. Soc. B: Biol. Sci. 368 (1621) (2013). 20130164.
[42] T. Kandemir, M.E. Schuster, A. Senyshyn, M. Behrens, R. Schlögl, The Haber–Bosch process revisited: on the real structure and stability of "ammonia iron" under working conditions, Angew. Chem. Int. (Ed.) 52 (48) (2013) 12723–12726.
[43] M.D. Fryzuk, S.A. Johnson, The continuing story of dinitrogen activation, Coord. Chem. Rev. 200 (2000) 379–409.
[44] I. Klopsch, E.Y. Yuzik-Klimova, S. Schneider, Functionalization of N 2 by mid to late transition metals via N–N bond cleavage, Nitro. Fix. (2017) 71–112.
[45] S. Hinrichsen, H. Broda, C. Gradert, L. Söncksen, F. Tuczek, Recent developments in synthetic nitrogen fixation, Annu. Rep. Sect. "A" (Inorg. Chem.) 108 (2012) 17–47.
[46] K.C. MacLeod, P.L. Holland, Recent developments in the homogeneous reduction of dinitrogen by molybdenum and iron, Nat. Chem. 5 (7) (2013) 559–565.
[47] S. Kuriyama, Y. Nishibayashi, Catalytic transformations of molecular dinitrogen by iron and cobalt–dinitrogen complexes as catalysts, Nitrogen Fixation, Springer, 2017, pp. 215–234.
[48] J.L. Crossland, D.R. Tyler, Iron–dinitrogen coordination chemistry: dinitrogen activation and reactivity, Coord. Chem. Rev. 254 (17–18) (2010) 1883–1894.
[49] Y. Tanabe, Y. Nishibayashi, Recent advances in catalytic silylation of dinitrogen using transition metal complexes, Coord. Chem. Rev. 389 (2019) 73–93.
[50] M.J. Chalkley, M.W. Drover, J.C. Peters, Catalytic N2-to-NH3 (or-N2H4) conversion by well-defined molecular coordination complexes, Chem. Rev. 120 (12) (2020) 5582–5636.
[51] S. Kim, F. Loose, P.J. Chirik, Beyond ammonia: nitrogen–element bond forming reactions with coordinated dinitrogen, Chem. Rev. 120 (12) (2020) 5637–5681.
[52] M. Mori, Activation of nitrogen for organic synthesis, J. Organomet. Chem. 689 (24) (2004) 4210–4227.
[53] M. Hidai, K. Komori, T. Kodama, D.-M. Jin, T. Takahashi, S. Sugiura, et al., Preparation and properties of molybdenum and tungsten dinitrogen complexes: XXI. Trimethylsilylation of coordinated dinitrogen, J. Organomet. Chem. 272 (2) (1984) 155–167.
[54] K. Komori, S. Sugiura, Y. Mizobe, M. Yamada, M. Hidai, Syntheses and some reactions of trimethylsilylated dinitrogen complexes of tungsten and molybdenum, Bull. Chem. Soc. Jpn. 62 (9) (1989) 2953–2959.
[55] K. Komori, H. Oshita, Y. Mizobe, M. Hidai, Preparation and properties of molybdenum and tungsten dinitrogen complexes. 25. Catalytic conversion of molecular nitrogen into silylamines using molybdenum and tungsten dinitrogen complexes, J. Am. Chem. Soc. 111 (5) (1989) 1939–1940.
[56] K. Shiina, Reductive silylation of molecular nitrogen via fixation to tris (trialkylsilyl) amine, J. Am. Chem. Soc. 94 (26) (1972) 9266–9267.
[57] T.A. Bazhenova, A.E. Shilov, Nitrogen fixation in solution, Coord. Chem. Rev. 144 (1995) 69–145.

[58] D.V. Yandulov, R.R. Schrock, Catalytic reduction of dinitrogen to ammonia at a single molybdenum center, Science 301 (5629) (2003) 76–78.
[59] K. Arashiba, Y. Miyake, Y. Nishibayashi, A molybdenum complex bearing PNP-type pincer ligands leads to the catalytic reduction of dinitrogen into ammonia, Nat. Chem. 3 (2) (2011) 120–125.
[60] Y. Ashida, K. Arashiba, K. Nakajima, Y. Nishibayashi, Molybdenum-catalysed ammonia production with samarium diiodide and alcohols or water, Nature 568 (7753) (2019) 536–540.
[61] N. Stucke, J. Krahmer, C. Näther, F. Tuczek, molybdenum complexes supported by PN3P pincer ligands: synthesis, characterization, and application to synthetic nitrogen fixation, Eur. J. Inorg. Chem. 2018 (47) (2018) 5108–5116.
[62] I. Vidyaratne, J. Scott, S. Gambarotta, P.H. Budzelaar, Dinitrogen activation, partial reduction, and formation of coordinated imide promoted by a chromium diimine-pyridine complex, Inorg. Chem. 46 (17) (2007) 7040–7049.
[63] S. Kuriyama, K. Arashiba, H. Tanaka, Y. Matsuo, K. Nakajima, K. Yoshizawa, et al., Direct transformation of molecular dinitrogen into ammonia catalyzed by cobalt dinitrogen complexes bearing anionic PNP pincer ligands, Angew. Chem. 128 (46) (2016) 14503–14507.
[64] S. Kuriyama, K. Arashiba, K. Nakajima, Y. Matsuo, H. Tanaka, K. Ishii, et al., Catalytic transformation of dinitrogen into ammonia and hydrazine by iron-dinitrogen complexes bearing pincer ligand, Nat. Commun. 7 (1) (2016) 1–9.
[65] Y. Sekiguchi, K. Arashiba, H. Tanaka, A. Eizawa, K. Nakajima, K. Yoshizawa, et al., Catalytic reduction of molecular dinitrogen to ammonia and hydrazine using vanadium complexes, Angew. Chem. Int. (Ed.) 57 (29) (2018) 9064–9068.
[66] B. Wang, G. Luo, M. Nishiura, S. Hu, T. Shima, Y. Luo, et al., Dinitrogen activation by dihydrogen and a PNP-ligated titanium complex, J. Am. Chem. Soc. 139 (5) (2017) 1818–1821.
[67] Y. Sekiguchi, F. Meng, H. Tanaka, A. Eizawa, K. Arashiba, K. Nakajima, et al., Synthesis and reactivity of titanium-and zirconium-dinitrogen complexes bearing anionic pyrrole-based PNP-type pincer ligands, Dalton Trans. 47 (33) (2018) 11322–11326.
[68] F. Schendzielorz, M. Finger, J. Abbenseth, C. Würtele, V. Krewald, S. Schneider, Metal-ligand cooperative synthesis of benzonitrile by electrochemical reduction and photolytic splitting of dinitrogen, Angew. Chem. Int. (Ed.) 58 (3) (2019) 830–834.
[69] I. Klopsch, M. Kinauer, M. Finger, C. Würtele, S. Schneider, Conversion of dinitrogen into acetonitrile under ambient conditions, Angew. Chem. Int. (Ed.) 55 (15) (2016) 4786–4789.
[70] I. Klopsch, M. Finger, C. Würtele, B. Milde, D.B. Werz, S. Schneider, Dinitrogen splitting and functionalization in the coordination sphere of rhenium, J. Am. Chem. Soc. 136 (19) (2014) 6881–6883.
[71] A. Cavaillé, B. Joyeux, N. Saffon-Merceron, N. Nebra, M. Fustier-Boutignon, N. Mézailles, Triphos–Fe dinitrogen and dinitrogen–hydride complexes: relevance to catalytic N 2 reductions, Chem. Commun. 54 (84) (2018) 11953–11956.
[72] Q. Liao, N. Saffon-Merceron, N. Mézailles, N2 reduction into silylamine at tridentate phosphine/Mo center: catalysis and mechanistic study, ACS Catal. 5 (11) (2015) 6902–6906.
[73] R. Imayoshi, K. Nakajima, J. Takaya, N. Iwasawa, Y. Nishibayashi, Synthesis and reactivity of iron–and cobalt–dinitrogen complexes bearing PSiP-type pincer ligands toward nitrogen fixation, Eur. J. Inorg. Chem. 2017 (32) (2017) 3769–3778.
[74] J. Zhang, G. Leitus, Y. Ben-David, D. Milstein, Efficient homogeneous catalytic hydrogenation of esters to alcohols, Angew. Chem. 118 (7) (2006) 1131–1133.

[75] K. Junge, B. Wendt, H. Jiao, M. Beller, Iridium-catalyzed hydrogenation of carboxylic acid esters, ChemCatChem 6 (10) (2014) 2810–2814.
[76] T. Zell, Y. Ben-David, D. Milstein, Unprecedented iron-catalyzed ester hydrogenation. Mild, selective, and efficient hydrogenation of trifluoroacetic esters to alcohols catalyzed by an iron pincer complex, Angew. Chem. 126 (18) (2014) 4773–4777.
[77] S. Werkmeister, K. Junge, B. Wendt, E. Alberico, H. Jiao, W. Baumann, et al., Hydrogenation of esters to alcohols with a well-defined iron complex, Angew. Chem. Int. (Ed.) 53 (33) (2014) 8722–8726.
[78] N.A. Espinosa-Jalapa, A. Nerush, L.J.W. Shimon, G. Leitus, L. Avram, Y. Ben-David, et al., Manganese-catalyzed hydrogenation of esters to alcohols, Chem.—A Eur. J. 23 (25) (2017) 5934–5938.
[79] D. Srimani, A. Mukherjee, A.F. Goldberg, G. Leitus, Y. Diskin-Posner, L.J. Shimon, et al., Cobalt-catalyzed hydrogenation of esters to alcohols: unexpected reactivity trend indicates ester enolate intermediacy, Angew. Chem. Int. (Ed.) 54 (42) (2015) 12357–12360.
[80] E. Balaraman, B. Gnanaprakasam, L.J. Shimon, D. Milstein, Direct hydrogenation of amides to alcohols and amines under mild conditions, J. Am. Chem. Soc. 132 (47) (2010) 16756–16758.
[81] S. Kar, M. Rauch, A. Kumar, G. Leitus, Y. Ben-David, D. Milstein, Selective room-temperature hydrogenation of amides to amines and alcohols catalyzed by a ruthenium pincer complex and mechanistic insight, ACS Catal. 10 (10) (2020) 5511–5515.
[82] J.R. Cabrero-Antonino, E. Alberico, H.-J. Drexler, W. Baumann, K. Junge, H. Junge, et al., Efficient base-free hydrogenation of amides to alcohols and amines catalyzed by well-defined pincer imidazolyl–ruthenium complexes, ACS Catal. 6 (1) (2016) 47–54.
[83] J.A. Garg, S. Chakraborty, Y. Ben-David, D. Milstein, Unprecedented iron-catalyzed selective hydrogenation of activated amides to amines and alcohols, Chem. Commun. 52 (30) (2016) 5285–5288.
[84] Y.-Q. Zou, S. Chakraborty, A. Nerush, D. Oren, Y. Diskin-Posner, Y. Ben-David, et al., Highly selective, efficient deoxygenative hydrogenation of amides catalyzed by a manganese pincer complex via metal–ligand cooperation, ACS Catal. 8 (9) (2018) 8014–8019.
[85] V. Papa, J.R. Cabrero-Antonino, E. Alberico, A. Spanneberg, K. Junge, H. Junge, et al., Efficient and selective hydrogenation of amides to alcohols and amines using a well-defined manganese–PNN pincer complex, Chem. Sci. 8 (5) (2017) 3576–3585.
[86] E. Balaraman, Y. Ben-David, D. Milstein, Unprecedented catalytic hydrogenation of urea derivatives to amines and methanol, Angew. Chem. Int. (Ed.) 50 (49) (2011) 11702–11705.
[87] Z. Han, L. Rong, J. Wu, L. Zhang, Z. Wang, K. Ding, Catalytic hydrogenation of cyclic carbonates: a practical approach from CO2 and epoxides to methanol and diols, Angew. Chem. Int. (Ed.) Engl. 51 (52) (2012) 13041–13045.
[88] A. Kumar, T. Janes, N.A. Espinosa-Jalapa, D. Milstein, Manganese catalyzed hydrogenation of organic carbonates to methanol and alcohols, Angew. Chem. Int. (Ed.) Engl. 57 (37) (2018) 12076–12080.
[89] U.K. Das, A. Kumar, Y. Ben-David, M.A. Iron, D. Milstein, Manganese catalyzed hydrogenation of carbamates and urea derivatives, J. Am. Chem. Soc. 141 (33) (2019) 12962–12966.
[90] A. Kumar, T. Janes, N.A. Espinosa-Jalapa, D. Milstein, Selective hydrogenation of cyclic imides to diols and amines and its application in the development of a liquid organic hydrogen carrier, J. Am. Chem. Soc. 140 (24) (2018) 7453–7457.

[91] D. Srimani, M. Feller, Y. Ben-David, D. Milstein, Catalytic coupling of nitriles with amines to selectively form imines under mild hydrogen pressure, Chem. Commun. 48 (97) (2012) 11853–11855.
[92] R. Adam, E. Alberico, W. Baumann, H.-J. Drexler, R. Jackstell, H. Junge, et al., NNP-type pincer imidazolylphosphine ruthenium complexes: efficient base-free hydrogenation of aromatic and aliphatic nitriles under mild conditions, Chem.—A Eur. J. 22 (14) (2016) 4991–5002.
[93] C. Bornschein, S. Werkmeister, B. Wendt, H. Jiao, E. Alberico, W. Baumann, et al., Mild and selective hydrogenation of aromatic and aliphatic (di)nitriles with a well-defined iron pincer complex, Nat. Commun. 5 (2014) 4111.
[94] S. Chakraborty, G. Leitus, D. Milstein, Iron-catalyzed mild and selective hydrogenative cross-coupling of nitriles and amines to form secondary aldimines, Angew. Chem. Int. (Ed.) Engl. 56 (8) (2017) 2074–2078.
[95] S. Chakraborty, D. Milstein, Selective hydrogenation of nitriles to secondary imines catalyzed by an iron pincer complex, ACS Catal. 7 (6) (2017) 3968–3972.
[96] S. Elangovan, C. Topf, S. Fischer, H. Jiao, A. Spannenberg, W. Baumann, et al., Selective catalytic hydrogenations of nitriles, ketones, and aldehydes by well-defined manganese pincer complexes, J. Am. Chem. Soc. 138 (28) (2016) 8809–8814.
[97] R.P. Yu, J.M. Darmon, J.M. Hoyt, G.W. Margulieux, Z.R. Turner, P.J. Chirik, High-activity iron catalysts for the hydrogenation of hindered, unfunctionalized alkenes, ACS Catal. 2 (8) (2012) 1760–1764.
[98] M. Ohff, A. Ohff, M.E. van der Boom, D. Milstein, Highly active Pd(II) PCP-type catalysts for the heck reaction, J. Am. Chem. Soc. 119 (48) (1997) 11687–11688.
[99] J. Liu, H. Wang, H. Zhang, X. Wu, H. Zhang, Y. Deng, et al., Identification of a highly efficient alkylated pincer thioimido–palladium(II) complex as the active catalyst in Negishi coupling, Chem.—A Eur. J. 15 (17) (2009) 4437–4445.
[100] H. Wang, J. Liu, Y. Deng, T. Min, G. Yu, X. Wu, et al., Pincer thioamide and pincer thioimide palladium complexes catalyze highly efficient Negishi coupling of primary and secondary alkyl zinc reagents at room temperature, Chem.—A Eur. J. 15 (6) (2009) 1499–1507.
[101] M.C. Lipke, R.A. Woloszynek, L. Ma, J.D. Protasiewicz, m-Terphenyl anchored palladium diphosphinite PCP-pincer complexes that promote the Suzuki − Miyaura reaction under mild conditions, Organometallics 28 (1) (2009) 188–196.
[102] J.L. Bolliger, O. Blacque, C.M. Frech, Short, facile, and high-yielding synthesis of extremely efficient pincer-type Suzuki catalysts bearing aminophosphine substituents, Angew. Chem. Int. (Ed.) 46 (34) (2007) 6514–6517.
[103] F. Churruca, R. SanMartin, B. Inés, I. Tellitu, E. Domínguez, Hydrophilic CNC-pincer palladium complexes: a source for highly efficient, recyclable homogeneous catalysts in Suzuki–Miyaura cross-coupling, Adv. Synth. Catal. 348 (14) (2006) 1836–1840.
[104] B. Inés, R. SanMartin, M.J. Moure, E. Domínguez, Insights into the role of new palladium pincer complexes as robust and recyclable precatalysts for Suzuki–Miyaura couplings in neat water, Adv. Synth. Catal. 351 (13) (2009) 2124–2132.
[105] R.B. Bedford, S.M. Draper, P. Noelle Scully, S.L. Welch, Palladium bis(phosphinite) 'PCP'-pincer complexes and their application as catalysts in the Suzuki reaction, N. J. Chem. 24 (10) (2000) 745–747.
[106] D. Olsson, O.F. Wendt, Suzuki reaction catalysed by a PCsp3P pincer Pd(II) complex: evidence for a mechanism involving molecular species, J. Organomet. Chem. 694 (19) (2009) 3112–3115.
[107] T. Takemoto, S. Iwasa, H. Hamada, K. Shibatomi, M. Kameyama, Y. Motoyama, et al., Highly efficient Suzuki–Miyaura coupling reactions catalyzed by bis(oxazolinyl)phenyl–Pd(II) complex, Tetrahedron Lett. 48 (19) (2007) 3397–3401.

[108] X.-Q. Zhang, Z.-X. Wang, Amido pincer nickel catalyzed Kumada cross-coupling of aryl, heteroaryl, and vinyl chlorides, Synlett 24 (16) (2013) 2081—2084.
[109] T. Di Franco, M. Stojanovic, S.C. Keller, R. Scopelliti, X. Hu, A structure—activity study of nickel NNN pincer complexes for alkyl-alkyl Kumada and Suzuki—Miyaura coupling reactions, Helv. Chim. Acta 99 (11) (2016) 830—847.
[110] D. Olsson, P. Nilsson, M. El Masnaouy, O.F. Wendt, A catalytic and mechanistic investigation of a PCP pincer palladium complex in the Stille reaction, Dalton Trans. 11 (2005) 1924—1929.
[111] F. Churruca, R. SanMartin, I. Tellitu, E. Domínguez, N-Heterocyclic NCN-pincer palladium complexes: a source for general, highly efficient catalysts in Heck, Suzuki, and Sonogashira coupling reactions, Synlett 2005 (20) (2005) 3116—3120.
[112] J.L. Bolliger, C.M. Frech, Highly convenient, clean, fast, and reliable Sonogashira coupling reactions promoted by aminophosphine-based pincer complexes of palladium performed under additive- and amine-free reaction conditions, Adv. Synth. Catal. 351 (6) (2009) 891—902.
[113] H.M. Lee, J.Y. Zeng, C.-H. Hu, M.-T. Lee, A new tridentate pincer phosphine/N-heterocyclic carbene ligand: palladium complexes, their structures, and catalytic activities, Inorg. Chem. 43 (21) (2004) 6822—6829.
[114] J.A. Loch, M. Albrecht, E. Peris, J. Mata, J.W. Faller, R.H. Crabtree, Palladium complexes with tridentate pincer bis-carbene ligands as efficient catalysts for C − C coupling, Organometallics 21 (4) (2002) 700—706.
[115] F.E. Hahn, M.C. Jahnke, T. Pape, Synthesis of pincer-type bis(benzimidazolin-2-ylidene) palladium complexes and their application in C − C coupling reactions, Organometallics 26 (1) (2007) 150—154.
[116] B. Inés, R. SanMartin, F. Churruca, E. Domínguez, M.K. Urtiaga, M.I. Arriortua, et al., Pincer-type palladium catalyst in Suzuki, Sonogashira, and Hiyama couplings in neat water, Organometallics 27 (12) (2008) 2833—2839.
[117] J. Kjellgren, J. Aydin, O.A. Wallner, I.V. Saltanova, K.J. Szabó, Palladium pincer complex catalyzed cross-coupling of vinyl epoxides and aziridines with organoboronic acids, Chem.—A Eur. J. 11 (18) (2005) 5260—5268.
[118] T. Tu, J. Malineni, K.H. Dötz, A novel pyridine-bridged bis-benzimidazolylidene pincer palladium complex: synthesis and catalytic properties, Adv. Synth. Catal. 350 (11—12) (2008) 1791—1795.
[119] D. Morales-Morales, R. Redón, C. Yung, C.M. Jensen, High yield olefination of a wide scope of aryl chlorides catalyzed by the phosphinito palladium PCP pincer complex: [PdCl{CH(OPPr)-2,6}], Chem. Commun. 17 (2000) 1619—1620.
[120] V. Leigh, W. Ghattas, H. Mueller-Bunz, M. Albrecht, Synthesis of pincer-type N-heterocyclic carbene palladium complexes with a hemilabile ligand and their application in cross-coupling catalysis, J. Organomet. Chem. 771 (2014) 33—39.
[121] V. Arora, H. Narjinari, P.G. Nandi, A. Kumar, Recent advances in pincer—nickel catalyzed reactions, Dalton Trans. 50 (10) (2021) 3394—3428.
[122] D.L. Broere, R. Plessius, J.I. van der Vlugt, New avenues for ligand-mediated processes—expanding metal reactivity by the use of redox-active catechol, o-aminophenol and o-phenylenediamine ligands, Chem. Soc. Rev. 44 (19) (2015) 6886—6915.
[123] P.J. Chirik, K. Wieghardt, Radical ligands confer nobility on base-metal catalysts, Science 327 (5967) (2010) 794—795.
[124] J.I. van der Vlugt, Radical-type reactivity and catalysis by single-electron transfer to or from redox-active ligands, Chem. (Weinh. an. der Bergstrasse, Ger.) 25 (11) (2019) 2651.
[125] O.R. Luca, R.H. Crabtree, Redox-active ligands in catalysis, Chem. Soc. Rev. 42 (4) (2013) 1440—1459.

[126] V. Lyaskovskyy, B. de Bruin, Redox non-innocent ligands: versatile new tools to control catalytic reactions, ACS Catal. 2 (2) (2012) 270–279.
[127] V.K. Praneeth, M.R. Ringenberg, T.R. Ward, Redox-active ligands in catalysis, Angew. Chem. Int. (Ed.) 51 (41) (2012) 10228–10234.
[128] J.L. Wong, R.H. Sánchez, J.G. Logan, R.A. Zarkesh, J.W. Ziller, A.F. Heyduk, Disulfide reductive elimination from an iron (III) complex, Chem. Sci. 4 (4) (2013) 1906–1910.
[129] M.W. Bouwkamp, E. Lobkovsky, P.J. Chirik, Bis (imino) pyridine iron (II) alkyl cations for olefin polymerization, J. Am. Chem. Soc. 127 (27) (2005) 9660–9661.
[130] M.W. Bouwkamp, S.C. Bart, E.J. Hawrelak, R.J. Trovitch, E. Lobkovsky, P.J. Chirik, Square planar bis (imino) pyridine iron halide and alkyl complexes, Chem. Commun. 27 (2005) 3406–3408.
[131] G.J. Britovsek, V.C. Gibson, S.J. McTavish, G.A. Solan, A.J. White, D.J. Williams, et al., Novel olefin polymerization catalysts based on iron and cobalt, Chem. Commun. (7)(1998) 849–850.
[132] B.L. Small, M. Brookhart, A.M. Bennett, Highly active iron and cobalt catalysts for the polymerization of ethylene, J. Am. Chem. Soc. 120 (16) (1998) 4049–4050.
[133] D.M. Spasyuk, D. Zargarian, A. van der Est, New POCN-type pincer complexes of nickel (II) and nickel (III), Organometallics 28 (22) (2009) 6531–6540.
[134] D. Adhikari, S. Mossin, F. Basuli, J.C. Huffman, R.K. Szilagyi, K. Meyer, et al., Structural, spectroscopic, and theoretical elucidation of a redox-active pincer-type ancillary applied in catalysis, J. Am. Chem. Soc. 130 (11) (2008) 3676–3682.
[135] A.I. Nguyen, K.J. Blackmore, S.M. Carter, R.A. Zarkesh, A.F. Heyduk, One-and two-electron reactivity of a tantalum (V) complex with a redox-active tris (amido) ligand, J. Am. Chem. Soc. 131 (9) (2009) 3307–3316.
[136] R.A. Zarkesh, J.W. Ziller, A.F. Heyduk, Four-electron oxidative formation of aryl diazenes using a tantalum redox-active ligand complex, Angew. Chem. Int. (Ed.) 47 (25) (2008) 4715–4718.
[137] A.I. Nguyen, R.A. Zarkesh, D.C. Lacy, M.K. Thorson, A.F. Heyduk, Catalytic nitrene transfer by a zirconium (IV) redox-active ligand complex, Chem. Sci. 2 (1) (2011) 166–169.
[138] F. Lu, R.A. Zarkesh, A.F. Heyduk, A redox-active ligand as a reservoir for protons and electrons: O2 reduction at zirconium (IV), Euro. J. Inorg. Chem. 2012 (3) (2012) 467–470.
[139] D. l L. Broere, B. De Bruin, J.N. Reek, M. Lutz, S. Dechert, J.I. Van Der Vlugt, Intramolecular redox-active ligand-to-substrate single-electron transfer: radical reactivity with a palladium (II) complex, J. Am. Chem. Soc. 136 (33) (2014) 11574–11577.
[140] D.L. Broere, L.L. Metz, B. de Bruin, J.N. Reek, M.A. Siegler, J.I. van der Vlugt, Redox-active ligand-induced homolytic bond activation, Angew. Chem. Int. (Ed.) 54 (5) (2015) 1516–1520.
[141] S.P. Rath, D. Sengupta, P. Ghosh, R. Bhattacharjee, M. Chakraborty, S. Samanta, et al., Effects of ancillary ligands on redox and chemical properties of ruthenium coordinated azoaromatic pincer, Inorg. Chem. 57 (19) (2018) 11995–12009.
[142] A. Mukherjee, D. Milstein, Homogeneous catalysis by cobalt and manganese pincer complexes, ACS Catal. 8 (12) (2018) 11435–11469.
[143] A. Peters, ISBN 3–527-20102-5. United States Ullmann's Encyclopedia of Industrial Chemistry. Vol. A2. VCH Verlagsgesellschaft, Weinheim, FRG, 1985. Xii + , Elsevier, 1986p. 553.
[144] M.W. Haenel, S. Oevers, K. Angermund, W.C. Kaska, H.-J. Fan, M.B. Hall, Thermally stable homogeneous catalysts for alkane dehydrogenation, Angew. Chem. Int. (Ed.) 40 (19) (2001) 3596–3600.

[145] M. Gupta, C. Hagen, R.J. Flesher, W.C. Kaska, C.M. Jensen, A highly active alkane dehydrogenation catalyst: stabilization of dihydrido rhodium and iridium complexes by a P–C–P pincer ligand, Chem. Commun. 17 (1996) 2083–2084.
[146] W.-w Xu, G. P Rosini, K. Krogh-Jespersen, A. S Goldman, M. Gupta, C. M Jensen, et al., Thermochemical alkane dehydrogenation catalyzed in solution without the use of a hydrogen acceptor, Chem. Commun. 23 (1997) 2273–2274.
[147] M. Gupta, C. Hagen, W.C. Kaska, R.E. Cramer, C.M. Jensen, Catalytic dehydrogenation of cycloalkanes to arenes by a dihydrido iridium P – C – P pincer complex, J. Am. Chem. Soc. 119 (4) (1997) 840–841.
[148] D.W. Lee, W.C. Kaska, C.M. Jensen, Mechanistic features of iridium pincer complex catalyzed hydrocarbon dehydrogenation reactions: inhibition upon formation of a μ-dinitrogen complex, Organometallics 17 (1) (1998) 1–3.
[149] M.A. McLoughlin, R.J. Flesher, W.C. Kaska, H.A. Mayer, Synthesis and reactivity of [IrH2(tBu2P)CH2CH2CHCH2CH2P(tBu2)], a dynamic iridium polyhydride complex, Organometallics 13 (10) (1994) 3816–3822.
[150] D. Morales-Morales, R. o Redón, C. Yung, C.M. Jensen, Dehydrogenation of alkanes catalyzed by an iridium phosphinito PCP pincer complex, Inorganica Chim. Acta 357 (10) (2004) 2953–2956.
[151] A. Kumar, J.D. Hackenberg, G. Zhuo, A.M. Steffens, O. Mironov, R.J. Saxton, et al., High yields of piperylene in the transfer dehydrogenation of pentane catalyzed by pincer-ligated iridium complexes, J. Mol. Catal. A: Chem. 426 (2017) 368–375.
[152] I. Göttker-Schnetmann, M. Brookhart, Mechanistic studies of the transfer dehydrogenation of cyclooctane catalyzed by iridium bis(phosphinite) p-XPCP pincer complexes, J. Am. Chem. Soc. 126 (30) (2004) 9330–9338.
[153] I. Göttker-Schnetmann, P.S. White, M. Brookhart, Synthesis and properties of iridium bis(phosphinite) pincer complexes (p-XPCP)IrH2, (p-XPCP)Ir(CO), (p-XPCP)Ir(H)(aryl), and {(p-XPCP)Ir}2{μ-N2} and their relevance in alkane transfer dehydrogenation, Organometallics 23 (8) (2004) 1766–1776.
[154] Y. Gao, C. Guan, M. Zhou, A. Kumar, T.J. Emge, A.M. Wright, et al., β-hydride elimination and C–H activation by an iridium acetate complex, catalyzed by Lewis acids. Alkane dehydrogenation cocatalyzed by Lewis acids and [2,6-bis(4,4-dimethyloxazolinyl)-3,5-dimethylphenyl]iridium, J. Am. Chem. Soc. 139 (18) (2017) 6338–6350.
[155] K.E. Allen, D.M. Heinekey, A.S. Goldman, K.I. Goldberg, Alkane dehydrogenation by C–H activation at iridium(III), Organometallics 32 (6) (2013) 1579–1582.
[156] K.E. Allen, D.M. Heinekey, A.S. Goldman, K.I. Goldberg, Regeneration of an iridium(III) complex active for alkane dehydrogenation using molecular oxygen, Organometallics 33 (6) (2014) 1337–1340.
[157] J.J. Adams, N. Arulsamy, D.M. Roddick, Acceptor CF3PCPH pincer reactivity with (PPh3)3Ir(CO)H, Dalton Trans. 40 (39) (2011) 10014–10019.
[158] D.M. Roddick, Tuning of PCP pincer ligand electronic and steric properties, in: G. van Koten, D. Milstein (Eds.), Organometallic Pincer Chemistry, Springer Berlin Heidelberg, Berlin, Heidelberg, 2013, pp. 49–88.
[159] J.J. Adams, N. Arulsamy, D.M. Roddick, Investigation of iridium CF3PCP pincer catalytic dehydrogenation and decarbonylation chemistry, Organometallics 31 (4) (2012) 1439–1447.
[160] A.R. Chianese, M.J. Drance, K.H. Jensen, S.P. McCollom, N. Yusufova, S.E. Shaner, et al., Acceptorless alkane dehydrogenation catalyzed by iridium CCC-pincer complexes, Organometallics 33 (2) (2014) 457–464.
[161] A.R. Chianese, A. Mo, N.L. Lampland, R.L. Swartz, P.T. Bremer, Iridium complexes of CCC-pincer N-heterocyclic carbene ligands: synthesis and catalytic C – H functionalization, Organometallics 29 (13) (2010) 3019–3026.

[162] A.R. Chianese, S.E. Shaner, J.A. Tendler, D.M. Pudalov, D.Y. Shopov, D. Kim, et al., Iridium complexes of bulky CCC-pincer N-heterocyclic carbene ligands: steric control of coordination number and catalytic alkene isomerization, Organometallics 31 (21) (2012) 7359–7367.
[163] W. Yao, Y. Zhang, X. Jia, Z. Huang, Selective catalytic transfer dehydrogenation of alkanes and heterocycles by an iridium pincer complex, Angew. Chem. Int. (Ed.) 53 (5) (2014) 1390–1394.
[164] X. Zhang, S.-B. Wu, X. Leng, L.W. Chung, G. Liu, Z. Huang, N-bridged pincer iridium complexes for highly efficient alkane dehydrogenation and the relevant linker effects, ACS Catal. (2020).
[165] Z. Huang, M. Brookhart, A.S. Goldman, S. Kundu, A. Ray, S.L. Scott, et al., Highly active and recyclable heterogeneous iridium pincer catalysts for transfer dehydrogenation of alkanes, Adv. Synth. Catal. 351 (1-2) (2009) 188–206.
[166] Z. Huang, E. Rolfe, E.C. Carson, M. Brookhart, A.S. Goldman, S.H. El-Khalafy, et al., Efficient heterogeneous dual catalyst systems for alkane metathesis, Adv. Synth. Catal. 352 (1) (2010) 125–135.
[167] Y. Shi, T. Suguri, C. Dohi, H. Yamada, S. Kojima, Y. Yamamoto, Highly active catalysts for the transfer dehydrogenation of alkanes: synthesis and application of novel 7–6–7 ring-based pincer iridium complexes, Chem.—A Eur. J. 19 (32) (2013) 10672–10689.
[168] K.B. Renkema, Y.V. Kissin, A.S. Goldman, Mechanism of alkane transfer-dehydrogenation catalyzed by a pincer-ligated iridium complex, J. Am. Chem. Soc. 125 (26) (2003) 7770–7771.
[169] S. Biswas, Z. Huang, Y. Choliy, D.Y. Wang, M. Brookhart, K. Krogh-Jespersen, et al., Olefin isomerization by iridium pincer catalysts. experimental evidence for an η3-Allyl pathway and an unconventional mechanism predicted by DFT calculations, J. Am. Chem. Soc. 134 (32) (2012) 13276–13295.
[170] S.M.M. Knapp, S.E. Shaner, D. Kim, D.Y. Shopov, J.A. Tendler, D.M. Pudalov, et al., Mechanistic studies of alkene isomerization catalyzed by CCC-pincer complexes of iridium, Organometallics 33 (2) (2014) 473–484.
[171] H. Fang, G. Liu, Z. Huang, Chapter 18—pincer iridium and ruthenium complexes for alkane dehydrogenation, in: D. Morales-Morales (Ed.), Pincer Compounds, Elsevier, 2018, pp. 383–399.
[172] B. Sheludko, M.T. Cunningham, A.S. Goldman, F.E. Celik, Continuous-flow alkane dehydrogenation by supported pincer-ligated iridium catalysts at elevated temperatures, ACS Catal. 8 (9) (2018) 7828–7841.
[173] O. Mironov, R.J. Saxton, A.S. Goldman, A. Kumar, Alkane-alkene coupling via tandem alkane-dehydrogenation/alkene-dimerization catalyzed by pincer iridium catalyst heterogenized on solid supports. United States 20180044261A1, 2018.
[174] J.J. Adams, N. Arulsamy, D.M. Roddick, Acceptor PCP pincer iridium(I) chemistry: stabilization of nonmeridional PCP coordination geometries, Organometallics 30 (4) (2011) 697–711.
[175] J.-i Ito, T. Kaneda, H. Nishiyama, Intermolecular C–H bond activation of alkanes and arenes by NCN pincer iridium (III) acetate complexes containing bis (oxazolinyl) phenyl ligands, Organometallics 31 (12) (2012) 4442–4449.
[176] J.J. Adams, B.C., Gruver, R. Donohoue, N. Arulsamy, D.M. Roddick, Acceptor pincer Ru(ii) chemistry, Dalton Trans. 41 (40) (2012) 12601–12611.
[177] J.D. Koola, D.M. Roddick, Activation of hydrocarbons by a ruthenium(II) (fluoroalkyl)phosphine hydride complex, J. Am. Chem. Soc. 113 (4) (1991) 1450–1451.
[178] B.C., Gruver, J.J. Adams, S.J. Warner, N. Arulsamy, D.M. Roddick, Acceptor pincer chemistry of ruthenium: catalytic alkane dehydrogenation by (CF3PCP)Ru (cod)(H), Organometallics 30 (19) (2011) 5133–5140.

[179] X. Zhou, S. Malakar, T. Zhou, S. Murugesan, C. Huang, T.J. Emge, et al., Catalytic alkane transfer dehydrogenation by PSP-pincer-ligated ruthenium. Deactivation of an extremely reactive fragment by formation of allyl hydride complexes, ACS Catal. 9 (5) (2019) 4072–4083.
[180] B.J. Eleazer, M.D. Smith, A.A. Popov, D.V. Peryshkov, Rapid reversible borane to boryl hydride exchange by metal shuttling on the carborane cluster surface, Chem. Sci. 8 (8) (2017) 5399–5407.
[181] Y. Zhang, H. Fang, W. Yao, X. Leng, Z. Huang, Synthesis of pincer hydrido ruthenium olefin complexes for catalytic alkane dehydrogenation, Organometallics 35 (2) (2016) 181–188.
[182] B.C., Gruver, J.J. Adams, N. Arulsamy, D.M. Roddick, Acceptor pincer chemistry of osmium: catalytic alkane dehydrogenation by (CF3PCP)Os(cod)(H), Organometallics 32 (21) (2013) 6468–6475.
[183] M.C. Haibach, D.Y. Wang, T.J. Emge, K. Krogh-Jespersen, A.S. Goldman, POP) Rh pincer hydride complexes: unusual reactivity and selectivity in oxidative addition and olefin insertion reactions, Chem. Sci. 4 (9) (2013) 3683–3692.
[184] K. Wang, M.E. Goldman, T.J. Emge, A.S. Goldman, Transfer-dehydrogenation of alkanes catalyzed by rhodium (I) phosphine complexes, J. Organomet. Chem. 518 (1–2) (1996) 55–68.
[185] D. Bézier, C. Guan, K. Krogh-Jespersen, A.S. Goldman, M. Brookhart, Experimental and computational study of alkane dehydrogenation catalyzed by a carbazolide-based rhodium PNP pincer complex, Chem. Sci. 7 (4) (2016) 2579–2586.
[186] J.-M. Basset, C. Coperet, D. Soulivong, M. Taoufik, J.T. Cazat, Metathesis of alkanes and related reactions, Acc. Chem. Res. 43 (2) (2010) 323–334.
[187] M.C. Haibach, S. Kundu, M. Brookhart, A.S. Goldman, Alkane Metathesis by tandem alkane-dehydrogenation–olefin-metathesis catalysis and related chemistry, Acc. Chem. Res. 45 (6) (2012) 947–958.
[188] L.V. Dinh, B. Li, A. Kumar, W. Schinski, K.D. Field, A. Kuperman, et al., Alkyl–aryl coupling catalyzed by tandem systems of pincer-ligated iridium complexes and zeolites, ACS Catal. 6 (5) (2016) 2836–2841.
[189] T.W. Lyons, D. Guironnet, M. Findlater, M. Brookhart, Synthesis of p-xylene from ethylene, J. Am. Chem. Soc. 134 (38) (2012) 15708–15711.
[190] R. Ahuja, B. Punji, M. Findlater, C. Supplee, W. Schinski, M. Brookhart, et al., Catalytic dehydroaromatization of n-alkanes by pincer-ligated iridium complexes, Nat. Chem. 3 (2) (2011) 167–171.
[191] G.E. Dobereiner, J. Yuan, R.R. Schrock, A.S. Goldman, J.D. Hackenberg, Catalytic synthesis of n-alkyl arenes through alkyl group cross-metathesis, J. Am. Chem. Soc. 135 (34) (2013) 12572–12575.
[192] X. Jia, Z. Huang, Conversion of alkanes to linear alkylsilanes using an iridium–iron-catalysed tandem dehydrogenation–isomerization–hydrosilylation, Nat. Chem. 8 (2) (2016) 157–161.
[193] X. Tang, X. Jia, Z. Huang, Thermal, catalytic conversion of alkanes to linear aldehydes and linear amines, J. Am. Chem. Soc. 140 (11) (2018) 4157–4163.
[194] G.A. Olah, Beyond oil and gas: the methanol economy, Angew. Chem. Int. (Ed.) 44 (18) (2005) 2636–2639.
[195] D. Prat, A. Wells, J. Hayler, H. Sneddon, C.R. McElroy, S. Abou-Shehada, et al., CHEM21 selection guide of classical- and less classical-solvents, Green. Chem. 18 (1) (2016) 288–296.
[196] D.R. Palo, R.A. Dagle, J.D. Holladay, Methanol steam reforming for hydrogen production, Chem. Rev. 107 (10) (2007) 3992–4021.
[197] J.-P. Lange, Methanol synthesis: a short review of technology improvements, Catal. Today 64 (1) (2001) 3–8.

[198] C.A. Huff, M.S. Sanford, Cascade catalysis for the homogeneous hydrogenation of CO2 to methanol, J. Am. Chem. Soc. 133 (45) (2011) 18122–18125.
[199] S. Wesselbaum, T. Vom Stein, J. Klankermayer, W. Leitner, Hydrogenation of carbon dioxide to methanol by using a homogeneous ruthenium-phosphine catalyst, Angew. Chem. Int. (Ed.) Engl. 51 (30) (2012) 7499–7502.
[200] V.L. Sushkevich, D. Palagin, M. Ranocchiari, J.A. van Bokhoven, Selective anaerobic oxidation of methane enables direct synthesis of methanol, Science 356 (6337) (2017) 523.
[201] F. Dalena, A. Senatore, A. Marino, A. Gordano, M. Basile, A. Basile, Methanol production and applications: an overview, Membranes 8 (2018) 3–28.
[202] R.M. Navarro, M.A. Peña, J.L. Fierro, Hydrogen production reactions from carbon feedstocks: fossil fuels and biomass, Chem. Rev. 107 (10) (2007) 3952–3991.
[203] A.F. Dalebrook, W. Gan, M. Grasemann, S. Moret, G. Laurenczy, Hydrogen storage: beyond conventional methods, Chem. Commun. 49 (78) (2013) 8735–8751.
[204] A. Sartbaeva, V.L. Kuznetsov, S.A. Wells, P.P. Edwards, Hydrogen nexus in a sustainable energy future, Energy Environ. Sci. 1 (1) (2008) 79–85.
[205] E.J. Barreiro, A.E. Kümmerle, C.A.M. Fraga, The methylation effect in medicinal chemistry, Chem. Rev. 111 (9) (2011) 5215–5246.
[206] J. Moran, A. Preetz, R.A. Mesch, M.J. Krische, Iridium-catalysed direct C-C coupling of methanol and allenes, Nat. Chem. 3 (4) (2011) 287–290.
[207] G.E. Dobereiner, R.H. Crabtree, Dehydrogenation as a substrate-activating strategy in homogeneous transition-metal catalysis, Chem. Rev. 110 (2) (2010) 681–703.
[208] M.H.S.A. Hamid, P.A. Slatford, J.M.J. Williams, Borrowing hydrogen in the activation of alcohols, Adv. Synth. Catal. 349 (10) (2007) 1555–1575.
[209] C. Gunanathan, D. Milstein, Applications of acceptorless dehydrogenation and related transformations in chemical synthesis, Science 341 (6143) (2013) 1229712.
[210] R.E. Rodríguez-Lugo, M. Trincado, M. Vogt, F. Tewes, G. Santiso-Quinones, H. Grützmacher, A homogeneous transition metal complex for clean hydrogen production from methanol-water mixtures, Nat. Chem. 5 (4) (2013) 342–347.
[211] M. Andérez-Fernández, L.K. Vogt, S. Fischer, W. Zhou, H. Jiao, M. Garbe, et al., manganese pincer catalyst for the selective dehydrogenation of methanol, Angew. Chem. Int. (Ed.) 56 (2) (2017) 559–562.
[212] M. Lei, Y. Pan, X. Ma, The nature of hydrogen production from aqueous-phase methanol dehydrogenation with ruthenium pincer complexes under mild conditions, Eur. J. Inorg. Chem. 2015 (5) (2015) 794–803.
[213] K.-i Fujita, R. Kawahara, T. Aikawa, R. Yamaguchi, Hydrogen production from a methanol–water solution catalyzed by an anionic iridium complex bearing a functional bipyridonate ligand under weakly basic conditions, Angew. Chem. Int. (Ed.) 54 (31) (2015) 9057–9060.
[214] E.A. Bielinski, M. Förster, Y. Zhang, W.H. Bernskoetter, N. Hazari, M.C. Holthausen, Base-free methanol dehydrogenation using a pincer-supported iron compound and lewis acid co-catalyst, ACS Catal. 5 (4) (2015) 2404–2415.
[215] A. Monney, E. Barsch, P. Sponholz, H. Junge, R. Ludwig, M. Beller, Base-free hydrogen generation from methanol using a bi-catalytic system, Chem. Commun. 50 (6) (2014) 707–709.
[216] E. Alberico, P. Sponholz, C. Cordes, M. Nielsen, H.-J. Drexler, W. Baumann, et al., Selective hydrogen production from methanol with a defined iron pincer catalyst under mild conditions, Angew. Chem. Int. (Ed.) 52 (52) (2013) 14162–14166.
[217] P. Hu, Y. Diskin-Posner, Y. Ben-David, D. Milstein, Reusable homogeneous catalytic system for hydrogen production from methanol and water, ACS Catal. 4 (8) (2014) 2649–2652.

[218] M. Nielsen, E. Alberico, W. Baumann, H.J. Drexler, H. Junge, S. Gladiali, et al., Low-temperature aqueous-phase methanol dehydrogenation to hydrogen and carbon dioxide, Nature 495 (7439) (2013) 85–89.
[219] R. Grigg, T.R.B. Mitchell, S. Sutthivaiyakit, N. Tongpenyai, Transition metal-catalysed N-alkylation of amines by alcohols, J. Chem. Soc., Chem. Commun. 12 (1981) 611–612.
[220] Y. Watanabe, Y. Tsuji, Y. Ohsugi, The ruthenium catalyzed N-alkylation and N-heterocyclization of aniline using alcohols and aldehydes, Tetrahedron Lett. 22 (1981) 2667–2670.
[221] K.-T. Huh, Y. Tsuji, M. Kobayashi, F. Okuda, Y. Watanabe, Ruthenium catalyzed N-methylation of aminoaranes using methanol, Chem. Lett. 17 (3) (1988) 449–452.
[222] A. Del Zotto, W. Baratta, M. Sandri, G. Verardo, P. Rigo, Cyclopentadienyl RuII complexes as highly efficient catalysts for the N-methylation of alkylamines by methanol, Eur. J. Inorg. Chem. 2004 (3) (2004) 524–529.
[223] F. Li, J. Xie, H. Shan, C. Sun, L. Chen, General and efficient method for direct N-monomethylation of aromatic primary amines with methanol, RSC Adv. 2 (23) (2012) 8645–8652.
[224] V.N. Tsarev, Y. Morioka, J. Caner, Q. Wang, R. Ushimaru, A. Kudo, et al., N-Methylation of amines with methanol at room temperature, Org. Lett. 17 (10) (2015) 2530–2533.
[225] L. Zhang, Y. Zhang, Y. Deng, F. Shi, Light-promoted N,N-dimethylation of amine and nitro compound with methanol catalyzed by Pd/TiO2 at room temperature, RSC Adv. 5 (19) (2015) 14514–14521.
[226] S. Elangovan, J. Neumann, J.-B. Sortais, K. Junge, C. Darcel, M. Beller, Efficient and selective N-alkylation of amines with alcohols catalysed by manganese pincer complexes, Nat. Commun. 7 (1) (2016) 12641.
[227] A. Bruneau-Voisine, D. Wang, V. Dorcet, T. Roisnel, C. Darcel, J.-B. Sortais, Mono-N-methylation of anilines with methanol catalyzed by a manganese pincer-complex, J. Catal. 347 (2017) 57–62.
[228] B. Paul, S. Shee, K. Chakrabarti, S. Kundu, Tandem transformation of nitro compounds into N-methylated amines: greener strategy for the utilization of methanol as a methylating agent, ChemSusChem 10 (11) (2017) 2370–2374.
[229] G. Choi, S.H. Hong, Selective N-formylation and N-methylation of amines using methanol as a sustainable C1 source, ACS Sustain. Chem. Eng. 7 (1) (2019) 716–723.
[230] K. Polidano, J.M.J. Williams, L.C. Morrill, Iron-catalyzed borrowing hydrogen β-C(sp3)-methylation of alcohols, ACS Catal. 9 (9) (2019) 8575–8580.
[231] R. Mamidala, P. Biswal, M.S. Subramani, S. Samser, K. Venkatasubbaiah, Palladacycle-phosphine catalyzed methylation of amines and ketones using methanol, J. Org. Chem. 84 (16) (2019) 10472–10480.
[232] K. Das, P.G. Nandi, K. Islam, H.K. Srivastava, A. Kumar, N–Alkylation of amines catalyzed by a ruthenium–pincer complex in the presence of in situ generated sodium alkoxide, Eur. J. Org. Chem. 2019 (40) (2019) 6855–6866.
[233] V. Arora, M. Dutta, K. Das, B. Das, H.K. Srivastava, A. Kumar, Solvent-free N-alkylation and dehydrogenative coupling catalyzed by a highly active pincer-nickel complex, Organometallics 39 (11) (2020) 2162–2176.
[234] P.S. Mahajan, V.T. Humne, S.D. Tanpure, S.B. Mhaske, Radical Beckmann rearrangement and its application in the formal total synthesis of antimalarial natural product isocryptolepine via C–H activation, Org. Lett. 18 (14) (2016) 3450–3453.
[235] B. Paul, S. Shee, D. Panja, K. Chakrabarti, S. Kundu, Direct synthesis of N,N-dimethylated and β-methyl N,N-dimethylated amines from nitriles using methanol: experimental and computational studies, ACS Catal. 8 (4) (2018) 2890–2896.

[236] B. Paul, D. Panja, S. Kundu, Ruthenium-catalyzed synthesis of N-methylated amides using methanol, Org. Lett. 21 (15) (2019) 5843–5847.
[237] B. Paul, M. Maji, D. Panja, S. Kundu, Tandem transformation of aldoximes to N-methylated amides using methanol, Adv. Synth. Catal. 361 (23) (2019) 5357–5362.
[238] B. Paul, M. Maji, S. Kundu, Atom-economical and tandem conversion of nitriles to N-methylated amides using methanol and water, ACS Catal. 9 (11) (2019) 10469–10476.
[239] S. Park, Y.A. Choi, H. Han, S.H. Yang, S. Chang, Rh-catalyzed one-pot and practical transformation of aldoximes to amides, Chem. Commun. (Camb.) 15 (2003) 1936–1937.
[240] C.L. Allen, R. Lawrence, L. Emmett, J.M.J. Williams, Mechanistic studies into metal-catalyzed aldoxime to amide rearrangements, Adv. Synth. Catal. 353 (18) (2011) 3262–3268.
[241] N. Ortega, C. Richter, F. Glorius, N-Formylation of amines by methanol activation, Org. Lett. 15 (7) (2013) 1776–1779.
[242] B. Kang, S.H. Hong, Hydrogen acceptor- and base-free N-formylation of nitriles and amines using methanol as C1 source, Adv. Synth. Catal. 357 (4) (2015) 834–840.
[243] S. Chakraborty, U. Gellrich, Y. Diskin-Posner, G. Leitus, L. Avram, D. Milstein, Manganese-catalyzed N-formylation of amines by methanol liberating H(2): a catalytic and mechanistic study, Angew. Chem. Int. (Ed.) Engl. 56 (15) (2017) 4229–4233.
[244] E.M. Lane, K.B. Uttley, N. Hazari, W. Bernskoetter, Iron-catalyzed amide formation from the dehydrogenative coupling of alcohols and secondary amines, Organometallics 36 (10) (2017) 2020–2025.
[245] L.K.M. Chan, D.L. Poole, D. Shen, M.P. Healy, T.J. Donohoe, Rhodium-catalyzed ketone methylation using methanol under mild conditions: formation of α-branched products, Angew. Chem. Int. (Ed.) 53 (3) (2014) 761–765.
[246] S. Ogawa, Y. Obora, Iridium-catalyzed selective α-methylation of ketones with methanol, Chem. Commun. 50 (19) (2014) 2491–2493.
[247] F. Li, J. Ma, N. Wang, α-Alkylation of ketones with primary alcohols catalyzed by a Cp*Ir complex bearing a functional bipyridonate ligand, J. Org. Chem. 79 (21) (2014) 10447–10455.
[248] X. Quan, S. Kerdphon, P.G. Andersson, C–C Coupling of ketones with methanol catalyzed by a N-heterocyclic carbene–phosphine iridium complex, Chem.—A Eur. J. 21 (9) (2015) 3576–3579.
[249] T.T. Dang, A.M. Seayad, A convenient ruthenium-catalysed α-methylation of carbonyl compounds using methanol, Adv. Synth. Catal. 358 (21) (2016) 3373–3380.
[250] K. Das, E. Yasmin, B. Das, H.K. Srivastava, A. Kumar, Phosphine-free pincer-ruthenium catalyzed biofuel production: high rates, yields and turnovers of solventless alcohol alkylation, Catal. Sci. Technol. 10 (24) (2020) 8347–8358.
[251] C. Carlini, M. Di Girolamo, A. Macinai, M. Marchionna, M. Noviello, A.M.R. Galletti, et al., Synthesis of isobutanol by the Guerbet condensation of methanol with n-propanol in the presence of heterogeneous and homogeneous palladium-based catalytic systems, J. Mol. Catal. A—Chem. 204 (2003) 721–728.
[252] Y. Li, H. Li, H. Junge, M. Beller, Selective ruthenium-catalyzed methylation of 2-arylethanols using methanol as C1 feedstock, Chem. Commun. 50 (95) (2014) 14991–14994.
[253] K. Oikawa, S. Itoh, H. Yano, H. Kawasaki, Y. Obora, Preparation and use of DMF-stabilized iridium nanoclusters as methylation catalysts using methanol as the C1 source, Chem. Commun. 53 (6) (2017) 1080–1083.
[254] R.L. Wingad, E.J.E. Bergström, M. Everett, K.J. Pellow, D.F. Wass, Catalytic conversion of methanol/ethanol to isobutanol—a highly selective route to an advanced biofuel, Chem. Commun. 52 (29) (2016) 5202–5204.

[255] Q. Liu, G. Xu, Z. Wang, X. Liu, X. Wang, L. Dong, et al., Iridium clusters encapsulated in carbon nanospheres as nanocatalysts for methylation of (bio)alcohols, ChemSusChem 10 (23) (2017) 4748–4755.
[256] S.M.A.H. Siddiki, A.S. Touchy, M.A.R. Jamil, T. Toyao, K.-i Shimizu, C-Methylation of alcohols, ketones, and indoles with methanol using heterogeneous platinum catalysts, ACS Catal. 8 (4) (2018) 3091–3103.
[257] S.-J. Chen, G.-P. Lu, C. Cai, Iridium-catalyzed methylation of indoles and pyrroles using methanol as feedstock, RSC Adv. 5 (86) (2015) 70329–70332.
[258] Z. Liu, Z. Yang, X. Yu, H. Zhang, B. Yu, Y. Zhao, et al., Methylation of C (sp3)–H/C(sp2)–H bonds with methanol catalyzed by cobalt system, Org. Lett. 19 (19) (2017) 5228–5231.
[259] K. Polidano, B.D.W. Allen, J.M.J. Williams, L.C. Morrill, Iron-catalyzed methylation using the borrowing hydrogen approach, ACS Catal. 8 (7) (2018) 6440–6445.
[260] A. Bruneau-Voisine, L. Pallova, S. Bastin, V. César, J.-B. Sortais, Manganese catalyzed α-methylation of ketones with methanol as a C1 source, Chem. Commun. 55 (3) (2019) 314–317.
[261] J. Sklyaruk, J.C. Borghs, O. El-Sepelgy, M. Rueping, Catalytic C1|alkylation with methanol and isotope-labeled methanol, Angew. Chem. Int. (Ed.) 58 (3) (2019) 775–779.
[262] J. Das, K. Singh, M. Vellakkaran, D. Banerjee, Nickel-catalyzed hydrogen-borrowing strategy for α-alkylation of ketones with alcohols: a new route to branched gem-bis(alkyl) ketones, Org. Lett. 20 (18) (2018) 5587–5591.
[263] M. Mastalir, M. Glatz, E. Pittenauer, G. Allmaier, K. Kirchner, Rhenium-catalyzed dehydrogenative coupling of alcohols and amines to afford nitrogen-containing aromatics and more, Org. Lett. 21 (4) (2019) 1116–1120.
[264] M. Mastalir, E. Pittenauer, G. Allmaier, K. Kirchner, Manganese-catalyzed aminomethylation of aromatic compounds with methanol as a sustainable C1 building block, J. Am. Chem. Soc. 139 (26) (2017) 8812–8815.
[265] S. Kim, S.H. Hong, Ruthenium-catalyzed aminomethylation and methylation of phenol derivatives utilizing methanol as the C1 source, Adv. Synth. Catal. 359 (5) (2017) 798–810.
[266] B.C., Roy, S. Debnath, K. Chakrabarti, B. Paul, M. Maji, S. Kundu, ortho-Amino group functionalized 2,2′-bipyridine based Ru(ii) complex catalysed alkylation of secondary alcohols, nitriles and amines using alcohols, Org. Chem. Front. 5 (6) (2018) 1008–1018.
[267] S. Thiyagarajan, C. Gunanathan, Facile ruthenium(II)-catalyzed α-alkylation of arylmethyl nitriles using alcohols enabled by metal–ligand cooperation, ACS Catal. 7 (8) (2017) 5483–5490.
[268] F. Li, L. Lu, P. Liu, Acceptorless dehydrogenative coupling of o-aminobenzamides with the activation of methanol as a C1 source for the construction of quinazolinones, Org. Lett. 18 (11) (2016) 2580–2583.
[269] S. Kerdphon, P. Sanghong, J. Chatwichien, V. Choommongkol, P. Rithchumpon, T. Singh, et al., Commercial copper-catalyzed aerobic oxidative synthesis of quinazolinones from 2-aminobenzamide and methanol, Eur. J. Org. Chem. 2020 (18) (2020) 2730–2734.
[270] B.C., Roy, S.A. Samim, D. Panja, S. Kundu, Tandem synthesis of quinazolinone scaffolds from 2-aminobenzonitriles using aliphatic alcohol–water system, Catal. Sci. Technol. 9 (21) (2019) 6002–6006.
[271] G. Satish, A. Polu, L. Kota, A. Ilangovan, Copper-catalyzed oxidative amination of methanol to access quinazolines, Org. Biomol. Chem. 17 (19) (2019) 4774–4782.

[272] Z. Sun, G. Bottari, K. Barta, Supercritical methanol as solvent and carbon source in the catalytic conversion of 1,2-diaminobenzenes and 2-nitroanilines to benzimidazoles, Green. Chem. 17 (12) (2015) 5172–5181.
[273] K. Tani, A. Iseki, T. Yamagata, Efficient transfer hydrogenation of alkynes and alkenes with methanol catalysed by hydrido(methoxo)iridium(III) complexes, Chem. Commun. 18 (1999) 1821–1822.
[274] N. Garg, S. Paira, B. Sundararaju, Efficient transfer hydrogenation of ketones using methanol as liquid organic hydrogen carrier, ChemCatChem 12 (13) (2020) 3472–3476.
[275] F. Bigi, R. Maggi, G. Sartori, Selected syntheses of ureas through phosgene substitutes, Green. Chem. 2 (4) (2000) 140–148.
[276] L. Tiwari, V. Kumar, B. Kumar, D. Mahajan, A practically simple, catalyst free and scalable synthesis of N-substituted ureas in water, RSC Adv. 8 (38) (2018) 21585–21595.
[277] S.H. Kim, S.H. Hong, Ruthenium-catalyzed urea synthesis using methanol as the C1 source, Org. Lett. 18 (2) (2016) 212–215.
[278] E.M. Lane, N. Hazari, W.H. Bernskoetter, Iron-catalyzed urea synthesis: dehydrogenative coupling of methanol and amines, Chem. Sci. 9 (16) (2018) 4003–4008.
[279] P. Lorusso, J. Coetzee, G.R. Eastham, D.J. Cole-Hamilton, α-Methylenation of methyl propanoate by the catalytic dehydrogenation of methanol, ChemCatChem 8 (1) (2016) 222–227.
[280] D. Shen, D.L. Poole, C.C. Shotton, A.F. Kornahrens, M.P. Healy, T.J. Donohoe, Hydrogen-borrowing and interrupted-hydrogen-borrowing reactions of ketones and methanol catalyzed by iridium, Angew. Chem. Int. (Ed.) Engl. 54 (5) (2015) 1642–1645.
[281] E.-A. Jo, J.-H. Lee, C.-H. Jun, Rhodium(i)-catalyzed one-pot synthesis of dialkyl ketones from methanol and alkenes through directed sp3 C–H bond activation of N-methylamine, Chem. Commun. 44 (2008) 5779–5781.
[282] C. Sun, X. Zou, F. Li, Direct use of methanol as an alternative to formaldehyde for the synthesis of 3,3′-bisindolylmethanes (3,3′-BIMs), Chem.—A Eur. J. 19 (42) (2013) 14030–14033.
[283] R.H. Crabtree, Homogeneous transition metal catalysis of acceptorless dehydrogenative alcohol oxidation: applications in hydrogen storage and to heterocycle synthesis, Chem. Rev. 117 (13) (2017) 9228–9246.
[284] R.A. Sheldon, Green chemistry and resource efficiency: towards a green economy, Green. Chem. 18 (11) (2016) 3180–3183.
[285] J. Zhang, M. Gandelman, L.J.W. Shimon, H. Rozenberg, D. Milstein, Electron-rich, bulky ruthenium PNP-type complexes. Acceptorless catalytic alcohol dehydrogenation, Organometallics 23 (17) (2004) 4026–4033.
[286] C. Gunanathan, L.J.W. Shimon, D. Milstein, Direct conversion of alcohols to acetals and H2 catalyzed by an acridine-based ruthenium pincer complex, J. Am. Chem. Soc. 131 (9) (2009) 3146–3147.
[287] M. Montag, J. Zhang, D. Milstein, Aldehyde binding through reversible C–C coupling with the pincer ligand upon alcohol dehydrogenation by a PNP–ruthenium catalyst, J. Am. Chem. Soc. 134 (25) (2012) 10325–10328.
[288] J. Zhang, E. Balaraman, G. Leitus, D. Milstein, Electron-rich PNP- and PNN-type ruthenium(II) hydrido borohydride pincer complexes. Synthesis, structure, and catalytic dehydrogenation of alcohols and hydrogenation of esters, Organometallics 30 (21) (2011) 5716–5724.
[289] J. Zhang, M. Gandelman, L.J.W. Shimon, D. Milstein, Electron-rich, bulky PNN-type ruthenium complexes: synthesis, characterization and catalysis of alcohol dehydrogenation, Dalton Trans. 1 (2007) 107–113.

[290] J. Zhang, G. Leitus, Y. Ben-David, D. Milstein, Facile conversion of alcohols into esters and dihydrogen catalyzed by new ruthenium complexes, J. Am. Chem. Soc. 127 (31) (2005) 10840—10841.
[291] M. Nielsen, H. Junge, A. Kammer, M. Beller, Towards a green process for bulk-scale synthesis of ethyl acetate: efficient acceptorless dehydrogenation of ethanol, Angew. Chem. Int. (Ed.) 51 (23) (2012) 5711—5713.
[292] M. Nielsen, A. Kammer, D. Cozzula, H. Junge, S. Gladiali, M. Beller, Efficient hydrogen production from alcohols under mild reaction conditions, Angew. Chem. Int. (Ed.) 50 (41) (2011) 9593—9597.
[293] S. De-Botton, R. Romm, G. Bensoussan, M. Hitrik, S. Musa, D. Gelman, Coordination versatility of p-hydroquinone-functionalized dibenzobarrelene-based PC(sp3)P pincer ligands, Dalton Trans. 45 (40) (2016) 16040—16046.
[294] S. Musa, I. Shaposhnikov, S. Cohen, D. Gelman, Ligand—metal cooperation in PCP pincer complexes: rational design and catalytic activity in acceptorless dehydrogenation of alcohols, Angew. Chem. Int. (Ed.) 50 (15) (2011) 3533—3537.
[295] K.-N.T. Tseng, J.W. Kampf, N.K. Szymczak, Base-free, acceptorless, and chemoselective alcohol dehydrogenation catalyzed by an amide-derived NNN-ruthenium (II) hydride complex, Organometallics 32 (7) (2013) 2046—2049.
[296] Q. Wang, H. Chai, Z. Yu, Dimeric ruthenium(II)-NNN complex catalysts bearing a pyrazolyl-pyridylamino-pyridine ligand for transfer hydrogenation of ketones and acceptorless dehydrogenation of alcohols, Organometallics 36 (18) (2017) 3638—3644.
[297] Q. Wang, H. Chai, Z. Yu, Acceptorless dehydrogenation of N-heterocycles and secondary alcohols by Ru(II)-NNC complexes bearing a pyrazoyl-indolyl-pyridine ligand, Organometallics 37 (4) (2018) 584—591.
[298] G. Zhang, S.K. Hanson, Cobalt-catalyzed acceptorless alcohol dehydrogenation: synthesis of imines from alcohols and amines, Org. Lett. 15 (3) (2013) 650—653.
[299] G. Zhang, K.V. Vasudevan, B.L. Scott, S.K. Hanson, Understanding the mechanisms of cobalt-catalyzed hydrogenation and dehydrogenation reactions, J. Am. Chem. Soc. 135 (23) (2013) 8668—8681.
[300] Y. Jing, X. Chen, X. Yang, Computational mechanistic study of the hydrogenation and dehydrogenation reactions catalyzed by cobalt pincer complexes, Organometallics 34 (24) (2015) 5716—5722.
[301] P.J. Bonitatibus, S. Chakraborty, M.D. Doherty, O. Siclovan, W.D. Jones, G.L. Soloveichik, Reversible catalytic dehydrogenation of alcohols for energy storage, Proc. Natl Acad. Sci. 112 (6) (2015) 1687.
[302] S. Chakraborty, P.O. Lagaditis, M. Förster, E.A. Bielinski, N. Hazari, M.C. Holthausen, et al., Well-defined iron catalysts for the acceptorless reversible dehydrogenation-hydrogenation of alcohols and ketones, ACS Catal. 4 (11) (2014) 3994—4003.
[303] D.H. Nguyen, X. Trivelli, F. Capet, J.-F. Paul, F. Dumeignil, R.M. Gauvin, Manganese pincer complexes for the base-free, acceptorless dehydrogenative coupling of alcohols to esters: development, scope, and understanding, ACS Catal. 7 (3) (2017) 2022—2032.
[304] P. Hu, D. Milstein, Conversion of alcohols to carboxylates using water and base with H 2 liberation, Organomet. Green. Catal. (2018) 175—192.
[305] E. Balaraman, E. Khaskin, G. Leitus, D. Milstein, Catalytic transformation of alcohols to carboxylic acid salts and H2 using water as the oxygen atom source, Nat. Chem. 5 (2) (2013) 122—125.
[306] P. Hu, Y. Ben-David, D. Milstein, General synthesis of amino acid salts from amino alcohols and basic water liberating H2, J. Am. Chem. Soc. 138 (19) (2016) 6143—6146.

[307] J.-H. Choi, L.E. Heim, M. Ahrens, M.H.G. Prechtl, Selective conversion of alcohols in water to carboxylic acids by in situ generated ruthenium trans dihydrido carbonyl PNP complexes, Dalton Trans. 43 (46) (2014) 17248–17254.
[308] P. Sponholz, D. Mellmann, C. Cordes, P.G. Alsabeh, B. Li, Y. Li, et al., Efficient and selective hydrogen generation from bioethanol using ruthenium pincer-type complexes, ChemSusChem 7 (9) (2014) 2419–2422.
[309] L. Zhang, D.H. Nguyen, G. Raffa, X. Trivelli, F. Capet, S. Desset, et al., Catalytic conversion of alcohols into carboxylic acid salts in water: scope, recycling, and mechanistic insights, ChemSusChem 9 (12) (2016) 1413–1423.
[310] Z. Dai, Q. Luo, X. Meng, R. Li, J. Zhang, T. Peng, Ru(II) complexes bearing 2,6-bis(benzimidazole-2-yl)pyridine ligands: a new class of catalysts for efficient dehydrogenation of primary alcohols to carboxylic acids and H2 in the alcohol/CsOH system, J. Organomet. Chem. 830 (2017) 11–18.
[311] E.W. Dahl, T. Louis-Goff, N.K. Szymczak, Second sphere ligand modifications enable a recyclable catalyst for oxidant-free alcohol oxidation to carboxylates, Chem. Commun. 53 (14) (2017) 2287–2289.
[312] H.-M. Liu, L. Jian, C. Li, C.-C. Zhang, H.-Y. Fu, X.-L. Zheng, et al., Dehydrogenation of alcohols to carboxylic acid catalyzed by in situ-generated facial ruthenium-CPP complex, J. Org. Chem. 84 (14) (2019) 9151–9160.
[313] Y. Li, M. Nielsen, B. Li, P.H. Dixneuf, H. Junge, M. Beller, Ruthenium-catalyzed hydrogen generation from glycerol and selective synthesis of lactic acid, Green. Chem. 17 (1) (2015) 193–198.
[314] L.S. Sharninghausen, B.Q. Mercado, R.H. Crabtree, N. Hazari, Selective conversion of glycerol to lactic acid with iron pincer precatalysts, Chem. Commun. 51 (90) (2015) 16201–16204.
[315] M. Dutta, K. Das, S.J. Prathapa, H.K. Srivastava, A. Kumar, Selective and high yield transformation of glycerol to lactic acid using NNN pincer ruthenium catalysts, Chem. Commun. 56 (68) (2020) 9886–9889.
[316] Z. Dai, Q. Luo, H. Jiang, Q. Luo, H. Li, J. Zhang, et al., Ni(ii)–N′NN′ pincer complexes catalyzed dehydrogenation of primary alcohols to carboxylic acids and H2 accompanied by alcohol etherification, Catal. Sci. Technol. 7 (12) (2017) 2506–2511.
[317] D.H. Nguyen, Y. Morin, L. Zhang, X. Trivelli, F. Capet, S. Paul, et al., Oxidative transformations of biosourced alcohols catalyzed by earth-abundant transition metals, ChemCatChem 9 (14) (2017) 2652–2660.
[318] Z. Shao, Y. Wang, Y. Liu, Q. Wang, X. Fu, Q. Liu, A general and efficient Mn-catalyzed acceptorless dehydrogenative coupling of alcohols with hydroxides into carboxylates, Org. Chem. Front. 5 (8) (2018) 1248–1256.
[319] D.R. Pradhan, S. Pattanaik, J. Kishore, C. Gunanathan, Cobalt-catalyzed acceptorless dehydrogenation of alcohols to carboxylate salts and hydrogen, Org. Lett. 22 (5) (2020) 1852–1857.
[320] A. Erkkilä, I. Majander, P.M. Pihko, Iminium catalysis, Chem. Rev. 107 (12) (2007) 5416–5470.
[321] F.F. Fleming, L. Yao, P.C. Ravikumar, L. Funk, B.C., Shook, Nitrile-containing pharmaceuticals: efficacious roles of the nitrile pharmacophore, J. Med. Chem. 53 (22) (2010) 7902–7917.
[322] S. Kobayashi, Y. Mori, J.S. Fossey, M.M. Salter, Catalytic enantioselective formation of C − C bonds by addition to imines and hydrazones: a ten-year update, Chem. Rev. 111 (4) (2011) 2626–2704.
[323] Z.-Y. Liu, Y.-M. Wang, Z.-R. Li, J.-D. Jiang, D.W. Boykin, Synthesis and anticancer activity of novel 3,4-diarylthiazol-2(3H)-ones (imines), Bioorg. Med. Chem. Lett. 19 (19) (2009) 5661–5664.

[324] S. Luo, E. Zhang, Y. Su, T. Cheng, C. Shi, A review of NIR dyes in cancer targeting and imaging, Biomaterials 32 (29) (2011) 7127—7138.
[325] S. Mukherjee, J.W. Yang, S. Hoffmann, B. List, Asymmetric enamine catalysis, Chem. Rev. 107 (12) (2007) 5471—5569.
[326] Z. Wang, J. Belli, C.M. Jensen, Homogeneous dehydrogenation of liquid organic hydrogen carriers catalyzed by an iridium PCP complex, Faraday Discuss. 151 (0) (2011) 297—305.
[327] W.H. Bernskoetter, M. Brookhart, Kinetics and mechanism of iridium-catalyzed dehydrogenation of primary amines to nitriles, Organometallics 27 (9) (2008) 2036—2045.
[328] X.-Q. Gu, W. Chen, D. Morales-Morales, C.M. Jensen, Dehydrogenation of secondary amines to imines catalyzed by an iridium PCP pincer complex: initial aliphatic or direct amino dehydrogenation? J. Mol. Catal. A: Chem. 189 (1) (2002) 119—124.
[329] L.-P. He, T. Chen, D. Gong, Z. Lai, K.-W. Huang, Enhanced reactivities toward amines by introducing an imine arm to the pincer ligand: direct coupling of two amines to form an imine without oxidant, Organometallics 31 (14) (2012) 5208—5211.
[330] K.-N.T. Tseng, A.M. Rizzi, N.K. Szymczak, Oxidant-free conversion of primary amines to nitriles, J. Am. Chem. Soc. 135 (44) (2013) 16352—16355.
[331] S. Chakraborty, W.W. Brennessel, W.D. Jones, A molecular iron catalyst for the acceptorless dehydrogenation and hydrogenation of N-heterocycles, J. Am. Chem. Soc. 136 (24) (2014) 8564—8567.
[332] B. Sawatlon, P. Surawatanawong, Mechanisms for dehydrogenation and hydrogenation of N-heterocycles using PNP-pincer-supported iron catalysts: a density functional study, Dalton Trans. 45 (38) (2016) 14965—14978.
[333] R. Xu, S. Chakraborty, H. Yuan, W.D. Jones, Acceptorless, reversible dehydrogenation and hydrogenation of N-heterocycles with a cobalt pincer catalyst, ACS Catal. 5 (11) (2015) 6350—6354.
[334] V. Zubar, J.C. Borghs, M. Rueping, Hydrogenation or dehydrogenation of N-containing heterocycles catalyzed by a single manganese complex, Org. Lett. 22 (10) (2020) 3974—3978.

Index

Note: Page numbers followed by "*f*" and "*t*" refer to figures and tables, respectively.

B

C

D

E

F

G

H

O

P

R

S

T

U

V

Z

PINCER-METAL COMPLEXES

Applications in Catalytic Dehydrogenation Chemistry

Edited by Akshai Kumar
Department of Chemistry, Centre for Nanotechnology, School of Health Science & Technology, Indian Institute of Technology, Guwahati, India

An overview of pincer-metal catalytic systems for transforming hydrocarbons and their derivatives

Pincer–Metal Complexes: Applications in Catalytic Dehydrogenation Chemistry provides an overview of pincer-metal catalytic systems transforming hydrocarbons and their derivatives, including methanol and related alcohols from a synthetic and mechanistic point of view. The book discusses success stories of pincer-metal systems as well as current and future challenges.

In recent years there has been a surge in the research on hydrocarbon dehydrogenation catalytic systems that are compatible with polar substituents. This helps facilitate the formulation of tandem processes that are not limited to hydrocarbon dehydrogenation but also to hydrocarbon functionalization in a single pot. This book provides thorough coverage of the operating mechanisms and the compatibility of catalytic dehydrogenation in both functionalized and unfunctionalized hydrocarbon systems.

The book is an ideal reference for researchers practicing synthetic organic chemistry, inorganic chemistry, organometallic chemistry, and catalysis in academia and industry.

Key Features

- Covers applications of pincer–metal complexes in organic transformations
- Includes pincer-group 8 and 9 metal complexes for alkane dehydrogenations
- Features a discussion of pincer–metal complexes for dehydrogenation of functionalized hydrocarbons including alcohols and methanol

About the Editor

Akshai Kumar earned his bachelor's degree in physics, chemistry, and mathematics, and later his master's degree in inorganic chemistry, from Mangalore University. He then earned his PhD at the Indian Institute of Science in Bangalore for his work on reductive and metathetic coupling reactions mediated by group (IV) metal alkoxides and continued his postdoctoral studies researching unusual titanium mediated reductive pathways. In 2010 he explored organofluorine chemistry during his postdoctoral studies at Goethe University. In 2012 at Rutgers—The State University of New Jersey, he focused his post-doctoral research on the design of tandem catalytic systems based on pincer–iridium complexes and zeolites for the catalytic transformation of alkanes to synthesize fuel chemicals. In 2015, he was appointed as Assistant Professor in Chemistry at IIT Guwahati. Currently, he is an Associate Professor in Chemistry at IIT Guwahati and his research focuses on transition-metal-catalyzed C–H and C–F activation reactions for the synthesis of fuel chemicals and heteroatom-doped π-conjugated organic materials.

ISBN 978-0-12-822091-7

9 780128 220917

ELSEVIER elsevier.com/books-and-journals